The heart of creatures is the foundation of life, the Prince of all, the sun of their microcosm, from where all vigor and strength does flow.

-William Harvey, *De Motu Cordis*, 1628

University of Alberta

The Role of TIMPs in Heart Disease

by

Vijay Saradhi Kandalam

A thesis submitted to the Faculty of Graduate Studies and Research

in partial fulfillment of the requirements for the degree of

Doctor of Philosophy

Department of Physiology

©Vijay Saradhi Kandalam

Fall 2012

Edmonton, Alberta

Permission is hereby granted to the University of Alberta Libraries to reproduce single copies of this thesis and to lend or sell such copies for private, scholarly or scientific research purposes only. Where the thesis is converted to, or otherwise made available in digital form, the University of Alberta will advise potential users of the thesis of these terms.

The author reserves all other publication and other rights in association with the copyright in the thesis and, except as herein before provided, neither the thesis nor any substantial portion thereof may be printed or otherwise reproduced in any material form whatsoever without the author's prior written permission.

DEDICATION

To family, friends, and colleagues who have supported my pursuit of realizing my potential. I would like to share this accomplishment with all of you, as without you I could not have achieved this.

ABSTRACT

Heart disease is a leading cause of morbidity and mortality in the world with a growing prevalence in a variety of manifestations. Many of the events that occur in the heart during the progression of disease have been explored to identify a causative mechanism to develop effective treatments and possibly a cure for heart disease. There is a growing body of evidence demonstrating the necessity for adaptive remodeling of the extracellular matrix (ECM) for proper cardiac function in response to disease through balanced regulation of its structure. Cardiac ECM serves as a structural framework for the myocardium, and its integrity is maintained by the function of matrix metalloproteinases (MMPs) which are kept under control by their physiological inhibitors, Tissue Inhibitor of Metalloproteinases (TIMPs). A balance between the MMPs and TIMPs is important for optimal degradation and replacement of the ECM either in physiological ECM turnover or in adverse ECM remodeling in disease.

The research presented in this thesis consists of our investigation of the role of two highly expressed TIMPs in the heart, TIMP2 and TIMP3, in response to two common models of human heart disease. Mice lacking TIMP2 or TIMP3 were subjected to myocardial infarction, while the outcome of TIMP2 deficiency was also studied in response to cardiac pressure overload. Myocardial infarction led to different outcomes in the $TIMP2^{-/-}$ and $TIMP3^{-/-}$ mice. While $TIMP3^{-/-}$ mice exhibited elevated rates of left ventricular rupture incidence and severely compromised survival, as well as significant cardiac dysfunction, lack of TIMP2 exacerbated cardiac function without compromising survival compared to parallel

wildtype mice. Following pressure overload, TIMP2$^{-/-}$ mice showed left ventricular dilation and dysfunction, hypertrophy and fibrosis which we found to be linked to impaired ECM-myocyte connection due to excess degradation of integrin-β1 via excess activity of membrane-type 1 MMP (MT1-MMP). We have therefore identified important and distinct roles for these TIMPs in heart disease.

The results presented in this thesis are important contributions to the study of the role of ECM remodeling in the adaptive cardiac response to injury, as demonstrated through a wide variety of physiological, histological, and molecular analyses of the development of heart disease in each model. These findings provide novel evidence identifying distinct mechanisms or pattern of events associated with TIMP2 and TIMP3 that can alter the current understanding of the role of each TIMP in the development and progression of heart disease.

ACKNOWLEDGEMENTS

I would like to acknowledge the many people who have made contributions to the work presented in this thesis, to other projects directly influencing the work presented within, and those who have contributed to this important phase of my development into a research scientist.

My supervisor Dr. Zamaneh Kassiri has been an ideal role model for me to learn from. From when we first started in the lab together to this day, we have shared many great accomplishments along the way. She has guided me through a variety of experiences, while always being available to provide me feedback to promote excellence in the work that I do. Her dedication and hardwork is inspirational and is why I strive to emulate her.

I would like to thank my Supervisory Committee members Dr. Jason Dyck and Dr. Richard Schulz. They have been available, approachable, and supportive to give me a different perspective for me to incorporate into my training. I admire each of them for their respective accomplishments, and appreciate the insight that they have shared with me, either formally or informally.

My laboratory has been the creative centre of great scientists with wonderful personalities and my professional and personal well-being in mind. We have accomplished quite a lot together and it has been very rewarding to have trained together with all of them, with each of them contributing to my life in some meaningful way. In particular I would like to acknowledge my fellow Ph.D. Candidate Ratnadeep Basu and Laboratory Technician Sue Wang. We have worked together since the beginning and they have been directly involved with all of the work you see in front of you.

Thank you to the Department of Physiology in the Faculty of Medicine and Dentistry for their support and direction. They have assisted me through guidance, to provide me opportunities to appreciate the wealth of knowledge available and the value of the scientific community. The Cardiovascular Research Centre has provided an excellent environment to establish the skills I need to

pursue my professional ambitions. I would like to give a special thank you to Alberta Innovates Health Solutions (AIHS) for rewarding my efforts and dedication with funding and opportunities to broaden my training. This exceptional training environment is what has made my time at the University of Alberta so influential for my future endeavors.

My family has supported me in pursuing challenges in my life unconditionally, and with that freedom to become who I would like to be, I wish to share my joy and a thank you.

TABLE OF CONTENTS

CHAPTER 2

LIST OF FIGURES

LIST OF TABLES

Formulas

Echocardiography

Ejection fraction: EF (%) = [LVEDV-LDESV] / LVEDV x 100

Fractional shortening: FS (%) = [LVEDD-LDESD] / LVEDD x 100

Velocity of circumferential

Shortening: VcFc = FS% / ET

VcFc = ([LVEDD-LDESD] / LVEDD x 100) / ET

ET	ejection time
LVEDD	left ventricular end-diastolic diameter
LVESD	left ventricular end-systolic diameter

Abbreviations

ADAM	a disintegrin and metalloproteinases
ATP	adenosine triphosphate
CSA	cross-sectional area
cDNA	complementary DNA
DNA	deoxyribonucleic acid
ECM	extracellular matrix
EF	ejection fraction
FAK	focal adhesion kinase
FS	fractional shortening
GPCR	G-protein coupled receptor
HIF	hypoxia-inducible factor
HPRT	hypoxanthine-guanine phosphoribosyltransferase-1
LAD	left anterior descending
LV	left ventricle
LVEDV	left ventricle end-diastolic volume
LVESV	left ventricular end-systolic volume
MHC	myosin heavy chain
MI	myocardial infarction
MMP	matrix metalloproteinase
MMPi	matrix metalloproteinase inhibitor (pharmacological)

MPEF	multiphoton excitation fluorescence
mRNA	messenger RNA
MT1-MMP	membrane type 1-matrix metalloproteinase
PBS	phosphate buffered saline
PCR	polymerase chain reaction
RECK	reversion-inducing-cysteine-rich protein with kazal motifs
RNA	ribonucleic acid
ROS	reactive oxygen species
RT-PCR	real-time polymerase chain reaction
SHG	second harmonic generation
SPARC	secreted protein acidic and rich in cysteine
TAC	transverse aortic constriction
TACE	TNF-alpha converting enzyme
TBS	Tris-buffered saline
TGF	transforming growth factor
TIMP	tissue inhibitor of metalloproteinase
TnC	troponin C
TNF	tumor necrosis factor
VEGF	vascular endothelial growth factor
VEGFR	vascular endothelial growth factor receptor
WT	wild-type

Prefix

M	mega ((10^6)
k	kilo (10^3)
c	centi (10^{-2})
m	milli (10^{-3})
μ	micro (10^{-6})
n	nano (10^{-9})

Units

Hz	hertz
L	litre
m	metre
g	gram
Da	dalton
°C	degree Celsius

Symbols

α	alpha
β	beta

CHAPTER 1

INTRODUCTION

1.1. Introduction overview

Heart disease a leading cause of mortality in North America, and the ensuing development of irreversible heart failure is a considerable burden for the healthcare system to cope with. The physical, psychological, social, and economic implications of inadequately managed heart disease are tremendous. According to the American Heart Association[1], coronary heart disease causes approximately one of every six deaths, and one in nine death certificates mentioned heart failure. The recent advancements of science and technology in the field of cardiovascular research, coupled with increasing cardiac-related morbidity and mortality, has demanded greater focus on uncovering the pathogenesis of heart disease for swift translation into the clinical setting. The cardiovascular circuit is a complex system. It is necessary to identify underlying mechanisms of heart disease in order to effectively incorporate novel therapies with existing options, which have historically been limited in their scope of preventing heart failure as mortality rates remain high[2]. There is a necessity to investigate potential novel targets to optimize heart disease treatment. Within the complexity of heart disease, preserving the integrity of the extracellular matrix (ECM) network for the structural foundation of the heart muscle presents an intriguing target for therapeutic interventions.

1.2. The fundamentals of cardiovascular physiology

The cardiovascular system is composed of the heart as the central pump, and the peripheral vasculature responsible for systemic perfusion. The heart is a four-chamber structure that can be divided into the right and left side. The right atrium and ventricle work as a unit to deliver blood to the lungs via the pulmonary artery for gas exchange and oxygenation, where blood proceeds to travel to the left atrium from the lungs through the pulmonary veins. It is in the pulmonary circuit that blood is reoxygenated and delivered back to the heart. The blood entering the left atrium is emptied into the left ventricle during diastole in both a

passive and active manner. The passive phase relies on left ventricle relaxation in order to maximally fill with blood followed by the ensuing active process involving atrial contraction to further empty the atrium, with both processes contributing to the left ventricle end-diastolic volume (LVEDV). Diastole is immediately followed by systolic contraction, where upon a fraction of the total blood in the left ventricle is ejected from the left ventricle through the aorta to the systemic circulation, with this fraction designated as the ejection fraction (EF). As blood circulates through the network of peripheral vasculature, the extensive microvascular capillary bed permits filtration and absorption and is the start of venous return to the heart.

1.3. The complex machinery of the heart

1.3.1. Structure of the heart muscle

The anatomy of the heart wall is composed of three distinguishable layers: the endocardium lining the heart chambers, the contracting muscular portion of the heart known as the myocardium, and the epicardium layer connecting to a fibrous pericardium surrounding the heart. The right ventricle wall is thinner than the left ventricle (LV) wall and is more compliant due to the lower afterload exerted by the pulmonary system and therefore requires less stroke work[3]. As with any muscle, the myocardium requires proper coronary circulation for delivery of nutrients and oxygen through a network of blood vessels originating at the aortic sinus off of the aortic root, and terminating in the coronary sinus emptying into the right atrium chamber, especially with increased physiological or pathological cardiovascular demands.

1.3.2. Cardiac cell types

The different cell types within the myocardium interact with one other through mechanical, electrical, and chemical means to support and sustain cardiac function[4]. The primary cell types that are found in the heart include the

cardiomyocytes, cardiac fibroblasts, endothelial cells, vascular smooth muscle cells, mast cells, and the recently identified cardiac stem cells[5, 6]. Cardiomyocytes and fibroblasts are the most abundant cells in the heart together comprising approximately 80% of the total number of cells[7], with the other cell types constituting a small fraction of the tissue composition.

Cardiomyocytes wrapped by the endomysium connective tissue are composed of bundles of myofibrils which are long chains of contractile sarcomeres[8, 9]. Computational models have depicted subendocardial and subepicardial muscle fibres of the ventricle arranged in counterdirectional helices, likely for the purpose of equal distribution of stress and strain on the heart wall[10]. There are also conductive cardiomyocytes[11] which are components of the electrical conduction system through the atria and ventricle walls. The sarcomere of the cardiomyocyte is the basic contractile unit of the heart. It is composed of the thick myosin and thin actin filaments[12, 13]. These myofilaments overlap with one another, and the cross-bridging generates force for the contraction of the myocyte. This action is mediated by the calcium released from the sarcoplasmic reticulum which then binds to the troponin complex, specifically troponin C[14] on the actin filament, subsequently removing the tropomyosin proteins from the actin molecule for exposure of myosin binding sites. The sarcomere is able to contract the myocyte as a unit as a result of its integral part in the cytoskeleton of the myocyte as it is connected through to the plasma membrane via the costamere unit. Cardiac fibroblasts are the source of the ECM structural proteins, mitogens, growth factors for paracrine signaling, and have direct communication with myocytes through cadherins and connexins, as they lie dispersed around the myocytes in the endomysium sheath[15, 16]. The endocardium lining the chambers consists of cells biologically similar to other endothelial cells, but embryologically distinct[17]. Endocardial cells are found in the aortic and pulmonary trunks, form the heart septa, and both the atrioventricular and semilunar valves of the heart[18]. The atrioventricular valves are located at the junction of the atrium and ventricle and are stabilized by the papillary muscles and the collagenous chordae tendinae to prevent prolapse.

There are various avenues for intercellular coupling among homogeneous or heterogeneous cells. Adjacent cardiomyocytes are held together by an intricate interdigitated region of attachment called an intercalated disc. Within the intercalated discs there exist three important junctions, or bridging structures. Neighbouring cardiomyocytes are mechanically coupled via the adherens junctions consisting of N-cadherins linked to the catenins, specifically β-catenin, connecting to the actin cytoskeleton of the cell via α-catenin[19-21]. The second adhesion complex is the desmosomes, which is a group of cadherin adhesion proteins. The cadherin and desmosome families are transmembrane proteins integrated into the cell membrane with an intracellular and extracellular portion of the complex. Intercellular electrical coupling is accomplished through gap junctions, which is a transmembrane complex consisting of integral proteins connexin-40[22], connexin-43[23], and to a lesser extent connexin-45. They allow movement of small molecules and ions especially important for communication after stretch-induced membrane depolarization[24].

1.4. Overview of heart disease

Heart disease can manifest itself in a variety of forms. Any disturbance to the function of one region can have a global impact as the heart operates as a single unit. The diversity of heart diseases is a result of the many variables associated with heart functioning. Cellular alterations can either be a cause or consequence of injury to the heart. Heart diseases can develop from a plethora of etiologies, including genetic mutations, congenital malformation, valvular disease, cardiomyopathies, ischemic heart disease, and many others. In 1996, the World Health Organization established that cardiomyopathies are defined as diseases of the myocardium associated with cardiac dysfunction. They are classified as dilated cardiomyopathy, hypertrophic cardiomyopathy, restrictive cardiomyopathy, and arrhythmogenic right ventricular cardiomyopathy, with a separate list of "specific cardiomyopathies" associated with specific cardiac or systemic disorders which includes ischemia, hypertension, valvular,

inflammation, and metabolism among others[25]. The limited scope of such a broad definition leaves room for debate[26, 27]. Impairment of the LV resulting from cardiomyopathy is a serious complication as it will compromise systemic perfusion to the organs of the body. The process in which the heart alters its size, shape, and function in response to stress is referred to as remodeling. Cardiac remodeling is a multidimensional process[28] that ultimately results in altered wall thickness (hypertrophy) and transformed chamber geometry (dilation), which loosely translates into a change in the architecture of the heart[28, 29]. Ventricular remodeling is a consequential adaptive measure to protect the heart and preserve cardiac function after injury. The degree of ventricular remodeling is contingent upon the extent of the injury involved in the disease. Two types of heart diseases, myocardial infarction and pressure overload-induced cardiomyopathy, will be the focus of this thesis and will be discussed in further detail.

1.4.1. Myocardial infarction

Etiology of myocardial infarction

Myocardial infarction (MI) is a cardiac event under the category of ischemic heart disease, and is commonly known as a heart attack. It occurs due to the complete blockage of blood flow through a major coronary artery causing ischemia to the downstream ventricular muscle. This leads to a scarcity of oxygen and nutrients delivered to this area. The ventricular remodeling that occurs after MI is an elaborate process with profound effects on cardiac function[30].

An ensuing type of cell death that occurs in infarcted myocardium is known as necrosis. The necrotic tissue becomes nonfunctional due to muscle death with subsequent replacement fibrosis, therefore losing its ability to contract. The severity and size of the infarction depends on the location of the occlusion and the area that is supplied by the occluded coronary artery. A blockage to a major trunk of the coronary artery would restrict flow to a larger region in comparison to that of a smaller branch. The heart could survive a coronary

occlusion due to the availability or establishment of a vast network of collateral arteries[31, 32] to maintain flow to the unaffected myocardium to preserve function.

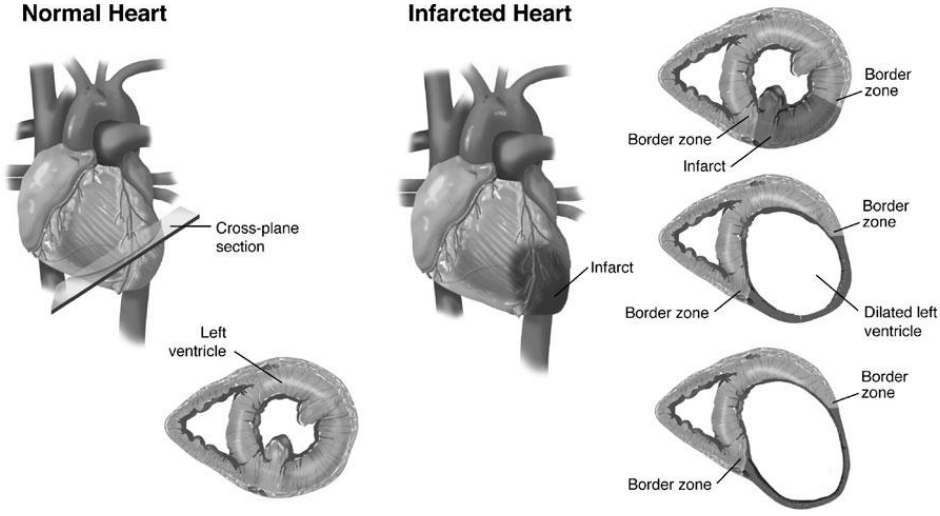

Figure 1.1. Left ventricular remodeling after myocardial infarction.

Cross-sections of the infarcted ventricle display the LV wall thinning and chamber dilation towards the apical region. Extracted from Gorman et al[33].

Cellular & molecular processes of myocardial infarction

Myocardial ischemia triggers many cellular and molecular events including cell death, oxidative stress, and inflammation of the necrotic and neighbouring myocardial regions, angiogenesis, cardiomyocyte growth, and myocardial fibrosis [34-37]. The presence or absence of these may combine to gradually develop a pathological dilated LV with considerable wall thinning, which could lead to heart failure, or to cardiac rhythm abnormalities[38] or infarct rupture resulting in sudden cardiac death[39].

Myocardial infarction: Ischemia-induced cellular necrosis

Ischemia following coronary artery occlusion generates a harsh environment for cardiomyocytes. The interrupted supply of oxygen and nutrients to the region creates a prime condition for cell death and destruction, leading to cellular necrosis which is generally termed as myocardial infarction. Necrosis can

have a drastic affect on the remodeling process as it is generally accepted that cardiomyocytes are postmitotic, or in other words terminally differentiated, therefore cannot be regenerated. The principle events describing the process of necrosis involve adenosine triphosphate (ATP) depletion, elevated reactive oxygen species (ROS)-induced mitochondrial damage, the influx of calcium into the mitochondria and cytosol, increased cellular acidosis, increased lysosomal rupture with intracellular protease release, and the inflow of water into the cell leading to the swelling and rupture of the plasma membrane [40-42]. The potential to minimize the expansion of necrotic injury at the cellular level is apparent, as pharmacological and genetic inhibition of necrosis-inducing factors has been found to lessen the infarct size and improve cardiac function post-MI[43].

Myocardial infarction: Oxidative stress

There exists a variety of oxidative agents that generate stress to the cardiomyocytes, which can be harmful to many features of the cell, including the nucleic acids, the sarcomere, ion channels and transporters, and the mitochondria[44]. Oxidative stress appears to have a causative or exacerbating role in many forms of heart diseases[45, 46], and is therefore an important contributor to the development of heart failure[47]. Oxidizing agents are molecules that oxidize other molecules, and in doing so withdraw electrons from the target molecule. These oxidizing agents generally fall into the families of ROS or reactive nitrogen species (RNS). ROS are a family of reactive oxidizing agents that consists of oxygen. These include the superoxide radical, peroxynitrite, hydroxyl radical, and hydrogen peroxide[48]. RNS overlaps with peroxynitrite and additionally consists of the nitric oxide radical. It is usually the concerted effect of ROS and RNS together that causes damage to the myocyte, such as in the generation of the powerful and unstable oxidant peroxynitrite from the reaction between superoxide and nitric oxide[49-51]. Nitric oxide is generated from L-arginine catalyzed by inducible nitric oxide synthase (iNOS) in the ischemic myocardium and possibly from infiltrating inflammatory cells.

Ischemia can damage the mitochondria, specifically the electron transport chain components[52], which generates reactive oxidizing species[53]. In addition to the electron transport chain in the mitochondria, other important cellular source of ROS[48, 54] is the superoxide producing plasma membrane-bound enzyme complex nicotinamide adenine dinucleotide phosphate (NADPH) oxidase, which has been strongly implicated in the transition from hypertrophy to the development of heart failure[55-57], and to a lesser extent a contribution from xanthine oxidase[58, 59]. Increased ROS has been found to activate matrix metalloproteinases (MMPs), which regulate extracellular matrix remodeling, and also initiating cellular necrosis post-MI by triggering calcium overload and increased permeability of the mitochondrial membrane (mitochondrial permeability transition)[60]. To combat these oxidative agents, the cells possess endogenous antioxidants, most notably superoxide dismutase, glutathione peroxidise, and catalase, which in many cases have been found to be suppressed or downregulated in heart failure[61, 62]. Maintaining a balance between oxidants and antioxidants is important to limit the damage that may occur from disproportionate oxidative reactions above physiological levels.

Myocardial infarction: Cardiac inflammation

MI results in the migration of monocytes, macrophages, and neutrophils responding to chemotactic factors in the infarct zone, initiating cytokine release and other molecular processes that localize the inflammatory response to the region of injury[37]. The recruitment of immune cells to the injured site has a reparative role that includes clearing dead cells and matrix debris and depositing granulation tissue at the site of injury[63, 64]. There is a delicate balance between the adaptive immune response and the adverse remodeling effects of prolonged inflammation in the cardiac response to disease[65]. The immune cells that have consistently been found to play an important role in cardiac remodeling are the neutrophils, macrophages, lymphocytes, and mast cells[66].

Neutrophil granulocytes are highly abundant, phagocytic, and are a hallmark of acute inflammation in response to trauma. Macrophages are

differentiated agranular monocytes and are the notable phagocytes, engulfing cellular necrotic debris[67]. The elicitors of inflammation are diverse. The pro-inflammatory cytokines[68] tumor necrosis factor alpha (TNFα), monocyte chemotactic protein-1 (MCP-1), and interleukins 1β, 6, and 8 (IL-1β, IL-6, and IL-8) are potent recruiters of immune cells to the region and are expressed by local cells, infiltrating immune cells, or through MMP processing. Interventions to restrict the activity of these cytokines involve neutralizing antibodies, soluble receptors, receptor antagonists and protease inhibitors[69]. Degraded ECM has been found to possess properties to serve as a chemoattractant for inflammatory cells at the injured region[70]. Infiltrating immune cells produce and activate MMPs [71, 72], which are the ECM proteolytic enzymes. Degraded ECM has a prominent role in inflammation, and therefore immune cell-mediated phagocytic clearance of matrix debris is necessary to arrest the inflammatory response. These effects collectively complicate the delicate balance involved in adaptive inflammation, and show how its dysregulation can have long-term repercussions on remodeling due to the immediate acute harmful effects of the inflammatory response.

Myocardial infarction: Fibrosis

In the infarcted heart, there is a need to differentiate between the infarcted ischemic area and the functional non-ischemic region when assessing the ECM remodeling process that is occurring. Fibrosis is generally defined as an excess increase in collagen content in the tissue. Fibrosis has been divided into two classes: reactive interstitial fibrosis and reparative/replacement scar formation[73]. Replacement fibrosis appears at sites of cardiomyocyte necrosis to preserve the structural integrity of the myocardium[40]. Tissue necrosis initiates a massive deposition of replacement fibrosis, likely due to targeted migration of fibroblasts to the necrotic region[74]. Fibroblasts characterized from the infarct area of the mouse heart exhibit increased proliferation, increased migration, altered adhesion, and increased collagen synthesis capacity compared to fibroblasts from the control hearts[75], likely due to cytokine-mediated chemotaxis[74, 76]. There is certainly a spatial and temporal pattern to MMP proteolysis of the ECM as part of

the scar formation process[77] by the degradation of damaged ECM in the early phase of scar formation. There is a delicate balance between the removal of the damaged ECM due to ischemia and the construction of new ECM. Suboptimal infarct remodeling can have profound effects on ventricular mechanics and can lead to LV rupture and death.

Myocardial infarction: Angiogenesis

The injury sustained in myocardial infarction is the result of impeded blood flow to a particular region of the myocardium, creating an ischemic environment where eventually an infarct will form in place of myocardial death. A protective mechanism in MI is myocardial angiogenesis to improve circulation to the infarct region and the neighboring tissue to ultimately reduce ischemic injury, restrict infarct expansion by preserving functional myocytes in the peri-infarct region, and improve overall cardiac function.

One approach of assessing the status of angiogenesis indirectly is to examine the expression of proangiogenic factors in the heart. In a rat MI model, it has been found that there is a rapid and prolonged increase in vascular endothelial growth factor (VEGF) and both VEGF receptors, VEGFR1 and VEGFR2 (also known as fms related tyrosine kinase-1 and fetal liver kinase-1/kinase insert domain receptor, respectively) after onset of an ischemic episode, initially throughout the heart but overtime localizing to the border region of the developed infarct[78]. Human heart tissue exposed to ischemia or infarction was biopsied and examined for early markers of angiogenesis, of which hypoxia-inducible factor 1 alpha (HIF-1α) was elevated early[79] supporting the rodent VEGF findings as HIF-1α is a known transcription activator of VEGF expression[80]. These findings suggest that in an ischemic state there is an intrinsic early response in the heart to promote angiogenesis.

An early study administered exogenous VEGF daily through an indwelling catheter to the distal site of the left circumflex artery which was constricted in a canine model. They discovered enhanced collateral blood flow and an increase in

the density of larger intramyocardial vessels, not capillaries, and similar infarct size as controls[81]. A later study demonstrated that intramyocardial injection of either HIF-1α or VEGF naked DNA immediately post-MI in a rat model in the left anterior free wall resulted in enhanced capillary density and regional blood flow that correlated with decreased infarct size[82]. As an alternative to the transfection of naked DNA, another study examined in a pig model the transduction of VEGF using multiple-site injections of an adenoviral vector at three weeks post-circumflex artery constriction, and observed an increase in myocardial perfusion and function[83]. A study using the adeno-associated viral vector immediately after left anterior descending coronary artery ligation in the rat model was also able to show effective infection of cardiomyocytes *in vivo* and an increase in new blood vessels around the infarcted myocardium region, although infarct size appeared the same compared to controls at two months of inoculation[84]. Additionally, the clinical trial in 2003[85] administering recombinant VEGF protein intramyocardially in patients with stable cardiac ischemia offered positive results after preliminary positive Phase I results[86, 87], although efficacy of delivery and risk of angioma are concerns in the patient trials that need to be closely observed.

There is a need to further assess the delivery strategies due to the perceived limitations of the intramyocardial (invasive approach and angioma formation risk) or intracoronary delivery (improbable complete delivery to the specific area of interest) of angiogenic factors[88]. Another limiting factor is the inherent flaw of VEGF-based therapy as it has been associated with highly permeable vessels and risk of tissue edema as reviewed by Weis and Cheresh[89]. There is also evidence that the ischemia-induced coronary collateral growth is a function of nitric oxide-dependent VEGF activity[90], thereby presenting the need to further investigate other potential important cofactors. The incorporation of cellular therapies, in particular mobilization of lineage-committed endothelial progenitor cells and their role in vasculogenesis and functional improvement [91, 92], is also a promising direction for therapy parallel to the angiogenesis approach of

expanding the capillary network by vascular endothelial cell proliferation and migration[93].

Experimental models of myocardial infarction

The surgical procedure that is traditionally used in the experimental animal model of myocardial infarction is the coronary artery occlusion procedure[94]. This can be accomplished by mechanically clamping or ligating a coronary artery at a specific location to occlude the vessel, thereby preventing blood flow to the downstream region. The most common site of ligation for left ventricular myocardial infarction is the left anterior descending artery, which is a prominent coronary artery that sustains a large region of the ventricle, or alternatively the circumflex artery particularly in the larger animal models[95]. This method creates a prolonged ischemic environment, where chronic occlusion will result in myocardial death and infarct formation, versus acute ischemic injury. This procedure has been performed on a number of different animal species[96-101].

1.4.2. Pressure overload cardiomyopathy

Etiology of pressure overload cardiomyopathy

Cardiac pressure overload is generated by elevated ventricular afterload. This increase in afterload is the pressure against which the heart must work in order to eject blood from the ventricles. In humans, increased afterload can result from two possible occurrences: increased resistance to outflow due to the incomplete opening of the semilunar valves, or from increased resistance to blood flow in the systemic or pulmonary arteries[102]. A stenotic aortic semilunar valve creates an obstruction to ventricular ejection of blood as it cannot open fully. The increased arterial resistance due to narrower and less compliant arteries requires the heart to work harder to pump blood against this resistance, such as in the state of chronic hypertension. For either of these conditions, the degree of increased workload on the heart depends upon the extent of restricted passage against

normal cardiac ejection. Increased afterload leading to amplified biomechanical stress is a common cause of left ventricular remodeling, which can lead to cardiac dysfunction and eventual heart failure[103].

Cellular and molecular processes of pressure overload

The pressure overloaded heart undergoes a compensatory phase followed by a decompensatory remodeling process[104]. The compensatory phase entails a hypertrophic adaptation of the myocardium to generate greater force and preserve cardiac function against a persistently detrimental increased afterload. Over time, it has been proposed that the gradual dilation of the ventricle and wall thinning under pressure alters the balance between ventricular wall stress, intraventricular pressure, ventricular radius, and ventricular wall thickness, parameters which are intrinsically related in the failing heart according to the Laplace Law[105]. The subsequent decompensatory process as a result of prolonged exposure further alters the myocardium with a gradual decline of cardiac performance. The major compensatory processes that occur are the growth of the cardiomyocytes, contractile regulation, creation of vessels to support the myocardial growth, and development of the ECM to support the increased workload of the heart.

Pressure overload: Cardiomyocyte hypertrophy

The early understanding of cardiomyocyte growth was able to clearly define the difference between physiological and pathological hypertrophy[106]. Physiological hypertrophy was described as having normal or augmented contractile state in which the maximum rate of ATP hydrolysis by myosin and the maximum velocity of muscle shortening are either normal or elevated; whereas pathological hypertrophy was associated with depressed contractility without necessarily concordant heart failure, in which case the rate of myosin ATPase activity and the velocity of muscle shortening are decreased[106]. More recently, physiological hypertrophy secondary to exercise has been described as having normal organization of cardiac structure, normal cardiac morphology, and normal or enhanced cardiac function[107, 108]. Pathological hypertrophy associated with

disease has been summarized as developing fibrosis, apoptosis, dysfunction, upregulation of fetal genes, and increased mortality[107, 108]. Pressure overload on the heart is a classic activator of hypertrophy due to the combination of mechanical cardiomyocyte stretch[109-111] and neurohormonal activation[112, 113]. The acute response to pressure overload is the development of concentric hypertrophy which involves parallel addition of sarcomeres increasing cardiomyocyte width, which in turn increases wall thickness[114]. This results in the left ventricle maintaining its overall size with a smaller chamber volume. The transition from early compensatory hypertrophy to the decompensatory dilation of the LV leading to heart failure was clearly evident and distinguishable in the hypertensive rat model[115].

There have been studies that challenge the "wall-stress" or "stress-correction" theory that states cardiac hypertrophy is compensatory in diseases with increased workload[116-119]. It has been suggested that the hypertrophic growth contributes to the disease state by demonstrating preserved function in the absence of hypertrophy, therefore not the increased wall stress related to an absence of hypertrophy which was classically attributed to dysfunction [120, 121].

Pressure overload: Fibrosis

Myocardial fibrosis is a well known cause of diastolic dysfunction and diastolic heart failure[122-124]. In heart failure there is an abnormally larger amount of collagen deposition in the interstitial space surrounding the failing yet functional cardiomyocytes. Collagen mRNA expression has been found to be increased four-five fold in the failing heart compared to the nonfailing hypertensive heart in the rat model[125], along with an increase in LV collagen concentration and interstitial fibrosis associated with increased passive muscle stiffness[126]. Collagen synthesis and deposition was also found to be elevated in patients with failing hypertensive heart, and was inversely correlated with EF[127]. The increased deposition of collagen within the functional myocardium can lead to restrictive ventricular filling, therefore diastolic dysfunction and in its severe form, diastolic failure[128]. Cardiac levels of profibrotic angiotensin II[129, 130] has

been found to be upregulated in patients with a failing heart[131]. At the point of decompensating cardiac remodeling, there is also a considerable upregulation of extracellular matrix regulatory proteins[132, 133], indicating that along with the increase in collagen the maladaptive upregulation of the major ECM remodeling components may contribute to the progression of heart failure.

Pressure overload: Calcium homeostasis

Many of the physiological processes that maintain ion homeostasis in the myocardium, including sensory and ion transport mechanisms, become faulty with progression to heart failure[134]. One critical ion of the many for which dysregulation has considerable pathological effects is calcium, as it is essential for myocyte excitation-contraction coupling. The influx of extracellular calcium leading to calcium release from the vast store of the sarcoplasmic reticulum is an initiating process for sarcomeric myofilament cross-bridging and cellular contraction. Two mechanisms that are pertinent to cardiac dysfunction from the systolic and diastolic failure perspectives are troponin C (TnC) calcium sensitivity and calcium handling by the sarcoplasmic reticulum, respectively.

Sensitivity of TnC to calcium is important for myosin binding to actin myofilaments during cardiomyocyte contraction. Calcium binding to TnC exposes the myosin binding site on actin by removal of the blocking tropomyosin. The stretch-induced loss of sensitivity that has been associated with heart disease impairs contractility of the myocyte, thereby impairing systolic performance[135]. The significance of TnC sensitivity for force generation is its relevance to the Frank-Starling mechanism and how this applies to the failing heart. The other aspect of calcium homeostasis involves the release and reuptake of calcium from the sarcoplasmic reticulum, a process known as calcium handling. Impaired calcium reuptake through the sarcoendoplasmic reticulum calcium ATPase-2a (SERCA2a) pump has been attributed to calcium overload and failure of ventricular relaxation[136]. The resultant impaired relaxation affects diastolic filling, and is a major contributor to diastolic heart failure. Calcium homeostasis

is a critical intracellular regulator of cardiac function, and is complementary to the various other remodeling processes occurring during heart failure.

Pressure overload: Angiogenesis

Cardiac microvascular angiogenesis is referred to as the creation of new vessels from existing vasculature. Angiogenesis during cardiac enlargement is variable based upon age, model, and duration of hypertrophy[137]. With pressure overload, the predicament with perfusion of the hypertrophied heart is at least three-fold: decreased coronary flow reserve (ratio of maximal flow to resting flow), increased muscle mass that requires nourishment, and the resultant decreased density of vessels[138]. Although there is usually growth of vasculature, it rarely compensates for the magnitude of hypertrophy[137]. Coronary flow has been demonstrated to be essential for functioning of the Akt kinase-induced hypertrophic heart as inhibition of angiogenesis impaired cardiac growth and functioning[139]. Stimulating angiogenesis in disease conditions with reduced perfusion can improve function by delivering oxygen and nutrients, especially to hypertrophic myocytes such as in pressure overload.

At the molecular level, the angiogenic factors that seem to have a prominent role in angiogenesis and vascular development are VEGF-A, platelet-derived growth factor, and angiopoeitin-1 & -2, with their respective receptors. VEGF-A has been found to be essential for differentiation and migration of the vascular endothelium[140] by binding to the VEGFR2 or with VEGFR1 receptor serving as a positive regulator of branching[141] and negative regulator to prevent vascular overgrowth[142] respectively. Platelet-derived growth factor primes vascular smooth muscle cells and pericytes to release proangiogenic factors, which have been found to be important for the vessel maturation process on which VEGF-dependent angiogenesis relies[143]. The angiopoeitins, Ang1 and Ang2, bind to their primary receptor Tie2 to stabilize mature vessels. Loss of Ang1 did not reduce angiogenesis, but instead made the vasculature nonfunctional in wound healing[144]. Ang2 was found to act as a competitive inhibitor of Ang1 at the Tie2 receptor binding site[145, 146].

The proteolytic actions of ECM regulatory proteins are important for the degradation and repair of the ECM for new vessel growth; however the findings of their role have been mixed[147-151], supporting the notion that ECM remodeling has a complex role in the angiogenesis process. Another element that may be involved in impaired vasculature in heart disease is the expression of the thrombospondin matricellular proteins, which are upregulated in tissue injury[152]. The TSPs are known angiogenic inhibitors in the tumour suppressor realm, through a variety of processes including promoting endothelial cell apoptosis, inhibition of endothelial cell migration, and impaired endothelial cell adhesion[153-156].

Experimental models of cardiac pressure overload

The most common method of inducing pressure overload in the experimental animal model is through coarctation of the aorta, commonly known as aortic banding. Aortic banding involves a surgical procedure to partially tie a suture or place a clip around the aorta of the animal to coarct the aorta to a certain extent in order to develop a pressure gradient for the heart to work against, thereby increasing the afterload of the heart. This is an effective model because it creates a cardiac pressure overload model with biomechanical stress localized to the heart. The severity of the model is dependent on two factors: the location and the degree of the constriction. Aortic banding can be done at the transverse aorta (closest to the heart), the descending aorta, the abdominal aorta, or at the suprarenal region (farthest from the heart). As pressure is maximum upon exiting the heart and dissipates as it travels through the vasculature, a similar constriction proximal to the heart would create a larger afterload on the heart compared to constriction further along the aorta. Choosing the appropriate constriction site is important for achieving the target level of afterload on the heart with consideration for ease of access to the aorta segment.

The increase in peripheral arterial resistance to blood flow, as it occurs in chronic hypertension, is another form of increased afterload. Genetic models of hypertension include the commonly used spontaneously hypertensive rat and

Dahl-salt sensitive rat among a wide array of hypertensive rat models[157]. Alternatively, another model involves delivering pressor doses of vasopressor agents such as angiotensin II or phenylephrine to the animal for an extended number of weeks. The pressor dose is the dose required to actively increase blood pressure in the animal. A lower dosage that does not increase the blood pressure is called a subpressor dose which can still exert other effects, such as cardiomyocyte hypertrophy by angiotensin II. These agents work through G protein- coupled receptors (GPCRs), with angiotensin II activating its AT1 receptor, and phenylephrine activating α1-adrenergic receptors. The agonist-induced hypertension can also be used as a model of increased afterload or pressure overload. However, it is important to note that systemic hypertension can also affect other organs such as the brain, liver and kidneys, which can in turn influence the heart function.

1.5. The extracellular matrix of the heart

1.5.1. Composition

The ECM is a network of proteins that structurally stabilizes the myocardium and enables it to contract synchronously. It is a dynamic structure that undergoes constant turnover, and its intact structure is essential for optimal cardiac structure and function. The ECM includes a diverse assortment of proteins categorized as fibrillar or nonfibrillar proteins. The fibrillar components of the ECM consists primarily of collagen I and III, with collagen I the predominant form. Proteins such as collagen IV, laminin, fibronectin, aggrecans, versican, tenascins along with various proteoglycans[158] constitute the diverse nonfibrillar portion of the ECM. These nonfibrillar proteins form the "basement membrane" that interacts with other fibrillar proteins, ligand molecules, and cellular adhesion molecules. These are the proteins with specific motifs which interact with the cardiac cells via the membrane-bound integrin proteins and other cell surface receptors which serve to transmit mechanical signals to the cytosolic

compartment for transduction to the sarcomere or nucleus. Collagen also maintains alignment of myofibrils within the myocytes through an ECM-integrin-cytoskeletal-myofibril connection[159, 160].

The ECM has been discovered to serve as a reservoir for growth factors and cytokines by containing binding sites for these molecules that can be released and activated upon degradation of the ECM, such as the potent procollagenic transforming growth factor (TGF)-β. Even ECM fragments can possibly serve as growth factor receptor agonists via the EGF-like domains that some possess[161, 162]. Proteolysis of the ECM can also have an inflammatory effect on the heart. Degraded ECM has been found to act as a chemokine, attracting inflammatory cells and permitting increased immune cell infiltration as mentioned previously. Disruption of the ECM network structure due to excess proteolytic activities can lead to wall thinning and LV dilation, whereas accumulation of collagen results in fibrosis and decreased compliance (increased stiffness) of the myocardium.

1.5.2. Synthesis

The fibroblasts are the primary cell type responsible for synthesizing the ECM components in the heart[163-167], although there is evidence of an indirect mechanical[168] as well as (small) direct contribution from myocytes[169]. Synthesis of the ECM is a regulated process in response to signals from ECM alteration, availability of profibrotic growth factors such as TGF-β[170, 171] and connective tissue growth factor[172], and angiotensin II signaling[173, 174]. The most abundant components of the ECM are the fibrillar collagens type I and III, as these proteins form the structural integrity of the heart with the added responsibility of absorbing tensile forces. Enhanced collagen synthesis has been found under certain mechanical shear, tensile , or compressive loading[175] and in various cardiovascular diseases[176, 177].

Collagen is initially produced in a procollagen form. In order for this to occur, individual alpha peptides undergo post-translation processing such as hydroxylation and glycosylation, after which three alpha peptides (two α1 and one

α2) bind together and twist into a triple helix procollagen molecule. Hydroxyproline is an essential component of collagen thought to be crucial to forming the helical shape and is highly abundant in collagen structure, while hydroxylysine has been identified as the target of glycosylation. Extracellular truncation of procollagen forms the lighter mature form known as tropocollagen. The cleaved procollagen amino (PINP and PIIINP) and carboxyl (PICP and PIIICP) terminal peptide ends have been used as biomarkers of collagen synthesis[178]. Appropriately, there is also a biomarker for quantifying degradation of collagen, the carboxyl-terminal telopeptide of collagen type I (CITP)[178, 179]. It is the polymer of tropocollagen formed with the assistance of extracellular enzymes such as lysyl oxidase which forms the structure known as the collagen fibril. Other agents that can contribute to stabilization of the ECM are the matricellular proteins, extracellular proteins that are not directly involved in the structural functions of the ECM.

The matricellular protein secreted protein acidic and rich in cysteine (SPARC; also known as osteonectin) is upregulated after cardiac injury and has been associated with ECM organization, collagen-binding, and potent regulation of growth factors[180] while interacting closely with other ECM components. Although SPARC deficient mice were reported to have initial protection against post-MI cardiac dilation[181], the early infarct rupture incidence and dysfunction suggests that SPARC is essential for cardiac ECM integrity[182]. SPARC was found to have an unfavourable role in pressure overload, with the cross-linking of collagen fibrils impairing cardiac function[183]. Similarly, the thrombospondin family of proteins are inconspicuous at baseline but increase expression with injury[152], with thrombospondin-1 shown to be a major activator of the latent profibrotic growth factor TGF-β *in vivo*[184], thereby contributing greatly to ECM synthesis[185, 186]. Thrombopondin-1 also has been found to be vital for cardiac remodeling post-MI[187].

1.5.3. ECM-cardiomyocyte adhesion and communication

Proper adhesion of the cardiomyocytes to an intact ECM is critical for optimal heart function. The transmembrane proteins of the integrin family are essential receptors for cellular communication with the ECM. The integrin heterodimer at the cell surface is composed of two isoforms, the α and β subunits. As reviewed by Ross & Borg[188], there are a total of 18 α-subunits and 8 β-subunits identified in mammals, of which 7 α-chains and one β-chain are predominantly expressed in cardiomyocytes. The β1 subunit, specifically the β1D splice variant unique to striated muscles[189], is most abundant in heterodimers present in the heart. The integrin complex is involved in adhesion, mechanosensation, cytoskeletal alignment, and force transmission of the cell[188]. Cardiac-specific lack of β1D integrin displayed myocardial fibrosis and heart failure by six months of age[190]. Integrins play a key role in the cardiac response to mechanical stress such as in chronic pressure overload, which results in upregulation of α1, α5, α7, and β1 integrins[191], and where the lack of β1D integrin resulted in considerably greater mortality[190]. The extracellular portion of the integrin complex binds to specific domains on the ECM proteins, in particular the basement membrane proteins such as laminin[192], fibronectin[193], collagen IV[194], and also with the fibrillar collagens[195]. The integrin heterodimer is a vital component of two major intracellular complexes, the focal adhesion complex and the costamere unit of the cell.

The focal adhesion complex is a conglomeration of basement membrane components, the integrin heterodimer, and a kinase complex that collectively transmits mechanical stimulus to biochemical signaling (Fig 1.2.). It serves as a key component of two major processes: force transmission and signal transduction for the initiation of gene transcription. The former is accomplished through direct attachment to cytoskeletal actin via alpha-actinin linkage. The focal adhesion complex primarily functions as a signaling cluster through an assembly of kinases which includes focal adhesion kinase (FAK), integrin-linked kinase, Src kinase, Ras kinase, Rho/ROCK kinase, Rac kinase[196-200] and others

which act through the combination of autophosphorylation and downstream phosphorylation to trigger an intracellular activation cascade. Integrins are also involved in the contraction of the cardiomyocytes through its incorporation in the costamere (Fig 1.2.), where it has direct interaction with intracellular cytoskeletal proteins and the sarcomere at the Z-disc[201-203]. The integrins are linked to the sarcomeric actin filaments through the assistance of alpha-actinin molecules. The focal adhesion complex and the costamere link with cytoskeletal elements such as vinculin, talin, paxillin, alpha-actinin, filamin, tensin, and others for cellular alignment with the ECM and neighbouring cells[204].

Cellular communication with the ECM also relies on the syndecan transmembrane proteins, in particular syndecan-1 and -4 in the heart, as it acts as a cofactor with integrins for connecting ECM proteins to the cytoskeleton[205]. Both integrins[190, 191] and syndecan-4[206] have essential roles for cardiac adaptation to pressure overload. There is also the transmembrane dystroglycan complex that binds to the intracellular cytoskeletal actin filaments via the dystrophin protein. The extracellular domain of dystroglycan binds to the ECM, although it is generally found to be localized with laminin of the basement membrane[207]. In addition to integrin signaling, the presence of the discoidin domain tyrosine-kinase receptors in fibroblasts, with the cardiac-specific isoform discoidin domain tyrosine-kinase receptor-2, is a unique and important feature of these cells[208]. The principle ligand of these receptors is fibrillar collagen[209-211], and can thereby act as an ECM sensor to modulate fibroblast proliferation and adjust synthesis of ECM components according to physiological or pathological signaling[212]. This illustrates the complexity of cellular interaction with its surrounding matrix environment, and how delicate changes in the environment or adhesion capacity can alter alignment, compromise mechanotransduction, and disrupt intercellular communication.

1.5.4. ECM remodeling

Adverse remodeling of the myocardial ECM is a result of an overall imbalance in its turnover, and is a key component of heart disease. Excessive

disruption or accumulation of ECM proteins has large-scale functional ramifications. The initial findings by Gross and Lapiere in the 1960's identified a unique protease that they classified as a collagenase, as it was able to process collagen and likely other structural components[213]. They elaborate that collagen in particular has an advantage over other proteins in that it is immune from attack from any commonly known proteolytic enzymes or cathepsins under physiological conditions. ECM integrity is regulated by the proteolytic actions of the MMPs and their physiological inhibitors, the tissue inhibitors of metalloproteinases (TIMPs). Other inhibitors of MMPs include α2-macroglobulin and reversion-inducing-cysteine-rich protein with kazal motifs (RECK). The inhibitory capacity of α2-macroglobulin involves irreversibly inhibiting

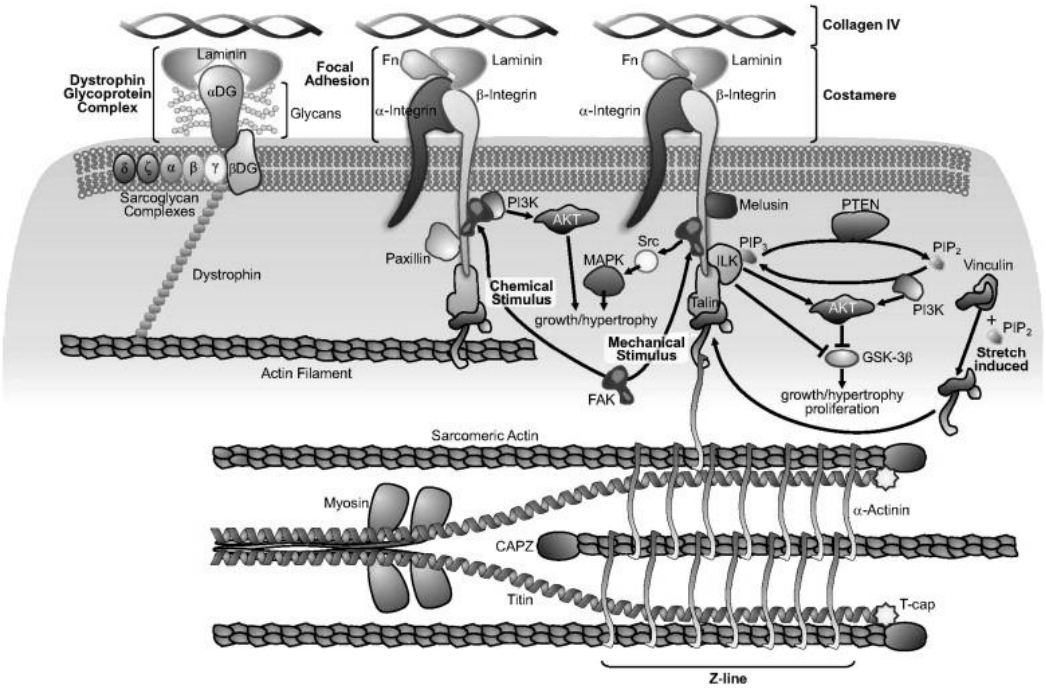

Figure 1.2. Complexes involved in cardiomyocyte mechanotransduction.

Membrane and cytosolic proteins involved in mechanosensation and transmitting mechanical force from the extracellular matrix through the cytoskeleton or through the signal transduction activation cascade. Extracted from Guo et al[214].

active MMPs followed by phagocytic elimination, and is mainly found in the plasma and liquid compartments with minimal tissue presence[162, 215, 216]. RECK is a membrane-bound inhibitor of MMPs which is modestly expressed in the heart[162, 217]. Since three-dimensional structures of the MMPs and TIMPs first were published in the mid-1990s and reviewed extensively[218-221], an understanding of their structure and interaction has become achievable.

1.6. MMP and TIMP balance in heart disease

1.6.1. Matrix metalloproteinases

Classification of MMPs

The MMPs belong to the family of zinc-dependent endopeptidases known as metzincins which are responsible for the proteolysis and turnover of the ECM. The MMPs are proteolytic enzymes that predominantly degrade extracellular proteins. The numbering and classification of MMPs is based loosely on their discovery sequence and substrate affinity respectively, with an additional category for the membrane anchored MMPs. MMPs have been traditionally recognized as extracellular proteases, although there has been evidence to credit them with degradation of intracellular proteins such as titin, the sarcomeric myofilaments, and the mitochondria architecture[222-227]. Of the 25 unique MMPs discovered to date[228, 229], nine have been found to have a major role in cardiac ECM remodeling. To date, the cardiac multidomain MMPs are MMP1, MMP2, MMP3, MMP8, MMP9, MMP12, MMP13, MMP28 and MT1-MMP (membrane-type 1 matrix metalloproteinase). The classification of these MMPs as collagenases (MMP1, MMP8, MMP13, and MT1-MMP) gelatinases (MMP2, and MMP9), stromelysins (MMP3), or elastases (MMP12) was based on initial findings of the preferred target substrate for each of these MMPs. Later discoveries have uncovered that although MMP substrate specificity is present, a number of MMPs are capable of degrading a broad-spectrum of ECM as well as non-ECM proteins .

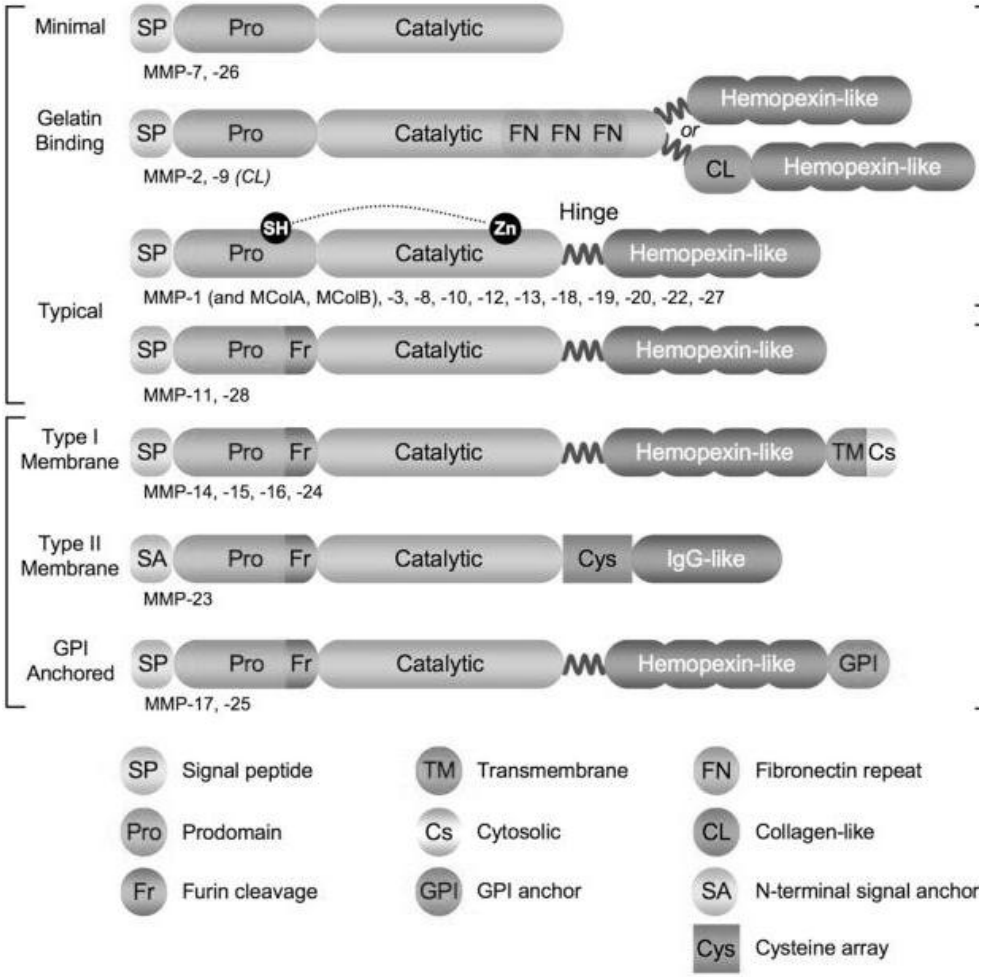

Figure 1.3. Structure and classification of MMPs.

Illustration of the various structural classes of MMPs with their constituent domains identified. Extracted from Ra & Parks[230].

Structure of MMPs

The MMPs are generally five-domain proteins, with the exception of the membrane-type class of MMPs (MT-MMPs) which includes an additional transmembrane segment, and MMP7 and MMP26 which do not possess the hinge or hemopexin domains[231, 232]. The five domains as listed from amino (N)-terminus to the carboxyl (C)-terminus are: the signal domain, the pro-domain, the

catalytic domain, the hinge region, and the hemopexin domain. In the MT-MMPs, the transmembrane domain is the end region at the C-terminus located partially in the cytosol of the cell as the rest of the protein is positioned extracellularly, while MMP7 and MMP26 end with the catalytic domain at the C-terminus. Each domain has a contributing role to the function of MMPs. The signal domain directs the MMP to cellular secretion to the extracellular environment. The pro-domain and the catalytic domain are connected via a cysteine switch from the pro-domain which forms a bond with the zinc ion embedded at the catalytic site. The hemopexin domain that is linked to the molecule via the hinge domain has been attributed to be involved in differential substrate affinity, stabilizing TIMP interaction, and is also implicated in proMMP binding to TIMPs[233].

In further detail, as reviewed by Bode[219, 220], N-terminus of the protein begins with the approximately 20-residue signal domain with the adjacent approximately 80-residue pro-domain. In addition to these, there is an extra region of approximately 11 residues after the pro-domain in the pro-membrane-type MMPs (proMT-MMPs) identified as a furin recognition site. MMPs are generally activated extracellularly after being secreted in their latent form through two primary steps: the bond disassociation between the cysteine residue of the pro-domain and the catalytic zinc of the catalytic domain, and also cleavage of the X99-Phe/Tyr100 activation cleavage peptide bond in the "rocker arm" linking the pro-domain with the catalytic domain. The catalytic domain is approximately 170 residues long, with the exception of the gelatinases (MMP2 and MMP9) which each contain a segment of approximately 175 residues of a triplet of collagen binding fibronectin-related type II modules. Continuing towards the C-terminus of the protein, there is a 10-70 residue long proline-rich hinge domain linking the catalytic domain with the hemopexin which itself is approximately 195 residues long. The hemopexin domain consists of four β-sheets around a central axis which actually takes the form of a propeller. The additional transmembrane region of the MT-MMPs that enables membrane anchoring is approximately 75-100 residues including the short cytoplasmic tail portion. The type of

transmembrane domain can classify the MMP as a type I transmembrane-type MMP (MT1, 2, 3, 5- MMP), glycosylphosphatidylinositol-linked MMP (MT4, 6-MMP), or type II transmembrane-type MMP (MMP23).

MMP pro-domain and catalytic domain interaction

Many segments of the primary MMP structures are homologous among different MMPs, meaning that the residue sequence at specific sites is the same in all MMPs. In the case of the pro-domain, there is the segment commonly known as the "switch" segment loop which is almost invariant with the residue sequence of Pro90-Arg91-Cys92-Gly-Val-Pro-Asp96, and the underlined residues identical among MMPs. This segment is identified as a 'kink' in the pro-domain which enters the active-site cleft of the catalytic domain, where it is the cysteine residue that interacts with the catalytic zinc and fixed water molecule. Additionally, the side chains of the Arg91 and Asp96 residues of the switch segment forms a salt bridge on top of His228 residue of the catalytic domain, which is the third zinc-ligand for His.

The catalytic domain consists of two zinc ions; one is identified as the catalytic zinc, and the other as the structural zinc which along with MMP-dependent two or three calcium ions, clamp the neighbouring S-loop which is thought to be involved in substrate and inhibitor binding. The active site helix contains the first two His residues (His 218 and His222) which interact with the catalytic zinc and the "catalytic Glu219". These three histidine residues are collectively included in the 11-residue long "zinc binding consensus sequence" identified as H218-EXX-H222-XXGXX-H228. Other major landmarks of the catalytic domain include: the end point of the active site helix is Gly225, followed by His228 and the MMP-invariant Ser 229. There is also a "Met-turn", which is a conserved sequence of Ala234-Leu-Met236-Tyr237 (although according to the sequence alignment it should be Ala-X-Met-X), and also the invariant Pro238-X-Tyr240 sequence.

MMP activation

MMPs can be regulated at three levels: gene expression, activation, and inhibition of the activated MMP. MMPs are produced as inactive zymogens. An abundant reserve of latent MMPs is ready to act upon activation[234, 235] which may occur in response to serine proteases, oxidative stress[9], or other MMPs and TIMPs[236-238]. A major method of MMP activation that has been described involves the cleavage of the prodomain of the MMP and truncation of the molecule in a stepwise process[239, 240], as exhibited in the activation of proMMP2[236] and proMMP13[241] through slightly different processes. This action removes the prodomain which is folded over the catalytic domain, thereby exposing the catalytic site for substrate degradation. It has been proposed that, unlike MMP activation which occurs in the extracellular space, another likely method that activates MT-MMPs is by furin proteases cleaving at the furin recognition site of MT-MMPs, mentioned previously, in the cytosolic compartment prior to localizing at the cell membrane[242]. Additionally, there is strong evidence that one of the methods of intracellular MMP activation that can occur is via induced reactive oxygen species disrupting the covalent bond between the pro- and catalytic-domain, thereby exposing the catalytic site for intracellular proteolytic activity[243, 244]. This process has been well described as the "cysteine switch" phenomenon involving the dissociation of the prodomain cysteine residue from the catalytic site of the adjacent catalytic domain[245]. The exposure of the catalytic site is the fundamental process to activate an MMP. Once activated, the primary physiological inhibitors of activated MMPs are the four TIMPs.

1.6.2. Tissue inhibitors of metalloproteinases

TIMPs are a group of four physiological MMP inhibitors that are 21-30 kDa proteins with 37-51% homology among the different TIMPs[246]. They consist of twelve conserved cysteine residues that form six disulfide bonds which fold the protein into six loops and two domains[247]. The N-terminus of the TIMPs is the inhibitory domain of the protein which reversibly inhibits activated MMPs[248], and the C-terminus has been credited with proMMP binding and possibly other MMP-

independent actions of TIMPs[249]. The N-terminus of the molecule also possesses the fully conserved five-amino acid "VIRAK" sequence which spans amino acids 18-22 in all TIMPs, which was first thought to have inhibitory functional significance, however later was found to be more involved structurally rather than any functional role[250]. The TIMPs are generally secreted proteins to the ECM, although there is evidence of an intracellular inhibitory role for TIMPs[224, 251]. The TIMPs are differentially expressed in the heart[252], with TIMP2 and TIMP3 having the highest mRNA expression followed by TIMP1 and TIMP4 in the heart. The last decade has brought a wealth of research to the forefront about the role of TIMPs in heart disease[162], the prospective diagnostic application[179], and therapeutic potential[253].

1.6.3. TIMP inhibition of MMPs

TIMPs reversibly inhibit active MMPs by forming noncovalent 1:1 stoichiometric complexes that are resistant to proteolytic degradation and heat denaturation[254]. The N-terminus of the TIMP protein has the five residue sequence of Cys1-Pro5 which binds directly to the active site cleft in a substrate-like manner. Cys1 is located directly above the catalytic zinc of the catalytic domain and in essence replaces the water molecule thereby also interacting with the catalytic Glu219 via hydrogen bond through its α-amino group. It has also been found that other portions of the N-terminus also may contribute to the intermolecular contact between the MMP and TIMP such as the sC-connector loop, sA-sB loop (in which the invariant VIRAK sequence is situated from residue 18-22 according to the sequence alignment[255]), and also disulfide bridging. In contrast to the general broad-spectrum inhibition of MMPs by the TIMPs, one interesting property of TIMP1 is its inability to inhibit the class of MT-MMPs[256]. Alteration of the N-terminus of TIMP1 by a single amino acid residue substitution rendered TIMP1 capable of inhibiting the MT-MMPs[257], shedding light onto the role of sequence variation in TIMP functional diversity at either domain.

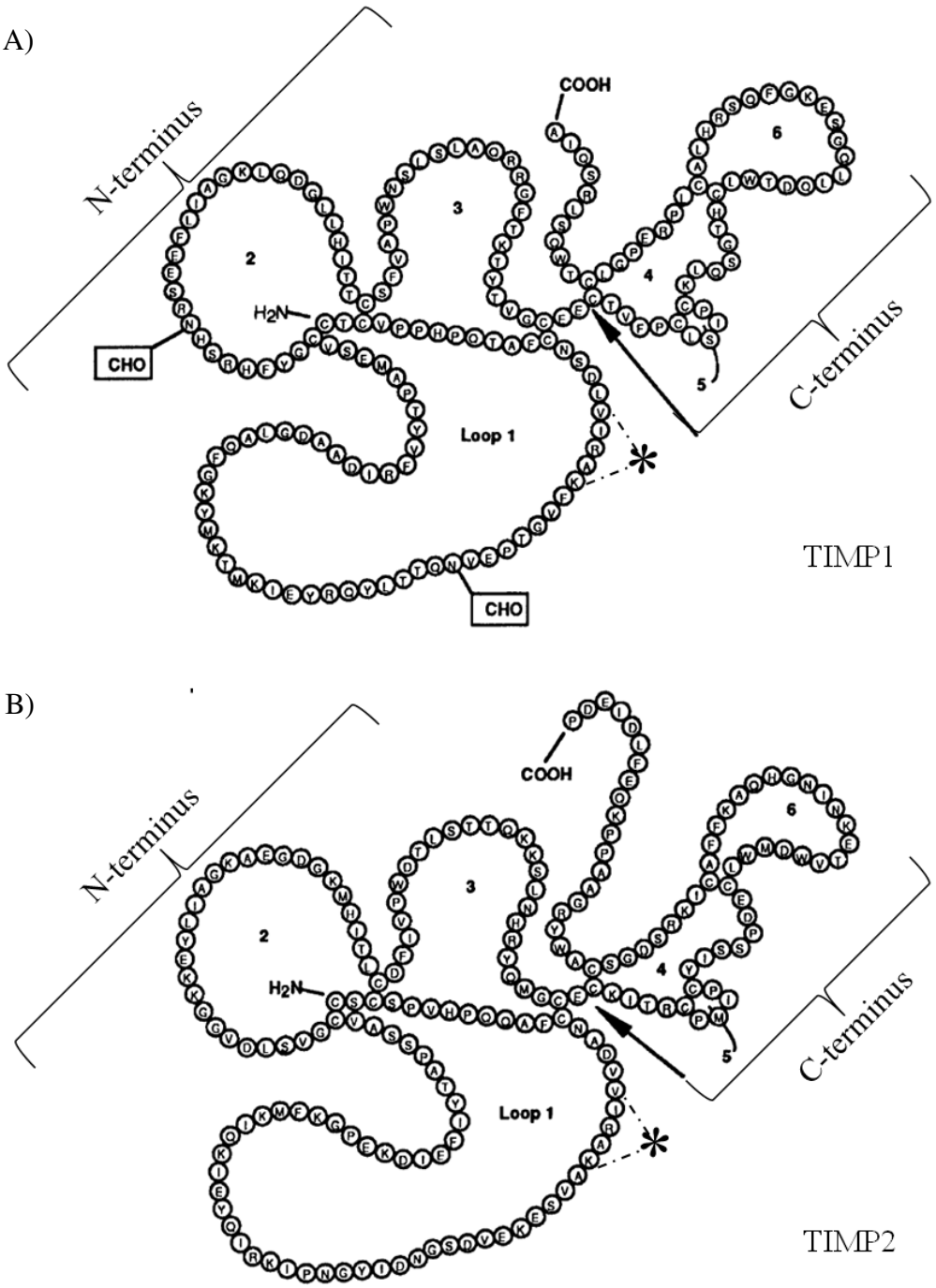

Figure 1.4. Primary structure of TIMP1 and TIMP2.

A, TIMP1 and TIMP2 (B) sequence. Arrow indicates N- and C-terminus junction (loops 1-3 and 4-6 respectively). The two boxed CHO represent the glycosylation sites of TIMP1 (A). "*" indicates the all-TIMP conserved "VIRAK" sequence. Adapted from Douglas et al[221].

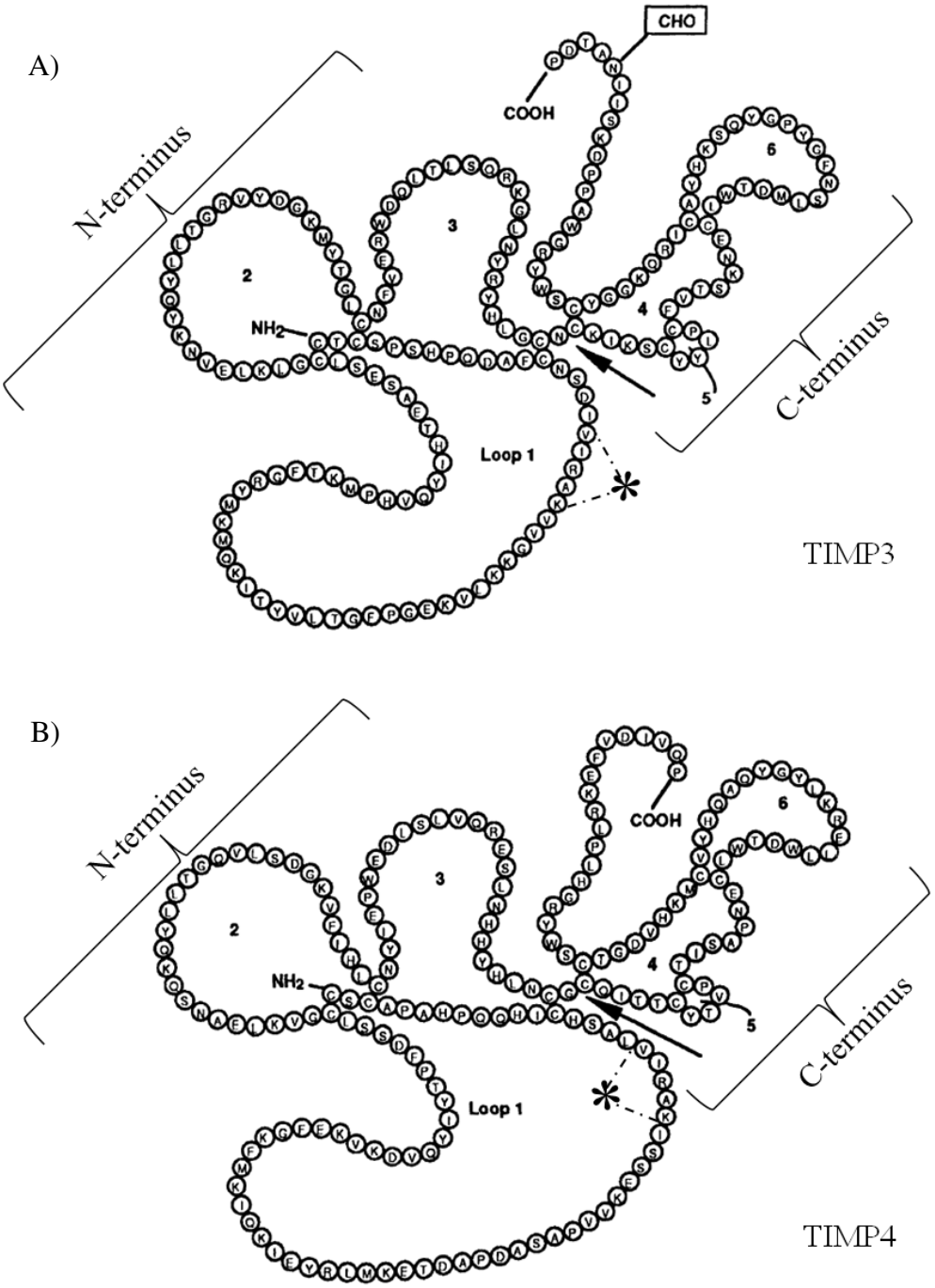

Figure 1.5. Primary structure of TIMP3 and TIMP4.

A, TIMP3 and TIMP4 (B) sequence. Arrow indicates N- and C-terminal junction (loops 1-3 and 4-6 respectively). The boxed CHO represents the proposed glycosylation site in TIMP3 (A). "*" indicates the all-TIMP conserved "VIRAK" sequence. Adapted from Douglas et al[221].

1.6.4. MMPs in animal models of heart disease

MMPs have been a focus of therapeutic intervention, as they have been implicated in heart disease through dysregulation of their proteolytic activity. MMPs are differentially expressed temporally and in response to different forms of heart disease. In rats, an upregulation of MMP2, MMP9, MMP13, as well as MMP8 and MMP14 has been reported post-MI[258] and in other MI animal models[259], differential increases in MMP levels with pressure or volume overload in dogs[260], and excessive MMP activity in the rat hypertensive failing heart[261, 262], which coincides with the dysregulation in human dilated cardiomyopathy[132] and in heart failure[159].

The studies that utilized genetically modified models best exemplify the causal role that the MMPs have in ECM remodeling and heart disease progression. Targeted deletion of MMP2[263, 264] or MMP9[148, 265, 266] in mice resulted in an ameliorated condition post-MI compared to control animals as both showed improvement in cardiac function and ventricular dilation. MMP2 deficiency greatly improved survival despite a similar infarct size compared to WT MI controls through a reduction of the incidence of infarct rupture[263, 264], which was also seen in one study with MMP9 deletion[266]. The deletion of MMP2[267] or MMP9[268] in the context of cardiac pressure overload due to aortic banding also was found to attenuate cardiac remodeling and dysfunction. In addition, cardiac-specific overexpression of MT1-MMP demonstrated adverse cardiac remodeling associated with dysregulated MMP activity, as poor survival, worsened function, and significant fibrosis were discovered post-MI in these mice[269].

1.6.5. The role of TIMPs in animal models of heart disease

TIMP1

The use of TIMP-deficient mice to investigate the role of TIMPs in heart disease after genetic deletion began with TIMP1. Mice with deletion of the gene for TIMP1 without any underlying conditions were found to have preserved

functional capacity with slight left ventricular dilation by 4 months of age[270]. MI in TIMP1-deficient mice led to increased LVEDV and dilation compared to WT mice[271], which was prevented with the use of a pharmacological MMP inhibitor[272]. Additionally, adenoviral overexpression of TIMP1 in the peri-infarct region of the rat infarcted heart resulted in preserved systolic and diastolic cardiac function, preserved ventricular geometry, and reduced fibrosis compared to control rats[273], along with abolished infarct rupture incidence after tail-vein adTIMP1 injection[266]. TIMP1 also demonstrated a protective role in the cardiac response to pressure overload; TIMP1 gene transfer into WT aortic-banded mice through tail-vein injection of TIMP1-overexpressing adenovirus (AdTIMP1), which considerably elevated plasma TIMP1 levels, showed minimal cardiac hypertrophy, fibrosis, or dilation at two weeks post-AB compared to control mice[268]. However, tail vein adenoviral injection presents two limitations that are not addressed in these two papers, the variable distribution of adenovirus and efficacy of myocardium uptake. The tail vein injection has a very high likelihood of nonuniform infection of passing cells and tissues as it follows venous return to the heart and remains in the blood, and also insufficient infection of the desired area of the left ventricle myocardium prior to inducing MI. As plasma concentration was the sole measurement of expression of the adenovirus, no evidence of increased tissue levels of TIMP1 was presented contrary to the study by Jayasankar on TIMP1$^{-/-}$-MI[273].

TIMP2

Previously, little work had been done to ascertain the *in vivo* role of TIMP2 in heart disease. TIMP2 is highly expressed in the heart[252]. Studies illustrating the MMP-dependent role of TIMP2 and the MMP-independent roles *in vivo* and *in vitro* are introduced in Section 1.7. This thesis will present and discuss our research uncovering the *in vivo* role of TIMP2 in heart disease that was the focus of this thesis[274, 275]. Subsequent to our paper demonstrating the critical role of TIMP2 post-MI[274], Ramani et al. reported that adenoviral TIMP2 overexpression in the peri-infarct region of the myocardium improved LV

dysfunction in only a couple of parameters compared to MI[276], indicating a potential protective role for TIMP2 against myocardial infarction. TIMP2 protein levels were confirmed to increase in MI myocardium after intramyocardial injection.

TIMP3

TIMP3$^{-/-}$ mice exhibit dilated cardiomyopathy by 21 months of age[277]. Cardiac pressure overload in the TIMP3-deficient mice perpetuated into exacerbated LV dilation and dysfunction, with severe hypertrophy and fibrosis contributing to early heart failure and greater mortality[278]. Combined inhibition of the proinflammatory cytokine TNF and MMP proteolysis was required for complete prevention of the TIMP3$^{-/-}$ phenotype. TIMP3$^{-/-}$ mice were also vulnerable to severe remodeling after post-MI as this translated into increased mortality[279]. The relatively high baseline expression level of TIMP3 in the heart compared to the other TIMPs[252] signifies its importance and the potential for effective heart disease therapy.

TIMP4

TIMP4 historically has been referred to as the cardiac inhibitor of metalloproteinases (CIMP)[280], likely due to restricted expression of TIMP4 to the heart, kidneys, pancreas, colon, testes, brain, and adipose[252, 281] unlike the other TIMPs which are generally thought to have a broad expression pattern. The TIMP4$^{-/-}$ mouse has similar heart structure and function at 5 months of age compared to the WT mouse, however by 20 months of age there is impaired heart function in the TIMP4$^{-/-}$ mouse accompanied by increased LV mass[282]. The lack of TIMP4 in the pressure overloaded heart did not impact cardiac remodeling or function, whereas MI in the TIMP4-deficient mice was more susceptible to LV rupture albeit without any further deterioration of cardiac function compared to WT MI control mice[282]. The mild phenotype exhibited with TIMP4 deficiency may be explained by the relatively low expression of the "heart TIMP" in the heart relative to the other TIMPs.

1.6.6. Pharmacological inhibition of MMPs

MMPs have been implicated in the adverse remodeling process in a variety of diseases such as cancer, arthritis, and heart disease. The purpose of developing pharmacological exogenous MMP inhibitors (MMPi) was to reduce the activity of MMPs which would considerably exceed that of the endogenous TIMPs in disease, thereby restoring the balance between the degradation and inhibition aspects of ECM remodeling. The scope of application was broad, as there was potential for cancer therapy by inhibiting tumour angiogenesis and cancer metastasis[283-285], reducing degradation of cartilage in arthritis[286, 287], as well as enabling adaptive reparative ECM remodeling in heart disease[288-290].

Development of a pharmacological MMPi was based on two approaches: zinc chelation and substrate mimicry for the substrate binding pockets of MMPs[291]. The limiting factors in MMPi development are the effective dosage required and toxicology of the compound, which together determine the therapeutic index[263]. One common side effect of MMPi treatment is musculoskeletal syndrome, characterized by joint pain and stiffness among others, which in most cases seems to be attributed to the collagenase-inhibitory characteristic of broad-spectrum MMP inhibition. This has led many to reduce the dosage. Others have instead looked at selective MMP inhibition as a possible alternative[149], in which case the selectivity and specificity of inhibition for certain MMPs may be variant. As hydroxamates in particular, but also carboxylates, are potent zinc chelators, their evolution into selective MMP inhibitors has been in part due to the growing body of MMP crystallographic studies for MMPi backbone design aimed at targeting the S1' pocket of specific MMPs[291]. There have been at least 56 MMPi compounds devised to date[263], with a majority of them discontinued and just a small group of them remaining in clinical development. Periostat (Doxycycline Hyclate) is the only FDA-approved MMP inhibitor for use on periodontal disease[292]. There has been a wide range of broad and selective MMP inhibitors used for animal models of cardiovascular disease, with only a short list of them including PD166793[293, 294], PGE530742[295, 296],

Doxycycline[297-299], and ONO-4187[300]. These have yielded positive, yet variable, effects in ameliorating heart disease in animal models. The PREMIER (Prevention of Myocardial Infarction Early Remodeling) trial using PG116800[301] for patients with ST-segment elevated myocardial infarction did not prove to be successful, as it did not improve clinical outcomes

1.7. Tissue inhibitor of metalloproteinases-2 (TIMP2)

Since the main focus of this thesis has been exploring the role of TIMP2 and TIMP3 in heart disease, TIMP2 and TIMP3 will be discussed in more details in the following sections.

1.7.1. Discovery & structure of TIMP2

TIMP2 was discovered in 1989 in the laboratory of William G. Stetler-Stevenson[302]. It was found after determining that it was a physiological inhibitor of the type IV collagenase, and was analogous structurally to the original TIMP (later named TIMP1). TIMP2 is a 21kDa protein that is 194 amino acids in length, and has a precursor form that is 220 amino acid residues in length[303], which is truncated into the mature form for secretion. The protein lacks glycosylation sites, as does TIMP4, which is evident by the low molecular weight compared to the other TIMPs, but has not been found to affect the inhibitory capacity of TIMP2. The TIMP2 gene is localized on human chromosome 17q25[304] and on mouse chromosome 11[305].

1.7.2. The interaction between TIMP2 and MMPs

The MMPs that have been found to be major targets for potent inhibition of TIMP2 include MMP2[306, 307] and MT1-MMP[308]. In addition to its inhibitory role of these MMPs, TIMP2 is capable of forming a complex with proMMP2[309, 310], which is required for the cell surface activation of proMMP2[236]. TIMP2 is the only TIMP that is involved in both of these processes and does so in a dose-dependent fashion. At higher concentrations TIMP2 inhibits MMP activity,

whereas at lower concentrations it activates proMMP2[311]. Cell surface activation of MMP2 occurs through TIMP2 forming a trimolecular complex with proMMP2 and MT1-MMP while an adjacent MT1-MMP cleaves the pro-domain of proMMP2[236, 312, 313]. In other words, TIMP2 serves as an anchor for MT1-MMP to cleave and activate the proMMP2. This is accomplished in a manner that is different from the typical inhibitory interaction between TIMP2 and MMP2. In the inhibitory relationship, the cysteine residue at the TIMP2 N-terminus binds to the catalytic domain at the N-terminus of active MMP2. The difference in the trimolecular complex formation is that the C-terminals of TIMP2 and proMMP2 bind together, thereby in essence presenting the proMMP2 N-terminus pro-domain to the adjacent membrane-bound MT1-MMP. The contradicting roles of TIMP2 in MMP2 regulation render it difficult to predict the role of TIMP2 in heart disease.

1.7.3. MMP-independent functions of TIMP2

TIMP2 regulates skeletal muscle integrin β1 expression

TIMP2 has also been reported to regulate expression of integrin β1 in skeletal muscle, in both oxidative and glycolytic muscle, but to a greater extent in the latter[314]. These findings suggest that TIMP2 colocalizes with the integrin β1 at the costamere, and as such deficiency of TIMP2 greatly reduced integrin β1 protein expression levels compromising neuromuscular junction development, for which the mechanism involved was not fully explored. This role of TIMP2 was found to be independent of its MMP inhibitory capacity, as there was an unexpected reduction of MMP activity in the muscle of the TIMP2-deficient mice[314].

TIMP2 inhibits angiogenesis

An important MMP-independent function of TIMP2 that could have considerable importance in cardiovascular disease is the inhibitory role on angiogenesis. In addition to the well-established MMP-dependent anti-angiogenic capacity that it and other TIMPs possess through MMP inhibition[315, 316], it has

been reported that TIMP2 in particular has a unique MMP-independent ability to inhibit angiogenesis through its indirect interaction with VEGFR2[317, 318]. It has been discovered that the noninhibitory C-terminus of TIMP2 interacts with an α3β1 integrin complex at the endothelial cell surface[319], which then through the release of phosphatases inactivates the adjacent VEGFR2 receptor, thereby diminishing endothelial cell proliferative capacity[317]. Retroviral overexpression of TIMP2 in mammary tumor development interestingly showed downregulation of VEGF mRNA expression in vitro and in vivo[320]. These processes combined illustrate a prominent role of TIMP2 in many diseases where vascular growth is implicated, in particular cancer and heart disease.

TIMP2 promotes collagen synthesis

Additionally, TIMP2 has exhibited a procollagenic affect through *in vitro* experiments using fibroblasts[321], the principle generator of collagen in the heart. Overexpression of TIMP2 via adenoviral transduction in cultured fibroblast demonstrated an increase in collagen synthesis from these cells, in addition to increased proliferative capacity of the fibroblasts. These findings provide insight into a complementary role that TIMP2 may have in ECM remodeling along with its inhibition of MMPs.

1.7.4. TIMP2 in heart disease

TIMP2 was initially thought to be constitutively expressed[246], although it has been found to be inducible in the myocardial tissue of patients with heart disease[322, 323], as well as in animal models of heart disease[274, 275]. It has been reported that TIMP2 myocardial protein levels are considerably increased in end-stage heart disease[133]. Other studies have reported an increase in myocardial TIMP2 protein levels in patients with aortic stenosis experiencing left ventricular pressure overload[323, 324], and in heart failure after experimental pressure overload [325]. Ischemic cardiomyopathy resulted in no change in myocardial TIMP2 levels[326], but plasma TIMP2 levels was increased in patients with myocardial infarction[327]. Patients with atrial fibrillation displayed an increase in TIMP2

levels as well[328]. There appears to be a trend of increased TIMP2 levels in heart disease, which needs to be further explored to interpret the role of TIMP2 in ECM remodeling in disease, as patients with aortic stenosis showed high correlation between elevated TIMP2 level and increased degree of fibrosis[323]. Additionally, the delayed pattern of the TIMP2 increase relative to early ECM proteolytic degradation also needs to be examined to understand the temporal relationship between MMPs and TIMPs during ECM remodeling.

1.8. Tissue inhibitor of metalloproteinases-3 (TIMP3)

1.8.1. Discovery & structure of TIMP3

TIMP3 was first discovered in 1991 as a metalloendopeptidase found in chicken[329, 330] which was homologous, yet unique, to the previously discovered TIMP and TIMP2 MMP inhibitors. TIMP3 shares 43-49% amino acid sequence homology with the other three TIMPs as reviewed by Lambert et al.[246]. TIMP3 has a molecular mass of 21kDa protein, although in the glycosylated form[331] it can increase to 27-29kDa, and in its mature form it is 188 amino acids in length. Gene mapping has identified the location of TIMP3 on human chromosome 22q12.1-q13.2[332] and on mouse chromosome 10[333]. Of the four TIMPs, TIMP3 is also distinct from the other TIMPs based on what is currently known about its ECM binding capacity[334]. TIMP3 has been found to possess two potential heparin binding sequences in the N-terminus domain, enabling tighter binding to sulfated glycosaminoglycans present in the ECM components[335]. This suggests that TIMP3 may potentially modulate MMP activity in a more focal manner than the other TIMPs[336].

1.8.2. The interaction between TIMP3 and MMPs

TIMP3 is ubiquitously expressed and is a potent inhibitor of a wide variety of metalloproteinases. With respect to its interaction with MMPs, in addition to the conventional targeting of the N-terminus catalytic domain of the activated

MMP, there has been examination of the potential interaction of TIMP3 with the inactive precursor pro-form of MMPs. Comparable to how TIMP2 is capable of binding to proMMP2 as previously mentioned (Section 1.7.2.), and how TIMP1 is able to form a complex with proMMP9[337], there is evidence that the C-terminus of TIMP3 is capable of binding to the hemopexin domain of both proMMP2 and proMMP9 in a similar fashion[338]. The function of these complexes has not yet fully been explored, as there is no evidence that TIMP3 is involved in any cell surface processing of these gelatinases[339], such as TIMP2.

1.8.3. Additional functions of TIMP3

TIMP3 inhibition of ADAM17 independent

In addition of inhibiting a broad-spectrum of MMPs, TIMP3 also inhibits another family of proteases, a disintegrin and metalloproteinases (ADAMs). A ADAM17, also known as TACE (TNF-alpha converting enzyme) is a protease responsible for the shedding of membrane-bound TNFα by converting it into its soluble active form [340]. The action of ADAM17 has been found to be inhibited primarily by TIMP3 [341, 342]. In human dilated cardiomyopathy, Satoh et al. found that both RNA and protein levels of both TACE and TNFα were positively correlated with left ventricular volume and negatively correlated with systolic function in the form of EF with more advanced dilated cardiomyopathy[343]. In addition to ADAM17, TIMP3 is able to inhibit other ADAMs, most notably ADAM10[344] and secreted soluble ADAM12[345]. ADAM10 can also be inhibited by TIMP1[344].

TIMP3-mediated inhibition of angiogenesis

It has been well-established that increased MMP activity is an important promoter of angiogenesis in a variety of physiological or pathological states[346, 347]. The inhibition of MMP activity that is provided by TIMPs is a principle regulator of the angiogenesis process. However, it has been suggested that the traditional MMP-dependent regulation of angiogenesis may only be a partial aspect of the anti-angiogenesis capacity of TIMP3. A novel mechanism has been proposed

whereby TIMP3 can inhibit angiogenesis independent of its MMP-inhibitory function but by directly competing with VEGF in binding to VEGFR2, thereby blocking downstream signaling[348]. By blocking VEGF from binding to its critical receptor, TIMP3 essentially blocks the signaling to the endothelial cells that would trigger the angiogenic response. These findings, along with the classical MMP-inhibition, as well as other findings of TIMP3 inhibiting the actions of endothelial cells *in vitro* and their response to other growth factors *in vivo*[349], suggests that TIMP3 likely has a multifaceted role as a potent anti-angiogenesis agent.

TIMP3 promotes apoptosis

The investigation of the affects of TIMPs on different cell types led to the discovery that the TIMPs have the potential to influence cells in different ways. One of the observations from earlier work was that overexpressing TIMP3 led to increased apoptosis *in vitro* in a variety of different cell types. Increased TIMP3 level was found to trigger substantial apoptosis in cardiac fibroblasts[321], vascular smooth muscle cells[350], and various cancer cells. This affect was not evident with TIMP1 or TIMP2. One approach that was proposed was to identify structural differences of TIMP3 that could explain this unique property, and to also determine if the proapoptotic affect was related to its MMP-inhibitory capacity[351]. They identified that the apoptotic and inhibition functions are related to the N-terminus and suggested that the apoptosis was possibly attributable to TIMP3's ADAM17/TACE regulatory function, which is unique to TIMP3. This was substantiated by another group identifying the conserved TNFα receptors remaining on the membrane in the presence of TIMP3 in human colon carcinoma cells as a mechanism of increased TNFα signaling and increased apoptosis of these cells[352]. More investigations into this aspect of TIMP3 function needs to be performed in order to determine the relationship between TIMP3 and cell survival, as future work using TIMP3$^{-/-}$ mice found increased apoptosis in the absence of TIMP3 in mammary gland epithelial cells *in vivo* supposedly attributable to increased MMP activity destabilizing surrounding ECM, thereby

creating an environment conducive to apoptosis[353]. Many variables were identified as factors that need to be accounted for, such as cell type and concentration of TIMP3, so it indicates that there is no established conclusion of the role of TIMP3 in apoptosis.

1.8.4. TIMP3 in heart disease

TIMP3 has been found to be downregulated during ischemic heart disease and in patients with dilated cardiomyopathy [326, 354] at the transcript and protein levels. Additionally, there is also evidence that this reduction in TIMP3 level in heart disease is sustained throughout the disease progression to the point of end-stage congestive heart failure[355]. These findings combined suggest that the reduction of TIMP3 may promote the transition from a compensated state to decompensated heart failure, and that its presence is in fact critical for proper cardiac response to disease.

1.9. General hypotheses and thesis objectives

General hypothesis

We hypothesized that TIMP2 and TIMP3 will affect cardiac response to disease differently. While lack of TIMP3 could impact extracelluar matrix remodeling and cell death, TIMP2 deficiency could prevent cell surface activation of MMP2 and thereby preserve the pathological ECM remodeling. In addition, based on the proposed anti-angiogenic functions of TIMP2 and TIMP3, lack of these TIMPs would improve the post-MI recovery and remodeling.

Rationale

The reasons for studying the role of TIMP2 and TIMP3 in different heart disease models are that these TIMPs show the highest mRNA expression levels in the mouse heart and it was important to determine if this resulted in a critical role for these TIMPs in the cardiac remodeling process. In addition, there had been no reports on the role of TIMP2 in heart disease models, and the role of TIMP3 in a model of MI was not fully explored. Meanwhile, the roles of TIMP1[268, 271, 272] and TIMP4[282] in both MI and in pressure overload cardiomyopathies has been reported. In addition, the role of TIMP2 in cell surface activation of pro-MMP2, and the reported anti-angiogentic functions of TIMP2 and TIMP3, provided the basis for examining the role of these TIMPs in models of heart disease where MMP2 activation and angiogenesis are major contributing factors to disease progression. These factors rationalized the studies described in this thesis.

Objectives

Given the multiple MMP-dependent and MMP-independent functions of TIMP2 and TIMP3 in the cardiovascular system and their high expression level in the heart, there is a strong possibility that they both play key roles in the cardiac response to disease. The following chapters will present research pertaining to our exploration of the role of TIMP2 and TIMP3 in heart disease, specifically MI and pressure overload cardiomyopathies using the $TIMP2^{-/-}$ and $TIMP3^{-/-}$ mouse. We aimed to investigate the importance of ECM proteolytic regulation for preventing pathological left ventricle remodeling and attenuating the decline of cardiac function in heart disease. Based on our findings and the reported changes of TIMP2 and TIMP3 levels in different diseases, ultimately we would like to identify the specific roles that TIMP2 and TIMP3 each have in heart disease and the conditions that dictate their necessity.

1.10. REFERENCES

1. Roger VL, Go AS, Lloyd-Jones DM, Benjamin EJ, Berry JD, Borden WB, Bravata DM, Dai S, Ford ES, Fox CS, Fullerton HJ, Gillespie C, Hailpern SM, Heit JA, Howard VJ, Kissela BM, Kittner SJ, Lackland DT, Lichtman JH, Lisabeth LD, Makuc DM, Marcus GM, Marelli A, Matchar DB, Moy CS, Mozaffarian D, Mussolino ME, Nichol G, Paynter NP, Soliman EZ, Sorlie PD, Sotoodehnia N, Turan TN, Virani SS, Wong ND, Woo D, Turner MB. Heart disease and stroke statistics--2012 update: A report from the american heart association. *Circulation*. 2012;125:e2-e220

2. Miller LW. Limitations of current medical therapies for the treatment of heart failure. *Rev Cardiovasc Med*. 2003;4 Suppl 2:S21-29

3. Voelkel NF, Quaife RA, Leinwand LA, Barst RJ, McGoon MD, Meldrum DR, Dupuis J, Long CS, Rubin LJ, Smart FW, Suzuki YJ, Gladwin M, Denholm EM, Gail DB. Right ventricular function and failure: Report of a national heart, lung, and blood institute working group on cellular and molecular mechanisms of right heart failure. *Circulation*. 2006;114:1883-1891

4. Tirziu D, Giordano FJ, Simons M. Cell communications in the heart. *Circulation*. 2010;122:928-937

5. Urbanek K, Torella D, Sheikh F, De Angelis A, Nurzynska D, Silvestri F, Beltrami CA, Bussani R, Beltrami AP, Quaini F, Bolli R, Leri A, Kajstura J, Anversa P. Myocardial regeneration by activation of multipotent cardiac stem cells in ischemic heart failure. *Proc Natl Acad Sci U S A*. 2005;102:8692-8697

6. Frangogiannis NG, Lindsey ML, Michael LH, Youker KA, Bressler RB, Mendoza LH, Spengler RN, Smith CW, Entman ML. Resident cardiac mast cells degranulate and release preformed tnf-alpha, initiating the cytokine cascade in experimental canine myocardial ischemia/reperfusion. *Circulation*. 1998;98:699-710

7. Banerjee I, Fuseler JW, Price RL, Borg TK, Baudino TA. Determination of cell types and numbers during cardiac development in the neonatal and adult rat and mouse. *Am J Physiol Heart Circ Physiol*. 2007;293:H1883-1891

8. Gregorio CC, Antin PB. To the heart of myofibril assembly. *Trends Cell Biol*. 2000;10:355-362

9. Weber KT, Sun Y, Tyagi SC, Cleutjens JP. Collagen network of the myocardium: Function, structural remodeling and regulatory mechanisms. *J Mol Cell Cardiol*. 1994;26:279-292

10. Sengupta PP, Korinek J, Belohlavek M, Narula J, Vannan MA, Jahangir A, Khandheria BK. Left ventricular structure and function: Basic science for cardiac imaging. *J Am Coll Cardiol*. 2006;48:1988-2001

11. Gorza L, Vettore S, Vitadello M. Molecular and cellular diversity of heart conduction system myocytes. *Trends Cardiovasc Med*. 1994;4:153-159

12. Stenger RJ, Spiro D. The ultrastructure of mammalian cardiac muscle. *J Biophys Biochem Cytol*. 1961;9:325-351

13. Millman BM. The filament lattice of striated muscle. *Physiol Rev*. 1998;78:359-391

14. Landesberg A, Sideman S. Coupling calcium binding to troponin c and cross-bridge cycling in skinned cardiac cells. *Am J Physiol*. 1994;266:H1260-1271

15. Ottaviano FG, Yee KO. Communication signals between cardiac fibroblasts and cardiac myocytes. *J Cardiovasc Pharmacol*. 2011;57:513-521

16. Kakkar R, Lee RT. Intramyocardial fibroblast myocyte communication. *Circ Res*. 2010;106:47-57

17. Misfeldt AM, Boyle SC, Tompkins KL, Bautch VL, Labosky PA, Baldwin HS. Endocardial cells are a distinct endothelial lineage derived from flk1+ multipotent cardiovascular progenitors. *Dev Biol*. 2009;333:78-89

18. Harris IS, Black BL. Development of the endocardium. *Pediatr Cardiol*. 2010;31:391-399

19. Pappas DJ, Rimm DL. Direct interaction of the c-terminal domain of alpha-catenin and f-actin is necessary for stabilized cell-cell adhesion. *Cell Commun Adhes*. 2006;13:151-170

20. Mege RM, Gavard J, Lambert M. Regulation of cell-cell junctions by the cytoskeleton. *Curr Opin Cell Biol*. 2006;18:541-548

21. Yamada S, Pokutta S, Drees F, Weis WI, Nelson WJ. Deconstructing the cadherin-catenin-actin complex. *Cell*. 2005;123:889-901

22. Louault C, Benamer N, Faivre JF, Potreau D, Bescond J. Implication of connexins 40 and 43 in functional coupling between mouse cardiac fibroblasts in primary culture. *Biochim Biophys Acta*. 2008;1778:2097-2104

23. Zhang Y, Kanter EM, Laing JG, Aprhys C, Johns DC, Kardami E, Yamada KA. Connexin43 expression levels influence intercellular coupling and cell proliferation of native murine cardiac fibroblasts. *Cell Commun Adhes*. 2008;15:289-303

24. Kamkin A, Kiseleva I, Lozinsky I, Scholz H. Electrical interaction of mechanosensitive fibroblasts and myocytes in the heart. *Basic Res Cardiol*. 2005;100:337-345

25. Richardson P, McKenna W, Bristow M, Maisch B, Mautner B, O'Connell J, Olsen E, Thiene G, Goodwin J, Gyarfas I, Martin I, Nordet P. Report of the 1995 world health organization/international society and federation of cardiology task force on the definition and classification of cardiomyopathies. *Circulation*. 1996;93:841-842

26. Giles TD, Chatterjee K, Cohn JN, Colucci WS, Feldman AM, Ferrans VJ, Roberts R. Definition, classification, and staging of the adult cardiomyopathies: A proposal for revision. *J Card Fail*. 2004;10:6-8

27. Thiene G, Corrado D, Basso C. Revisiting definition and classification of cardiomyopathies in the era of molecular medicine. *Eur Heart J*. 2008;29:144-146

28. Cohn JN, Ferrari R, Sharpe N. Cardiac remodeling--concepts and clinical implications: A consensus paper from an international forum on cardiac remodeling. Behalf of an international forum on cardiac remodeling. *J Am Coll Cardiol*. 2000;35:569-582

29. Gaasch WH, Zile MR. Left ventricular structural remodeling in health and disease: With special emphasis on volume, mass, and geometry. *J Am Coll Cardiol*. 2011;58:1733-1740

30. Pfeffer MA, Braunwald E. Ventricular remodeling after myocardial infarction. Experimental observations and clinical implications. *Circulation*. 1990;81:1161-1172

31. Seiler C. The human coronary collateral circulation. *Eur J Clin Invest*. 2010;40:465-476

32. Berry C, Balachandran KP, L'Allier PL, Lesperance J, Bonan R, Oldroyd KG. Importance of collateral circulation in coronary heart disease. *Eur Heart J*. 2007;28:278-291

33. Gorman RC, Jackson BM, Burdick JA, Gorman JH. Infarct restraint to limit adverse ventricular remodeling. *J Cardiovasc Transl Res*. 2011;4:73-81

34. McCall K. Genetic control of necrosis - another type of programmed cell death. *Curr Opin Cell Biol*. 2010;22:882-888

35. Kanamori H, Takemura G, Goto K, Maruyama R, Tsujimoto A, Ogino A, Takeyama T, Kawaguchi T, Watanabe T, Fujiwara T, Fujiwara H, Seishima M, Minatoguchi S. The role of autophagy emerging in postinfarction cardiac remodelling. *Cardiovasc Res*. 2011;91:330-339

36. Swynghedauw B. Molecular mechanisms of myocardial remodeling. *Physiol Rev*. 1999;79:215-262

37. Sutton MG, Sharpe N. Left ventricular remodeling after myocardial infarction: Pathophysiology and therapy. *Circulation*. 2000;101:2981-2988

38. St John Sutton M, Lee D, Rouleau JL, Goldman S, Plappert T, Braunwald E, Pfeffer MA. Left ventricular remodeling and ventricular arrhythmias after myocardial infarction. *Circulation*. 2003;107:2577-2582

39. Takada A, Saito K, Nagai T, Hamamatsu A, Murai T. When does an infarcted heart rupture? A pathological study of 148 out-of-hospital sudden death cases. *Int J Cardiol*. 2008;129:447-448

40. Gandhi MS, Kamalov G, Shahbaz AU, Bhattacharya SK, Ahokas RA, Sun Y, Gerling IC, Weber KT. Cellular and molecular pathways to myocardial necrosis and replacement fibrosis. *Heart Fail Rev*. 2011;16:23-34

41. Golstein P, Kroemer G. Cell death by necrosis: Towards a molecular definition. *Trends Biochem Sci*. 2007;32:37-43

42. Nakayama H, Chen X, Baines CP, Klevitsky R, Zhang X, Zhang H, Jaleel N, Chua BH, Hewett TE, Robbins J, Houser SR, Molkentin JD. Ca2+- and

mitochondrial-dependent cardiomyocyte necrosis as a primary mediator of heart failure. *J Clin Invest*. 2007;117:2431-2444

43. Chiong M, Wang ZV, Pedrozo Z, Cao DJ, Troncoso R, Ibacache M, Criollo A, Nemchenko A, Hill JA, Lavandero S. Cardiomyocyte death: Mechanisms and translational implications. *Cell Death Dis*. 2011;2:e244

44. Giordano FJ. Oxygen, oxidative stress, hypoxia, and heart failure. *J Clin Invest*. 2005;115:500-508

45. Hori M, Nishida K. Oxidative stress and left ventricular remodelling after myocardial infarction. *Cardiovasc Res*. 2009;81:457-464

46. Henderson BC, Tyagi N, Ovechkin A, Kartha GK, Moshal KS, Tyagi SC. Oxidative remodeling in pressure overload induced chronic heart failure. *Eur J Heart Fail*. 2007;9:450-457

47. McMurray J, Chopra M, Abdullah I, Smith WE, Dargie HJ. Evidence of oxidative stress in chronic heart failure in humans. *Eur Heart J*. 1993;14:1493-1498

48. Sorescu D, Griendling KK. Reactive oxygen species, mitochondria, and nad(p)h oxidases in the development and progression of heart failure. *Congest Heart Fail*. 2002;8:132-140

49. Packer MA, Porteous CM, Murphy MP. Superoxide production by mitochondria in the presence of nitric oxide forms peroxynitrite. *Biochem Mol Biol Int*. 1996;40:527-534

50. Ishida H, Ichimori K, Hirota Y, Fukahori M, Nakazawa H. Peroxynitrite-induced cardiac myocyte injury. *Free Radic Biol Med*. 1996;20:343-350

51. Schulz R, Dodge KL, Lopaschuk GD, Clanachan AS. Peroxynitrite impairs cardiac contractile function by decreasing cardiac efficiency. *Am J Physiol*. 1997;272:H1212-1219

52. Chen Q, Moghaddas S, Hoppel CL, Lesnefsky EJ. Ischemic defects in the electron transport chain increase the production of reactive oxygen species from isolated rat heart mitochondria. *Am J Physiol Cell Physiol*. 2008;294:C460-466

53. Kowaltowski AJ, de Souza-Pinto NC, Castilho RF, Vercesi AE. Mitochondria and reactive oxygen species. *Free Radic Biol Med*. 2009;47:333-343

54. Santos CX, Anilkumar N, Zhang M, Brewer AC, Shah AM. Redox signaling in cardiac myocytes. *Free Radic Biol Med*. 2011;50:777-793

55. Li JM, Gall NP, Grieve DJ, Chen M, Shah AM. Activation of nadph oxidase during progression of cardiac hypertrophy to failure. *Hypertension*. 2002;40:477-484

56. Kuroda J, Ago T, Matsushima S, Zhai P, Schneider MD, Sadoshima J. Nadph oxidase 4 (nox4) is a major source of oxidative stress in the failing heart. *Proc Natl Acad Sci U S A*. 2010;107:15565-15570

57. Heymes C, Bendall JK, Ratajczak P, Cave AC, Samuel JL, Hasenfuss G, Shah AM. Increased myocardial nadph oxidase activity in human heart failure. *J Am Coll Cardiol*. 2003;41:2164-2171

58. Gonzalez DR, Treuer AV, Castellanos J, Dulce RA, Hare JM. Impaired s-nitrosylation of the ryanodine receptor caused by xanthine oxidase activity contributes to calcium leak in heart failure. *J Biol Chem*. 2010;285:28938-28945

59. Hayashi K, Kimata H, Obata K, Matsushita A, Fukata A, Hashimoto K, Noda A, Iwase M, Koike Y, Yokota M, Nagata K. Xanthine oxidase inhibition improves left ventricular dysfunction in dilated cardiomyopathic hamsters. *J Card Fail*. 2008;14:238-244

60. Shanmuganathan S, Hausenloy DJ, Duchen MR, Yellon DM. Mitochondrial permeability transition pore as a target for cardioprotection in the human heart. *Am J Physiol Heart Circ Physiol*. 2005;289:H237-242

61. Hill MF, Singal PK. Right and left myocardial antioxidant responses during heart failure subsequent to myocardial infarction. *Circulation*. 1997;96:2414-2420

62. Dhalla AK, Singal PK. Antioxidant changes in hypertrophied and failing guinea pig hearts. *Am J Physiol*. 1994;266:H1280-1285

63. Frangogiannis NG. The immune system and cardiac repair. *Pharmacol Res*. 2008;58:88-111

64. Jiang B, Liao R. The paradoxical role of inflammation in cardiac repair and regeneration. *J Cardiovasc Transl Res*. 2010;3:410-416

65. Frangogiannis NG. Regulation of the inflammatory response in cardiac repair. *Circ Res*. 2012;110:159-173

66. Frangogiannis NG, Smith CW, Entman ML. The inflammatory response in myocardial infarction. *Cardiovasc Res*. 2002;53:31-47

67. Lambert JM, Lopez EF, Lindsey ML. Macrophage roles following myocardial infarction. *Int J Cardiol*. 2008;130:147-158

68. Nian M, Lee P, Khaper N, Liu P. Inflammatory cytokines and postmyocardial infarction remodeling. *Circ Res*. 2004;94:1543-1553

69. Kelso A. Cytokines: Principles and prospects. *Immunol Cell Biol*. 1998;76:300-317

70. Ren G, Dewald O, Frangogiannis NG. Inflammatory mechanisms in myocardial infarction. *Curr Drug Targets Inflamm Allergy*. 2003;2:242-256

71. Lindsey M, Wedin K, Brown MD, Keller C, Evans AJ, Smolen J, Burns AR, Rossen RD, Michael L, Entman M. Matrix-dependent mechanism of neutrophil-mediated release and activation of matrix metalloproteinase 9 in myocardial ischemia/reperfusion. *Circulation*. 2001;103:2181-2187

72. Shapiro SD, Kobayashi DK, Ley TJ. Cloning and characterization of a unique elastolytic metalloproteinase produced by human alveolar macrophages. *J Biol Chem*. 1993;268:23824-23829

73. Weber KT, Brilla CG. Factors associated with reactive and reparative fibrosis of the myocardium. *Basic Res Cardiol*. 1992;87 Suppl 1:291-301

74. Brown RD, Jones GM, Laird RE, Hudson P, Long CS. Cytokines regulate matrix metalloproteinases and migration in cardiac fibroblasts. *Biochem Biophys Res Commun*. 2007;362:200-205

75. Squires CE, Escobar GP, Payne JF, Leonardi RA, Goshorn DK, Sheats NJ, Mains IM, Mingoia JT, Flack EC, Lindsey ML. Altered fibroblast function following myocardial infarction. *J Mol Cell Cardiol*. 2005;39:699-707

76. Leask A, Abraham DJ. Tgf-beta signaling and the fibrotic response. *FASEB J*. 2004;18:816-827

77. Wilson EM, Moainie SL, Baskin JM, Lowry AS, Deschamps AM, Mukherjee R, Guy TS, St John-Sutton MG, Gorman JH, 3rd, Edmunds LH, Jr., Gorman RC, Spinale FG. Region- and type-specific induction of matrix metalloproteinases in post-myocardial infarction remodeling. *Circulation*. 2003;107:2857-2863

78. Li J, Brown LF, Hibberd MG, Grossman JD, Morgan JP, Simons M. Vegf, flk-1, and flt-1 expression in a rat myocardial infarction model of angiogenesis. *Am J Physiol*. 1996;270:H1803-1811

79. Lee SH, Wolf PL, Escudero R, Deutsch R, Jamieson SW, Thistlethwaite PA. Early expression of angiogenesis factors in acute myocardial ischemia and infarction. *N Engl J Med*. 2000;342:626-633

80. Pugh CW, Ratcliffe PJ. Regulation of angiogenesis by hypoxia: Role of the hif system. *Nat Med*. 2003;9:677-684

81. Banai S, Jaklitsch MT, Shou M, Lazarous DF, Scheinowitz M, Biro S, Epstein SE, Unger EF. Angiogenic-induced enhancement of collateral blood flow to ischemic myocardium by vascular endothelial growth factor in dogs. *Circulation*. 1994;89:2183-2189

82. Shyu KG, Wang MT, Wang BW, Chang CC, Leu JG, Kuan P, Chang H. Intramyocardial injection of naked DNA encoding hif-1alpha/vp16 hybrid to enhance angiogenesis in an acute myocardial infarction model in the rat. *Cardiovasc Res*. 2002;54:576-583

83. Mack CA, Patel SR, Schwarz EA, Zanzonico P, Hahn RT, Ilercil A, Devereux RB, Goldsmith SJ, Christian TF, Sanborn TA, Kovesdi I, Hackett N, Isom OW, Crystal RG, Rosengart TK. Biologic bypass with the use of adenovirus-mediated gene transfer of the complementary deoxyribonucleic acid for vascular endothelial growth factor 121 improves myocardial perfusion and function in the ischemic porcine heart. *J Thorac Cardiovasc Surg*. 1998;115:168-176; discussion 176-167

84. Su H, Lu R, Kan YW. Adeno-associated viral vector-mediated vascular endothelial growth factor gene transfer induces neovascular formation in ischemic heart. *Proc Natl Acad Sci U S A*. 2000;97:13801-13806

85. Henry TD, Annex BH, McKendall GR, Azrin MA, Lopez JJ, Giordano FJ, Shah PK, Willerson JT, Benza RL, Berman DS, Gibson CM, Bajamonde

A, Rundle AC, Fine J, McCluskey ER. The viva trial: Vascular endothelial growth factor in ischemia for vascular angiogenesis. *Circulation*. 2003;107:1359-1365

86. Hendel RC, Henry TD, Rocha-Singh K, Isner JM, Kereiakes DJ, Giordano FJ, Simons M, Bonow RO. Effect of intracoronary recombinant human vascular endothelial growth factor on myocardial perfusion: Evidence for a dose-dependent effect. *Circulation*. 2000;101:118-121

87. Henry TD, Rocha-Singh K, Isner JM, Kereiakes DJ, Giordano FJ, Simons M, Losordo DW, Hendel RC, Bonow RO, Eppler SM, Zioncheck TF, Holmgren EB, McCluskey ER. Intracoronary administration of recombinant human vascular endothelial growth factor to patients with coronary artery disease. *Am Heart J*. 2001;142:872-880

88. Kornowski R, Fuchs S, Leon MB, Epstein SE. Delivery strategies to achieve therapeutic myocardial angiogenesis. *Circulation*. 2000;101:454-458

89. Weis SM, Cheresh DA. Pathophysiological consequences of vegf-induced vascular permeability. *Nature*. 2005;437:497-504

90. Matsunaga T, Warltier DC, Weihrauch DW, Moniz M, Tessmer J, Chilian WM. Ischemia-induced coronary collateral growth is dependent on vascular endothelial growth factor and nitric oxide. *Circulation*. 2000;102:3098-3103

91. Shintani S, Murohara T, Ikeda H, Ueno T, Honma T, Katoh A, Sasaki K, Shimada T, Oike Y, Imaizumi T. Mobilization of endothelial progenitor cells in patients with acute myocardial infarction. *Circulation*. 2001;103:2776-2779

92. Kawamoto A, Gwon HC, Iwaguro H, Yamaguchi JI, Uchida S, Masuda H, Silver M, Ma H, Kearney M, Isner JM, Asahara T. Therapeutic potential of ex vivo expanded endothelial progenitor cells for myocardial ischemia. *Circulation*. 2001;103:634-637

93. Freedman SB, Isner JM. Therapeutic angiogenesis for coronary artery disease. *Ann Intern Med*. 2002;136:54-71

94. Klocke R, Tian W, Kuhlmann MT, Nikol S. Surgical animal models of heart failure related to coronary heart disease. *Cardiovasc Res*. 2007;74:29-38

95. Mann DL, Foale RA, Gillam LD, Schoenfeld D, Newell J, Weyman AE. Early natural history of regional left ventricular dysfunction after experimental myocardial infarction. *Am Heart J*. 1988;115:538-546

96. Salto-Tellez M, Yung Lim S, El-Oakley RM, Tang TP, ZA AL, Lim SK. Myocardial infarction in the c57bl/6j mouse: A quantifiable and highly reproducible experimental model. *Cardiovasc Pathol*. 2004;13:91-97

97. Samsamshariat SA, Samsamshariat ZA, Movahed MR. A novel method for safe and accurate left anterior descending coronary artery ligation for research in rats. *Cardiovasc Revasc Med*. 2005;6:121-123

98. Kramer CM, Rogers WJ, Park CS, Seibel PS, Shaffer A, Theobald TM, Reichek N, Onodera T, Gerdes AM. Regional myocyte hypertrophy parallels regional myocardial dysfunction during post-infarct remodeling. *J Mol Cell Cardiol*. 1998;30:1773-1778

99. Driesen RB, Verheyen FK, Dijkstra P, Thone F, Cleutjens JP, Lenders MH, Ramaekers FC, Borgers M. Structural remodelling of cardiomyocytes in the border zone of infarcted rabbit heart. *Mol Cell Biochem*. 2007;302:225-232

100. Wolf T, Gepstein L, Dror U, Hayam G, Shofti R, Zaretzky A, Uretzky G, Oron U, Ben-Haim SA. Detailed endocardial mapping accurately predicts the transmural extent of myocardial infarction. *J Am Coll Cardiol*. 2001;37:1590-1597

101. Mukherjee R, Brinsa TA, Dowdy KB, Scott AA, Baskin JM, Deschamps AM, Lowry AS, Escobar GP, Lucas DG, Yarbrough WM, Zile MR, Spinale FG. Myocardial infarct expansion and matrix metalloproteinase inhibition. *Circulation*. 2003;107:618-625

102. Schwartzkopff B, Frenzel H, Dieckerhoff J, Betz P, Flasshove M, Schulte HD, Mundhenke M, Motz W, Strauer BE. Morphometric investigation of human myocardium in arterial hypertension and valvular aortic stenosis. *Eur Heart J*. 1992;13 Suppl D:17-23

103. Drazner MH. The progression of hypertensive heart disease. *Circulation*. 2011;123:327-334

104. Cohn JN. Structural basis for heart failure. Ventricular remodeling and its pharmacological inhibition. *Circulation*. 1995;91:2504-2507

105. Diwan A, Dorn GW, 2nd. Decompensation of cardiac hypertrophy: Cellular mechanisms and novel therapeutic targets. *Physiology (Bethesda)*. 2007;22:56-64

106. Wikman-Coffelt J, Parmley WW, Mason DT. The cardiac hypertrophy process. Analyses of factors determining pathological vs. Physiological development. *Circ Res*. 1979;45:697-707

107. McMullen JR, Jennings GL. Differences between pathological and physiological cardiac hypertrophy: Novel therapeutic strategies to treat heart failure. *Clin Exp Pharmacol Physiol*. 2007;34:255-262

108. Bernardo BC, Weeks KL, Pretorius L, McMullen JR. Molecular distinction between physiological and pathological cardiac hypertrophy: Experimental findings and therapeutic strategies. *Pharmacol Ther*. 2010;128:191-227

109. DiMichele LA, Doherty JT, Rojas M, Beggs HE, Reichardt LF, Mack CP, Taylor JM. Myocyte-restricted focal adhesion kinase deletion attenuates pressure overload-induced hypertrophy. *Circ Res*. 2006;99:636-645

110. De Acetis M, Notte A, Accornero F, Selvetella G, Brancaccio M, Vecchione C, Sbroggio M, Collino F, Pacchioni B, Lanfranchi G, Aretini A, Ferretti R, Maffei A, Altruda F, Silengo L, Tarone G, Lembo G. Cardiac overexpression of melusin protects from dilated cardiomyopathy due to long-standing pressure overload. *Circ Res*. 2005;96:1087-1094

111. Russell B, Curtis MW, Koshman YE, Samarel AM. Mechanical stress-induced sarcomere assembly for cardiac muscle growth in length and width. *J Mol Cell Cardiol*. 2010;48:817-823

112. Wettschureck N, Rutten H, Zywietz A, Gehring D, Wilkie TM, Chen J, Chien KR, Offermanns S. Absence of pressure overload induced myocardial hypertrophy after conditional inactivation of galphaq/galpha11 in cardiomyocytes. *Nat Med*. 2001;7:1236-1240

113. Kiriazis H, Wang K, Xu Q, Gao XM, Ming Z, Su Y, Moore XL, Lambert G, Gibbs ME, Dart AM, Du XJ. Knockout of beta(1)- and beta(2)-adrenoceptors attenuates pressure overload-induced cardiac hypertrophy and fibrosis. *Br J Pharmacol*. 2008;153:684-692

114. Lorell BH, Carabello BA. Left ventricular hypertrophy: Pathogenesis, detection, and prognosis. *Circulation*. 2000;102:470-479

115. Inoko M, Kihara Y, Morii I, Fujiwara H, Sasayama S. Transition from compensatory hypertrophy to dilated, failing left ventricles in dahl salt-sensitive rats. *Am J Physiol*. 1994;267:H2471-2482

116. Esposito G, Rapacciuolo A, Naga Prasad SV, Takaoka H, Thomas SA, Koch WJ, Rockman HA. Genetic alterations that inhibit in vivo pressure-overload hypertrophy prevent cardiac dysfunction despite increased wall stress. *Circulation*. 2002;105:85-92

117. Hill JA, Karimi M, Kutschke W, Davisson RL, Zimmerman K, Wang Z, Kerber RE, Weiss RM. Cardiac hypertrophy is not a required compensatory response to short-term pressure overload. *Circulation*. 2000;101:2863-2869

118. Clemente CF, Tornatore TF, Theizen TH, Deckmann AC, Pereira TC, Lopes-Cendes I, Souza JR, Franchini KG. Targeting focal adhesion kinase with small interfering rna prevents and reverses load-induced cardiac hypertrophy in mice. *Circ Res*. 2007;101:1339-1348

119. Marano G, Palazzesi S, Vergari A, Catalano L, Gaudi S, Testa C, Canese R, Carpinelli G, Podo F, Ferrari AU. Inhibition of left ventricular remodelling preserves chamber systolic function in pressure-overloaded mice. *Pflugers Arch*. 2003;446:429-436

120. Muiesan ML, Salvetti M, Monteduro C, Bonzi B, Paini A, Viola S, Poisa P, Rizzoni D, Castellano M, Agabiti-Rosei E. Left ventricular concentric geometry during treatment adversely affects cardiovascular prognosis in hypertensive patients. *Hypertension*. 2004;43:731-738

121. Muiesan ML, Salvetti M, Paini A, Monteduro C, Galbassini G, Bonzi B, Poisa P, Belotti E, Agabiti Rosei C, Rizzoni D, Castellano M, Agabiti Rosei E. Inappropriate left ventricular mass changes during treatment adversely affects cardiovascular prognosis in hypertensive patients. *Hypertension*. 2007;49:1077-1083

122. Weidemann F, Herrmann S, Stork S, Niemann M, Frantz S, Lange V, Beer M, Gattenlohner S, Voelker W, Ertl G, Strotmann JM. Impact of myocardial fibrosis in patients with symptomatic severe aortic stenosis. *Circulation*. 2009;120:577-584

123. Towbin JA. Scarring in the heart--a reversible phenomenon? *N Engl J Med*. 2007;357:1767-1768

124. Jellis C, Martin J, Narula J, Marwick TH. Assessment of nonischemic myocardial fibrosis. *J Am Coll Cardiol*. 2010;56:89-97

125. Boluyt MO, O'Neill L, Meredith AL, Bing OH, Brooks WW, Conrad CH, Crow MT, Lakatta EG. Alterations in cardiac gene expression during the transition from stable hypertrophy to heart failure. Marked upregulation of genes encoding extracellular matrix components. *Circ Res*. 1994;75:23-32

126. Conrad CH, Brooks WW, Hayes JA, Sen S, Robinson KG, Bing OH. Myocardial fibrosis and stiffness with hypertrophy and heart failure in the spontaneously hypertensive rat. *Circulation*. 1995;91:161-170

127. Querejeta R, Lopez B, Gonzalez A, Sanchez E, Larman M, Martinez Ubago JL, Diez J. Increased collagen type i synthesis in patients with heart failure of hypertensive origin: Relation to myocardial fibrosis. *Circulation*. 2004;110:1263-1268

128. Martos R, Baugh J, Ledwidge M, O'Loughlin C, Conlon C, Patle A, Donnelly SC, McDonald K. Diastolic heart failure: Evidence of increased myocardial collagen turnover linked to diastolic dysfunction. *Circulation*. 2007;115:888-895

129. Kawano H, Do YS, Kawano Y, Starnes V, Barr M, Law RE, Hsueh WA. Angiotensin ii has multiple profibrotic effects in human cardiac fibroblasts. *Circulation*. 2000;101:1130-1137

130. Hao J, Wang B, Jones SC, Jassal DS, Dixon IM. Interaction between angiotensin ii and smad proteins in fibroblasts in failing heart and in vitro. *Am J Physiol Heart Circ Physiol*. 2000;279:H3020-3030

131. Serneri GG, Boddi M, Cecioni I, Vanni S, Coppo M, Papa ML, Bandinelli B, Bertolozzi I, Polidori G, Toscano T, Maccherini M, Modesti PA. Cardiac angiotensin ii formation in the clinical course of heart failure and its relationship with left ventricular function. *Circ Res*. 2001;88:961-968

132. Spinale FG, Coker ML, Heung LJ, Bond BR, Gunasinghe HR, Etoh T, Goldberg AT, Zellner JL, Crumbley AJ. A matrix metalloproteinase induction/activation system exists in the human left ventricular myocardium and is upregulated in heart failure. *Circulation*. 2000;102:1944-1949

133. Thomas CV, Coker ML, Zellner JL, Handy JR, Crumbley AJ, 3rd, Spinale FG. Increased matrix metalloproteinase activity and selective upregulation

in lv myocardium from patients with end-stage dilated cardiomyopathy. *Circulation*. 1998;97:1708-1715

134. Doshi D, Marx SO. Ion channels, transporters, and pumps as targets for heart failure therapy. *J Cardiovasc Pharmacol*. 2009;54:273-278

135. Fuchs F, Smith SH. Calcium, cross-bridges, and the frank-starling relationship. *News Physiol Sci*. 2001;16:5-10

136. Gianni D, Chan J, Gwathmey JK, del Monte F, Hajjar RJ. Serca2a in heart failure: Role and therapeutic prospects. *J Bioenerg Biomembr*. 2005;37:375-380

137. Tomanek RJ, Torry RJ. Growth of the coronary vasculature in hypertrophy: Mechanisms and model dependence. *Cell Mol Biol Res*. 1994;40:129-136

138. Breisch EA, Houser SR, Carey RA, Spann JF, Bove AA. Myocardial blood flow and capillary density in chronic pressure overload of the feline left ventricle. *Cardiovasc Res*. 1980;14:469-475

139. Shiojima I, Sato K, Izumiya Y, Schiekofer S, Ito M, Liao R, Colucci WS, Walsh K. Disruption of coordinated cardiac hypertrophy and angiogenesis contributes to the transition to heart failure. *J Clin Invest*. 2005;115:2108-2118

140. Bautch VL, Redick SD, Scalia A, Harmaty M, Carmeliet P, Rapoport R. Characterization of the vasculogenic block in the absence of vascular endothelial growth factor-a. *Blood*. 2000;95:1979-1987

141. Kearney JB, Kappas NC, Ellerstrom C, DiPaola FW, Bautch VL. The vegf receptor flt-1 (vegfr-1) is a positive modulator of vascular sprout formation and branching morphogenesis. *Blood*. 2004;103:4527-4535

142. Roberts DM, Kearney JB, Johnson JH, Rosenberg MP, Kumar R, Bautch VL. The vascular endothelial growth factor (vegf) receptor flt-1 (vegfr-1) modulates flk-1 (vegfr-2) signaling during blood vessel formation. *Am J Pathol*. 2004;164:1531-1535

143. Greenberg JI, Shields DJ, Barillas SG, Acevedo LM, Murphy E, Huang J, Scheppke L, Stockmann C, Johnson RS, Angle N, Cheresh DA. A role for vegf as a negative regulator of pericyte function and vessel maturation. *Nature*. 2008;456:809-813

144. Jeansson M, Gawlik A, Anderson G, Li C, Kerjaschki D, Henkelman M, Quaggin SE. Angiopoietin-1 is essential in mouse vasculature during development and in response to injury. *J Clin Invest*. 2011;121:2278-2289

145. Tuo QH, Zeng H, Stinnett A, Yu H, Aschner JL, Liao DF, Chen JX. Critical role of angiopoietins/tie-2 in hyperglycemic exacerbation of myocardial infarction and impaired angiogenesis. *Am J Physiol Heart Circ Physiol*. 2008;294:H2547-2557

146. Tsigkos S, Koutsilieris M, Papapetropoulos A. Angiopoietins in angiogenesis and beyond. *Expert Opin Investig Drugs*. 2003;12:933-941

147. Cheng XW, Kuzuya M, Nakamura K, Maeda K, Tsuzuki M, Kim W, Sasaki T, Liu Z, Inoue N, Kondo T, Jin H, Numaguchi Y, Okumura K, Yokota M, Iguchi A, Murohara T. Mechanisms underlying the impairment of ischemia-induced neovascularization in matrix metalloproteinase 2-deficient mice. *Circ Res*. 2007;100:904-913

148. Lindsey ML, Escobar GP, Dobrucki LW, Goshorn DK, Bouges S, Mingoia JT, McClister DM, Jr., Su H, Gannon J, MacGillivray C, Lee RT, Sinusas AJ, Spinale FG. Matrix metalloproteinase-9 gene deletion facilitates angiogenesis after myocardial infarction. *Am J Physiol Heart Circ Physiol*. 2006;290:H232-239

149. Lindsey ML, Gannon J, Aikawa M, Schoen FJ, Rabkin E, Lopresti-Morrow L, Crawford J, Black S, Libby P, Mitchell PG, Lee RT. Selective matrix metalloproteinase inhibition reduces left ventricular remodeling but does not inhibit angiogenesis after myocardial infarction. *Circulation*. 2002;105:753-758

150. Aplin AC, Zhu WH, Fogel E, Nicosia RF. Vascular regression and survival are differentially regulated by mt1-mmp and timps in the aortic ring model of angiogenesis. *Am J Physiol Cell Physiol*. 2009;297:C471-480

151. Devy L, Huang L, Naa L, Yanamandra N, Pieters H, Frans N, Chang E, Tao Q, Vanhove M, Lejeune A, van Gool R, Sexton DJ, Kuang G, Rank D, Hogan S, Pazmany C, Ma YL, Schoonbroodt S, Nixon AE, Ladner RC, Hoet R, Henderikx P, Tenhoor C, Rabbani SA, Valentino ML, Wood CR, Dransfield DT. Selective inhibition of matrix metalloproteinase-14 blocks tumor growth, invasion, and angiogenesis. *Cancer Res*. 2009;69:1517-1526

152. Schellings MW, Pinto YM, Heymans S. Matricellular proteins in the heart: Possible role during stress and remodeling. *Cardiovasc Res*. 2004;64:24-31

153. Iruela-Arispe ML, Lombardo M, Krutzsch HC, Lawler J, Roberts DD. Inhibition of angiogenesis by thrombospondin-1 is mediated by 2 independent regions within the type 1 repeats. *Circulation*. 1999;100:1423-1431

154. Murphy-Ullrich JE, Hook M. Thrombospondin modulates focal adhesions in endothelial cells. *J Cell Biol*. 1989;109:1309-1319

155. Greenwood JA, Murphy-Ullrich JE. Signaling of de-adhesion in cellular regulation and motility. *Microsc Res Tech*. 1998;43:420-432

156. Murphy-Ullrich JE, Gurusiddappa S, Frazier WA, Hook M. Heparin-binding peptides from thrombospondins 1 and 2 contain focal adhesion-labilizing activity. *J Biol Chem*. 1993;268:26784-26789

157. Pinto YM, Paul M, Ganten D. Lessons from rat models of hypertension: From goldblatt to genetic engineering. *Cardiovasc Res*. 1998;39:77-88

158. Kassiri Z, Khokha R. Myocardial extra-cellular matrix and its regulation by metalloproteinases and their inhibitors. *Thromb Haemost*. 2005;93:212-219

159. Spinale FG. Matrix metalloproteinases: Regulation and dysregulation in the failing heart. *Circ Res*. 2002;90:520-530

160. Parker KK, Ingber DE. Extracellular matrix, mechanotransduction and structural hierarchies in heart tissue engineering. *Philos Trans R Soc Lond B Biol Sci*. 2007;362:1267-1279

161. Hynes RO. The extracellular matrix: Not just pretty fibrils. *Science*. 2009;326:1216-1219

162. Moore L, Fan D, Basu R, Kandalam V, Kassiri Z. Tissue inhibitor of metalloproteinases (timps) in heart failure. *Heart Fail Rev*. 2011

163. Postlethwaite AE, Holness MA, Katai H, Raghow R. Human fibroblasts synthesize elevated levels of extracellular matrix proteins in response to interleukin 4. *J Clin Invest*. 1992;90:1479-1485

164. Siwik DA, Chang DL, Colucci WS. Interleukin-1beta and tumor necrosis factor-alpha decrease collagen synthesis and increase matrix metalloproteinase activity in cardiac fibroblasts in vitro. *Circ Res*. 2000;86:1259-1265

165. Siwik DA, Pagano PJ, Colucci WS. Oxidative stress regulates collagen synthesis and matrix metalloproteinase activity in cardiac fibroblasts. *Am J Physiol Cell Physiol*. 2001;280:C53-60

166. Carver W, Nagpal ML, Nachtigal M, Borg TK, Terracio L. Collagen expression in mechanically stimulated cardiac fibroblasts. *Circ Res*. 1991;69:116-122

167. Eghbali M. Cardiac fibroblasts: Function, regulation of gene expression, and phenotypic modulation. *Basic Res Cardiol*. 1992;87 Suppl 2:183-189

168. Pathak M, Sarkar S, Vellaichamy E, Sen S. Role of myocytes in myocardial collagen production. *Hypertension*. 2001;37:833-840

169. Eghbali M, Blumenfeld OO, Seifter S, Buttrick PM, Leinwand LA, Robinson TF, Zern MA, Giambrone MA. Localization of types i, iii and iv collagen mrnas in rat heart cells by in situ hybridization. *J Mol Cell Cardiol*. 1989;21:103-113

170. Petrov VV, Fagard RH, Lijnen PJ. Stimulation of collagen production by transforming growth factor-beta1 during differentiation of cardiac fibroblasts to myofibroblasts. *Hypertension*. 2002;39:258-263

171. Butt RP, Laurent GJ, Bishop JE. Collagen production and replication by cardiac fibroblasts is enhanced in response to diverse classes of growth factors. *Eur J Cell Biol*. 1995;68:330-335

172. Chen MM, Lam A, Abraham JA, Schreiner GF, Joly AH. Ctgf expression is induced by tgf- beta in cardiac fibroblasts and cardiac myocytes: A potential role in heart fibrosis. *J Mol Cell Cardiol*. 2000;32:1805-1819

173. Gao X, He X, Luo B, Peng L, Lin J, Zuo Z. Angiotensin ii increases collagen i expression via transforming growth factor-beta1 and extracellular signal-regulated kinase in cardiac fibroblasts. *Eur J Pharmacol*. 2009;606:115-120

174. Chen K, Chen J, Li D, Zhang X, Mehta JL. Angiotensin ii regulation of collagen type i expression in cardiac fibroblasts: Modulation by ppar-gamma ligand pioglitazone. *Hypertension*. 2004;44:655-661

175. Gupta V, Grande-Allen KJ. Effects of static and cyclic loading in regulating extracellular matrix synthesis by cardiovascular cells. *Cardiovasc Res*. 2006;72:375-383

176. Diez J, Gonzalez A, Lopez B, Querejeta R. Mechanisms of disease: Pathologic structural remodeling is more than adaptive hypertrophy in hypertensive heart disease. *Nat Clin Pract Cardiovasc Med*. 2005;2:209-216

177. Zannad F, Rossignol P, Iraqi W. Extracellular matrix fibrotic markers in heart failure. *Heart Fail Rev*. 2009

178. Lopez B, Gonzalez A, Diez J. Circulating biomarkers of collagen metabolism in cardiac diseases. *Circulation*. 2010;121:1645-1654

179. Lindsay MM, Maxwell P, Dunn FG. Timp-1: A marker of left ventricular diastolic dysfunction and fibrosis in hypertension. *Hypertension*. 2002;40:136-141

180. Bradshaw AD, Sage EH. Sparc, a matricellular protein that functions in cellular differentiation and tissue response to injury. *J Clin Invest*. 2001;107:1049-1054

181. McCurdy SM, Dai Q, Zhang J, Zamilpa R, Ramirez TA, Dayah T, Nguyen N, Jin YF, Bradshaw AD, Lindsey ML. Sparc mediates early extracellular matrix remodeling following myocardial infarction. *Am J Physiol Heart Circ Physiol*. 2011;301:H497-505

182. Schellings MW, Vanhoutte D, Swinnen M, Cleutjens JP, Debets J, van Leeuwen RE, d'Hooge J, Van de Werf F, Carmeliet P, Pinto YM, Sage EH, Heymans S. Absence of sparc results in increased cardiac rupture and dysfunction after acute myocardial infarction. *J Exp Med*. 2009;206:113-123

183. Bradshaw AD, Baicu CF, Rentz TJ, Van Laer AO, Boggs J, Lacy JM, Zile MR. Pressure overload-induced alterations in fibrillar collagen content and myocardial diastolic function: Role of secreted protein acidic and rich in cysteine (sparc) in post-synthetic procollagen processing. *Circulation*. 2009;119:269-280

184. Crawford SE, Stellmach V, Murphy-Ullrich JE, Ribeiro SM, Lawler J, Hynes RO, Boivin GP, Bouck N. Thrombospondin-1 is a major activator of tgf-beta1 in vivo. *Cell*. 1998;93:1159-1170

185. Tomita H, Egashira K, Ohara Y, Takemoto M, Koyanagi M, Katoh M, Yamamoto H, Tamaki K, Shimokawa H, Takeshita A. Early induction of transforming growth factor-beta via angiotensin ii type 1 receptors contributes to cardiac fibrosis induced by long-term blockade of nitric oxide synthesis in rats. *Hypertension*. 1998;32:273-279

186. Liu X, Sun SQ, Hassid A, Ostrom RS. Camp inhibits transforming growth factor-beta-stimulated collagen synthesis via inhibition of extracellular signal-regulated kinase 1/2 and smad signaling in cardiac fibroblasts. *Mol Pharmacol*. 2006;70:1992-2003

187. Frangogiannis NG, Ren G, Dewald O, Zymek P, Haudek S, Koerting A, Winkelmann K, Michael LH, Lawler J, Entman ML. Critical role of endogenous thrombospondin-1 in preventing expansion of healing myocardial infarcts. *Circulation*. 2005;111:2935-2942

188. Ross RS, Borg TK. Integrins and the myocardium. *Circ Res*. 2001;88:1112-1119

189. van der Flier A, Kuikman I, Baudoin C, van der Neut R, Sonnenberg A. A novel beta 1 integrin isoform produced by alternative splicing: Unique expression in cardiac and skeletal muscle. *FEBS Lett*. 1995;369:340-344

190. Shai SY, Harpf AE, Babbitt CJ, Jordan MC, Fishbein MC, Chen J, Omura M, Leil TA, Becker KD, Jiang M, Smith DJ, Cherry SR, Loftus JC, Ross RS. Cardiac myocyte-specific excision of the beta1 integrin gene results in myocardial fibrosis and cardiac failure. *Circ Res*. 2002;90:458-464

191. Babbitt CJ, Shai SY, Harpf AE, Pham CG, Ross RS. Modulation of integrins and integrin signaling molecules in the pressure-loaded murine ventricle. *Histochem Cell Biol*. 2002;118:431-439

192. von der Mark H, Williams I, Wendler O, Sorokin L, von der Mark K, Poschl E. Alternative splice variants of alpha 7 beta 1 integrin selectively recognize different laminin isoforms. *J Biol Chem*. 2002;277:6012-6016

193. Wu X, Sun Z, Foskett A, Trzeciakowski JP, Meininger GA, Muthuchamy M. Cardiomyocyte contractile status is associated with differences in fibronectin and integrin interactions. *Am J Physiol Heart Circ Physiol*. 2010;298:H2071-2081

194. Vandenberg P, Kern A, Ries A, Luckenbill-Edds L, Mann K, Kuhn K. Characterization of a type iv collagen major cell binding site with affinity to the alpha 1 beta 1 and the alpha 2 beta 1 integrins. *J Cell Biol*. 1991;113:1475-1483

195. Terracio L, Rubin K, Gullberg D, Balog E, Carver W, Jyring R, Borg TK. Expression of collagen binding integrins during cardiac development and hypertrophy. *Circ Res*. 1991;68:734-744

196. Laser M, Willey CD, Jiang W, Cooper Gt, Menick DR, Zile MR, Kuppuswamy D. Integrin activation and focal complex formation in cardiac hypertrophy. *J Biol Chem*. 2000;275:35624-35630

197. Kuppuswamy D, Kerr C, Narishige T, Kasi VS, Menick DR, Cooper Gt. Association of tyrosine-phosphorylated c-src with the cytoskeleton of hypertrophying myocardium. *J Biol Chem*. 1997;272:4500-4508

198. White DE, Coutu P, Shi YF, Tardif JC, Nattel S, St Arnaud R, Dedhar S, Muller WJ. Targeted ablation of ilk from the murine heart results in dilated cardiomyopathy and spontaneous heart failure. *Genes Dev*. 2006;20:2355-2360

199. Torsoni AS, Marin TM, Velloso LA, Franchini KG. Rhoa/rock signaling is critical to fak activation by cyclic stretch in cardiac myocytes. *Am J Physiol Heart Circ Physiol*. 2005;289:H1488-1496

200. Sussman MA, Welch S, Walker A, Klevitsky R, Hewett TE, Price RL, Schaefer E, Yager K. Altered focal adhesion regulation correlates with cardiomyopathy in mice expressing constitutively active rac1. *J Clin Invest*. 2000;105:875-886

201. Hoshijima M. Mechanical stress-strain sensors embedded in cardiac cytoskeleton: Z disk, titin, and associated structures. *Am J Physiol Heart Circ Physiol*. 2006;290:H1313-1325

202. Samarel AM. Costameres, focal adhesions, and cardiomyocyte mechanotransduction. *Am J Physiol Heart Circ Physiol*. 2005;289:H2291-2301

203. Danowski BA, Imanaka-Yoshida K, Sanger JM, Sanger JW. Costameres are sites of force transmission to the substratum in adult rat cardiomyocytes. *J Cell Biol*. 1992;118:1411-1420

204. Jockusch BM, Bubeck P, Giehl K, Kroemker M, Moschner J, Rothkegel M, Rudiger M, Schluter K, Stanke G, Winkler J. The molecular architecture of focal adhesions. *Annu Rev Cell Dev Biol*. 1995;11:379-416

205. Saoncella S, Echtermeyer F, Denhez F, Nowlen JK, Mosher DF, Robinson SD, Hynes RO, Goetinck PF. Syndecan-4 signals cooperatively with integrins in a rho-dependent manner in the assembly of focal adhesions and actin stress fibers. *Proc Natl Acad Sci U S A*. 1999;96:2805-2810

206. Finsen AV, Lunde IG, Sjaastad I, Ostli EK, Lyngra M, Jarstadmarken HO, Hasic A, Nygard S, Wilcox-Adelman SA, Goetinck PF, Lyberg T, Skrbic B, Florholmen G, Tonnessen T, Louch WE, Djurovic S, Carlson CR, Christensen G. Syndecan-4 is essential for development of concentric myocardial hypertrophy via stretch-induced activation of the calcineurin-nfat pathway. *PLoS One*. 2011;6:e28302

207. Klietsch R, Ervasti JM, Arnold W, Campbell KP, Jorgensen AO. Dystrophin-glycoprotein complex and laminin colocalize to the sarcolemma and transverse tubules of cardiac muscle. *Circ Res*. 1993;72:349-360

208. Camelliti P, Borg TK, Kohl P. Structural and functional characterisation of cardiac fibroblasts. *Cardiovasc Res*. 2005;65:40-51

209. Leitinger B. Molecular analysis of collagen binding by the human discoidin domain receptors, ddr1 and ddr2. Identification of collagen binding sites in ddr2. *J Biol Chem*. 2003;278:16761-16769

210. Xu H, Raynal N, Stathopoulos S, Myllyharju J, Farndale RW, Leitinger B. Collagen binding specificity of the discoidin domain receptors: Binding sites on collagens ii and iii and molecular determinants for collagen iv recognition by ddr1. *Matrix Biol*. 2011;30:16-26

211. Ichikawa O, Osawa M, Nishida N, Goshima N, Nomura N, Shimada I. Structural basis of the collagen-binding mode of discoidin domain receptor 2. *EMBO J*. 2007;26:4168-4176

212. Blissett AR, Garbellini D, Calomeni EP, Mihai C, Elton TS, Agarwal G. Regulation of collagen fibrillogenesis by cell-surface expression of kinase dead ddr2. *J Mol Biol*. 2009;385:902-911

213. Gross J, Lapiere CM. Collagenolytic activity in amphibian tissues: A tissue culture assay. *Proc Natl Acad Sci U S A*. 1962;48:1014-1022

214. Guo D, Kassiri Z, Basu R, Chow FL, Kandalam V, Damilano F, Liang W, Izumo S, Hirsch E, Penninger JM, Backx PH, Oudit GY. Loss of pi3kgamma enhances camp-dependent mmp remodeling of the myocardial n-cadherin adhesion complexes and extracellular matrix in response to early biomechanical stress. *Circ Res*. 2010;107:1275-1289

215. Nagase H, Itoh Y, Binner S. Interaction of alpha 2-macroglobulin with matrix metalloproteinases and its use for identification of their active forms. *Ann N Y Acad Sci*. 1994;732:294-302

216. Woessner JF, Jr. Matrix metalloproteinase inhibition. From the jurassic to the third millennium. *Ann N Y Acad Sci*. 1999;878:388-403

217. Oh J, Takahashi R, Kondo S, Mizoguchi A, Adachi E, Sasahara RM, Nishimura S, Imamura Y, Kitayama H, Alexander DB, Ide C, Horan TP, Arakawa T, Yoshida H, Nishikawa S, Itoh Y, Seiki M, Itohara S, Takahashi C, Noda M. The membrane-anchored mmp inhibitor reck is a key regulator of extracellular matrix integrity and angiogenesis. *Cell*. 2001;107:789-800

218. Bode W, Fernandez-Catalan C, Grams F, Gomis-Ruth FX, Nagase H, Tschesche H, Maskos K. Insights into mmp-timp interactions. *Ann N Y Acad Sci*. 1999;878:73-91

219. Bode W, Fernandez-Catalan C, Tschesche H, Grams F, Nagase H, Maskos K. Structural properties of matrix metalloproteinases. *Cell Mol Life Sci*. 1999;55:639-652

220. Bode W, Maskos K. Structural basis of the matrix metalloproteinases and their physiological inhibitors, the tissue inhibitors of metalloproteinases. *Biol Chem*. 2003;384:863-872

221. Douglas DA, Shi YE, Sang QA. Computational sequence analysis of the tissue inhibitor of metalloproteinase family. *J Protein Chem*. 1997;16:237-255

222. Schulz R. Intracellular targets of matrix metalloproteinase-2 in cardiac disease: Rationale and therapeutic approaches. *Annu Rev Pharmacol Toxicol*. 2007;47:211-242

223. Sung MM, Schulz CG, Wang W, Sawicki G, Bautista-Lopez NL, Schulz R. Matrix metalloproteinase-2 degrades the cytoskeletal protein alpha-actinin in peroxynitrite mediated myocardial injury. *J Mol Cell Cardiol*. 2007;43:429-436

224. Gao CQ, Sawicki G, Suarez-Pinzon WL, Csont T, Wozniak M, Ferdinandy P, Schulz R. Matrix metalloproteinase-2 mediates cytokine-induced myocardial contractile dysfunction. *Cardiovasc Res*. 2003;57:426-433

225. Sawicki G, Leon H, Sawicka J, Sariahmetoglu M, Schulze CJ, Scott PG, Szczesna-Cordary D, Schulz R. Degradation of myosin light chain in isolated rat hearts subjected to ischemia-reperfusion injury: A new intracellular target for matrix metalloproteinase-2. *Circulation*. 2005;112:544-552

226. Ali MA, Cho WJ, Hudson B, Kassiri Z, Granzier H, Schulz R. Titin is a target of matrix metalloproteinase-2: Implications in myocardial ischemia/reperfusion injury. *Circulation*. 2010;122:2039-2047

227. Rouet-Benzineb P, Buhler JM, Dreyfus P, Delcourt A, Dorent R, Perennec J, Crozatier B, Harf A, Lafuma C. Altered balance between matrix gelatinases (mmp-2 and mmp-9) and their tissue inhibitors in human dilated cardiomyopathy: Potential role of mmp-9 in myosin-heavy chain degradation. *Eur J Heart Fail*. 1999;1:337-352

228. Spinale FG. Myocardial matrix remodeling and the matrix metalloproteinases: Influence on cardiac form and function. *Physiol Rev*. 2007;87:1285-1342

229. Greenlee KJ, Werb Z, Kheradmand F. Matrix metalloproteinases in lung: Multiple, multifarious, and multifaceted. *Physiol Rev*. 2007;87:69-98

230. Ra HJ, Parks WC. Control of matrix metalloproteinase catalytic activity. *Matrix Biol*. 2007;26:587-596

231. Uria JA, Lopez-Otin C. Matrilysin-2, a new matrix metalloproteinase expressed in human tumors and showing the minimal domain organization required for secretion, latency, and activity. *Cancer Res*. 2000;60:4745-4751

232. de Coignac AB, Elson G, Delneste Y, Magistrelli G, Jeannin P, Aubry JP, Berthier O, Schmitt D, Bonnefoy JY, Gauchat JF. Cloning of mmp-26. A novel matrilysin-like proteinase. *Eur J Biochem*. 2000;267:3323-3329

233. Overall CM. Molecular determinants of metalloproteinase substrate specificity: Matrix metalloproteinase substrate binding domains, modules, and exosites. *Mol Biotechnol*. 2002;22:51-86

234. Janicki JS, Brower GL, Gardner JD, Forman MF, Stewart JA, Jr., Murray DB, Chancey AL. Cardiac mast cell regulation of matrix metalloproteinase-related ventricular remodeling in chronic pressure or volume overload. *Cardiovasc Res*. 2006;69:657-665

235. Li YY, McTiernan CF, Feldman AM. Interplay of matrix metalloproteinases, tissue inhibitors of metalloproteinases and their regulators in cardiac matrix remodeling. *Cardiovasc Res*. 2000;46:214-224

236. Wang Z, Juttermann R, Soloway PD. Timp-2 is required for efficient activation of prommp-2 in vivo. *J Biol Chem*. 2000;275:26411-26415

237. Knauper V, Will H, Lopez-Otin C, Smith B, Atkinson SJ, Stanton H, Hembry RM, Murphy G. Cellular mechanisms for human procollagenase-3 (mmp-13) activation. Evidence that mt1-mmp (mmp-14) and gelatinase a (mmp-2) are able to generate active enzyme. *J Biol Chem*. 1996;271:17124-17131

238. Murphy G, Cockett MI, Stephens PE, Smith BJ, Docherty AJ. Stromelysin is an activator of procollagenase. A study with natural and recombinant enzymes. *Biochem J*. 1987;248:265-268

239. Nagase H. Activation mechanisms of matrix metalloproteinases. *Biol Chem*. 1997;378:151-160

240. Visse R, Nagase H. Matrix metalloproteinases and tissue inhibitors of metalloproteinases: Structure, function, and biochemistry. *Circ Res*. 2003;92:827-839

241. Knauper V, Bailey L, Worley JR, Soloway P, Patterson ML, Murphy G. Cellular activation of prommp-13 by mt1-mmp depends on the c-terminal domain of mmp-13. *FEBS Lett*. 2002;532:127-130

242. Remacle AG, Rozanov DV, Fugere M, Day R, Strongin AY. Furin regulates the intracellular activation and the uptake rate of cell surface-associated mt1-mmp. *Oncogene*. 2006;25:5648-5655

243. Viappiani S, Nicolescu AC, Holt A, Sawicki G, Crawford BD, Leon H, van Mulligen T, Schulz R. Activation and modulation of 72kda matrix metalloproteinase-2 by peroxynitrite and glutathione. *Biochem Pharmacol*. 2009;77:826-834

244. Okamoto T, Akaike T, Sawa T, Miyamoto Y, van der Vliet A, Maeda H. Activation of matrix metalloproteinases by peroxynitrite-induced protein s-glutathiolation via disulfide s-oxide formation. *J Biol Chem*. 2001;276:29596-29602

245. Van Wart HE, Birkedal-Hansen H. The cysteine switch: A principle of regulation of metalloproteinase activity with potential applicability to the entire matrix metalloproteinase gene family. *Proc Natl Acad Sci U S A*. 1990;87:5578-5582

246. Lambert E, Dasse E, Haye B, Petitfrere E. Timps as multifacial proteins. *Crit Rev Oncol Hematol*. 2004;49:187-198

247. Bodden MK, Harber GJ, Birkedal-Hansen B, Windsor LJ, Caterina NC, Engler JA, Birkedal-Hansen H. Functional domains of human timp-1 (tissue inhibitor of metalloproteinases). *J Biol Chem*. 1994;269:18943-18952

248. Murphy G, Houbrechts A, Cockett MI, Williamson RA, O'Shea M, Docherty AJ. The n-terminal domain of tissue inhibitor of metalloproteinases retains metalloproteinase inhibitory activity. *Biochemistry*. 1991;30:8097-8102

249. Vanhoutte D, Heymans S. Timps and cardiac remodeling: 'Embracing the mmp-independent-side of the family'. *J Mol Cell Cardiol*. 2010;48:445-453

250. Williamson RA, Martorell G, Carr MD, Murphy G, Docherty AJ, Freedman RB, Feeney J. Solution structure of the active domain of tissue inhibitor of metalloproteinases-2. A new member of the ob fold protein family. *Biochemistry*. 1994;33:11745-11759

251. Schulze CJ, Wang W, Suarez-Pinzon WL, Sawicka J, Sawicki G, Schulz R. Imbalance between tissue inhibitor of metalloproteinase-4 and matrix metalloproteinases during acute myocardial [correction of myoctardial] ischemia-reperfusion injury. *Circulation*. 2003;107:2487-2492

252. Nuttall RK, Sampieri CL, Pennington CJ, Gill SE, Schultz GA, Edwards DR. Expression analysis of the entire mmp and timp gene families during mouse tissue development. *FEBS Lett*. 2004;563:129-134

253. Tian H, Huang ML, Liu KY, Jia ZB, Sun L, Jiang SL, Liu W, Kinkaid HY, Wu J, Li RK. Inhibiting matrix metalloproteinase by cell-based timp-

3 gene transfer effectively treats acute and chronic ischemic cardiomyopathy. *Cell Transplant*. 2011

254. Gomez DE, Alonso DF, Yoshiji H, Thorgeirsson UP. Tissue inhibitors of metalloproteinases: Structure, regulation and biological functions. *Eur J Cell Biol*. 1997;74:111-122

255. Zhu WH, Guo X, Villaschi S, Francesco Nicosia R. Regulation of vascular growth and regression by matrix metalloproteinases in the rat aorta model of angiogenesis. *Lab Invest*. 2000;80:545-555

256. Will H, Atkinson SJ, Butler GS, Smith B, Murphy G. The soluble catalytic domain of membrane type 1 matrix metalloproteinase cleaves the propeptide of progelatinase a and initiates autoproteolytic activation. Regulation by timp-2 and timp-3. *J Biol Chem*. 1996;271:17119-17123

257. Lee MH, Rapti M, Murphy G. Unveiling the surface epitopes that render tissue inhibitor of metalloproteinase-1 inactive against membrane type 1-matrix metalloproteinase. *J Biol Chem*. 2003;278:40224-40230

258. Peterson JT, Li H, Dillon L, Bryant JW. Evolution of matrix metalloprotease and tissue inhibitor expression during heart failure progression in the infarcted rat. *Cardiovasc Res*. 2000;46:307-315

259. Lindsey ML. Mmp induction and inhibition in myocardial infarction. *Heart Fail Rev*. 2004;9:7-19

260. Nagatomo Y, Carabello BA, Coker ML, McDermott PJ, Nemoto S, Hamawaki M, Spinale FG. Differential effects of pressure or volume overload on myocardial mmp levels and inhibitory control. *Am J Physiol Heart Circ Physiol*. 2000;278:H151-161

261. Iwanaga Y, Aoyama T, Kihara Y, Onozawa Y, Yoneda T, Sasayama S. Excessive activation of matrix metalloproteinases coincides with left ventricular remodeling during transition from hypertrophy to heart failure in hypertensive rats. *J Am Coll Cardiol*. 2002;39:1384-1391

262. Sakata Y, Yamamoto K, Mano T, Nishikawa N, Yoshida J, Hori M, Miwa T, Masuyama T. Activation of matrix metalloproteinases precedes left ventricular remodeling in hypertensive heart failure rats: Its inhibition as a primary effect of angiotensin-converting enzyme inhibitor. *Circulation*. 2004;109:2143-2149

263. Matsumura S, Iwanaga S, Mochizuki S, Okamoto H, Ogawa S, Okada Y. Targeted deletion or pharmacological inhibition of mmp-2 prevents cardiac rupture after myocardial infarction in mice. *J Clin Invest*. 2005;115:599-609

264. Hayashidani S, Tsutsui H, Ikeuchi M, Shiomi T, Matsusaka H, Kubota T, Imanaka-Yoshida K, Itoh T, Takeshita A. Targeted deletion of mmp-2 attenuates early lv rupture and late remodeling after experimental myocardial infarction. *Am J Physiol Heart Circ Physiol*. 2003;285:H1229-1235

265. Ducharme A, Frantz S, Aikawa M, Rabkin E, Lindsey M, Rohde LE, Schoen FJ, Kelly RA, Werb Z, Libby P, Lee RT. Targeted deletion of matrix metalloproteinase-9 attenuates left ventricular enlargement and collagen accumulation after experimental myocardial infarction. *J Clin Invest*. 2000;106:55-62

266. Heymans S, Luttun A, Nuyens D, Theilmeier G, Creemers E, Moons L, Dyspersin GD, Cleutjens JP, Shipley M, Angellilo A, Levi M, Nube O, Baker A, Keshet E, Lupu F, Herbert JM, Smits JF, Shapiro SD, Baes M, Borgers M, Collen D, Daemen MJ, Carmeliet P. Inhibition of plasminogen activators or matrix metalloproteinases prevents cardiac rupture but impairs therapeutic angiogenesis and causes cardiac failure. *Nat Med*. 1999;5:1135-1142

267. Matsusaka H, Ide T, Matsushima S, Ikeuchi M, Kubota T, Sunagawa K, Kinugawa S, Tsutsui H. Targeted deletion of matrix metalloproteinase 2 ameliorates myocardial remodeling in mice with chronic pressure overload. *Hypertension*. 2006;47:711-717

268. Heymans S, Lupu F, Terclavers S, Vanwetswinkel B, Herbert JM, Baker A, Collen D, Carmeliet P, Moons L. Loss or inhibition of upa or mmp-9 attenuates lv remodeling and dysfunction after acute pressure overload in mice. *Am J Pathol*. 2005;166:15-25

269. Spinale FG, Mukherjee R, Zavadzkas JA, Koval CN, Bouges S, Stroud RE, Dobrucki LW, Sinusas AJ. Cardiac restricted overexpression of membrane type-1 matrix metalloproteinase causes adverse myocardial remodeling following myocardial infarction. *J Biol Chem*. 2010;285:30316-30327

270. Roten L, Nemoto S, Simsic J, Coker ML, Rao V, Baicu S, Defreyte G, Soloway PJ, Zile MR, Spinale FG. Effects of gene deletion of the tissue

inhibitor of the matrix metalloproteinase-type 1 (timp-1) on left ventricular geometry and function in mice. *J Mol Cell Cardiol*. 2000;32:109-120

271. Creemers EE, Davis JN, Parkhurst AM, Leenders P, Dowdy KB, Hapke E, Hauet AM, Escobar PG, Cleutjens JP, Smits JF, Daemen MJ, Zile MR, Spinale FG. Deficiency of timp-1 exacerbates lv remodeling after myocardial infarction in mice. *Am J Physiol Heart Circ Physiol*. 2003;284:H364-371

272. Ikonomidis JS, Hendrick JW, Parkhurst AM, Herron AR, Escobar PG, Dowdy KB, Stroud RE, Hapke E, Zile MR, Spinale FG. Accelerated lv remodeling after myocardial infarction in timp-1-deficient mice: Effects of exogenous mmp inhibition. *Am J Physiol Heart Circ Physiol*. 2005;288:H149-158

273. Jayasankar V, Woo YJ, Bish LT, Pirolli TJ, Berry MF, Burdick J, Bhalla RC, Sharma RV, Gardner TJ, Sweeney HL. Inhibition of matrix metalloproteinase activity by timp-1 gene transfer effectively treats ischemic cardiomyopathy. *Circulation*. 2004;110:II180-186

274. Kandalam V, Basu R, Abraham T, Wang X, Soloway PD, Jaworski DM, Oudit GY, Kassiri Z. Timp2 deficiency accelerates adverse post-myocardial infarction remodeling because of enhanced mt1-mmp activity despite lack of mmp2 activation. *Circ Res*. 2010;106:796-808

275. Kandalam V, Basu R, Moore L, Fan D, Wang X, Jaworski DM, Oudit GY, Kassiri Z. Lack of tissue inhibitor of metalloproteinases 2 leads to exacerbated left ventricular dysfunction and adverse extracellular matrix remodeling in response to biomechanical stress. *Circulation*. 2011;124:2094-2105

276. Ramani R, Nilles K, Gibson G, Burkhead B, Mathier M, McNamara D, McTiernan CF. Tissue inhibitor of metalloproteinase-2 gene delivery ameliorates postinfarction cardiac remodeling. *Clin Transl Sci*. 2011;4:24-31

277. Fedak PW, Smookler DS, Kassiri Z, Ohno N, Leco KJ, Verma S, Mickle DA, Watson KL, Hojilla CV, Cruz W, Weisel RD, Li RK, Khokha R. Timp-3 deficiency leads to dilated cardiomyopathy. *Circulation*. 2004;110:2401-2409

278. Kassiri Z, Oudit GY, Sanchez O, Dawood F, Mohammed FF, Nuttall RK, Edwards DR, Liu PP, Backx PH, Khokha R. Combination of tumor necrosis factor-alpha ablation and matrix metalloproteinase inhibition

prevents heart failure after pressure overload in tissue inhibitor of metalloproteinase-3 knock-out mice. *Circ Res*. 2005;97:380-390

279. Tian H, Cimini M, Fedak PW, Altamentova S, Fazel S, Huang ML, Weisel RD, Li RK. Timp-3 deficiency accelerates cardiac remodeling after myocardial infarction. *J Mol Cell Cardiol*. 2007;43:733-743

280. Cox MJ, Hawkins UA, Hoit BD, Tyagi SC. Attenuation of oxidative stress and remodeling by cardiac inhibitor of metalloproteinase protein transfer. *Circulation*. 2004;109:2123-2128

281. Melendez-Zajgla J, Del Pozo L, Ceballos G, Maldonado V. Tissue inhibitor of metalloproteinases-4. The road less traveled. *Mol Cancer*. 2008;7:85

282. Koskivirta I, Kassiri Z, Rahkonen O, Kiviranta R, Oudit GY, McKee TD, Kyto V, Saraste A, Jokinen E, Liu PP, Vuorio E, Khokha R. Mice with tissue inhibitor of metalloproteinases 4 (timp4) deletion succumb to induced myocardial infarction but not to cardiac pressure overload. *J Biol Chem*. 2010;285:24487-24493

283. Zucker S, Cao J, Chen WT. Critical appraisal of the use of matrix metalloproteinase inhibitors in cancer treatment. *Oncogene*. 2000;19:6642-6650

284. Coussens LM, Fingleton B, Matrisian LM. Matrix metalloproteinase inhibitors and cancer: Trials and tribulations. *Science*. 2002;295:2387-2392

285. Hidalgo M, Eckhardt SG. Development of matrix metalloproteinase inhibitors in cancer therapy. *J Natl Cancer Inst*. 2001;93:178-193

286. Vincenti MP, Clark IM, Brinckerhoff CE. Using inhibitors of metalloproteinases to treat arthritis. Easier said than done? *Arthritis Rheum*. 1994;37:1115-1126

287. Burrage PS, Mix KS, Brinckerhoff CE. Matrix metalloproteinases: Role in arthritis. *Front Biosci*. 2006;11:529-543

288. Peterson JT. Matrix metalloproteinase inhibitor development and the remodeling of drug discovery. *Heart Fail Rev*. 2004;9:63-79

289. Creemers EE, Cleutjens JP, Smits JF, Daemen MJ. Matrix metalloproteinase inhibition after myocardial infarction: A new approach to prevent heart failure? *Circ Res*. 2001;89:201-210

290. Lee RT. Matrix metalloproteinase inhibition and the prevention of heart failure. *Trends Cardiovasc Med*. 2001;11:202-205

291. Jacobsen JA, Major Jourden JL, Miller MT, Cohen SM. To bind zinc or not to bind zinc: An examination of innovative approaches to improved metalloproteinase inhibition. *Biochim Biophys Acta*. 2010;1803:72-94

292. Golub LM. Introduction and background. *Pharmacol Res*. 2011;63:99-101

293. Yarbrough WM, Mukherjee R, Brinsa TA, Dowdy KB, Scott AA, Escobar GP, Joffs C, Lucas DG, Crawford FA, Jr., Spinale FG. Matrix metalloproteinase inhibition modifies left ventricular remodeling after myocardial infarction in pigs. *J Thorac Cardiovasc Surg*. 2003;125:602-610

294. Kaludercic N, Lindsey ML, Tavazzi B, Lazzarino G, Paolocci N. Inhibiting metalloproteases with pd 166793 in heart failure: Impact on cardiac remodeling and beyond. *Cardiovasc Ther*. 2008;26:24-37

295. Apple KA, Yarbrough WM, Mukherjee R, Deschamps AM, Escobar PG, Mingoia JT, Sample JA, Hendrick JW, Dowdy KB, McLean JE, Stroud RE, O'Neill TP, Spinale FG. Selective targeting of matrix metalloproteinase inhibition in post-infarction myocardial remodeling. *J Cardiovasc Pharmacol*. 2006;47:228-235

296. Yarbrough WM, Mukherjee R, Escobar GP, Mingoia JT, Sample JA, Hendrick JW, Dowdy KB, McLean JE, Lowry AS, O'Neill TP, Spinale FG. Selective targeting and timing of matrix metalloproteinase inhibition in post-myocardial infarction remodeling. *Circulation*. 2003;108:1753-1759

297. Villarreal FJ, Griffin M, Omens J, Dillmann W, Nguyen J, Covell J. Early short-term treatment with doxycycline modulates postinfarction left ventricular remodeling. *Circulation*. 2003;108:1487-1492

298. Garcia RA, Go KV, Villarreal FJ. Effects of timed administration of doxycycline or methylprednisolone on post-myocardial infarction inflammation and left ventricular remodeling in the rat heart. *Mol Cell Biochem*. 2007;300:159-169

299. Tessone A, Feinberg MS, Barbash IM, Reich R, Holbova R, Richmann M, Mardor Y, Leor J. Effect of matrix metalloproteinase inhibition by doxycycline on myocardial healing and remodeling after myocardial infarction. *Cardiovasc Drugs Ther*. 2005;19:383-390

300. Takai S, Jin D, Inagaki S, Yamamoto D, Tanaka K, Miyazaki M. Significance of matrix metalloproteinase-9 in cardiac dysfunction during the very acute phase after myocardial infarction in hamsters. *Eur J Pharmacol*. 2007;572:57-60

301. Hudson MP, Armstrong PW, Ruzyllo W, Brum J, Cusmano L, Krzeski P, Lyon R, Quinones M, Theroux P, Sydlowski D, Kim HE, Garcia MJ, Jaber WA, Weaver WD. Effects of selective matrix metalloproteinase inhibitor (pg-116800) to prevent ventricular remodeling after myocardial infarction: Results of the premier (prevention of myocardial infarction early remodeling) trial. *J Am Coll Cardiol*. 2006;48:15-20

302. Stetler-Stevenson WG, Krutzsch HC, Liotta LA. Tissue inhibitor of metalloproteinase (timp-2). A new member of the metalloproteinase inhibitor family. *J Biol Chem*. 1989;264:17374-17378

303. Stetler-Stevenson WG, Brown PD, Onisto M, Levy AT, Liotta LA. Tissue inhibitor of metalloproteinases-2 (timp-2) mrna expression in tumor cell lines and human tumor tissues. *J Biol Chem*. 1990;265:13933-13938

304. De Clerck Y, Szpirer C, Aly MS, Cassiman JJ, Eeckhout Y, Rousseau G. The gene for tissue inhibitor of metalloproteinases-2 is localized on human chromosome arm 17q25. *Genomics*. 1992;14:782-784

305. Stetler-Stevenson WG, Liotta LA, Seldin MF. Linkage analysis demonstrates that the timp-2 locus is on mouse chromosome 11. *Genomics*. 1992;14:828-829

306. Itoh Y, Ito A, Iwata K, Tanzawa K, Mori Y, Nagase H. Plasma membrane-bound tissue inhibitor of metalloproteinases (timp)-2 specifically inhibits matrix metalloproteinase 2 (gelatinase a) activated on the cell surface. *J Biol Chem*. 1998;273:24360-24367

307. Bernardo MM, Fridman R. Timp-2 (tissue inhibitor of metalloproteinase-2) regulates mmp-2 (matrix metalloproteinase-2) activity in the extracellular environment after pro-mmp-2 activation by mt1 (membrane type 1)-mmp. *Biochem J*. 2003;374:739-745

308. Zucker S, Drews M, Conner C, Foda HD, DeClerck YA, Langley KE, Bahou WF, Docherty AJ, Cao J. Tissue inhibitor of metalloproteinase-2 (timp-2) binds to the catalytic domain of the cell surface receptor, membrane type 1-matrix metalloproteinase 1 (mt1-mmp). *J Biol Chem*. 1998;273:1216-1222

309. Goldberg GI, Marmer BL, Grant GA, Eisen AZ, Wilhelm S, He CS. Human 72-kilodalton type iv collagenase forms a complex with a tissue inhibitor of metalloproteases designated timp-2. *Proc Natl Acad Sci U S A*. 1989;86:8207-8211

310. Morgunova E, Tuuttila A, Bergmann U, Tryggvason K. Structural insight into the complex formation of latent matrix metalloproteinase 2 with tissue inhibitor of metalloproteinase 2. *Proc Natl Acad Sci U S A*. 2002;99:7414-7419

311. Caterina JJ, Yamada S, Caterina NC, Longenecker G, Holmback K, Shi J, Yermovsky AE, Engler JA, Birkedal-Hansen H. Inactivating mutation of the mouse tissue inhibitor of metalloproteinases-2(timp-2) gene alters prommp-2 activation. *J Biol Chem*. 2000;275:26416-26422

312. Strongin AY, Collier I, Bannikov G, Marmer BL, Grant GA, Goldberg GI. Mechanism of cell surface activation of 72-kda type iv collagenase. Isolation of the activated form of the membrane metalloprotease. *J Biol Chem*. 1995;270:5331-5338

313. English JL, Kassiri Z, Koskivirta I, Atkinson SJ, Di Grappa M, Soloway PD, Nagase H, Vuorio E, Murphy G, Khokha R. Individual timp deficiencies differentially impact pro-mmp-2 activation. *J Biol Chem*. 2006;281:10337-10346

314. Lluri G, Langlois GD, McClellan B, Soloway PD, Jaworski DM. Tissue inhibitor of metalloproteinase-2 (timp-2) regulates neuromuscular junction development via a beta1 integrin-mediated mechanism. *J Neurobiol*. 2006;66:1365-1377

315. Burbridge MF, Coge F, Galizzi JP, Boutin JA, West DC, Tucker GC. The role of the matrix metalloproteinases during in vitro vessel formation. *Angiogenesis*. 2002;5:215-226

316. Seandel M, Noack-Kunnmann K, Zhu D, Aimes RT, Quigley JP. Growth factor-induced angiogenesis in vivo requires specific cleavage of fibrillar type i collagen. *Blood*. 2001;97:2323-2332

317. Seo DW, Li H, Guedez L, Wingfield PT, Diaz T, Salloum R, Wei BY, Stetler-Stevenson WG. Timp-2 mediated inhibition of angiogenesis: An mmp-independent mechanism. *Cell*. 2003;114:171-180

318. Stetler-Stevenson WG, Seo DW. Timp-2: An endogenous inhibitor of angiogenesis. *Trends Mol Med*. 2005;11:97-103

319. Fernandez CA, Butterfield C, Jackson G, Moses MA. Structural and functional uncoupling of the enzymatic and angiogenic inhibitory activities of tissue inhibitor of metalloproteinase-2 (timp-2): Loop 6 is a novel angiogenesis inhibitor. *J Biol Chem*. 2003;278:40989-40995

320. Hajitou A, Sounni NE, Devy L, Grignet-Debrus C, Lewalle JM, Li H, Deroanne CF, Lu H, Colige A, Nusgens BV, Frankenne F, Maron A, Yeh P, Perricaudet M, Chang Y, Soria C, Calberg-Bacq CM, Foidart JM, Noel A. Down-regulation of vascular endothelial growth factor by tissue inhibitor of metalloproteinase-2: Effect on in vivo mammary tumor growth and angiogenesis. *Cancer Res*. 2001;61:3450-3457

321. Lovelock JD, Baker AH, Gao F, Dong JF, Bergeron AL, McPheat W, Sivasubramanian N, Mann DL. Heterogeneous effects of tissue inhibitors of matrix metalloproteinases on cardiac fibroblasts. *Am J Physiol Heart Circ Physiol*. 2005;288:H461-468

322. Fielitz J, Leuschner M, Zurbrugg HR, Hannack B, Pregla R, Hetzer R, Regitz-Zagrosek V. Regulation of matrix metalloproteinases and their inhibitors in the left ventricular myocardium of patients with aortic stenosis. *J Mol Med*. 2004;82:809-820

323. Heymans S, Schroen B, Vermeersch P, Milting H, Gao F, Kassner A, Gillijns H, Herijgers P, Flameng W, Carmeliet P, Van de Werf F, Pinto YM, Janssens S. Increased cardiac expression of tissue inhibitor of metalloproteinase-1 and tissue inhibitor of metalloproteinase-2 is related to cardiac fibrosis and dysfunction in the chronic pressure-overloaded human heart. *Circulation*. 2005;112:1136-1144

324. Polyakova V, Hein S, Kostin S, Ziegelhoeffer T, Schaper J. Matrix metalloproteinases and their tissue inhibitors in pressure-overloaded human myocardium during heart failure progression. *J Am Coll Cardiol*. 2004;44:1609-1618

325. Tozzi R, Palladini G, Fallarini S, Nano R, Gatti C, Presotto C, Schiavone A, Micheletti R, Ferrari P, Fogari R, Perlini S. Matrix metalloprotease activity is enhanced in the compensated but not in the decompensated

phase of pressure overload hypertrophy. *Am J Hypertens*. 2007;20:663-669

326. Li YY, Feldman AM, Sun Y, McTiernan CF. Differential expression of tissue inhibitors of metalloproteinases in the failing human heart. *Circulation*. 1998;98:1728-1734

327. Kelly D, Squire IB, Khan SQ, Dhillon O, Narayan H, Ng KH, Quinn P, Davies JE, Ng LL. Usefulness of plasma tissue inhibitors of metalloproteinases as markers of prognosis after acute myocardial infarction. *Am J Cardiol*. 2010;106:477-482

328. Polyakova V, Miyagawa S, Szalay Z, Risteli J, Kostin S. Atrial extracellular matrix remodelling in patients with atrial fibrillation. *J Cell Mol Med*. 2008;12:189-208

329. Staskus PW, Masiarz FR, Pallanck LJ, Hawkes SP. The 21-kda protein is a transformation-sensitive metalloproteinase inhibitor of chicken fibroblasts. *J Biol Chem*. 1991;266:449-454

330. Pavloff N, Staskus PW, Kishnani NS, Hawkes SP. A new inhibitor of metalloproteinases from chicken: Chimp-3. A third member of the timp family. *J Biol Chem*. 1992;267:17321-17326

331. Apte SS, Olsen BR, Murphy G. The gene structure of tissue inhibitor of metalloproteinases (timp)-3 and its inhibitory activities define the distinct timp gene family. *J Biol Chem*. 1995;270:14313-14318

332. Apte SS, Mattei MG, Olsen BR. Cloning of the cdna encoding human tissue inhibitor of metalloproteinases-3 (timp-3) and mapping of the timp3 gene to chromosome 22. *Genomics*. 1994;19:86-90

333. Apte SS, Hayashi K, Seldin MF, Mattei MG, Hayashi M, Olsen BR. Gene encoding a novel murine tissue inhibitor of metalloproteinases (timp), timp-3, is expressed in developing mouse epithelia, cartilage, and muscle, and is located on mouse chromosome 10. *Dev Dyn*. 1994;200:177-197

334. Lee MH, Atkinson S, Murphy G. Identification of the extracellular matrix (ecm) binding motifs of tissue inhibitor of metalloproteinases (timp)-3 and effective transfer to timp-1. *J Biol Chem*. 2007;282:6887-6898

335. Yu WH, Yu S, Meng Q, Brew K, Woessner JF, Jr. Timp-3 binds to sulfated glycosaminoglycans of the extracellular matrix. *J Biol Chem*. 2000;275:31226-31232

336. Mann DL, Spinale FG. Activation of matrix metalloproteinases in the failing human heart: Breaking the tie that binds. *Circulation*. 1998;98:1699-1702

337. O'Connell JP, Willenbrock F, Docherty AJ, Eaton D, Murphy G. Analysis of the role of the cooh-terminal domain in the activation, proteolytic activity, and tissue inhibitor of metalloproteinase interactions of gelatinase b. *J Biol Chem*. 1994;269:14967-14973

338. Butler GS, Apte SS, Willenbrock F, Murphy G. Human tissue inhibitor of metalloproteinases 3 interacts with both the n- and c-terminal domains of gelatinases a and b. Regulation by polyanions. *J Biol Chem*. 1999;274:10846-10851

339. Nagase H, Visse R, Murphy G. Structure and function of matrix metalloproteinases and timps. *Cardiovasc Res*. 2006;69:562-573

340. Black RA, Rauch CT, Kozlosky CJ, Peschon JJ, Slack JL, Wolfson MF, Castner BJ, Stocking KL, Reddy P, Srinivasan S, Nelson N, Boiani N, Schooley KA, Gerhart M, Davis R, Fitzner JN, Johnson RS, Paxton RJ, March CJ, Cerretti DP. A metalloproteinase disintegrin that releases tumour-necrosis factor-alpha from cells. *Nature*. 1997;385:729-733

341. Amour A, Slocombe PM, Webster A, Butler M, Knight CG, Smith BJ, Stephens PE, Shelley C, Hutton M, Knauper V, Docherty AJ, Murphy G. Tnf-alpha converting enzyme (tace) is inhibited by timp-3. *FEBS Lett*. 1998;435:39-44

342. Lee MH, Rapti M, Murphy G. Delineating the molecular basis of the inactivity of tissue inhibitor of metalloproteinase-2 against tumor necrosis factor-alpha-converting enzyme. *J Biol Chem*. 2004;279:45121-45129

343. Satoh M, Nakamura M, Saitoh H, Satoh H, Maesawa C, Segawa I, Tashiro A, Hiramori K. Tumor necrosis factor-alpha-converting enzyme and tumor necrosis factor-alpha in human dilated cardiomyopathy. *Circulation*. 1999;99:3260-3265

344. Amour A, Knight CG, Webster A, Slocombe PM, Stephens PE, Knauper V, Docherty AJ, Murphy G. The in vitro activity of adam-10 is inhibited by timp-1 and timp-3. *FEBS Lett*. 2000;473:275-279

345. Loechel F, Fox JW, Murphy G, Albrechtsen R, Wewer UM. Adam 12-s cleaves igfbp-3 and igfbp-5 and is inhibited by timp-3. *Biochem Biophys Res Commun*. 2000;278:511-515

346. Haas TL, Milkiewicz M, Davis SJ, Zhou AL, Egginton S, Brown MD, Madri JA, Hudlicka O. Matrix metalloproteinase activity is required for activity-induced angiogenesis in rat skeletal muscle. *Am J Physiol Heart Circ Physiol*. 2000;279:H1540-1547

347. Rundhaug JE. Matrix metalloproteinases and angiogenesis. *J Cell Mol Med*. 2005;9:267-285

348. Qi JH, Ebrahem Q, Moore N, Murphy G, Claesson-Welsh L, Bond M, Baker A, Anand-Apte B. A novel function for tissue inhibitor of metalloproteinases-3 (timp3): Inhibition of angiogenesis by blockage of vegf binding to vegf receptor-2. *Nat Med*. 2003;9:407-415

349. Anand-Apte B, Pepper MS, Voest E, Montesano R, Olsen B, Murphy G, Apte SS, Zetter B. Inhibition of angiogenesis by tissue inhibitor of metalloproteinase-3. *Invest Ophthalmol Vis Sci*. 1997;38:817-823

350. Baker AH, Zaltsman AB, George SJ, Newby AC. Divergent effects of tissue inhibitor of metalloproteinase-1, -2, or -3 overexpression on rat vascular smooth muscle cell invasion, proliferation, and death in vitro. Timp-3 promotes apoptosis. *J Clin Invest*. 1998;101:1478-1487

351. Bond M, Murphy G, Bennett MR, Amour A, Knauper V, Newby AC, Baker AH. Localization of the death domain of tissue inhibitor of metalloproteinase-3 to the n terminus. Metalloproteinase inhibition is associated with proapoptotic activity. *J Biol Chem*. 2000;275:41358-41363

352. Smith MR, Kung H, Durum SK, Colburn NH, Sun Y. Timp-3 induces cell death by stabilizing tnf-alpha receptors on the surface of human colon carcinoma cells. *Cytokine*. 1997;9:770-780

353. Fata JE, Leco KJ, Voura EB, Yu HY, Waterhouse P, Murphy G, Moorehead RA, Khokha R. Accelerated apoptosis in the timp-3-deficient mammary gland. *J Clin Invest*. 2001;108:831-841

354. Fedak PW, Moravec CS, McCarthy PM, Altamentova SM, Wong AP, Skrtic M, Verma S, Weisel RD, Li RK. Altered expression of disintegrin metalloproteinases and their inhibitor in human dilated cardiomyopathy. *Circulation*. 2006;113:238-245

355. Fedak PW, Altamentova SM, Weisel RD, Nili N, Ohno N, Verma S, Lee TY, Kiani C, Mickle DA, Strauss BH, Li RK. Matrix remodeling in experimental and human heart failure: A possible regulatory role for timp-3. *Am J Physiol Heart Circ Physiol*. 2003;284:H626-634

CHAPTER 2

MATERIALS AND METHODS

2.1. Animal care

WT, TIMP2-deficient ($TIMP2^{-/-}$)[1] and TIMP3-deficient ($TIMP3^{-/-}$)[2] mice are in C57BL/6 background (The Jackson Laboratory; Bar Harbor, MN, USA) and were housed in our animal facility at University of Alberta. WT and either $TIMP2^{-/-}$ or $TIMP3^{-/-}$ mice were bred to generate WT, knockout, and heterozygous age-matched littermates. Mice were weaned at 3 weeks of age. All animal experiments were carried out in accordance with Canadian Council on Animal Care Guidelines and regulations of Animal Policy and Welfare committee at University of Alberta (under the Animal Use Protocol numbers 555, 572, 609), as well as the Guide for the Care and Use of Laboratory Animals published by the US National Institute of Health.

2.2. Experimental animal disease models

2.2.1. MI: left anterior descending coronary artery ligation

Male 11-12 weeks old WT and $TIMP2^{-/-}$ mice were subjected to MI induced by ligation of the left anterior descending artery (LAD)[3]. Mice anesthetized with 1% isoflurane with 100% oxygen and intubated underwent left thoracotamy in the fifth intercostal space. The pericardium was opened to expose the left ventricle of the heart, and then the LAD was encircled and ligated under the tip of the left atrial appendage (Figure 2.1.A) using a 7-0 silk suture. Once the LAD ligation was complete, the muscle and skin was closed in layers with the use of a 6-0 silk suture and the mice were allowed to recover on a warming pad until they were fully awake. The sham-operated mice from each genotype underwent the exact same procedure but their LAD was not ligated. Sham-operated mice were used as baseline controls.

2.2.2. *In vivo* pressure overload by TAC

Eight-week old male WT and TIMP2$^{-/-}$ mice underwent transverse aortic constriction (TAC) to generate pressure overload[4]. The mice were anesthetized with 1% isoflurane using 100% oxygen. A horizontal skin incision of 1 cm was made at the level of second intercostal space. A 6-0 silk suture was passed under the aortic arch. A bent 27-gauge needle was then placed next to the aortic arch and the suture was snugly tied around the needle and the aorta, between the brachiocephalic trunk (first branch) and the left carotid artery (second branch) (Figure 2.1.B). The needle was quickly removed allowing the suture to constrict the aorta to a fixed diameter. The incision was closed in layers and the mice were allowed to recover on a warming pad until they were fully awake. Mice received buprenorphine for the first 24 hours. The sham-operated animals underwent the same procedure without the constriction of aorta.

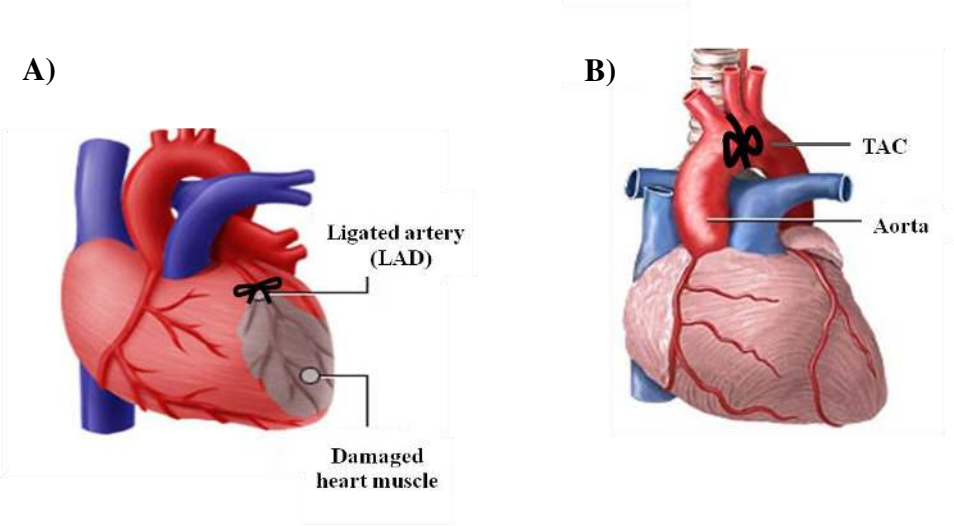

Figure 2.1. Experimental animal disease models.

A) Experimental myocardial infarction model, the left anterior descending (LAD) coronary artery is ligated, thereby occluding the artery and preventing blood flow to the target myocardium. B) Transverse aortic constriction (TAC) generates pressure overload on the heart by constricting the aorta which increases resistance against which the heart is required to work against.

2.3. Pharmacological MMP inhibitor (MMPi) administration in vivo

A broad-spectrum MMP inhibitor, PD-166793 (Pfizer Inc.), with the chemical name (S)-2-(4'-bromo-biphenyl-4-sulfonylamino)-3-methyl-butyric acid, was prepared by suspending in a 0.5% methylcellulose vehicle solution[5], as it has been found to be soluble predominantly in DMSO or ethanol[6]. TIMP3$^{-/-}$-sham and MI mice received PD-166793 (30 mg·kg^{-1}·day^{-1}) by daily gavage that began 2 days before MI and was continued for 2 days post-MI. For TAC studies, TIMP2$^{-/-}$ mice received PD166793 (30 mg·kg^{-1}·day^{-1}) by daily gavage one day before TAC surgery and through the course of the study. PD166793 is a broad-spectrum MMP inhibitor, yet is selective as it is not known to inhibit other families of enzymes[6].

2.4. Tissue collection

2.4.1. Mortality and autopsy

Autopsy was performed on each mouse found dead throughout the course of the study. Survival was recorded as the total number of live animals from each genotype remaining each day after surgery, and plotted as a percentage of the total number of animals included in the study. In the MI model, cardiac rupture was confirmed by the presence of blood clot in the pericardium or in the chest cavity, and rupture-induced mortality was specially recorded.

2.4.2. Tissue collection

2.4.2.1. MI mice

At 1 day, 3 days, 1 week, or 4 weeks post-MI, surviving mice were anesthetized and the hearts were quickly excised, the atria and right ventricle were removed and discarded, the LV was dissected into infarct, peri-infarct, and non-infarct regions, and then flash-frozen separately in liquid nitrogen and stored at -80°C for further protein and RNA analyses. In order to dissect the LV into the

three regions, after removal of the right ventricle and the atria, LV was opened by cutting longitudinally from the base to the apex along the septal wall. The LV was laid flat and the infarct region at the apex was identified as whiter in color due to infarction. The infarct region was visible at 1 day post-MI and more evident at later time points. This region was dissected first as a strip of tissue. Immediately following this, the peri-infarct region which we defined and consistently targeted as the 1-2mm region adjacent to the infarct region, was dissected and temporarily stored by flash-freezing, followed by storage of the previously isolated infarct region. Lastly, the remaining tissue was stored as the non-infarct tissue.

For histology and immunohistochemical analyses, whole hearts were arrested in diastole with 1 M KCl and then fixed in 10% neutral buffered formalin. The purpose of this method is to arrest the heart in diastole in order to maintain the end-diastolic maximum dimensions of the ventricle for qualitative histological assessment of ventricle dilation and other chamber and ventricular wall properties. The hearts were fixed in 10% formalin for a minimum of 48 hours. Using a sharp blade, the hearts were cut along a longitudinal axis and paraffin-embedded, and processed for histological analyses.

Additionally, lung tissue was collected and wet and dry weights were recorded. After recording the wet weight, the lungs were allowed to dry for 48 hours at room temperature, after which lung dry weight was recorded. Lung water content was calculated as the difference between wet and dry lung weights. A greater difference between lung wet weight and dry weight meant a larger amount of water accumulation, indicating pulmonary edema. For each mouse, we recorded the identification number, the genotype, time-point post-surgery of tissue collection, body weight, wet and dry lung weight, and tibial length (Table 2.1.)

2.4.2.2. TAC mice

At 2 weeks or 5 weeks post-TAC, sham and TAC mice from either genotype were sub-lethally anesthetized, the heart tissue was excised and either

flash-frozen in liquid nitrogen and stored in -80°C or formalin-fixed until use for molecular and histological experiments respectively. The LV was isolated, weighed and frozen for molecular experiments. For histology, the LV was cut in half using a blade along the transverse plane through the mid-ventricle region for a cross-sectional view of the LV. The data recorded from these animals included body weight, heart weight, LV weight, lung weights, and the length of the tibia bone in the leg as a measure of body size which was used to normalize the heart and LV weights.

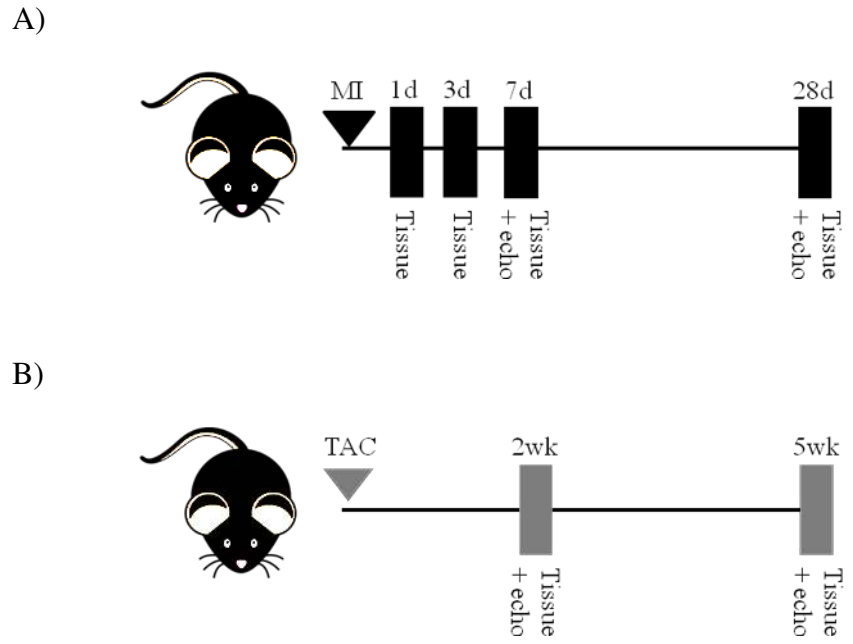

Figure 2.2. Tissue collection and imaging timeline.

A, Tissue was collected at 1, 3, 7, and 28 days post-MI, with *in vivo* imaging conducted at 7 and 28 days. B, At 2 and 5 weeks post-TAC, imaging was completed and was followed by tissue collection.

Table 2.1. Mouse data collection form

Date	Genotype	Time point	BW	HW	LVW	TL	Lung Wwt.	Lung Dwt.	Notes

BW= Body weight; HW= Heart weight; LVW= Left ventricle weight; TL Tibial length; Lung Wwt= Lung wet weight; Lung Dwt= Lung dry weight

2.5. *In vivo* cardiac structure and function assessment

2.5.1. Echocardiography imaging

In vivo systolic and diastolic cardiac functions were measured by noninvasive transthoracic echocardiography at 1 week and 4 weeks post-MI, or at 2 weeks and 5 weeks post-TAC, using a Vevo 770 high-resolution imaging system equipped with a 30-MHz transducer (RMV- 707B; VisualSonics, Toronto, ON, Canada) as previously described[7] and conducted[8, 9]. Mice were placed on a heating pad and a nose cone with 0.75-1% isoflurane in 100% oxygen was applied. The temperature was maintained at 36.5°C to 37.5°C. Ultrasound gel was placed on the chest of the anesthetized mouse. The ultrasound probe was placed in contact with the ultrasound gel and scanning was performed over 30 minutes. The temperature, heart rate, and blood pressure were constantly monitored during the ultrasound recording.

M-mode images were obtained for measurements of left ventricle (LV) wall thickness (LVWT), and chamber sizes using such parameters as LV end-diastolic diameter (LVEDD) and LV end-systolic diameter (LVESD). Qualitative and quantitative measurements were made offline using analytic software (VisualSonics, Toronto, ON, Canada). LV EF was calculated using the following equation:

$$EF(\%) = [LVEDV-LDESV/LVEDV] \times 100$$

Specifically for post-MI function, the wall motion score index (WMSI) was calculated based on the *American Society of Echocardiography* recommended assessment of wall motion function of the 17-segment LV model whereby 1=normal wall motion, 2=hypokinetic segment, 3=akinetic segment, 4=dyskinetic segment and 5=aneurysmal segment[10-12]. In the murine model, the use of WMSI and analysis of segmental wall motion abnormalities in the infarction models has been validated despite the small heart size and fast heart rate[10, 13, 14]. The classical 16-segments (6 basal segments, 6 mid-ventricular segments and 4 apical segments) were assessed using the short axis views while the apical cap was evaluated based on the parasternal long-axis view. An increase in WMSI (>1) indicates suppressed LV systolic wall motion.

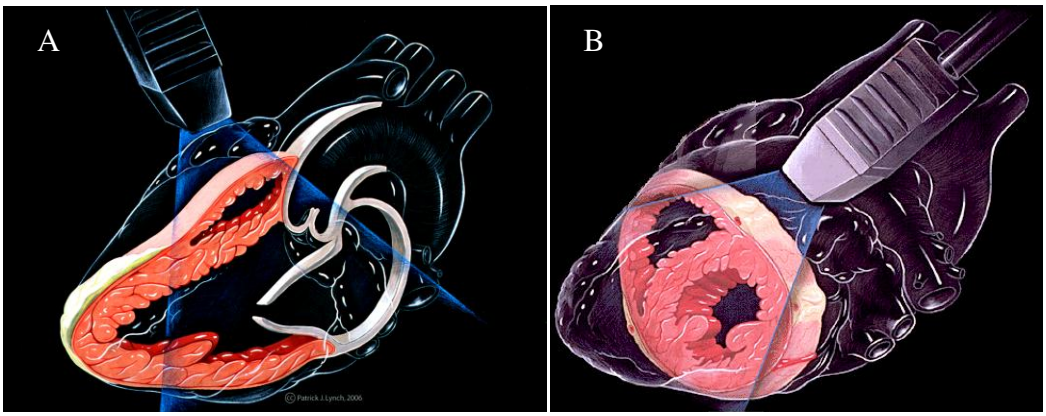

Figure 2.3. Echocardiogram imaging views for cardiac structure and function assessment.

Two different imaging views were utilized, the long-axis or parasternal view (A), which presents the longitudinal view of the heart, and the short-axis view (B) displaying the cross-sectional cardiac features.

2.5.2. Transmitral doppler (TMD)

Diastolic function was assessed using pulsed-wave Doppler imaging of the transmitral filling pattern with the early transmitral filling wave (E-wave) followed by the late filling wave due to atrial contraction (A-wave). Isovolumic relaxation time (IVRT) was calculated as the time from closure of the aortic valve to initiation of the E-wave. The deceleration time of the E-wave deceleration time (DT) was determined by measuring the time needed for the down-slope of the peak of the E-wave to reach the baseline while the rate of E-wave deceleration rate (EWDR) was calculated as the E-wave divided by the DT.

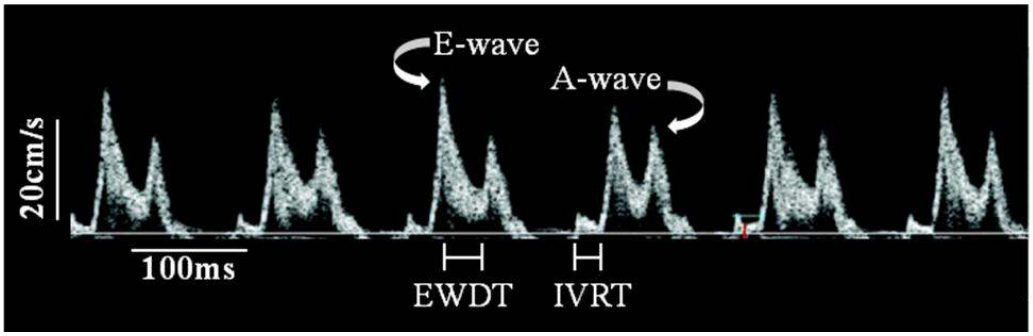

Figure 2.4. Representative image of the transmitral Doppler (TMD) imaging signal detecting diastolic transmitral flow velocity.

The transmitral flow velocity signal pattern is generated from the blood flow velocity across the mitral valve (also known as the bicuspid or left atrioventricular valve) during diastolic ventricular filling. It is useful in assessing the biphasic flow pattern of diastole, which is early flow and late flow. A few of the pertinent parameters are displayed above: E-wave of the early filling phase, A-wave from atrial contraction, isovolumetric relaxation time (IVRT), and E-wave deceleration time (EWDT).

2.5.3. Tissue doppler imaging (TDI)

Tissue Doppler imaging (TDI) is a novel and validated technique to assess systolic and diastolic function with a reduction in E' and an elevation in E/E' being considered valid markers of elevated LV filling pressure and diastolic dysfunction[8, 9]. TDI was made at the inferolateral region in the radial short axis at the base of the LV with the assessment of early diastolic (E') and late diastolic (A') myocardial velocities, as well as for the assessment of peak systolic annular motion (S').

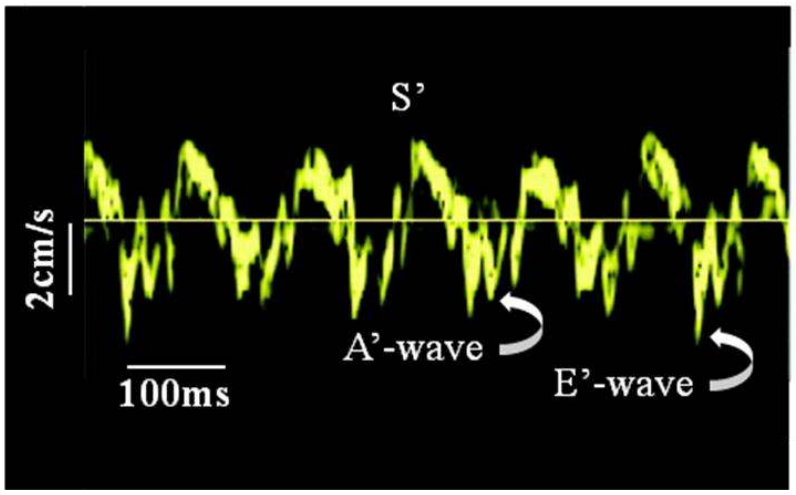

Figure 2.5. Representative image of the tissue Doppler imaging (TDI) signal detecting myocardium motion.

The TDI signal is generated from the ventricular myocardial tissue motion adjacent to the mitral valve annulus (a fibrous ring attached to the leaflets of the mitral valve) during systolic and diastolic ventricular action. A few of the pertinent parameters are displayed above: E'-wave of the early filling phase, A'-wave from atrial contraction, and peak systolic annular motion (S').

2.5.4. ECG-gated kilohertz visualization (EKV)

Electrocardiogram kilohertz-based visualization (EKV™) software analysis produced offline reconstruction for simulated 250 to 1,000 Hz static and cine loop images. This method that provides the highest temporal resolution versus typical two-dimensional B-mode imaging. Modified parasternal long axis EKV loops were also used to measure EF using Simpson's method.

2.6. Morphological analysis

2.6.1. Myocardium

2.6.1.1. Masson's trichrome stain

Freshly excised hearts were arrested in diastole with 1M KCl, fixed in 10% neutral buffered formalin, paraffin-embedded (Alberta Diabetes Institute Histology Core; University of Alberta, Edmonton, AB, Canada), and sectioned for Masson's trichrome staining (University of Alberta Department of Laboratory Medicine and Pathology; Edmonton, AB, Canada). All images were captured on a Leica DM4000B microscope using Infinity Capture software (Lumenera; Ottawa, ON, Canada). Qualitative assessment of overall LV hypertrophy or chamber dilation was achievable by sectioning of the WT and TIMP2$^{-/-}$ sham and disease mouse heart.

Formalin-fixed, paraffin-embedded isolated left ventricles were cross-sectioned (4μm) and processed with Masson's trichrome stain for quantitative measurement of myocyte cross-sectional area (CSA) as an indicator of hypertrophy. The CSA of myocytes was measured using a 40x objective and ImageJ software (National Institute of Health, NIH) for analysis. CSA was determined by tracing the outline of the cross-sectioned myocytes and recording the area measured. Measurements were converted from pixels to μm^2 through calibration of the system, which was done with the use of a micrometer. The

number of cells measured was 40-60 cells from each heart with a total of three hearts per group from each time-point.

2.6.1.2. Triphenyl tetrazolium chloride (TTC)

Infarct size was measured at 1 week post-MI by perfusing the hearts at a constant pressure (60 mmHg) first with phosphate-buffered saline (PBS) to clear out the blood, then with 2% triphenyl tetrazolium chloride (Sigma-Aldrich, Oakville, ON, Canada) which stains the live cells red, while infarcted myocardium appears white. Cross sections were then sliced from apex to the base in 2mm sections. The infarct region per slice was measured using ImageJ software as surface area, and reported as percentage of total area of slices when combined.

2.6.2. ECM structure

2.6.2.1. Picrosirius red

Left ventricular cross-sections (4µm) were stained with Picrosirius red (PSR) to visualize collagen fibrosis in the heart (University of Alberta Department of Laboratory Medicine and Pathology; Edmonton, AB, Canada). Sham, 2 weeks, 5 weeks, and MMPi-treated TAC hearts were formalin-fixed and paraffin-embedded for sectioning (Alberta Diabetes Institute Histology Core; University of Alberta, Edmonton, AB, Canada). Slides were protected from light and stored at 4°C. Images were captured on a Leica DM4000B microscope using Infinity Capture software.

2.6.2.2. Quantification of fibrillar collagen content

Fibrillar collagen was quantified in the infarct and non-infarct myocardium of WT and TIMP2$^{-/-}$ mice at 3 days post-MI using the QuickZyme Collagen Assay kit that recognizes only the fibrillar collagen (QuickZyme Biosciences, Netherlands). Fibrillar collagen was extracted[15] by homogenizing infarct or non-infarct heart tissues in 0.5M acetic acid and pepsin (1:10 weight/tissue wet weight). The homogenate was incubated overnight at 4°C on a roller table. The next day the samples were centrifuged (14,000rpm for 10

minutes), the supernatant was collected and total protein was quantified using Bio Rad DC protein assay. Samples (200μg) and collagen standard (0, 0.5, 1, 2, 4, 6, 8, and 10 μg) were added to assigned wells in a 96-well plate. Dilution buffer was added to each sample to a final volume of 140μL/wells. Sirius Red dye solution was added to each well and mixed gently and thoroughly. The plate was sealed and incubated on ice (to avoid degradation of the collagen fibres). The samples were centrifuged (as in the 96-well plate) at 3000 x *g* at 4°C. The collagen fibre (which is bound to Sirius Red dye) forms a pellet at the bottom of the well. The pellets were washed three times with washing buffer. Detection buffer was added to the pellets and mixed thoroughly and the signal was read at 540nm. A standard curve was generated using the collagen standard samples (A540 against [collagen]), a best-fit linearized curve was generated and collagen content per well was calculated for the samples from the A540 values, and reported as μg fibrillar collagen/ 200μg total protein. All steps were performed on ice (or at 4°C) to avoid degradation of the collagen fibres.

2.6.2.3. Multiphoton and second harmonic generation imaging.

Collagen fibers in unfixed and unstained heart tissue were visualized by using the novel second harmonic generation (SHG) and multiphoton excitation fluorescence (MPEF) microscopy imaging technique[16]. The laser used for SHG as well as the MPEF signals was a mode-locked femto-second Ti:Sapphire Tsunami (Spectra-Physics, Mountain View, CA) synchronously pumped by a Millenia Xs J (Spectra-Physics) diode-pumped solid-state laser. The Tsunami laser, consistently produced pulses of 100-fs width between 790 and 950 nm. Wavelength identification and selection was achieved by an IST laser spectrum analyzer (IST, Horseheads, NY) coupled to a TDS 210 oscilloscope (Tektronix, Beaverton, OR). The laser output was attenuated using neutral density filters (New Focus, San Jose, CA) and the average power was consistently maintained below the damage threshold for the tissue. The power attenuated laser was directed to a Leica AOBS RS scan head (4000 Hz) coupled with Leica upright microscope system (Heidelberg, Germany). The laser beam was focused on the

specimen through an Olympus XLUMPlanFl 20X/0.95 NA water-immersion objective. The backscattered SHG and MPEF emissions from the sample were collected through the objective lens. Leica Confocal Software TCS SP2 was used for the image acquisition. Non-de-scanned detectors and spectral scanning mode both in the reflection geometry were used for capturing the 3-dimensional images as well as for the spectral signal characterizations respectively. A broad range of infrared laser wavelength of excitation (800 to 900-nm) with a scan interval of 10 nm was employed to detect the SHG signals, which peaked at an excitation wavelength of 880-nm. In the Non-de-scanned photomultiplier tube (PMT) detectors (R6357, Hamamatsu, Shizuoka, Japan), a 700nm short pass filter (E700SP, Chroma Technology; Bellow Falls, VT, USA) was used to prevent the scattered IR laser radiation from reaching the detector, and a 455 DCXRU dichroic beam splitter was used to separate the SHG signal from the other endogenously fluorescent signals emitting from other tissue components. All SHG and MPEF spectral data were generated using the de-scanned PMT detector (R6357, Hamamatsu) located inside the scan-head with a maximum confocal pinhole setting at 600 μm. The gain and the offset of the photomultiplier tubes were adjusted for optimized detection using the color gradient to avoid pixel intensity saturation and background. Images (8 bit) acquired at scan speed of 5 sec per 512 X 512 pixels. Three dimensional stack of images with optical section thickness of 0.7μM were captured from 120 μm thick tissue. For each tissue volume, z-section images were compiled and the 3-dimensional image restoration was performed using Volocity software (Improvisions; UK).

2.6.2.4. Scanning electron microscopy

Scanning electron microscopy (SEM)[17] was performed by manually slicing the LV into 2-3mm pieces and fixing them in 2.5% glutaraldehyde and 2% paraformaldehyde in 0.1 M PBS for 48 hrs at room temperature. Samples were washed in 0.1M PBS (3X15 min), followed by quick distilled water rinse. Dehydration was carried out by a series of ethanol washes. Hexamethyldisilazane (HMDS) was used (instead of critical point drying) for tissue preparation.

Samples were air dried overnight, mounted on SEM stubs, sputter coated with Au/Pd, and imaged using Phillips Scanning Electron Microscope (FEI Company, Model: XL30).

2.7. Immunohistochemistry (IHC)

2.7.1. Integrin-β1 immunostaining

Fluorescent staining for integrin-β1 was performed on OCT-frozen tissue as described[18]. Transverse sections (20 μm) were direct mounted onto gelatin coated slides, and after being hydrated and blocked, sections were incubated with rabbit α-human integrin β1 primary antibody (1:500, AB 1952; Millipore; Billerica, MA, USA), and Cy3-conjugated goat α-rabbit IgG secondary antibody (1:500, Jackson ImmunoResearch, West Grove, PA, USA). Slides were cover slipped with Citifluor (Electron Microscopy Sciences; Hatfield, PA, USA), immunoreactivity was visualized with a Nikon Eclipse C1confocal microscope (MicroVideo Instruments; Avon, MA, USA), and images were acquired with identical settings for all samples. Specificity of labeling was verified by exclusion of primary antibody and use of control IgG.

2.7.2. Immunostaining for neutrophils and macrophages

Hearts were fixed in 10% buffered formalin for 48 hours followed by 80% ethanol. Paraffin sections (4 μm thick) were de-waxed in 5 changes of xylenes and brought down to water through graded alcohols. For neutrophil staining, sections were then pretreated with 1% pepsin in 0.01N HCl at pH 2.0 for 15 minutes at 37°C. Endogenous biotin activities were blocked using an avidin-biotin blocking kit (Lab Vision). Sections were then blocked with 10% normal rabbit serum (Vector Labs) for 10 minutes before incubating with the rat anti mouse neutrophils antibody (Serotec: MCA771GA) overnight at 1/600 dilution. After washing well in Tris-base saline (TBS), staining was finished with 30 minutes each of a biotinylated rabbit anti-rat IgG linking antibody followed by alkaline

phosphatase streptavidin (Vector Labs: SA-5100). Color development was performed using a freshly prepared solution of Vector Red from an alkaline phosphatise substrate kit (Vector Labs.: SK-5100). After washing well in tap water, sections were counterstained lightly with Mayer's hematoxylin solution. Sections were then dehydrated in alcohols, cleared in xylenes and mounted in Permount (Fisher).

For macrophage staining (Mac 3), sections were heat-retrieved using Tris-ethylenediaminetetraacetic acid (EDTA) buffer at pH 9.0. Endogenous biotin activities were blocked using an avidin-biotin blocking kit (Lab Vision). Sections were then blocked with 10% normal rabbit serum (Vector Labs) for 10 minutes before incubating with the rat anti- mouse F4/80 antibody (Serotec: cat#MCA497GA, clone CI:A3-1) at 1/50 or rat anti-mouse Mac-3 antibody (BD Pharmingen: cat#550292, clone M3/84) at 1/50 overnight. After washing well in TBS, staining was finished with 30 minutes each of a biotinylated rabbit anti-rat IgG linking antibody (Vector Labs) followed by horseradish peroxidise (HRP)-conjugated streptavidin labeling reagent (ID Labs). Color development was performed using a freshly prepared solution of Nova Red (Vector Labs). After washing well in tap water, sections were counterstained lightly with Mayer's hematoxylin solution. Finally, sections were dehydrated in alcohols, cleared in xylenes and mounted in Permount (Fisher).

2.8. RNA expression analysis

2.8.1. RNA extraction and purification

RNA was extracted using Trizol (Invitrogen; Burlington, ON, Canada), followed by reverse transcription to generate cDNA for TaqMan Realtime polymerase chain reaction (RT-PCR) for mRNA expression analysis[17, 19]. The RNA extraction protocol involved homogenization of the tissue sample in 500µL of Trizol reagent (Invitrogen; Burlingtion, ON, Canada) in an RNAase-free 1.5mL microcentrifuge tube. The homogenized tissue was kept at room temperature for

five minutes, and following centrifugation at 12,000 x g at 4°C for 10 minutes the supernatant was transferred to another RNAase-free microtube. The pellet was resuspended in another 500µL of Trizol, with homogenization and centrifuge repeated according to the preceding step. The two collections of supernatant were combined and 200µL of chloroform was added using a glass pipette as it is a strong solvent. The tubes were vigorously shaken manually for 15 seconds and then incubated at room temperature for three minutes. The samples were centrifuged at 12,000 x g at 4°C for 15 minutes, which separated the contents into three distinct layers. The RNA-containing upper colorless aqueous phase was carefully transferred to a new RNAase-free centrifuge tube, with the interphase and pink organic phenol phases discarded. Subsequently, 500µL of 2-propanol (isopropanol) was added to each tube and gently inverted several times, after which the tubes were incubated at -20°C overnight. On the following day, the sample was centrifuged at 12,000 x g at 4°C for 10 minutes, after discarding the supernatant, 1mL of 75% ethanol (prepared from 100% ethanol and RNAase-free water) was added to the pellet. After dislodging the pellet by gently pipetting, the sample was centrifuged at 7,500 x g at 4°C for five minutes. The supernatant was removed, the pellet was air-dried for 10 minutes, and the RNA pellet was then resuspended in 12µL of RNAase-free water for quantification using the Nanodrop 1000 spectrophotometer (Nanodrop; Willmington, DE, USA).

2.8.2. Taqman RT-PCR

The RNA samples were reverse-transcribed to generate complementary DNA (cDNA) . For each gene, a standard curve was generated using known concentrations of mouse brain cDNA (0.625, 9 1.25, 2.5, 5, 10 and 20µg) as a function of cycle threshold (CT). The standard curve of $[cDNA]_{brain}$ as a function of CT is fit to a linear regression: Y=aX+b, where Y=cycle threshold, a=slope of the standard curve, X=[cDNA]experimental sample. The SDS2.2 software (integral to ABI7900 real-time machine) fits the CT values for the experimental samples in this formula and generates values for cDNA levels. Subsequently, these values are normalized by our internal controls, 18S (ribosomal RNA) or

HPRT (hypoxanthine-guanine phosphoribosyltransferase-1) which has been shown to be an appropriate housekeeping gene for myocardial tissue[20], and the values are expressed as relative expression (R.E.). All samples were run in triplicates in 384 well plates.

Table 2.2. Taqman primers and probe sequences.

Gene	Primer/ Probe	Sequence
TIMP1	Forward:	5'-CAT GGA AAG CCT CTG TGG ATA TG-3'
	Reverse:	5'-AAG CTG CAG GCA CTG ATG TG-3'
	Probe:	5'-FAM-CTC ATC ACG GGC CGC CTA AGG AAC-TAM RA-3'
TIMP2	Forward:	5'-CCA GAA GAA GAG CCT GAA CCA-3'
	Reverse:	5'-GTC CAT CCA GAG GCA CTC ATC-3'
	Probe:	5'-FAM-ACT CGCT GTC CCA TGA TCC CTT GC-TAM RA-3'
TIMP3	Forward:	5'-GGC CTC AAT TAC CGC TAC CA-3'
	Reverse:	5'-CTG ATA GCC AGG GTA CCC AAA A-3'
	Probe:	5'-FAM-TGC TAC TAC TTG CCT TGT TTT GTG ACC TCC A-TAM RA-3'
TIMP4	Forward:	5'-TGC AGA GGG AGA GCC TGA A-3'
	Reverse:	5'-GGT ACA TGG CAC TGC ATA GCA-3'
	Probe:	5'-FAM-CCA CCA GAA CTG TGG CTG CCA AAT C-TAMRA-3'
MMP2	Forward:	5'-AAC TAC GAT GAT GAC CGG AAG TG-3'
	Reverse:	5'-TGG CAT GGC CGA ACT CA-3'
	Probe:	5'-FAM-TCT GTC CTG ACC AAG GAT ATA GCC TAT TCC TCG-TAM RA-3'
MMP8	Forward:	5'- GAT TCA GAA GAA ACG TGG ACT CAA-3'
	Reverse:	5'- CAT CAA GGC ACC AGG ATC AGT -3'

	Probe:	5’-FAM-CAT GAA TTT GGA CAT TCT TTG GGA-CTC TCT CAC-TAM RA-3’
MMP9	Forward:	5’-CGA ACT TCG ACA CTG ACA AGA AGT -3’
	Reverse:	5’- GCA CGC TGG AAT GAT CTA AGC-3’
	Probe:	5’-FAM-TCT GTC CAG ACC AAG GGT ACA GCC TGT TC-TAM RA-3’
MMP13	Forward:	5’-GGG CTC TGA ATG GTT ATG ACA TTC -3’
	Reverse:	5’-AGC GCT CAG TCT CTT CAC CTC TT -3’
	Probe:	5’-FAM-AAG GTT ATC CCA GAA AAA TAT CTG ACC TGG GAT TC-TAM RA-3’
MT1-MMP	Forward:	5’- AGG AGA CAG AGG TGA TCA TCA TTG -3’
	Reverse:	5’- GTC CCA TGG CGT CTG AAG A -3’
	Probe:	5’-FAM-CCT GCC GGT ACT ACT GCT GCT CCT G-TAM RA-3’
BNP	Forward:	5'-CTG CTG GAG CTG ATA AGA GA-3'
	Reverse:	5'-TGC CCA AAG CAG CTT GAG AT-3'
	Probe:	5'-FAM-CTC AAG GCA GCA CCC TCC GGG-TAMRA-3'
β-MHC	Forward:	5'-GTGCCAAGGGCCTGAATGAG-3'
	Reverse:	5'-GCAAAGGCTCCAGGTCTGA-3'
	Probe:	5'-ATCTTGTGCTACCCAGCTCTAA-3'
α- SkMA	Forward:	5'-CAGCCGGCGCCTGTT-3'
	Reverse:	5'-CCACAGGGCTTTGTTTGAAAA-3'
	Probe:	5'-FAM-TTGACGTGTACATAGATTGACTCGTTTTACCTC ATTTTG- TAMRA-3'
pro-collagen I-α1	Forward:	5’-CTTCACCTACAGCACCCTTGTG-3’
	Reverse:	5’-TGACTGTCTTGCCCCAAGTTC-3’
	Probe:	5’-FAM-CTGCACGAGTCACACC-TAMRA-3’

pro-collagen III-α1 type II	Forward: Reverse: Probe:	5'- TGTCCTTTGCGATGACATAATCTG-3' 5'- AATGGGATCTCTGGGTTGGG-3' 5'-FAM- ATGAGGAGCCACTAGACT-TAMRA-3'
Integrin-β1		Mm01253230_m1 (premixed primers/probe)
18S		Kit from Applied Biosystems (ABI; Carlsbad, CA, USA)
HPRT	Forward: Reverse: Probe:	5'-AGC TTG CTG GTG AAA AGG AC-3' 5'-CAA CTT GCG CTC ATC TTA GG-3' 5'-FAM-CAA CAA AGT CTG GCC TGT ATC CAA C-TAM RA-3'

2.9. Protein analysis

2.9.1. Tissue protein extraction

Total protein was extracted from frozen tissue by gentle manual homogenization in EDTA-free RIPA buffer (Table 2.3. for western blot; Table 2.4. for zymography) including protease inhibitor (Table 2.5.; Calbiochem, San Diego, CA, USA) and phosphatase inhibitor cocktails (Table 2.6.;. Sigma-Aldrich, Oakville, ON, Canada) (Table 2.7. Calbiochem, San Diego, CA, USA). The homogenized tissue was kept on ice for one hour with one minute intervals of high-speed vortex every 15 minutes. The sample was centrifuged at 14,000 x g for 12 minutes and the protein-containing supernatant transferred to a new tube. Protein content concentration was determined using the Bio-Rad DC protein assay (Bio-Rad; Missisauga, ON, Canada) using a clear flat-bottom 96-well plate and a spectrophotometric plate-reader at 750nm. Protein extracted using Cytobuster Protein Extraction Buffer (Novagen, Madison, WI, USA) followed the same process, with the exception of the extraction buffer used.

Table 2.3. RIPA protein extraction buffer pH 7.4 in ddH_2O - Western blot

RIPA Protein extraction buffer pH 7.4- Western blot				
	Chemical name	M.W. (g/mol)	$Conc._{stock}$	$Conc._{final}$
1	Tris-HCl	121.14	N/A	50 mM
2	Sodium chloride (NaCl)	58.44	N/A	120 mM
3	EDTA	372.24	N/A	1 mM
4	Triton X-100 (detergent)	624.00	N/A	1%

Table 2.4. RIPA Protein extraction buffer pH 7.4 in ddH_2O - Zymography

RIPA Protein extraction buffer pH 7.4- Zymography				
	Chemical name	M.W. (g/mol)	$Conc._{stock}$	$Conc._{final}$
1	Tris-HCl	121.14	N/A	50 mM
2	Sodium chloride (NaCl)	58.44	N/A	150 mM
3	Triton X-100 (detergent)	624.00	N/A	1%
4	SDS (detergent)	288.38	N/A	0.1%
5	NP40 (detergent)	N/A	N/A	1%
6	Sodium deoxycholate (detergent)	414.55	N/A	1%

Table 2.5. Protease inhibitor cocktail

Protease inhibitor cocktail III, EDTA-free (Calbiochem; cat# 539134)				
	Chemical name	M.W. (g/mol)	$Conc._{stock}$	$Conc._{final}$
1	AEBSF, hydrochloride	239.50	100x	1x
2	Aprotinin	6512.00	100x	1x
3	Bestatin	308.37	100x	1x
4	E-64	357.40	100x	1x
5	Leupeptin	475.59	100x	1x
6	Pepstatin A	685.89	100x	1x

Table 2.6. Phosphatase inhibitor cocktail- Tyr, acidic, & alkaline phosphatases

Phosphatase inhibitor cocktail 2- Tyr, acidic, & alkaline (Sigma; pdt# 5726)				
	Chemical name	M.W. (g/mol)	$Conc._{stock}$	$Conc._{final}$
1	Sodium-orthovanadate	183.91	100x	1x
2	Sodium-molybdate	241.95	100x	1x
3	Sodium-tartrate	230.08	100x	1x
4	Imidazole	68.08	100x	1x

Table 2.7. Phosphatase inhibitor cocktail- Ser/Thr & alkaline phosphatases

Phosphatase inhibitor cocktail IV- Ser/Thr & alkaline (Calbiochem; cat# 524628)				
	Chemical name	M.W. (g/mol)	$Conc._{stock}$	$Conc._{final}$
1	(-)-p-Bromotetramisole oxalate	373.22	100x	1x
2	Cantharidin	196.20	100x	1x
3	Calyculin A	1009.20	100x	1x

Membrane fraction was extracted from sham, infarct, peri- and non-infarct myocardial tissue. Frozen tissue was homogenized in RIPA buffer (Table 2.8.), and protease inhibitor (Table 2.5. Calbiochem, San Diego, CA, USA) and phosphatase inhibitors (Table 2.6. Sigma-Aldrich, Oakville, ON, Canada; Table 2.7. Calbiochem, San Diego, CA, USA) cocktails. The homogenized tissue was kept on ice for one hour with one minute intervals of high-speed vortex every 15 minutes, which was subsequently centrifuged at 2,900 x g for 20 minutes. The supernatant containing the cytosolic and membrane proteins was transferred to a new ultracentrifuge tube. The pellet containing the nuclear protein was discarded. The supernatant containing the cytosolic and membrane proteins was centrifuged at 29,000 x g for 45 minutes. This high speed centrifugation separated the cytosolic protein (supernatant) from the membrane protein (pellet). The pellet was

resuspended in 50µL RIPA buffer containing detergents (Table 2.9.) and centrifuged at 15,000 x g for 20 minutes. This supernatant was stored at -80°C as the membrane fraction.

Table 2.8. RIPA Protein extraction buffer pH 7.4 in ddH_2O – Cytosol+Membrane protein fraction

RIPA Protein extraction buffer pH 7.4- Cytosol-Membrane fraction				
	Chemical name	M.W. (g/mol)	$Conc._{stock}$	$Conc._{final}$
1	Tris-HCl	121.14	N/A	50 mM
2	Sodium chloride (NaCl)	58.44	N/A	150 mM
3	EDTA	372.24	N/A	1 mM
4	Dithiothreitol (DTT)	154.25	100 mM	1 mM
5	Phenylmethylsulfonyl fluoride (PMSF)	174.19	100 mM	1 mM

Table 2.9. RIPA Protein extraction buffer pH 7.4 in ddH_2O –Membrane protein fraction

RIPA Protein extraction buffer pH 7.4- Membrane fraction				
	Chemical name	M.W. (g/mol)	$Conc._{stock}$	$Conc._{final}$
1	Tris-HCl	121.14	N/A	50 mM
2	Sodium chloride (NaCl)	58.44	N/A	150 mM
3	EDTA	372.24	N/A	1 mM
4	Dithiothreitol (DTT)	154.25	100 mM	1 mM
5	PMSF	174.19	100 mM	1 mM
6	NP40 (detergent)	N/A	N/A	1%
7	Sodium deoxycholate (detergent)	414.55	2.5%	0.25%

2.9.2. Western blot

The sodium dodecyl sulphate-based polyacrylamide (SDS) gel was used for transfer of loaded protein onto a polyvinylidene fluoride (PVDF) membrane for binding of an antibody to a specific epitope on the protein of interest that resides on the membrane. Each sample to be loaded per well was prepared by combining the volume for 40µg of sample protein with the appropriate volume of 2x protein loading buffer (Table 2.10.) and PBS (Table 2.11.), boiled for 5 minutes to denature the protein, and traveled through the gel via electrophoresis (at 100V; Bio Rad; Mississauga, ON, Canada) in the presence of a electrophoresis running buffer solution (Table 2.12.) , and through electrophoresis was transferred onto the PVDF membrane for blotting using a transfer buffer solution (Table 2.13). After transfer, the membrane was blocked with 5% skim milk for two hours at room temperature and primary antibody was applied overnight as a specific dilution ranging from 1:100 to 1:5000 in 5% skim milk depending on the antibody and the protein of interest. The membrane was washed 3x15 minutes with TBS (Table 2.14.) with 0.1% Tween (TBST), followed by the application of the appropriate species-based horse radish peroxidase (HRP) linked-secondary antibody in 5% skim milk at a dilution of 1:5000 for two hours at room temperature which binds to the primary antibody. After another 3x15 minutes washing of the membrane with TBST, Enhanced Chemiluminescence (ECL; GE Amersham; Baie d'Urfe, QC, Canada) was applied to the membrane according to manufacturer's instructions for 5 minutes which binds specifically to the HRP segment on the secondary antibody. An image of the membrane was taken by either developing x-ray film (Fuji Medical X-Ray Film Super Rx; Fujifilm) which was exposed to the chemiluminescent membrane, or by imaging the chemiluminescent membrane using a luminescent image analyzer housing a chemiluminescence-sensitive camera (GE ImageQuant LAS 4000; GE). The PVDF membrane was then stripped with a mild stripping buffer (Table 2.15.) for 30 min at 55^{o}C for subsequent immunoblotting of the membrane. For all western blots, the Coomassie-stained gel (2% Coomassie blue, 25% methanol, 10% acetic acid) or the Ponceau-stained membrane (0.1% Ponceau S (w/v) in 1% acetic acid)

were used as the loading controls. Coomassie blue is a permanent stain that is applied to the gel after transfer to qualitatively assess the loading of the gel with the assumption of proper transfer. Ponceau stain is red in color and can be applied to the membrane immediately after transfer as it is a reversible staining procedure of the final product, which is the membrane. Upon washing the membrane with TBST after imaging the Ponceau staining, it is ready to continue the process of the blocking of the membrane.

Table 2.10. Sample loading buffer pH 6.8 in ddH_2O - Western blot

Sample loading buffer pH 6.8- Western blot				
	Chemical name	M.W. (g/mol)	$Conc._{stock}$	$Conc._{final}$
1	Tris-HCl	121.14	130 mM	65 mM
2	SDS	288.38	4.6%	2.3%
3	Bromophenol Blue	669.96	0.2%	0.1%
4	Glycerol	92.09	20%	10%
5	Dithiothreitol (DTT)	154.25	2%	1%

Table 2.11. Phosphate-buffered Saline (PBS) pH 7.4 in double-distilled water (ddH_2O)

Phosphate-buffered Saline (PBS) pH 7.4				
	Chemical name	M.W. (g/mol)	$Conc._{stock}$	$Conc._{final}$
1	Sodium chloride (NaCl)	58.44	1370 mM	137mM
2	Potassium chloride (KCl)	74.55	27 mM	2.7 mM
3	Sodium phosphate dibasic (Na_2HPO_4)	141.96	100 mM	10 mM
4	Potassium phosphate monobasic (KH_2PO_4)	136.09	18 mM	1.8 mM

Table 2.12. Running buffer pH 8.3 in ddH_2O

Running buffer pH 8.3				
	Chemical name	M.W. (g/mol)	$Conc._{stock}$	$Conc._{final}$
1	Tris-HCl	121.14	250 mM	25 mM
2	Glycine	75.07	1920 mM	192 mM
3	Sodium dodecyl sulfate (SDS)	288.38	10%	1%

Table 2.13. Transfer buffer pH 8.3 in ddH_2O

Transfer buffer pH 8.3				
	Chemical name	M.W. (g/mol)	$Conc._{stock}$	$Conc._{final}$
1	Tris- HCl	121.14	200 mM	20 mM
2	Glycine	75.07	1500 mM	150 mM
3	Methanol	32.04	N/A	20%

Table 2.14. Tris-buffered Saline (TBS) pH 8.0 in ddH_2O

Tris-buffered Saline (TBS) pH 8.0				
	Chemical name	M.W. (g/mol)	$Conc._{stock}$	$Conc._{final}$
1	Sodium chloride (NaCl)	58.44	1250 mM	125 mM
2	Tris-HCl	121.14	250 mM	25 mM

Table 2.15. Western blot Membrane Stripping buffer pH 6.8 in ddH_2O

Western blot Membrane Stripping buffer pH 6.8				
	Chemical name	M.W. (g/mol)	$Conc._{stock}$	$Conc._{final}$
1	Tris-HCl	121.14	1000 mM (pH 6.8)	62.5 mM
2	SDS	288.38	20%	2%
3	β-mercaptoethanol	78.13	14300mM	100mM

Western blot analyses were performed on a 10% polyacrylamide gel to detect protein levels of TIMP1 (26 kDa; 1:500 dilution, monoclonal rat anti-mouse; R&D Systems; Minneapolis, MN, USA), TIMP2 (21 kDa; 1:1000 dilution, monoclonal mouse anti-mouse; Abcam; Cambridge, MA, USA), TIMP3 (30 kDa; 1:1000 dilution, monoclonal rabbit anti-mouse; Santa Cruz; Santa Cruz, CA, USA) and TIMP4 (26 kDa; 1:1000 dilution, monoclonal rabbit anti-mouse; Novus Biologicals; Oakville, ON, Canada) [9, 21]. An 8% gel was used for higher molecular weight proteins, generally 70 kDa and larger, such as integrin β1D (116 kDa; 1:500 dilution, monoclonal rabbit anti-mouse; Millipore; Billerica, MA, USA)[22], phospho-FAK (125 kDa; Tyr397; 1:500 dilution, monoclonal rabbit anti-mouse; Millipore; Billerica, MA, USA) total FAK (125 kDa; 1:1000 dilution, monoclonal rabbit anti-mouse Santa Cruz; Santa Cruz, CA, USA), and SPARC (42 kDa; 1:500 dilution, monoclonal rat anti-mouse; R&D Systems; Minneapolis, MN, USA).

Western blot analysis for MT1-MMP was performed on the membrane protein fractions using a MT1-MMP antibody (65 kDa; 1:1000 dilution polyclonal rabbit anti-mouse; SantaCruz, Santa Cruz, CA, USA) using a 10% acrylamide gel, and after blocking with 5% skim milk the membrane was blotted for toll-like receptor 4 (TLR-4) (1:500 dilution monoclonal rabbit anti-mouse; Santa Cruz, Santa Cruz, CA, USA), and subsequently for caspase-3 (1:3000 dilution monoclonal rabbit anti-mouse; Cell Signaling; Davers, MA, USA).

2.9.3. Gelatin zymography

Gelatin zymography was performed to detect pro- and cleaved active MMP2 and MMP9. Protein was extracted as previously mentioned using an EDTA-free RIPA buffer as EDTA is a known metal-ion chelator, which would interfere with MMP activity. Preparation of the polyacrylamide gel included adding gelatin to the mixture at a final concentration of 2 mg/mL. Each sample to be loaded per well was prepared by combining the volume for 50µg of sample protein with the appropriate volume of nondenaturing loading dye (Table 2.16) and PBS (Table 2.11.).

Table 2.16. Sample loading buffer pH 6.8 in ddH_2O - Zymography

Sample loading buffer pH 6.8- Zymography				
	Chemical name	M.W. (g/mol)	$Conc._{stock}$	$Conc._{final}$
1	Tris-HCl	121.14	125 mM	62.5 mM
2	Glycerol	92.09	20%	10%
3	SDS	288.38	4%	2%
4	Bromophenol Blue	669.96	0.02%	0.01%

After electrophoresis of 40µg-contaning sample protein mixture per well, the gelatin-based polyacrylamide gel was washed in Triton-X 3 x 20 minutes. The gel was then washed 3x10 minutes in incubation substrate buffer (Table 2.17). The gelatin zymography gel was incubated in the incubation substrate buffer for 24 hours at 37°C, after which the buffer was replaced with fresh substrate buffer. Following another 24 hours of incubation (a total of 48 hours), the gel was stained with Coomassie Blue (2% Coomassie Blue; Table 2.18.) overnight for visualization of white or clear bands on a dark blue background. A destaining solution was used to clear any residual stain from the gel (Table 2.19.) The remaining 10µg-containing portion of the protein mixture that was not loaded for the zymography was run on a 10% polyacrylamide gel and Coomassie-Blue stained and used as a loading and protein dilution control.

Table 2.17. Substrate buffer in ddH_2O - Zymography

Substrate buffer- Zymography				
	Chemical name	M.W. (g/mol)	$Conc._{stock}$	$Conc._{final}$
1	Tris-HCl	121.14	2000 mM	50 mM
2	Calcium chloride $(CaCl_2)•2H_2O$	147.02	2000 mM	5 mM
3	Sodium chloride (NaCl)	58.44	N/A	150 mM
4	Sodium azide (NaN_3)	65.01	5%	0.05%

Table 2.18 Polyacrylamide Gel Staining solution in ddH_2O

Polyacrylamide Gel Staining solution				
	Chemical name	M.W. (g/mol)	$Conc._{stock}$	$Conc._{final}$
1	Coomassie blue	854.00	N/A	2%
2	Methanol	32.04	N/A	25%
3	Acetic acid	60.05	N/A	10%

Table 2.19. Polyacrylamide Gel Destaining solution in ddH_2O

Polyacrylamide Gel Destaining solution				
	Chemical name	M.W. (g/mol)	$Conc._{stock}$	$Conc._{final}$
1	Methanol	32.04	N/A	30%
2	Acetic acid	60.05	N/A	1%

2.9.4. Qualitative analysis of protein levels

Quantification of the protein bands on either the western blot or zymography was achieved using densitometry analysis software (ImageJ; NIH). ImageJ allowed for measurement of band density by producing histograms with respect to the band density relative to the background for a set of selected bands. The areas of the histograms were individually obtained and represented the density of the band. The value obtained for each band was an arbitrary value; hence this value was normalized first to the density obtained from the relevant band on the loading control. After normalization to the loading control, the density was further normalized to one specific sample, either the WT sham protein band or to a specified control band (ie. the 64kDa cleaved MMP2 band of the HT1080 positive control for the zymography). HT1080 is a fibrosarcoma cell line which produce high levels of MMPs, in particular MMP2 and MMP9. This presented a relative value of protein present in each loaded sample.

2.10. ECM-myocyte adhesion

2.10.1. In vitro ECM-myocyte adhesion assay

Adhesion of adult cardiomyocytes to ECM proteins were assessed by using an in situ CytoSelect Cell Adhesion Assay (ECM Array, Colorimetric Format, Cell Biolabs; Burlington, ON, Canada) according the manufacturer's instructions[4]. Using Collagenase, Type 2 (Worthington Biochemical; Lakewood, NJ, USA) recommended for heart, cardiomyocytes were isolated from mice of either genotype at 2 weeks after sham or TAC–operation and were plated (20,000 cells/well) in wells coated with different ECM proteins, specifically laminin, fibronectin, collagen I, collagen IV, fibrin, and BSA as control. After 1hr of incubation (2% CO_2, 37^{o}C), cells were washed with PBS to remove the nonadherent cells prior to adding Cell Stain solution. The excess staining solution was washed with PBS, and extraction solution was added to redissolve the dye. The solution was transferred to a fresh plate and optical density (OD) was recorded at 560 nm.

2.11. MMP enzyme *in vitro* activity assay

2.11.1. MMP activity assay

Total gelatinase and collagenase activities were measured using EnzChek fluorescent-based gelatinase/collagenase activity assay kit (Invitrogen; Burlingtion, ON, Canada) according to the manufacturer's instructions, and proteins were extracted using Cytobuster Protein Extraction Buffer. The assay involves *in vitro* analysis of gelatinase/collagenase activity using the extracted protein sample. The fluorescein isothiocyanate (FITC) conjugate-substrate (gelatin or collagen) was added to each well, after which 100µg of protein sample was added to each well. The assay was incubated at room temperature and fluorescence intensity from degraded substrate was measured after six hours on a fluorescence microplate reader at absorption at 495nm and fluorescence emission at 515nm. The slope of the curve indicates the rate of fluorescence, which is an indication of the amount of MMP enzyme available. A steeper slope would

represent a greater amount of active enzyme, thereby generating a greater rate of increase in fluorescence over time.

2.11.2. MT1-MMP specific activity assay

Activity of MT1-MMP was measured in the membrane fraction of the myocardium using the Amersham Biotrak activity assay (RPN2637, GE Healthcare), an antibody based assay that ensures measurement of MT1-MMP-specific activity. According to manufacturer's instructions, samples and standards were incubated in microplates coated with MT1-MMP antibody overnight, the wells were then washed and an MT1-MMP substrate provided with the assay (S-2444 peptide substrate, GE Healthcare) was added to the wells and incubated at 37°C for 6 hours, and absorbance optical density values were read at 405nm using a spectrophotometric plate-reader. MT1-MMP activity was blocked with 5ng/mL of recombinant TIMP2 (rTIMP2) but not rTIMP1 (R&D System; Minneapolis, MN, USA).

A variation of this assay was used for post-TAC analysis of MT1-MMP activity measurement[23, 24] using a specific MT1-MMP fluorogenic substrate (catalog #444258, Calbiochem, San Diego, CA, USA). LV myocardial protein extracts using Cytobuster Extraction buffer (100µg), or alternatively a cacodylic acid-based extraction buffer (Table 2.20.) that has been shown to be effective and commonly used[25, 26], were incubated along with the MT1-MMP substrate at 37^{o}C, and excitation/emission (328/400nm, Spectramax M5 microplate reader) were recorded over 5 hours. The negative controls did not include the MT1-MMP substrate or protein extract. Fluorescence readings were converted to MT1-MMP activity by using a recombinant active MT1-MMP construct (MT1-MMP Catalytic Domain, catalog #475935, Calbiochem, San Diego, CA, USA) as a standard curve in a parallel set of reactions. Concentrations of MT1-MMP catalytic domain for the standard curve included 12.5, 25, 50, 100, 200, and 400 ng/mL. The formula for the conversion of the optical density reading indicating the magnitude of fluorescence to the concentration of MT1-MMP present in the test sample was derived from the standard curve linear relationship between

fluorescence and the known concentrations of the MT1-MMP catalytic domain construct standards. An alternate protein extraction method that has been shown to be effective for MMP activity assays purposes consists of using

Table 2.20. Protein extraction buffer pH 5.0 in ddH_2O - MMP activity assay

Protein extraction buffer pH 5.0- MMP activity assay				
	Chemical name	M.W. (g/mol)	$Conc._{stock}$	$Conc._{final}$
1	Cacodylic acid	138.01	N/A	10mM
2	Sodium chloride (NaCl)	58.44	N/A	150mM
3	Zinc chloride($ZnCl_2$)	136.29	N/A	0.1mM
4	Sodium azide (NaN3)	65.01	N/A	2mM
5	Triton X-100	624.00	N/A	0.1%

2.12. Statistical analyses

All statistical analyses were performed using the SPSS Statistics software (version 19; IBM; Chicago, Ill). Reported averaged values are presented as the mean ± standard error of the mean (SEM). Statistical significance is recognized at $p<0.05$. Post-MI, mortality and rupture incidents were compared using the Kaplan–Meier curves and the log rank test for statistical significance in the survival distribution. As there were generally two factors involved, comparisons between the sham, infarct, peri-infarct, and non-infarct tissues of the two genotypes were performed using the two-way analysis of variance (ANOVA) followed by Student–Neuman–Keuls test for multiple comparison testing. Comparisons were made between the WT and $TIMP2^{-/-}$ sham, 2 week-TAC, and 5 week-TAC groups also using the two-way ANOVA. Normal distribution of data sets to perform ANOVA was determined using the Shapiro-Wilk test for normality, after which we then performed the statistical analyses as noted above. Further analysis of data sets required use of Student's t-test. The appropriate symbols to indicate significance are included in the graph as part of the analysis where applicable, with description in the respective figure legend.

2.13. REFERENCES

1. Wang Z, Juttermann R, Soloway PD. Timp-2 is required for efficient activation of prommp-2 in vivo. *J Biol Chem*. 2000;275:26411-26415

2. Kawamoto H, Yasuda O, Suzuki T, Ozaki T, Yotsui T, Higuchi M, Rakugi H, Fukuo K, Ogihara T, Maeda N. Tissue inhibitor of metalloproteinase-3 plays important roles in the kidney following unilateral ureteral obstruction. *Hypertens Res*. 2006;29:285-294

3. Kassiri Z, Zhong J, Guo D, Basu R, Wang X, Liu PP, Scholey JW, Penninger JM, Oudit GY. Loss of angiotensin-converting enzyme 2 accelerates maladaptive left ventricular remodeling in response to myocardial infarction. *Circ Heart Fail*. 2009;2:446-455

4. Guo D, Kassiri Z, Basu R, Chow FL, Kandalam V, Damilano F, Liang W, Izumo S, Hirsch E, Penninger JM, Backx PH, Oudit GY. Loss of pi3kgamma enhances camp-dependent mmp remodeling of the myocardial n-cadherin adhesion complexes and extracellular matrix in response to early biomechanical stress. *Circ Res*. 2010;107:1275-1289

5. Chancey AL, Brower GL, Peterson JT, Janicki JS. Effects of matrix metalloproteinase inhibition on ventricular remodeling due to volume overload. *Circulation*. 2002;105:1983-1988

6. Kaludercic N, Lindsey ML, Tavazzi B, Lazzarino G, Paolocci N. Inhibiting metalloproteases with pd 166793 in heart failure: Impact on cardiac remodeling and beyond. *Cardiovasc Ther*. 2008;26:24-37

7. Zhou YQ, Foster FS, Nieman BJ, Davidson L, Chen XJ, Henkelman RM. Comprehensive transthoracic cardiac imaging in mice using ultrasound biomicroscopy with anatomical confirmation by magnetic resonance imaging. *Physiol Genomics*. 2004;18:232-244

8. Basu R, Oudit GY, Wang X, Zhang L, Ussher JR, Lopaschuk GD, Kassiri Z. Type 1 diabetic cardiomyopathy in the akita (ins2wt/c96y) mouse model is characterized by lipotoxicity and diastolic dysfunction with preserved systolic function. *Am J Physiol Heart Circ Physiol*. 2009;297:H2096-2108

9. Kandalam V, Basu R, Abraham T, Wang X, Awad A, Wang W, Lopaschuk GD, Maeda N, Oudit GY, Kassiri Z. Early activation of matrix metalloproteinases underlies the exacerbated systolic and diastolic

dysfunction in mice lacking timp3 following myocardial infarction. *Am J Physiol Heart Circ Physiol*. 2010;299:H1012-1023

10. Zhang Y, Takagawa J, Sievers RE, Khan MF, Viswanathan MN, Springer ML, Foster E, Yeghiazarians Y. Validation of the wall motion score and myocardial performance indexes as novel techniques to assess cardiac function in mice after myocardial infarction. *Am J Physiol Heart Circ Physiol*. 2007;292:H1187-1192

11. Schiller NB, Shah PM, Crawford M, DeMaria A, Devereux R, Feigenbaum H, Gutgesell H, Reichek N, Sahn D, Schnittger I, et al. Recommendations for quantitation of the left ventricle by two-dimensional echocardiography. American society of echocardiography committee on standards, subcommittee on quantitation of two-dimensional echocardiograms. *J Am Soc Echocardiogr*. 1989;2:358-367

12. Cerqueira MD, Weissman NJ, Dilsizian V, Jacobs AK, Kaul S, Laskey WK, Pennell DJ, Rumberger JA, Ryan T, Verani MS. Standardized myocardial segmentation and nomenclature for tomographic imaging of the heart: A statement for healthcare professionals from the cardiac imaging committee of the council on clinical cardiology of the american heart association. *Circulation*. 2002;105:539-542

13. Scherrer-Crosbie M, Steudel W, Hunziker PR, Liel-Cohen N, Ullrich R, Zapol WM, Picard MH. Three-dimensional echocardiographic assessment of left ventricular wall motion abnormalities in mouse myocardial infarction. *J Am Soc Echocardiogr*. 1999;12:834-840

14. Suehiro K, Takuma S, Cardinale C, Hozumi T, Shimizu J, Yano H, Di Tullio MR, Wang J, Smith CR, Burkhoff D, Homma S. Assessment of segmental wall motion abnormalities using contrast two-dimensional echocardiography in awake mice. *Am J Physiol Heart Circ Physiol*. 2001;280:H1729-1735

15. Mancuso P, Rahman A, Hershey SD, Dandu L, Nibbelink KA, Simpson RU. 1,25-dihydroxyvitamin-d3 treatment reduces cardiac hypertrophy and left ventricular diameter in spontaneously hypertensive heart failure-prone (cp/+) rats independent of changes in serum leptin. *J Cardiovasc Pharmacol*. 2008;51:559-564

16. Abraham T, Carthy J, McManus B. Collagen matrix remodeling in 3-dimensional cellular space resolved using second harmonic generation and multiphoton excitation fluorescence. *J Struct Biol*. 2010;169:36-44

17. Kassiri Z, Oudit GY, Sanchez O, Dawood F, Mohammed FF, Nuttall RK, Edwards DR, Liu PP, Backx PH, Khokha R. Combination of tumor necrosis factor-alpha ablation and matrix metalloproteinase inhibition prevents heart failure after pressure overload in tissue inhibitor of metalloproteinase-3 knock-out mice. *Circ Res*. 2005;97:380-390

18. Perez-Martinez L, Jaworski DM. Tissue inhibitor of metalloproteinase-2 promotes neuronal differentiation by acting as an anti-mitogenic signal. *J Neurosci*. 2005;25:4917-4929

19. Kassiri Z, Defamie V, Hariri M, Oudit GY, Anthwal S, Dawood F, Liu P, Khokha R. Simultaneous transforming growth factor beta-tumor necrosis factor activation and cross-talk cause aberrant remodeling response and myocardial fibrosis in timp3-deficient heart. *J Biol Chem*. 2009;284:29893-29904

20. Noutsias M, Rohde M, Block A, Klippert K, Lettau O, Blunert K, Hummel M, Kuhl U, Lehmkuhl H, Hetzer R, Rauch U, Poller W, Pauschinger M, Schultheiss HP, Volk HD, Kotsch K. Preamplification techniques for real-time rt-pcr analyses of endomyocardial biopsies. *BMC Mol Biol*. 2008;9:3

21. Kandalam V, Basu R, Abraham T, Wang X, Soloway PD, Jaworski DM, Oudit GY, Kassiri Z. Timp2 deficiency accelerates adverse post-myocardial infarction remodeling because of enhanced mt1-mmp activity despite lack of mmp2 activation. *Circ Res*. 2010;106:796-808

22. Jaworski DM, Soloway P, Caterina J, Falls WA. Tissue inhibitor of metalloproteinase-2(timp-2)-deficient mice display motor deficits. *J Neurobiol*. 2006;66:82-94

23. Deschamps AM, Yarbrough WM, Squires CE, Allen RA, McClister DM, Dowdy KB, McLean JE, Mingoia JT, Sample JA, Mukherjee R, Spinale FG. Trafficking of the membrane type-1 matrix metalloproteinase in ischemia and reperfusion: Relation to interstitial membrane type-1 matrix metalloproteinase activity. *Circulation*. 2005;111:1166-1174

24. Spinale FG, Escobar GP, Mukherjee R, Zavadzkas JA, Saunders SM, Jeffords LB, Leone AM, Beck C, Bouges S, Stroud RE. Cardiac-restricted overexpression of membrane type-1 matrix metalloproteinase in mice: Effects on myocardial remodeling with aging. *Circ Heart Fail*. 2009;2:351-360

25. Zile MR, Baicu CF, Stroud RE, Van Laer A, Arroyo J, Mukherjee R, Jones JA, Spinale FG. Pressure overload-dependent membrane type 1-matrix metalloproteinase induction: Relationship to lv remodeling and fibrosis. *Am J Physiol Heart Circ Physiol*. 2012;302:H1429-1437

26. Jones JA, Ruddy JM, Bouges S, Zavadzkas JA, Brinsa TA, Stroud RE, Mukherjee R, Spinale FG, Ikonomidis JS. Alterations in membrane type-1 matrix metalloproteinase abundance after the induction of thoracic aortic aneurysm in a murine model. *Am J Physiol Heart Circ Physiol*. 2010;299:H114-124

CHAPTER 3

Early activation of matrix metalloproteinases underlies the exacerbated systolic and diastolic dysfunction in mice lacking TIMP3 following myocardial infarction

Vijay Kandalam[1,4], Ratnadeep Basu[1,4], Thomas Abraham[5], Xiuhua Wang[1,5], Ahmed Awad[1,4], Wei Wang[3,4], Gary D. Lopaschuk[3,4], Nobuyo Maeda[6], Gavin Y. Oudit[2,4], and Zamaneh Kassiri[1,4]

1*Department of Physiology,* 2*Department of Medicine/Division of Cardiology,* 3*Department of Pediatrics, and* 4*Cardiovascular Research Center and The Mazankowski Alberta Heart Institute, University of Alberta, Edmonton, Alberta,* 5*James Hogg iCAPTURE Centre, University of British Columbia, Vancouver, British Columbia, Canada, and* 6*University of North Carolina at Chapel Hill, Chapel Hill, North Carolina*

Contributions:

VK (40%): Cared for and monitored the animals, scheduled procedures, tissue collection, data collection, and project planning. Collected all tissue, processed all tissue, and conducted the majority of experiments and all data analysis. VK had a primary role in the writing of the manuscript and assembly of final figures.

RB: Analysis of all acquired raw echocardiography data and project planning, TA: performed SHG imaging, XW: performed LAD-ligation surgeries and Taqman RT-PCR, AA: assisted in zymography of 3 day post-MI samples, WW: performed the pilot LAD-ligation surgeries on a small set of animals, GL: input regarding surgical model with WW, NM: provided us with TIMP3$^{-/-}$ mice, GYO: worked in conjunction with RB to manage echocardiography analysis and interpretation, ZK: supervisor of VK, overall project planning and corresponding author.

A version of this chapter has been published. Kandalam et al. 2010. American Journal of Physiology- Heart and Circulatory Physiology. 299(4): H1012-23.

3.1. Introduction

Coronary artery disease is the most common cause of heart failure and remains a major cause of morbidity and mortality worldwide[1]. MI leads to a region and time-dependent adverse myocardial remodeling resulting in ventricular dilation, dysfunction, and infarct rupture that can result in sudden cardiac death and/or heart failure[2-4]. Free wall myocardial rupture is a fatal complication of acute MI and is associated with a high mortality[5, 6]. Impaired remodeling of the ECM is a critical contributor to postinfarction dilation, dysfunction, and myocardial rupture[7, 8]. ECM integrity is maintained by a balance in the function of MMPs, which degrade ECM proteins, and their physiological inhibitors, the TIMPs. Altered plasma profiles of MMPs/TIMPs correlate with adverse post-MI ventricular remodeling in patients[9]. MMPs have been shown to play a key role in post-MI LV rupture in animal models[10, 11], as well as in patients who died of LV rupture[12]. Among the TIMPs, TIMP3 is ECM bound, is highly expressed in the heart[13], can inhibit a broad spectrum of metalloproteinases, and is downregulated in the ischemic myocardium of animals[14], as well as in patients with ischemic heart failure[15]. TIMP3 deficiency severely compromises cardiac response to pressure overload, resulting in the early development of dilated cardiomyopathy[16] and excess myocardial fibrosis[17], as well as accelerated adverse LV remodeling post-MI[18].

3.2. Objectives

Myocardial remodeling following infarction is a complex process orchestrated by a number of cellular and extracellular events[4, 19]. Hence, identifying the early events that lead to activation of multiple factors in mediating adverse cardiac response to MI can provide new potential therapies to lessen the resulting complications. For this we examined the remodeling process in specified regions of the LV myocardium at an early timepoint with great relevance to the expected phenotype and which has only been briefly explored

previously. TIMP3 is highly expressed in the heart, and is markedly downregulated in patients with ischemic cardiomyopathy[15]. We therefore examined the time- and region-dependent role of TIMP3 in the cardiac response to MI.

3.3. Methods

3.3.1. LAD coronary artery ligation

Mice that were 11-12 weeks old were anesthetized and underwent surgical LAD ligation according to protocol in Chapter 2.2.1 to generate a state of ischemia leading to myocardial infarction. Sham-operated mice were used as controls. Mice were allowed to recover and monitored as described in Chapter 2.4.1.

3.3.2. *In vivo* imaging and analysis

Echocardiography was conducted to examine parameters pertaining to MI analysis as described in Chapter 2.5.1. TMD (Chapter 2.5.2), TDI (Chapter 2.5.3), and EKV (Chapter 2.5.4) modes were also utilized for complete *in vivo* analysis of cardiac function.

3.3.3. Molecular and cellular analysis

Sham and post-MI tissue was collected as described in Chapter 2.4.2.1., and processed for molecular (RNA in Chapter 2.8., protein in Chapter 2.9., and MMP activity in Chapter 2.11.1.), histological (neutrophils staining in Chapter 2.7.2), and morphological (left ventricle morphology in Chapter 2.6.1.1., infarct size in Chapter 2.6.1.2., and collagen organization in Chapter 2.6.2.3.) analysis.

3.3.4. *In vivo* MMPi treatment of MI

A broad-spectrum MMPi, PD-166793 (Pfizer Inc.) was administered by daily gavage as described in Chapter 2.3. PD-166793 treatment (30 $mg \cdot kg^{-1} \cdot day^{-1}$) of the $TIMP3^{-/-}$ MI mice began 2 days before MI and was continued until 2 days post-MI.

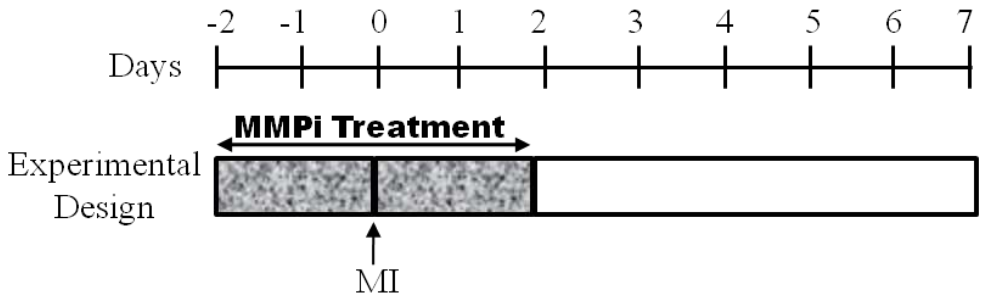

Figure 3.1. Pharmacological MMPi administration in experimental MI.

Pharmacological MMPi PD166793 (Pfizer) was delivered through daily gavage (30mg/kg•day) to $TIMP3^{-/-}$ mice starting 2 days prior to MI, and was continued until two days post-MI in order to examine the effect of early MMP inhibition in post-MI cardiac remodeling in the $TIMP3^{-/-}$ mice.

3.4. Results

3.4.1. Myocardial infarction alters TIMP levels in a region and time-dependent fashion

The mRNA (Figure 3.4.) and protein levels (Figure 3.2. and Figure 3.3) were measured for all TIMPs in the infarct, peri-infarct and non-infarct regions of WT mice at 3 days (Figure 3.2.) and 1 week post-MI (Figure 3.3.). At 3 days post-MI, TIMP1 protein levels were significantly increased in the infarct and peri-infarct myocardium, while its levels in the non-infarct region was additionally increased by 1 week post-MI. TIMP2 levels were decreased in the peri- and non-infarct myocardium at both time points. TIMP3 and TIMP4 levels were markedly reduced in the infarct region at both time points, while TIMP3 levels were also reduced in the peri- and non-infarct regions at 3 days post-MI. Changes in the mRNA levels (Figure 3.4.), however, did not directly correspond to the alterations in protein levels, as also reported previously[20, 21]. For instance, at 1 week post-MI, TIMP3 mRNA levels were elevated in the infarct region, but unaltered in the peri-infarct and infarct regions, while its protein levels remained markedly reduced in the infarct and peri-infarct areas. This could represent a compensatory response to the loss of the TIMP3 protein, and/or the TIMP3 mRNA synthesized by infiltrating fibroblasts.

Among all TIMPs, TIMP3 showed a marked reduction in all regions of myocardium early post-MI, with the greatest reduction in the infarct followed by peri- and non-infarct regions, suggesting a region and time sensitive loss of TIMP3 protein during the early cardiac response to MI. Next, we examined if TIMP3 deficiency impacted the alterations in TIMP levels post-MI (Figures 3.2. and 3.3.). Compared to WT mice, $TIMP3^{-/-}$ mice showed a markedly smaller increase in TIMP levels in the peri-infarct area at 3 days and in all regions at 1 week post-MI, but greater TIMP2 and TIMP4 protein levels in the infarct area at 3 days post-MI, which persisted for TIMP4 at 1week post-MI (Figures 3.2. and 3.3.).

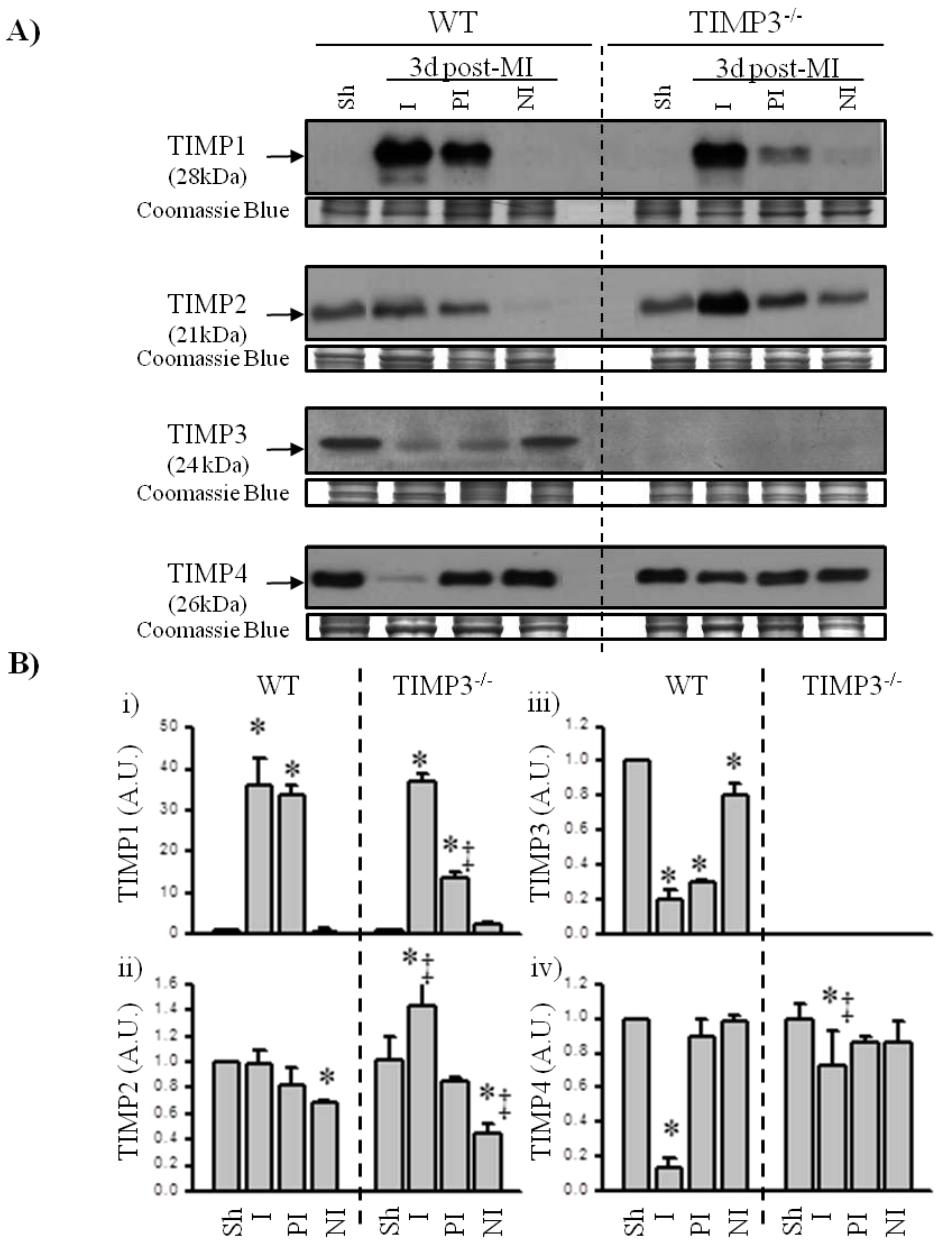

Figure 3.2. TIMP levels are altered in response to MI.

Representative western blots (A), and averaged protein levels (B.i-iv) for TIMP1, TIMP2, TIMP3 and TIMP4 in sham (sh), infarct (I), peri-infarct (PI), and non-infarct (NI) myocardium of WT and TIMP3$^{-/-}$ mice at 3 days post-MI. (n=4/group/genotype). Coomassie blue was used as internal control. A.U.= Arbitrary Units. Values are presented as mean ± SEM. *$p<0.05$ compared to sham, ‡$p<0.05$ compared to WT using two-way ANOVA analysis.

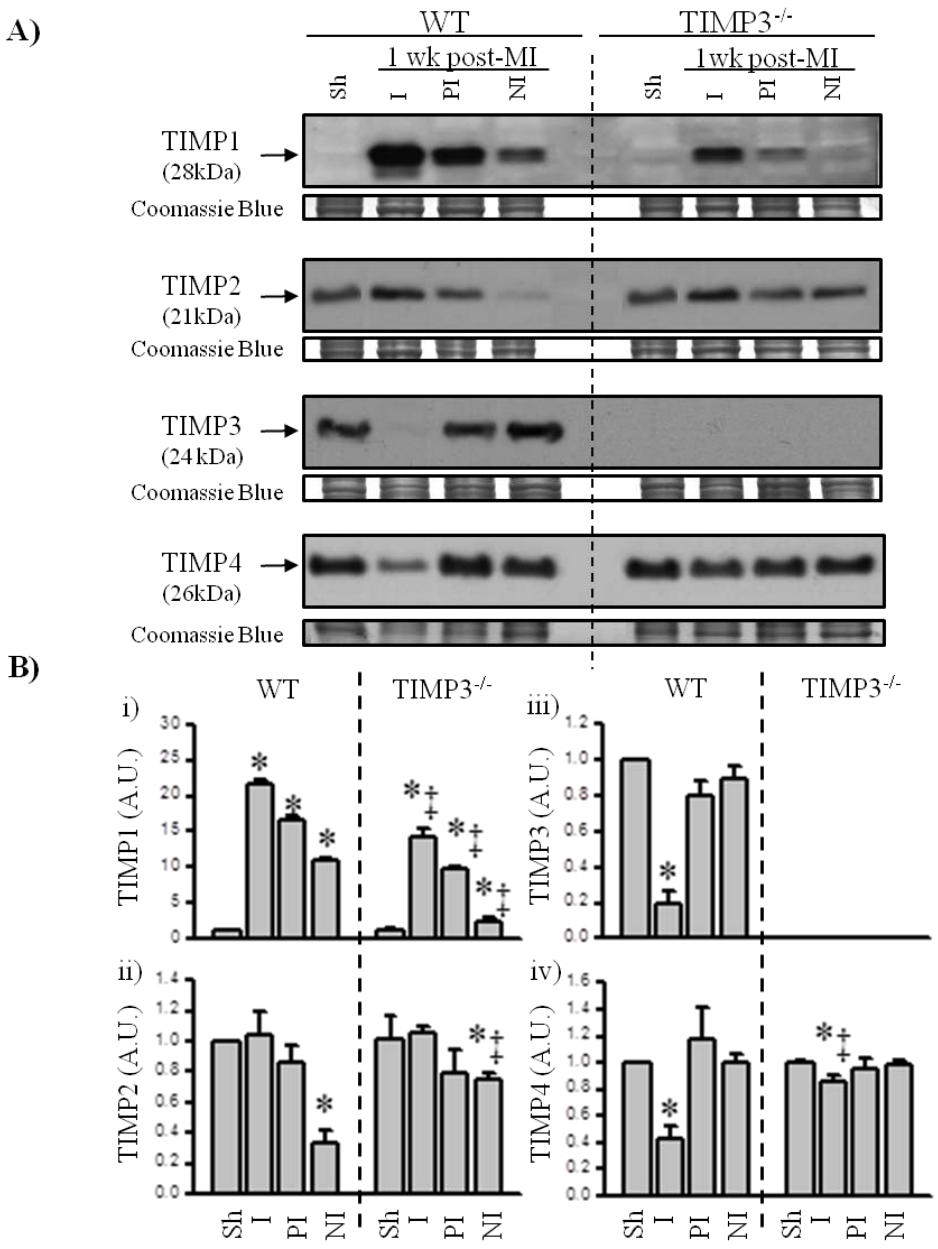

Figure 3.3. Differential protein levels of TIMPs following MI.

Representative western blots (A), and averaged protein levels (B.i-iv) for TIMP1, TIMP2, TIMP3 and TIMP4 in sham (sh), infarct (I), peri-infarct (PI), and non-infarct (NI) myocardium of WT and TIMP3$^{-/-}$ mice at 1 week post-MI. (n=4/group/genotype). Coomassie blue was used as internal control. A.U.= Arbitrary Units. Values are presented as mean ± SEM. *p<0.05 compared to sham, ‡p<0.05 compared to WT using two-way ANOVA analysis.

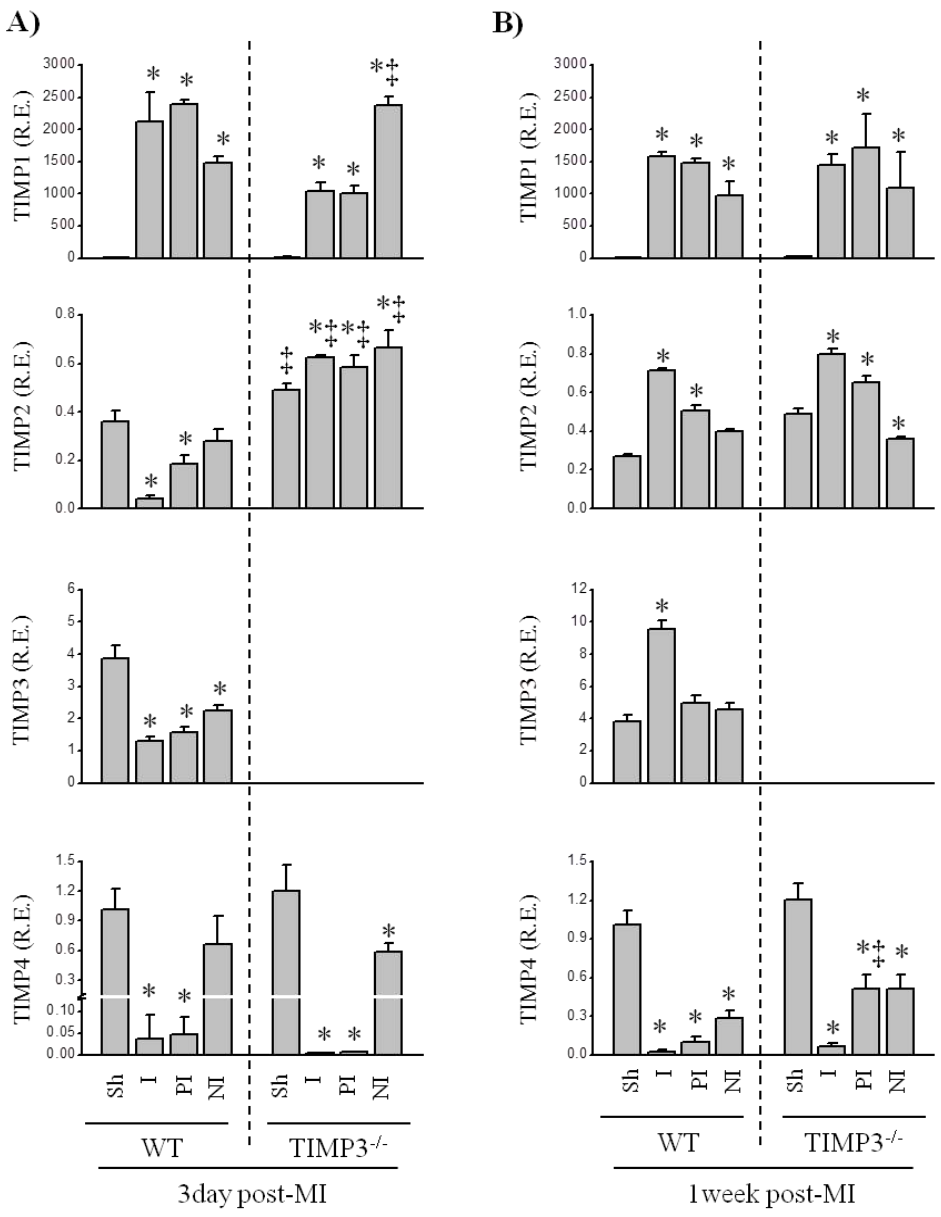

Figure 3.4. Expression of TIMPs is altered differentially between WT and TIMP3$^{-/-}$ mice post-MI.

mRNA expression of TIMP1, TIMP2, TIMP3 and TIMP4 in sham, infarct (I), peri-infarct (PI) and non-infarct (NI) regions of WT and TIMP3$^{-/-}$ heart at 3 days (A) and 1 week post-MI (B). R.E.=Relative Expression, MI=myocardial infarction. Presented values are Mean ± SEM. *$p<0.05$ compared to sham, ‡$p<0.05$ compared to WT using two-way ANOVA analysis.

3.4.2. Suppressed post-MI survival in TIMP3$^{-/-}$ mice due to excess LV rupture

To determine if the reduction in TIMP3 post-MI underlies the disease progression, and if the early rise in TIMP2 and TIMP4 in the infarct myocardium of TIMP3$^{-/-}$ mice compensate for the absence of TIMP3, we examined the cardiac response of TIMP3-deficient to MI compared to age-matched WT mice over 4 weeks. TIMP3$^{-/-}$ mice showed a significantly decreased rate of survival compared to WT mice over 4 weeks post-MI (Figure 3.5.A). Autopsy results revealed that majority of the mice had died due to LV rupture that lead to hemopericardium and/or hemothorax. Left ventricular rupture occurred in 81% of TIMP3$^{-/-}$ mice at 3-7 days post-MI compared to 32% in WT mice (Figure 3.5.B). Gross histological analysis of WT and TIMP3$^{-/-}$ hearts at 3 days, 1 week and 4 weeks post-MI showed greater LV dilation and larger infarct expansion in the TIMP3$^{-/-}$ mice (Figure 3.6.A). Our findings further demonstrate that the increased TIMP2 and TIMP4 protein in the infarct area was not sufficient to compensate for the absence of TIMP3 and to improve the rate of post-MI rupture. Further analysis of the infarct size showed that despite comparable initial infarct sizes at 1 day post-MI, TIMP3$^{-/-}$ mice developed a 25% greater infarct expansion compared to WT mice by 1 week post-MI (Fig. 3.6.B).

3.4.3. TIMP3-deficiency leads to greater LV dilation, exacerbated systolic and diastolic dysfunction post-MI associated with aberrant ECM remodeling

Echocardiographic imaging at 1 week (Table 3.1.) and 4 weeks post-MI (Table 3.2.) revealed markedly greater LV dilation, and lower EF indicating marked suppression in systolic function in TIMP3$^{-/-}$ compared to WT mice. WMSI is a validated method of evaluating regional LV wall motion abnormalities and correlates with the degree of adverse ventricular remodeling post-MI[20, 22, 23]. A WMSI value of 1 indicates intact LV wall motion and contractility, as found in sham-operated mice. At 1 week post-MI, TIMP3$^{-/-}$ hearts showed significantly higher WMSI indicating more severe adverse regional remodeling in the ventricles compared to WT mice, due primarily to worsening of mid-ventricular

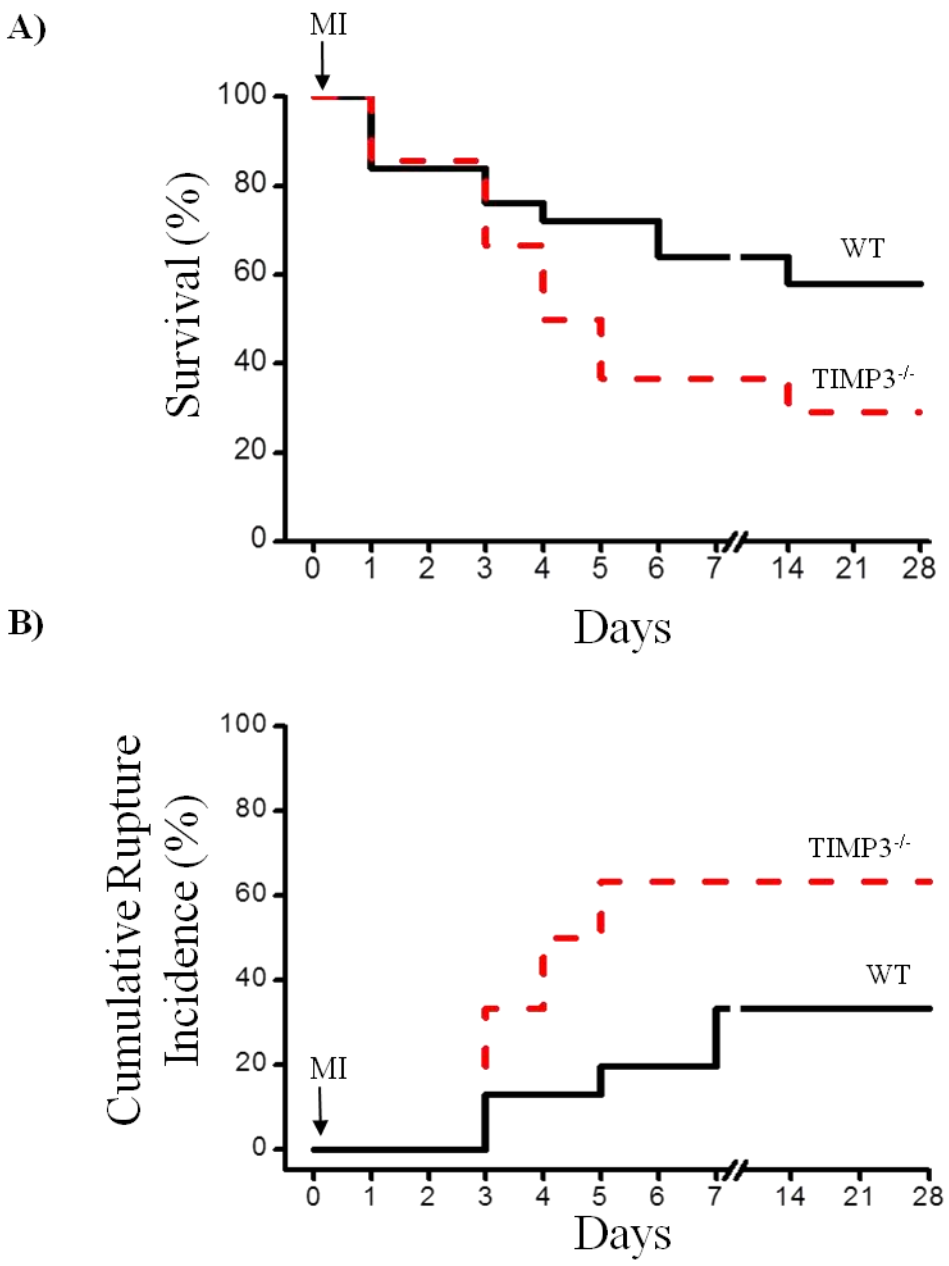

Figure 3.5. Severely compromised rate of survival post-MI in the absence of TIMP3.

Rate of total survival (A) and cumulative rate of rupture incidence (B) in WT (solid line, n=35) and TIMP3$^{-/-}$ mice (dashed line, n=50) over 4 weeks following MI.

Table 3.1. Echocardiographic parameters show more severe structural and functional deterioration in TIMP3$^{-/-}$ compared to WT mice at 1 week post-MI.

	WT-Sham	WT-MI	TIMP3$^{-/-}$-Sham	TIMP3$^{-/-}$-MI
Sample size (n)	6	8	6	8
HR (bpm)	489±17	494±20	482±18	499±20
LVEDV (µL)	65.9±2.1	133.1±14.5*	66.1±4.6	165.4±20.2*‡
LVESV (µL)	28.4±3.0	95.4±14.4*	30.8±2.6	135.8±23.9*‡
LVPWTd (mm)	0.75±0.02	0.64±0.06*	0.73±0.01	0.52±0.02*
EF (%)	66.7±0.2	37.1±6.2*	60.4±0.3	17.4±2.6*‡
WMSI	1	1.67±0.09*	1	2.48±0.06*‡
E'/A'	1.3±0.2	0.9±0.1*	1.1±0.1	0.7±0.1*‡
LA size (mm)	1.5±0.1	2.2±0.2*	1.6±0.1	2.5±0.1*‡
IVRT (ms)	14.7±0.5	17.5±1.1*	14.2±0.7	21.9±2.1*‡
DT (ms)	22.7±0.6	24.4±2.3	23.3±0.8	29.3±3.6*‡

HR= Heart Rate; LVEDV= LV End-Diastolic Pressure; LVESV= LV End-Systolic Volume; LVPWTd= LV posterior wall thickness in diastole; EF= Ejection Fraction; WMSI= Wall motion score index; E'/A'= ratio of early tissue Doppler velocity (E') to tissue Doppler velocity due to atrial contraction (A'); LA size= left atrium size; IVRT= isovolumetric relaxation time (of the LV); DT= deceleration time of the E-wave . *$p<0.05$ compared to corresponding sham-operated group; Values are presented as mean±SEM; ‡ $p<0.05$ compared with WT-MI group using two-way ANOVA analysis.

Table 3.2. Echocardiographic parameters show greater structural and functional deterioration in TIMP3$^{-/-}$ compared to WT mice at 4 week after MI.

	WT-Sham	WT-MI	TIMP3$^{-/-}$-Sham	TIMP3$^{-/-}$-MI
Sample size (n)	6	10	6	10
HR (bpm)	489±17	492±14	490±9	499±20
LVEDV (µL)	68.5±5.4	167.5±15.2*	66.8±3.7	190.4±15.5*‡
LVESV (µL)	31.8±2.1	138.3±14.2*	29.4±3.1	165.2±5.5*‡
EF (%)	61.4±1.3	25.5±3.2*	63.7±2.1	12.2±4.3*‡
E'/A'	1.1±0.1	0.8±0.1*	1.2±0.1	0.6±0.1*
LA size (mm)	1.5±0.2	2.3±0.2*	1.6±0.1	2.6±0.3*
IVRT (ms)	14.2±0.7	19.2±1.2*	14.7±0.5	25.1±2.3*‡
DT (ms)	23.3±0.9	25.9±1.3	25.5±2.1	32.4±1.9*‡

HR= Heart Rate; LVEDV= LV End-Diastolic Pressure; LVESV= LV End-Systolic Volume; LVPWTd= LV posterior wall thickness in diastole; EF= Ejection Fraction; WMSI= Wall motion score index; E'/A'= ratio of early tissue Doppler velocity (E') to tissue Doppler velocity due to atrial contraction (A'); LA size= left atrium size; IVRT= isovolumetric relaxation time (of the LV); DT= deceleration time of the E-wave . *$p<0.05$ compared to corresponding sham-operated group; Values are presented as mean±SEM; ‡ $p<0.05$ compared with WT-MI group using two-way ANOVA analysis.

and apical wall motion. TDI further revealed that mice lacking TIMP3 developed a more severe diastolic dysfunction as indicated by markedly lower ratio of E'-wave to A'-wave, larger left atrium, elevated LV isovolumetric relaxation time and increased deceleration time which indicate impaired relaxation (Table 3.1. and Table 3.2.). These results demonstrate that loss of TIMP3 leads to greater LV dilation and worsening of LV wall motion, systolic and diastolic dysfunction following MI.

TIMP3 is a potent inhibitor of a number of MMPs that degrade the ECM structural proteins. In addition, the severe LV dilation in TIMP3$^{-/-}$ mice indicates structural instability that could result from disrupted ECM structure. We assessed ECM structure in the infarct and non-infarct myocardium of WT and TIMP3$^{-/-}$ mice at 3 days post-MI by second harmonic generation imaging of unfixed and unstained hearts as before[20]. We found that TIMP3-deficient mice exhibited lower density and greater disarray of collagen fibers in the infarct area compared to WT hearts (Figure 3.7.B), while expression of procollagen type I and procollagen type III were comparable between the genotypes (Fig. 3.7.Ci-ii) suggesting that excess MMP activity and collagen degradation in TIMP3$^{-/-}$ mice.

3.4.4. Early post-MI proteolysis is markedly elevated in the TIMP3$^{-/-}$ mice

MMPs have been linked to LV dilation, rupture and inflammation post-MI[10-12, 24]. We therefore performed gelatin zymography to determine the levels of MMP2 and MMP9, the two MMPs that have been associated with LV rupture post-MI[11, 24]. We assessed the total proteolytic activity in the infarct, peri-infarct and non-infarct myocardial tissue by using gelatinase and collagenase activity assays from EnzChek. At 1 day post-MI, MMP9 and active MMP2 were detectable in the infarct and peri-infarct regions of TIMP3$^{-/-}$ but not WT hearts (Figure 3.8.A & 3.8.B). Consistently, total gelatinase (Figure 3.8.C.i) and collagenase activities (Figure 3.8.C.ii) were significantly greater in TIMP3$^{-/-}$ compared to WT myocardium. Interestingly, by 3 days post-MI, gelatin zymography showed elevated MMP9 and active MMP2 only in the non-infarct myocardium of TIMP3$^{-/-}$ compared to WT hearts (Figure 3.9.A. and 3.9.B.).

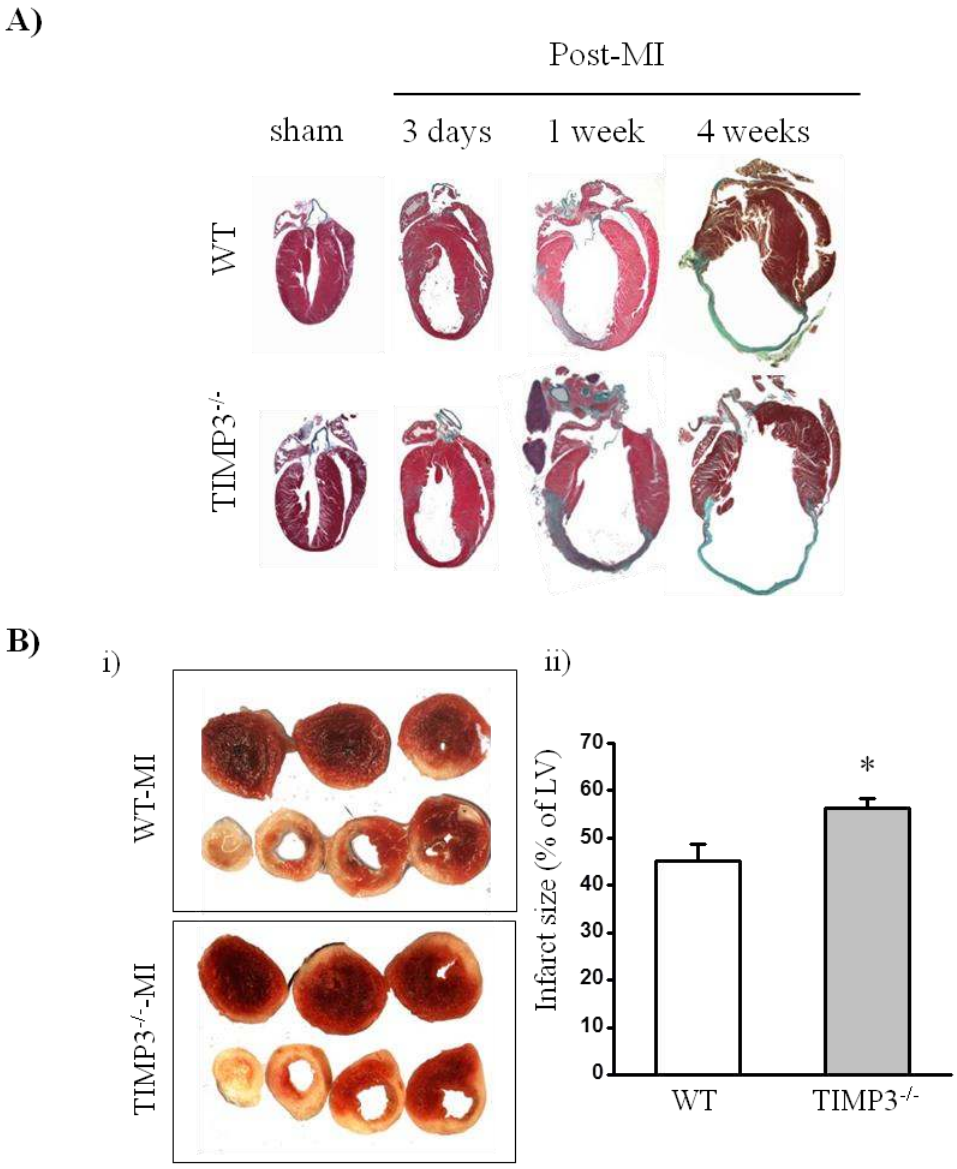

Figure 3.6. Lack of TIMP3 results in increased left ventricular dilation and infarct expansion post-MI.

A) Gross morphology of WT and TIMP3$^{-/-}$ hearts following sham operation or 3 days, 1 week and 4 weeks after MI. B) Representative TTC-stained WT and TIMP3$^{-/-}$ hearts (i), and averaged infarct size (ii, n=8/genotype) at 1 week post-MI. LV=left ventricle. *$p<0.05$ compared to WT using Student's T-test analysis.

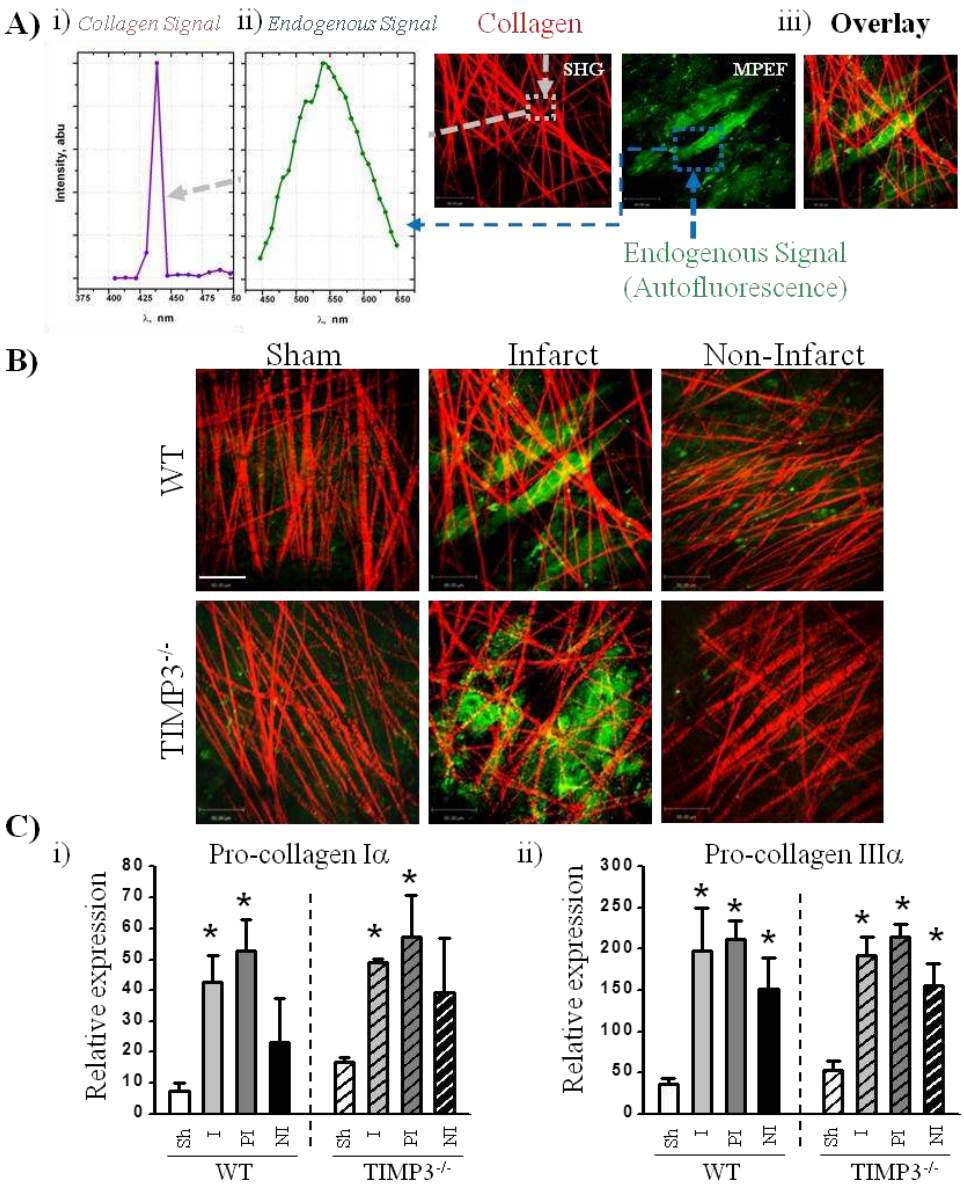

Figure 3.7. Lack of TIMP3 results in aberrant degradation of the fibrillar structure of the extracellular matrix.

A) SHG (red) (i) and MPEF (green) imaging (ii) were used to visualize the collagen fibers and endogenous autofluorescence, respectively. iii) Superimposed SHG and MPEF images. B) Representative images showing the density and organization of the collagen fibers in the infarct and non-infarct myocardium of WT and TIMP3$^{-/-}$ mice at 3 days post-MI. Scale bar=80μm. C) Taqman mRNA expression of procollagen type I (i) and procollagen type III (ii) in WT and TIMP3$^{-/-}$ mice at 3 days post-MI, n=5/group, *p<0.05 compared to sham, ‡p<0.05 compared to WT-MI using two-way ANOVA analysis.

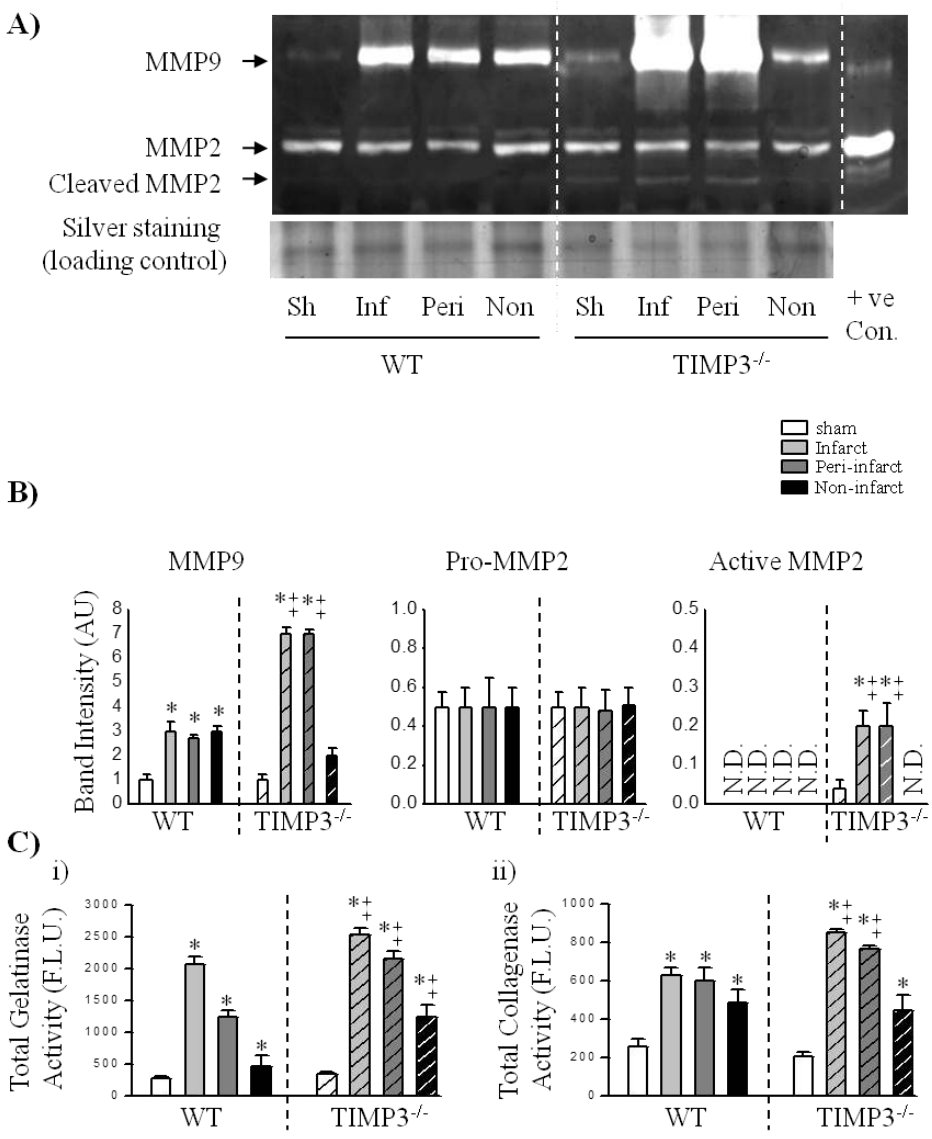

Figure 3.8. TIMP3 deficiency triggers a rapid and transient increase in MMP levels and activity 1 day post-MI

Representative gelatin zymography (A) and averaged band intensities for MMP9, proMMP2 and active MMP2 (B), total gelatinase activity (C-i) and total collagenase activity (C-ii) in WT and TIMP3$^{-/-}$ hearts at 1 day post-MI. sh=sham, inf=infarct, peri=peri-infarct, non=non-infarct. A.U.=Arbitrary Units, R.E.=Relative Expression, F.L.U.=Fluorescent Light Unit, n=6/group/genotype. *p<0.05 compared to sham, ‡p<0.05 compared to WT using two-way ANOVA analysis.

Total gelatinase activity (Figure 3.9.C.i), but not collagenase activity (Figure 3.9.C.ii), was higher in the peri-infarct TIMP3$^{-/-}$ myocardium. A similar pattern was observed at 1 week post-MI (Figure 3.10). These data indicate that myocardial infarction results in time and region-specific alterations including a very early rise in MMP activities, which could be a key determinant of the subsequent LV remodeling and dysfunction.

3.4.5. Increased rate of LV rupture in TIMP3$^{-/-}$-MI mice is associated with heightened inflammation

Myocardial infarction triggers a rapid inflammatory response that involves the influx of leukocytes in the infarct and peri-infarct regions of the myocardium[25, 26]. Among the leukocytes, neutrophils are the first responders[24], and neutrophil influx in the infarct area of myocardium has been linked to LV rupture post-MI[27, 28]. TIMP3 deficiency has been shown to result in increased inflammation in other disease models[29, 30]. Staining for neutrophils revealed a significantly greater population of these cells in the infarct and peri-infarct regions of TIMP3$^{-/-}$ compared to WT hearts at 3 days post-MI (Figure 3.11). In addition, expression of inflammatory MMPs was increased in these hearts. MMP8 mRNA levels were significantly higher in all regions, and MMP12 in the infarct area of TIMP3$^{-/-}$ hearts (Figure 3.12.A.i and 3.12.A.*ii*). The severe inflammation and expression of inflammatory MMPs in TIMP3-deficient mice at 3 days post-MI coincides with the peak of LV rupture post-MI. In addition, MT1-MMP, a major collagenase in the heart was significantly elevated in TIMP3$^{-/-}$ myocardium (Figure 3.12.A.iii).

3.4.6. Early inhibition of MMPs blunts the adverse outcomes of TIMP3-deficiency

Next, we aimed to determine if the early rise in total MMP activities is in fact the underlying mechanism for the more severe LV remodeling, dysfunction and rupture in TIMP3$^{-/-}$ mice. We treated TIMP3$^{-/-}$ mice with PD166793, a broad-

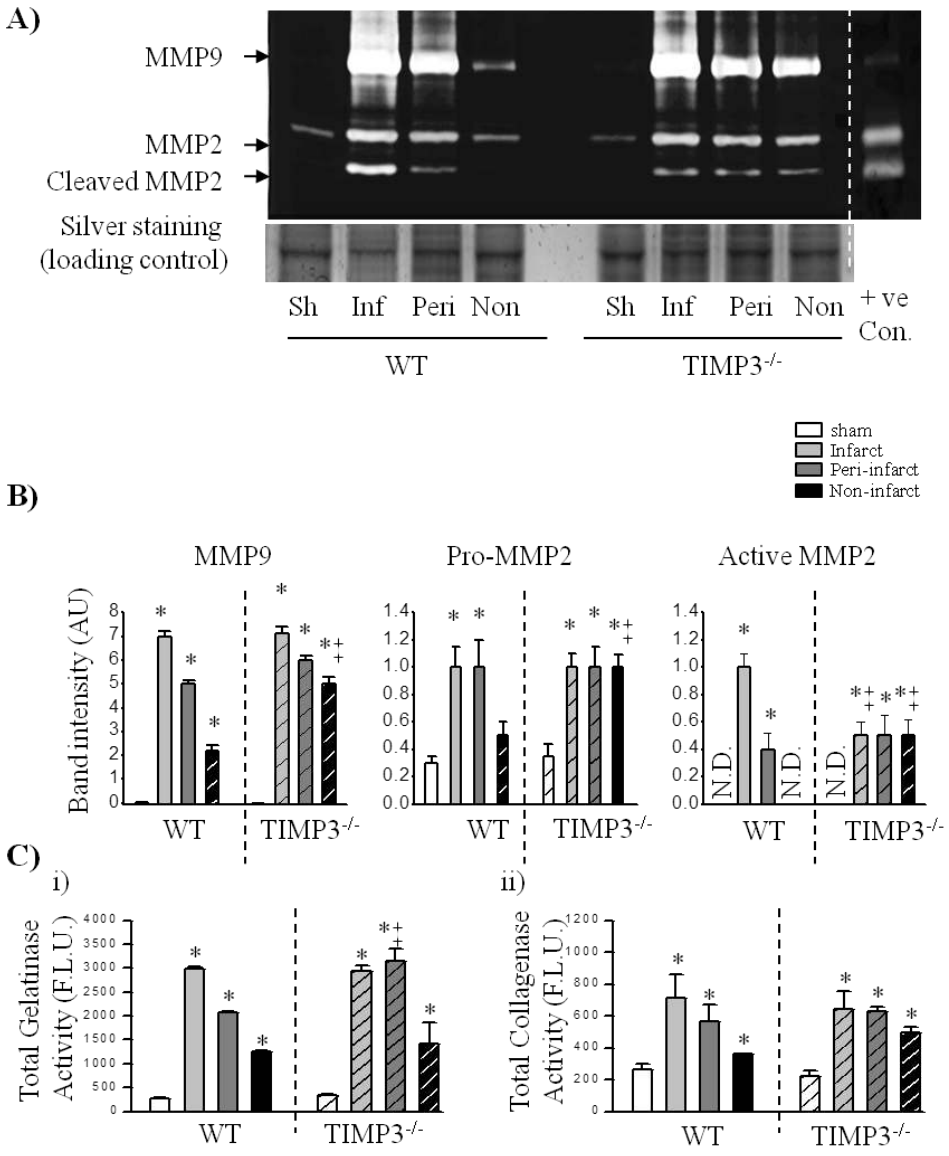

Figure 3.9. Lack of TIMP3 sustains an early increase in MMP levels and activity at 3 days following MI.

Representative gelatin zymography (A) and averaged band intensities for MMP9, proMMP2 and active MMP2 (B), total gelatinase activity (C-i) and total collagenase activity (C-ii) in WT and TIMP3$^{-/-}$ hearts at 3 day post-MI. sh=sham, inf=infarct, peri=peri-infarct, non=non-infarct. A.U.=Arbitrary Units, R.E.=Relative Expression, F.L.U.=Fluorescent Light Unit, n=6/group/genotype. *p<0.05 compared to sham, ‡p<0.05 compared to WT using two-way ANOVA analysis.

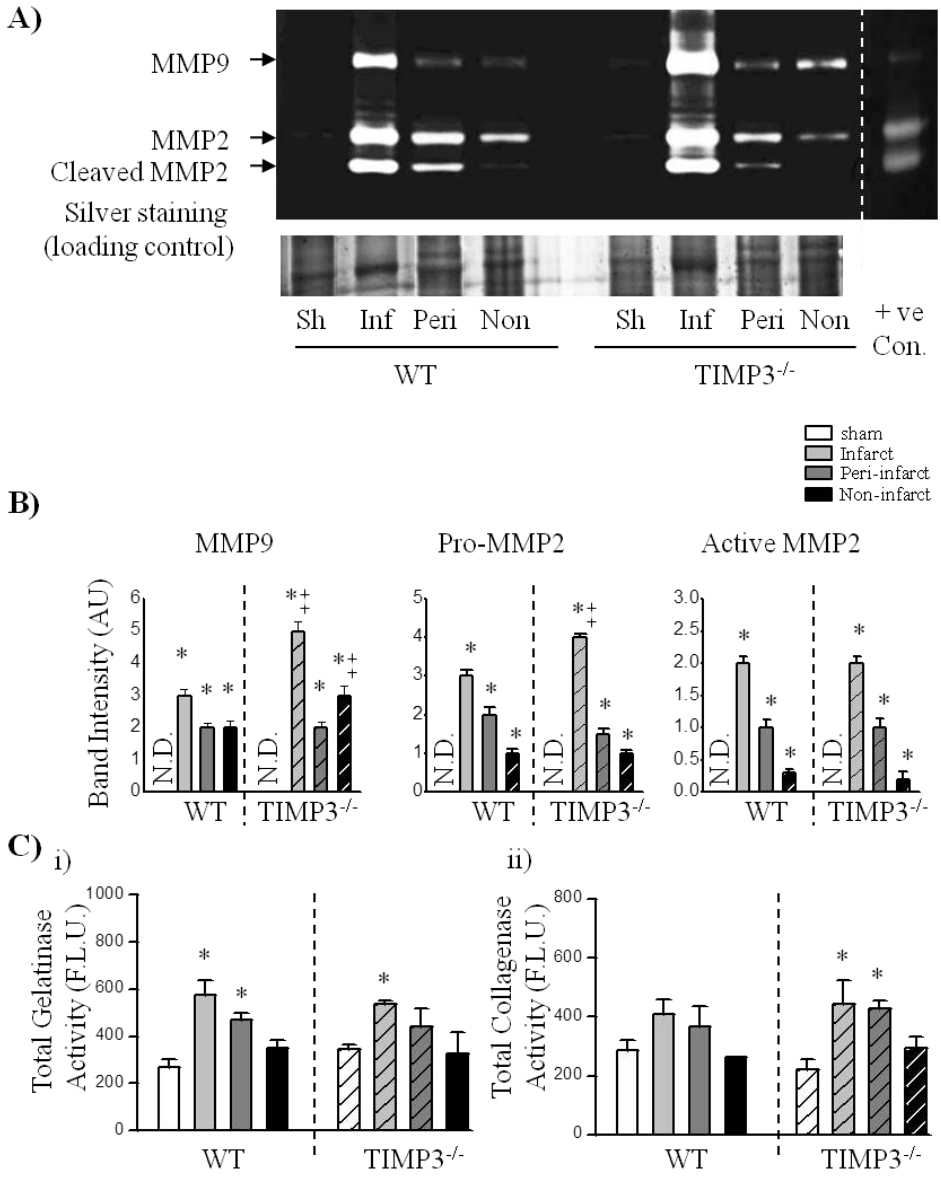

Figure 3.10. TIMP3 deficiency exhibits a diminished difference in MMP levels and activity by 1 week after MI.

Representative gelatin zymography (A) and averaged band intensities for MMP9, proMMP2 and active MMP2 (B), total gelatinase activity (C-i) and total collagenase activity (C-ii) in WT and TIMP3$^{-/-}$ hearts at 1 week post-MI. sh=sham, inf=infarct, peri=peri-infarct, non=non-infarct. A.U.=Arbitrary Units, R.E.=Relative Expression, F.L.U.=Fluorescent Light Unit, n=6/group/genotype. *p<0.05 compared to sham, ‡p<0.05 compared to WT using two-way ANOVA analysis.

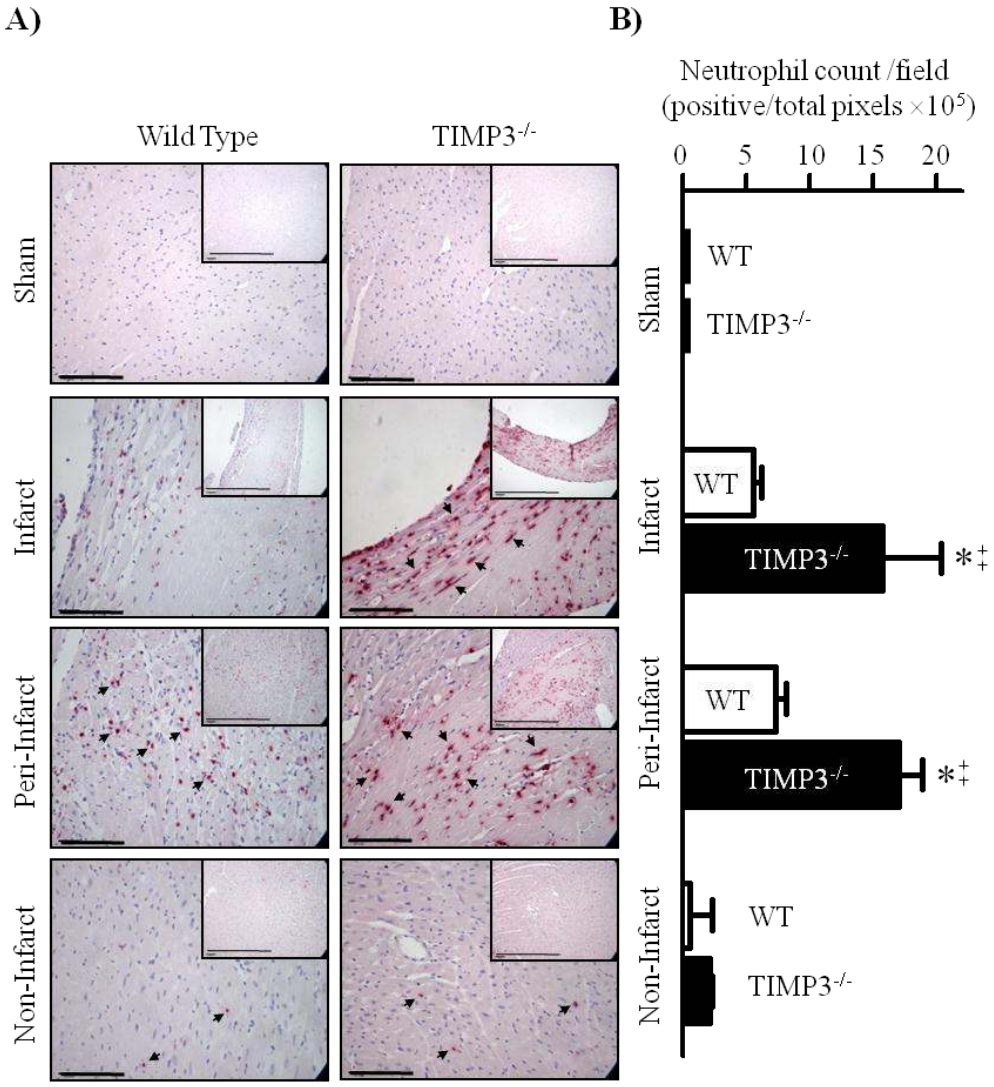

Figure 3.11. Enhanced neutrophil infiltration in the TIMP3-deficient infarct and peri-infarct myocardium at 3 days post-MI.

A) Immunostaining for mouse neutrophils in WT and TIMP3$^{-/-}$ hearts after sham or MI (red). Scale bar=100μm. Inset shows a lower magnification, Scale bar=200 μm. B) Averaged neutrophil counts in sham, infarct, peri-infarct and non-infarct myocardium in WT and TIMP3$^{-/-}$ mice. Neutrophil counts were performed on 6 fields/cross-section, 3 cross-sections/ heart, and 5 hearts/genotype. *$p<0.05$ compared to sham, ‡$p<0.05$ compared to WT using two-way ANOVA analysis.

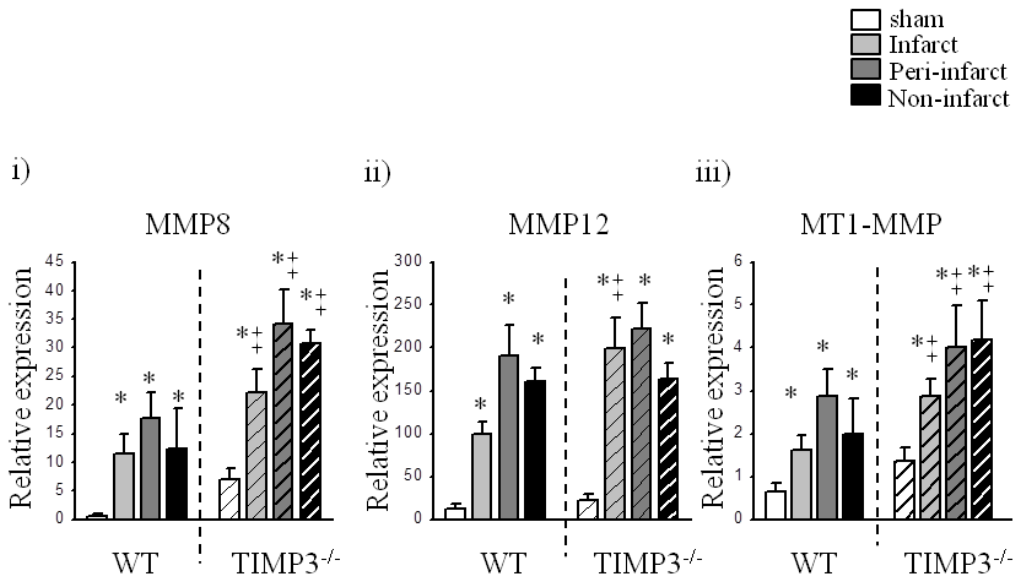

Figure 3.12. Enhanced collagenase expression levels in the TIMP3-deficient infarct and peri-infarct myocardium at 3 days post-MI.

Expression levels of inflammatory MMPs, MMP8 (i) and MMP12 (ii), and collagenase MT1-MMP (iii) in WT and TIMP3$^{-/-}$ hearts, n=6/group/ genotype. *p<0.05 compared to sham, ‡p<0.05 compared to WT using two-way ANOVA analysis.

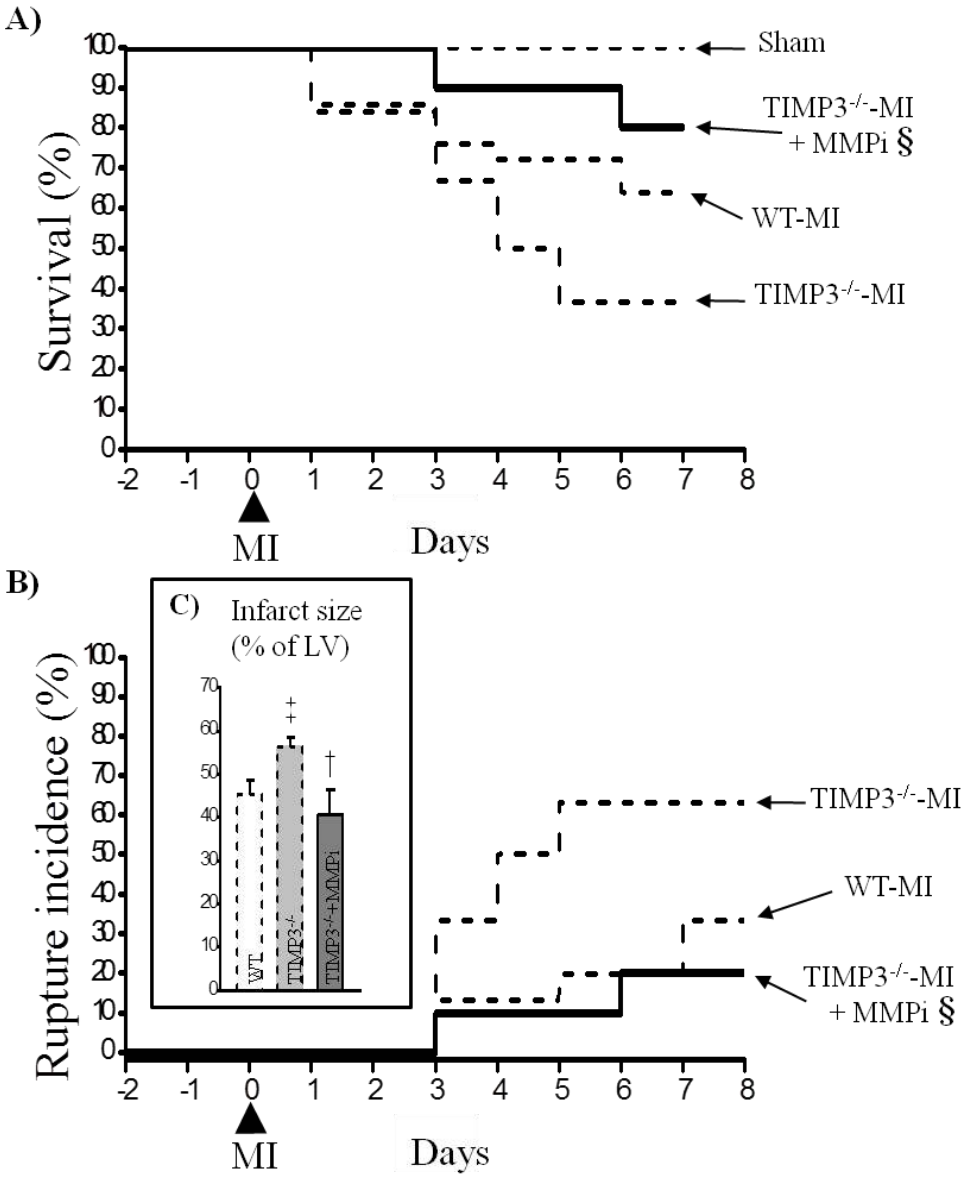

Figure 3.13. Early treatment with an MMP inhibitor (PD166793) improved post-MI survival in TIMP3$^{-/-}$ mice.

Total survival (A) and cumulative rate of LV rupture (B) in sham-WT/TIMP3$^{-/-}$ (n=10/genotype), WT-MI (n=35), TIMP3$^{-/-}$-MI (n=50), and TIMP3$^{-/-}$-MI+MMPi (n=20) groups. C) Infarct size at 1 week post-MI for WT (n=8), TIMP3$^{-/-}$ (n=8) and TIMP3$^{-/-}$+MMPi (n=6) groups. ‡ $p<0.05$ compared to WT-MI, † $p<0.05$ compared to TIMP3$^{-/-}$-MI using one-way ANOVA analysis, § $p<0.05$ compared to TIMP3$^{-/-}$-MI using Kaplan-Meier curve and log rank test.

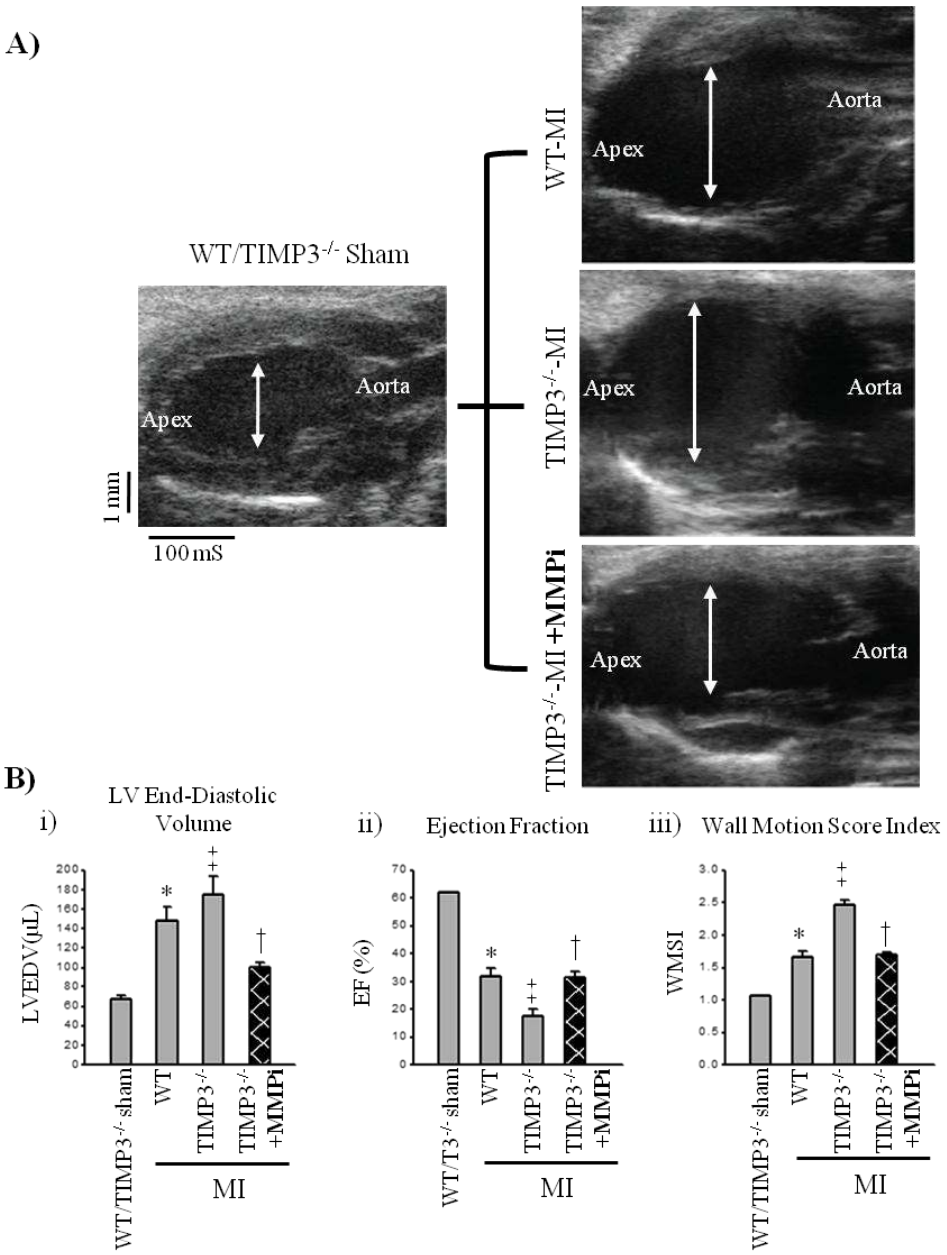

Figure 3.14. Early MMP inhibition markedly improved LV dilation and systolic dysfunction in TIMP3$^{-/-}$ mice post-MI.

Representative parasternal long axis view (A) from sham of either genotype, WT-MI, TIMP3$^{-/-}$-MI and TIMP3$^{-/-}$-MI hearts with MMPi treatment at 1 week post-MI. B) Averaged left ventricular end-diastolic volume (LVEDV) (i), ejection fraction (EF) (ii), and wall motion score index (WMSI) (iii) in sham-operated (n=5/group), WT-MI, TIMP3$^{-/-}$-MI and TIMP3$^{-/-}$-MI+MMPi groups (n=8/group). *p<0.05 compared to sham, ‡p<0.05 compared to WT-MI, † p<0.05 compared to TIMP3$^{-/-}$-MI using one-way ANOVA analysis.

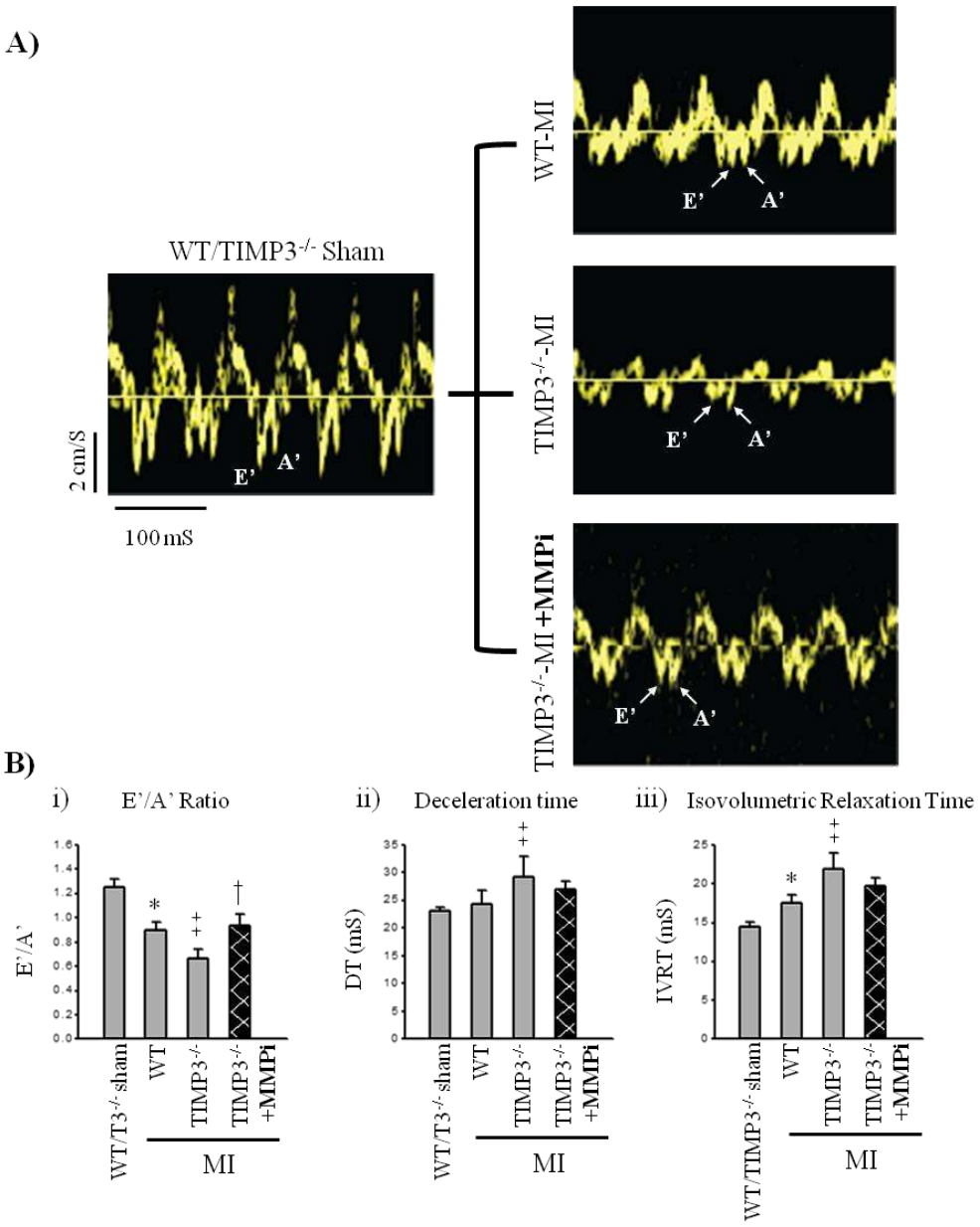

Figure 3.15. Early MMP inhibition exhibits subtle improvement in LV diastolic function in TIMP3$^{-/-}$ mice after MI.

Representative tissue Doppler images (A) from sham of either genotype, WT-MI, TIMP3$^{-/-}$-MI and TIMP3$^{-/-}$-MI hearts with MMPi treatment at 1 week post-MI. B) Averaged diastolic parameters, E'/A' ratio (i), deceleration time of the E-wave (DT) (ii), and isovolumetric relaxation time of LV (IVRT) (iii) in sham-operated (n=5/group), WT-MI, TIMP3$^{-/-}$-MI and TIMP3$^{-/-}$-MI+MMPi groups (n=8/group). *p<0.05 compared to sham, ‡p<0.05 compared to WT-MI, † p<0.05 compared to TIMP3$^{-/-}$-MI using one-way ANOVA analysis.

spectrum MMP-inhibitor that does not inhibit ADAM17/TACE[31], 2 days prior to and 2 days after induction of MI (Figure 3.1.). This treatment significantly improved total survival (Figure 3.13.A.) and the rate of LV rupture incidence (Figure 3.13.B) in TIMP3$^{-/-}$ mice. In addition, this early MMPi-treatment decreased the infarct expansion (Figure 3.13.C), reduced LV dilation (Figure 3.14.A. and 3.14.B.i), improved the systolic dysfunction as indicated by increased EF (Figure 3.14.B.ii) and lowered WMSI (Figure 3.14.B.iii), and improved diastolic dysfunction as shown by increased E'/A' ratio (Figure 3.15.B.i) in TIMP3$^{-/-}$ mice. This experiment illustrates that MMP activation very early post-MI is a key determinant of the subsequent outcome, and that the beneficial effects of MMP inhibition outlasts the treatment.

3.5. Discussion

3.5.1. Early MMP activity precedes the deleterious outcomes of TIMP3 deficiency

TIMP3-deficient mice have been reported to develop accelerated remodeling following MI[18], however, the molecular analyses in this study was performed at or after 1week post-MI. We and others[20, 28, 32, 33] have found that post-MI LV rupture peaks at 3 days with no incident of LV rupture after 7 days post-MI. In light of these mortality findings, the interest to look at the molecular mechanisms of cardiac rupture has directed us to investigate earlier timepoints, as early as one day post-MI. In parallel with the increased mortality, there was a noticeable difference in total gelatinase MMP activity at 3 days post-MI, which was even less evident by 1week post-MI, indicating that a major determining phase may have been missed. The rapid presence of a variety of active MMP species, along with correlating inflammation associated with MMP regulation, in this case notably neutrophils, has also been implicated in this process with the early phase involved in the destabilization of the ECM. The protective effects of MMPi treatment early post-MI in TIMP3$^{-/-}$ mice indicates that the early rise in MMP

activities post-MI is a major determinant of subsequent LV remodeling and dysfunction. These data provide a thorough analysis of the early molecular events that lead to deteriorated cardiac remodeling, morphometry and dysfunction by 1 week post-MI.

3.5.2. The imbalance between MMPs and TIMP3 creates a vulnerable destabilized environment for further ECM degradation, inflammation, and rupture

In patients with myocardial infarction, the adverse ventricular remodeling has been linked to an imbalance in MMP/TIMP activity[9]. This is supported by the presence of increased inflammation in the infarct and peri-infarct regions, predisposing this area to rapid turnover at the risk of an excess of MMP activity, which was clearly evident at 1 day. We used second harmonic generation imaging on unfixed and unstained heart tissue to visualize the ECM fibrillar structure. The advantage of this technique is that it excludes the tissue alterations resulting from manipulations such as fixing or staining. The markedly greater rate of LV rupture in TIMP3-deficient mice is associated with a greater infarct expansion in these mice, which is consistent with a recent report that infarct size determines the risk of LV rupture post-MI[28].

3.5.3. Time and regional-specific MMP activities

We examined the time- and region-specific MMP activities and found that MMP9 and MMP2 levels, as well as total collagenase and gelatinase activities, were elevated in the infarct and peri-infarct regions by 1 day post-MI in TIMP3$^{-/-}$ mice. This is also consistent with reports showing that MMP9 increases early post-MI in patients[34] and in experimental models[35]. An increase in MMP activities and collagen degradation within hours of MI also has been reported in rat hearts[36]. Tian *et al.* reported increased MMP2 activity in TIMP3$^{-/-}$ mice at 1week post-MI[18], whereas we found the rise in MMP2 activity only at 1 day post-MI but not at later time points. Tian *et al.*'s finding is most likely because it was measured in the whole LV and the region-dependent (infarct, peri-infarct vs. non-infarct)

alterations in MMP2 activation were not taken into consideration. A region-specific MMP expression and TIMP downregulation in sheep heart post-MI has also been reported[37]. Mice lacking MMP2 are protected against LV rupture[11], while mice overexpressing MMP2 develop LV dilation and dysfunction[38]. The early increase in proteolytic activities in the infarct and peri-infarct regions could explain the greater rate of LV rupture in TIMP3$^{-/-}$ mice, while the increased MMP levels and proteolytic activity in the non-infarct myocardium could explain the exacerbated LV dilation and dysfunction in these mice compared to the parallel WT group.

3.5.4. Conclusions

In this study we examine the early molecular events post-MI and demonstrate a region- and time-specific function for TIMP3 in cardiac recovery from MI. We further demonstrate that LAD-ligation triggers early downregulation of TIMP3 in WT mice, and that TIMP3-deficient mice show a very early increase in MMP activities post-MI, aberrant degradation of ECM fibrillar structure and enhanced inflammation, leading to exacerbated LV dilation, systolic and diastolic dysfunction at 1 week and 4 weeks post-MI. Our data demonstrate that the initial rise in proteolytic activities early post-MI is a triggering factor for subsequent LV adverse remodeling and LV rupture. Hence, timing of treatments to improve cardiac response to MI may be critical in producing favorable outcome. We provide evidence that the MMP-inhibitory function of TIMP3 is critical during early stages of recovery from myocardial infarction. Since TIMP3 levels are significantly reduced in the hearts of patients with ischemic cardiomyopathy, overexpressing or supplementing TIMP3 in myocardial ischemic injury may prove to be a promising therapeutic approach.

3.6. References

1. Hunt SA, Abraham WT, Chin MH, Feldman AM, Francis GS, Ganiats TG, Jessup M, Konstam MA, Mancini DM, Michl K, Oates JA, Rahko PS, Silver MA, Stevenson LW, Yancy CW, Antman EM, Smith SC, Jr., Adams CD, Anderson JL, Faxon DP, Fuster V, Halperin JL, Hiratzka LF, Jacobs AK, Nishimura R, Ornato JP, Page RL, Riegel B. Acc/aha 2005 guideline update for the diagnosis and management of chronic heart failure in the adult: A report of the american college of cardiology/american heart association task force on practice guidelines (writing committee to update the 2001 guidelines for the evaluation and management of heart failure): Developed in collaboration with the american college of chest physicians and the international society for heart and lung transplantation: Endorsed by the heart rhythm society. *Circulation*. 2005;112:e154-235

2. Cohn JN, Ferrari R, Sharpe N. Cardiac remodeling--concepts and clinical implications: A consensus paper from an international forum on cardiac remodeling. Behalf of an international forum on cardiac remodeling. *J Am Coll Cardiol*. 2000;35:569-582

3. Pfeffer MA, Braunwald E. Ventricular remodeling after myocardial infarction. Experimental observations and clinical implications. *Circulation*. 1990;81:1161-1172

4. Sutton MG, Sharpe N. Left ventricular remodeling after myocardial infarction: Pathophysiology and therapy. *Circulation*. 2000;101:2981-2988

5. Davis N, Sistino JJ. Review of ventricular rupture: Key concepts and diagnostic tools for success. *Perfusion*. 2002;17:63-67

6. Figueras J, Cortadellas J, Soler-Soler J. Left ventricular free wall rupture: Clinical presentation and management. *Heart*. 2000;83:499-504

7. Jugdutt BI. Ventricular remodeling after infarction and the extracellular collagen matrix: When is enough enough? *Circulation*. 2003;108:1395-1403

8. Spinale FG. Myocardial matrix remodeling and the matrix metalloproteinases: Influence on cardiac form and function. *Physiol Rev*. 2007;87:1285-1342

9. Webb CS, Bonnema DD, Ahmed SH, Leonardi AH, McClure CD, Clark LL, Stroud RE, Corn WC, Finklea L, Zile MR, Spinale FG. Specific temporal profile of matrix metalloproteinase release occurs in patients after myocardial infarction: Relation to left ventricular remodeling. *Circulation*. 2006;114:1020-1027

10. Heymans S, Luttun A, Nuyens D, Theilmeier G, Creemers E, Moons L, Dyspersin GD, Cleutjens JP, Shipley M, Angellilo A, Levi M, Nube O, Baker A, Keshet E, Lupu F, Herbert JM, Smits JF, Shapiro SD, Baes M, Borgers M, Collen D, Daemen MJ, Carmeliet P. Inhibition of plasminogen activators or matrix metalloproteinases prevents cardiac rupture but impairs therapeutic angiogenesis and causes cardiac failure. *Nat Med*. 1999;5:1135-1142

11. Matsumura S, Iwanaga S, Mochizuki S, Okamoto H, Ogawa S, Okada Y. Targeted deletion or pharmacological inhibition of mmp-2 prevents cardiac rupture after myocardial infarction in mice. *J Clin Invest*. 2005;115:599-609

12. van den Borne SW, Cleutjens JP, Hanemaaijer R, Creemers EE, Smits JF, Daemen MJ, Blankesteijn WM. Increased matrix metalloproteinase-8 and -9 activity in patients with infarct rupture after myocardial infarction. *Cardiovasc Pathol*. 2009;18:37-43

13. Nuttall RK, Sampieri CL, Pennington CJ, Gill SE, Schultz GA, Edwards DR. Expression analysis of the entire mmp and timp gene families during mouse tissue development. *FEBS Lett*. 2004;563:129-134

14. Sawicki G, Menon V, Jugdutt BI. Improved balance between timp-3 and mmp-9 after regional myocardial ischemia-reperfusion during at1 receptor blockade. *J Card Fail*. 2004;10:442-449

15. Li YY, Feldman AM, Sun Y, McTiernan CF. Differential expression of tissue inhibitors of metalloproteinases in the failing human heart. *Circulation*. 1998;98:1728-1734

16. Kassiri Z, Oudit GY, Sanchez O, Dawood F, Mohammed FF, Nuttall RK, Edwards DR, Liu PP, Backx PH, Khokha R. Combination of tumor necrosis factor-alpha ablation and matrix metalloproteinase inhibition prevents heart failure after pressure overload in tissue inhibitor of metalloproteinase-3 knock-out mice. *Circ Res*. 2005;97:380-390

17. Kassiri Z, Defamie V, Hariri M, Oudit GY, Anthwal S, Dawood F, Liu P, Khokha R. Simultaneous transforming growth factor beta-tumor necrosis

factor activation and cross-talk cause aberrant remodeling response and myocardial fibrosis in timp3-deficient heart. *J Biol Chem*. 2009;284:29893-29904

18. Tian H, Cimini M, Fedak PW, Altamentova S, Fazel S, Huang ML, Weisel RD, Li RK. Timp-3 deficiency accelerates cardiac remodeling after myocardial infarction. *J Mol Cell Cardiol*. 2007;43:733-743

19. Zamilpa R, Lindsey ML. Extracellular matrix turnover and signaling during cardiac remodeling following mi: Causes and consequences. *J Mol Cell Cardiol*. 2010;48:558-563

20. Kandalam V, Basu R, Abraham T, Wang X, Soloway PD, Jaworski DM, Oudit GY, Kassiri Z. Timp2 deficiency accelerates adverse post-myocardial infarction remodeling because of enhanced mt1-mmp activity despite lack of mmp2 activation. *Circ Res*. 2010;106:796-808

21. Peterson JT, Li H, Dillon L, Bryant JW. Evolution of matrix metalloprotease and tissue inhibitor expression during heart failure progression in the infarcted rat. *Cardiovasc Res*. 2000;46:307-315

22. Moller JE, Hillis GS, Oh JK, Reeder GS, Gersh BJ, Pellikka PA. Wall motion score index and ejection fraction for risk stratification after acute myocardial infarction. *Am Heart J*. 2006;151:419-425

23. Zhang Y, Takagawa J, Sievers RE, Khan MF, Viswanathan MN, Springer ML, Foster E, Yeghiazarians Y. Validation of the wall motion score and myocardial performance indexes as novel techniques to assess cardiac function in mice after myocardial infarction. *Am J Physiol Heart Circ Physiol*. 2007;292:H1187-1192

24. Kawakami R, Saito Y, Kishimoto I, Harada M, Kuwahara K, Takahashi N, Nakagawa Y, Nakanishi M, Tanimoto K, Usami S, Yasuno S, Kinoshita H, Chusho H, Tamura N, Ogawa Y, Nakao K. Overexpression of brain natriuretic peptide facilitates neutrophil infiltration and cardiac matrix metalloproteinase-9 expression after acute myocardial infarction. *Circulation*. 2004;110:3306-3312

25. Frangogiannis NG. Targeting the inflammatory response in healing myocardial infarcts. *Curr Med Chem*. 2006;13:1877-1893

26. Frangogiannis NG, Smith CW, Entman ML. The inflammatory response in myocardial infarction. *Cardiovasc Res*. 2002;53:31-47

27. Fang L, Gao XM, Moore XL, Kiriazis H, Su Y, Ming Z, Lim YL, Dart AM, Du XJ. Differences in inflammation, mmp activation and collagen damage account for gender difference in murine cardiac rupture following myocardial infarction. *J Mol Cell Cardiol*. 2007;43:535-544

28. Gao XM, Ming Z, Su Y, Fang L, Kiriazis H, Xu Q, Dart AM, Du XJ. Infarct size and post-infarct inflammation determine the risk of cardiac rupture in mice. *Int J Cardiol*. 2010;143:20-28

29. Mohammed FF, Smookler DS, Taylor SE, Fingleton B, Kassiri Z, Sanchez OH, English JL, Matrisian LM, Au B, Yeh WC, Khokha R. Abnormal tnf activity in timp3-/- mice leads to chronic hepatic inflammation and failure of liver regeneration. *Nat Genet*. 2004;36:969-977

30. Smookler DS, Mohammed FF, Kassiri Z, Duncan GS, Mak TW, Khokha R. Tissue inhibitor of metalloproteinase 3 regulates tnf-dependent systemic inflammation. *J Immunol*. 2006;176:721-725

31. Peterson JT, Hallak H, Johnson L, Li H, O'Brien PM, Sliskovic DR, Bocan TM, Coker ML, Etoh T, Spinale FG. Matrix metalloproteinase inhibition attenuates left ventricular remodeling and dysfunction in a rat model of progressive heart failure. *Circulation*. 2001;103:2303-2309

32. Kassiri Z, Zhong J, Guo D, Basu R, Wang X, Liu PP, Scholey JW, Penninger JM, Oudit GY. Loss of angiotensin-converting enzyme 2 accelerates maladaptive left ventricular remodeling in response to myocardial infarction. *Circ Heart Fail*. 2009;2:446-455

33. Yang Y, Ma Y, Han W, Li J, Xiang Y, Liu F, Ma X, Zhang J, Fu Z, Su YD, Du XJ, Gao XM. Age-related differences in postinfarct left ventricular rupture and remodeling. *Am J Physiol Heart Circ Physiol*. 2008;294:H1815-1822

34. Kaden JJ, Dempfle CE, Sueselbeck T, Brueckmann M, Poerner TC, Haghi D, Haase KK, Borggrefe M. Time-dependent changes in the plasma concentration of matrix metalloproteinase 9 after acute myocardial infarction. *Cardiology*. 2003;99:140-144

35. Lindsey M, Wedin K, Brown MD, Keller C, Evans AJ, Smolen J, Burns AR, Rossen RD, Michael L, Entman M. Matrix-dependent mechanism of neutrophil-mediated release and activation of matrix metalloproteinase 9 in myocardial ischemia/reperfusion. *Circulation*. 2001;103:2181-2187

36. Takahashi S, Barry AC, Factor SM. Collagen degradation in ischaemic rat hearts. *Biochem J*. 1990;265:233-241

37. Wilson EM, Moainie SL, Baskin JM, Lowry AS, Deschamps AM, Mukherjee R, Guy TS, St John-Sutton MG, Gorman JH, 3rd, Edmunds LH, Jr., Gorman RC, Spinale FG. Region- and type-specific induction of matrix metalloproteinases in post-myocardial infarction remodeling. *Circulation*. 2003;107:2857-2863

38. Bergman MR, Teerlink JR, Mahimkar R, Li L, Zhu BQ, Nguyen A, Dahi S, Karliner JS, Lovett DH. Cardiac matrix metalloproteinase-2 expression independently induces marked ventricular remodeling and systolic dysfunction. *Am J Physiol Heart Circ Physiol*. 2007;292:H1847-1860

CHAPTER 4

TIMP2 deficiency accelerates adverse post-myocardial infarction remodeling because of enhanced MT1-MMP activity despite the lack of MMP2 activation

Vijay Kandalam[1,2,3], Ratnadeep Basu[1,2,3], Thomas Abraham[5], Xiuhua Wang[1,2,3], Paul D. Soloway[6], Diane M. Jaworski[7], Gavin Y. Oudit[2,3,4], Zamaneh Kassiri[1,2,3]

1Department of Physiology, 2Cardiovascular Research Centre, 3Mazankowski Alberta Heart Institute, and 4Department of Medicine/Cardiology, University of Alberta, Edmonton, Canada; 5James Hogg iCAPTURE Centre, University of British Columbia, Vancouver, Canada; 6Division of Nutritional Sciences, Cornell University, New York; and 7Department of Anatomy and Neurobiology, University of Vermont, Burlington.

Contributions:

VK (70%): Monitoring of all animals, scheduling surgeries and functional analyses, tissue collection, data collection, and project planning. Collected all tissue, processed all tissue, and conducted majority of experiments and all data analysis. VK had a primary role in the writing of the manuscript and assembly of final figures.

RB: analysis of all acquired raw echocardiography data, TA: performed SHG imaging, XW: performed LAD-ligation surgeries and Taqman RT-PCR. PDS & DMJ: provided TIMP2$^{-/-}$ mice, GYO: worked in conjunction with RB to manage echocardiography analysis and interpretation, ZK: supervisor of VK, overall project planning and corresponding author.

A version of this chapter has been published. Kandalam et al. 2010. Circulation Research. 106(4): 796-808.

4.1. Introduction

MI results in adverse remodeling of the myocardium including the ECM.[1] The ECM is a dynamic structure which undergoes constant turnover, and its intact structure is essential for optimal cardiac structure and function. TIMPs play a critical role in regulating the activity of the ECM-degrading enzymes, the MMPs.[2, 3] In patients with ischemic or idiopathic dilated cardiomyopathy, myocardial protein levels of TIMP2 remained unaltered,[4, 5] or increased in end-stage dilated cardiomyopathy patients,[6] while plasma analyses revealed a rise in TIMP2 levels in late stages of MI.[7] TIMP2 is unique among TIMPs since in addition to inhibiting a number of MMPs, it mediates MMP2 activation. MMP2 has been linked to a number of cardiomyopathies.[3, 8, 9] Given this multidimensional biochemical function of TIMP2 (an activator and an inhibitor of MMPs), the impact of altered TIMP2 levels in disease is quite unpredictable.

In this study, we are the first to directly examine the role of TIMP2 in cardiac response to MI by subjecting mice lacking TIMP2 and age-matched WT mice to MI using the LAD artery ligation model. TIMP2 deficiency markedly exacerbated LV dilation and systolic dysfunction compared to WT mice. TIMP2$^{-/-}$ hearts exhibited excess degradation of the ECM collagen fibres due to enhanced activity of collagenases, particularly MT1-MMP. Activation of proMMP2 was completely abrogated in TIMP2$^{-/-}$ hearts. Collectively, the MMP-inhibitory function of TIMP2, but not its MMP-activating function, is critical in cardiac response to MI.

4.2. Objectives

The importance of TIMPs in post-MI remodeling has been studied in detail, with studies examining the role of TIMP1[10], TIMP3[11, 12], and TIMP4[13] in MI using the TIMP-knockout mouse. No previous work examining the role of TIMP2 through the use of the TIMP2$^{-/-}$ mouse is present. In light of its general high cardiac expression level relative to the other TIMPs, the objective of this

study is to investigate TIMP2 involvement in the cardiac response to MI. We will achieve this by utilizing the LAD ligation experimental MI model in the background of the TIMP2$^{-/-}$ mouse to determine the extent and mechanism of ECM remodeling in the absence of TIMP2 compared to WT mice. The opposing actions of MMP inhibition and MMP2 activation by TIMP2 in the setting of MI makes it difficult to predict if TIMP2 has a protective or unfavourable role in disease progression, which needs to be clarified to determine the therapeutic potential of TIMP2.

4.3. Methods

4.3.1. LAD coronary artery ligation

At 11-12 weeks of age, mice were anesthetized and underwent surgical LAD ligation according to protocol in Section 2.2.1 to generate an ischemic state. Sham-operated mice were used as controls. Mice were allowed to recover and monitored as described in Section 2.4.1.

4.3.2. *In vivo* imaging and analysis

Echocardiography was conducted to examine parameters pertaining to MI analysis as described in Section 2.5.1. TMD (Section 2.5.2), TDI (Section 2.5.3), and EKV (Section 2.5.4) modes were also utilized for complete *in vivo* analysis of cardiac function.

4.3.3. Molecular and cellular analysis

Sham and post-MI tissue was collected as described in Section 2.4.2., and processed for molecular (collagen in Section 2.6.2.2., RNA in Section 2.8., protein in section 2.9., and MMP activity in Section 2.11.), histological (neutrophils and macrophages in Section 2.7.2), and morphological (left ventricle morphology in Section 2.6.1.1., infarct size in Section 2.6.1.2., and collagen organization in Section 2.6.2.3.) analysis.

4.4. Results

4.4.1. MI alters TIMPs differently in WT versus TIMP2$^{-/-}$ mice

We first examined if MI affects TIMP2 mRNA and protein levels in WT hearts. TIMP2 mRNA levels showed a significant and transient decrease in the infarct area at 3 days (Figure 4.1.Ai) followed by a marked increase at 1 week post-MI (Figure 4.1.Aii). *Timp2* mRNA levels also increased in the peri- and non-infarct regions (Figure 4.1.Ai-Aii). TIMP2 protein levels, however, showed a persistent and significant reduction in infarct, peri- and non-infarct regions at 3 days and 1 week post-MI compared to sham-operated hearts (Figure 4.1.B). This dissociation between mRNA and protein levels suggests a post-transcriptional regulation of myocardial TIMP2 protein levels in response to MI. In addition, the rise in *Timp2* mRNA could be a compensatory attempt by the tissue to replace the loss of TIMP2 protein. These data raised the question of whether this altered TIMP2 levels could improve or adversely impact the cardiac recovery following MI.

Before investigating how TIMP2 deficiency impacts cardiac response to MI, we examined if TIMP2-deficient myocardium exhibits upregulation of other TIMPs which could compensate for its absence. TIMP1 levels were significantly higher, but TIMP3 and TIMP4 levels remain unaltered, compared to WT (Figure 4.2.Bi-Biv), except for a significantly higher TIMP4 protein level in the TIMP2$^{-/-}$-

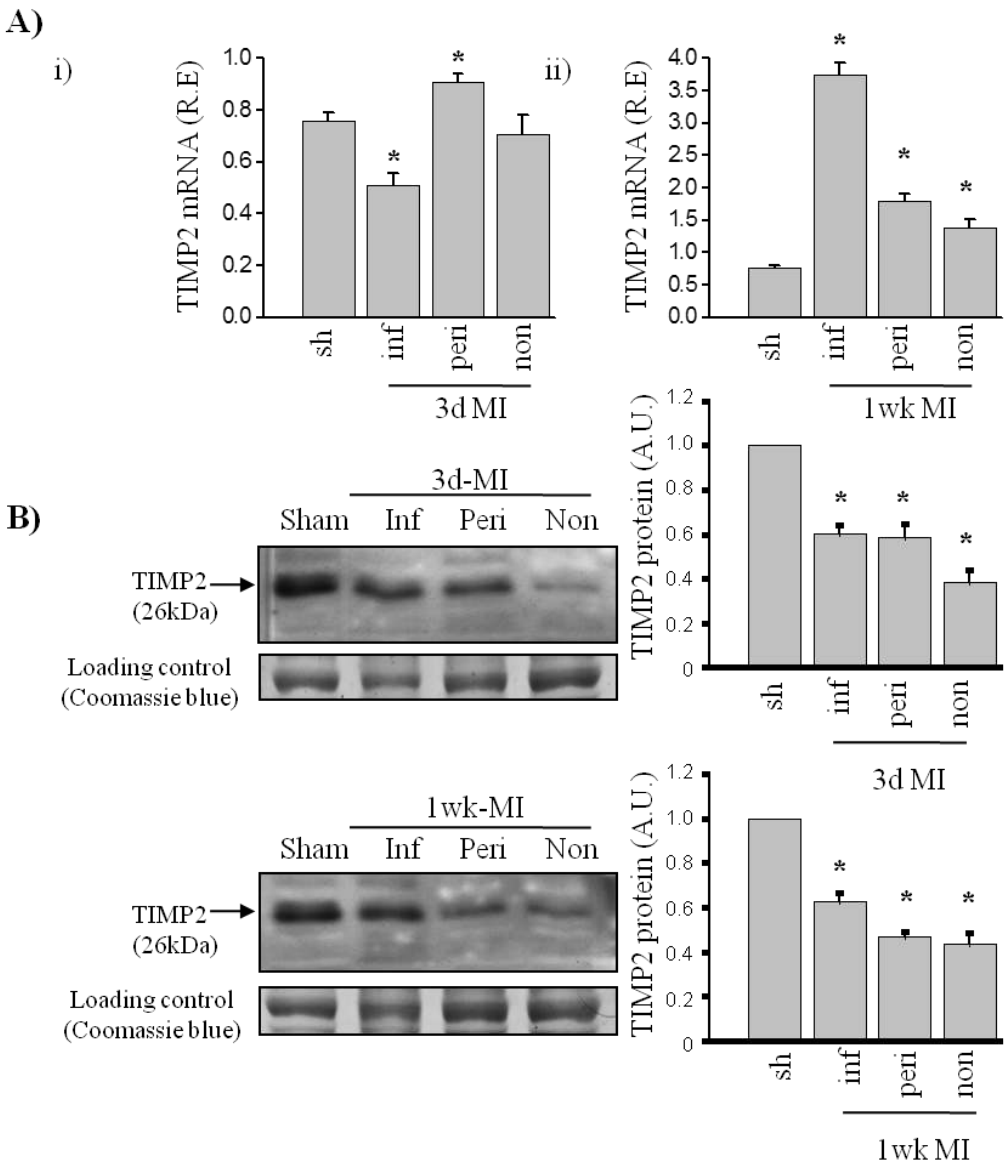

Figure 4.1. TIMP2 mRNA and protein levels in WT mice following MI.

A, TIMP2 mRNA levels in the infarct, peri-infarct and non-infarct myocardium compared to sham at 3 days (i) and 1 week (ii) post-MI (n=6/group/genotype). B, Representative western blot (left) and quantified protein levels (right) show TIMP2 protein levels in the sham heart compared to the infarct, peri-infarct, and non-infarct regions at 3 days and 1 week post-MI. Representative blots are shown on the left, and quantified protein levels are shown on the right (n=4/group/genotype). R.E= Relative Expression, A.U. Arbitrary Units. *$p<0.05$ compared to sham using one-way ANOVA analysis.

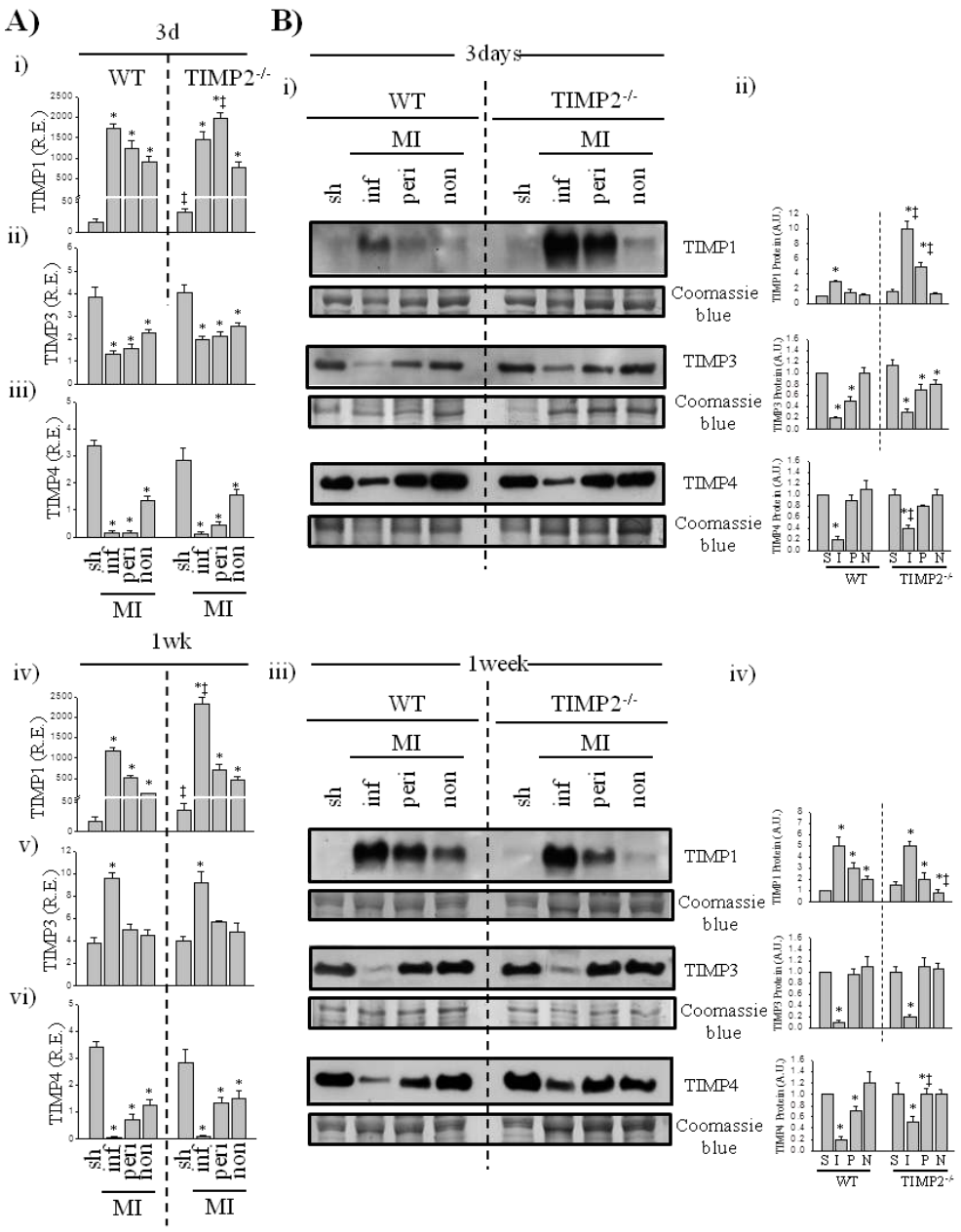

Figure 4.2. RNA and protein levels of TIMPs in WT and TIMP2$^{-/-}$ myocardium post-MI.

A, Relative mRNA expression levels of TIMPs 1, 3, and 4 at 3 days (i-iii) and 1 week (iv-vi) post-MI in the infarct (inf), peri-infarct (peri), and non-infarct (non) myocardium (n=6/group/genotype). B, Representative Western blots at 3 days (i) and 1 week (iii) and protein quantification of TIMPs at 3 days (ii) and 1 week (iv) post-MI (n=4/group/genotype). Coomassie blue used as loading control. A.U., arbitrary units; I, infarct; N, non-infarct; P, peri-infarct; R.E., relative expression; S, sham. *P<0.05 compared to corresponding sham; ‡P<0.05 compared to WT using two-way ANOVA analysis.

peri- infarct myocardium at 1 week post-MI (Figure 4.2.Bii and Biv). The increase in TIMP1 (and the smaller increase in TIMP4) in TIMP2$^{-/-}$-MI hearts could compensate for the absence of TIMP2.

4.4.2. TIMP2 deficiency increases severity of disease following MI

Following MI, WT and TIMP2$^{-/-}$ mice exhibited a similar rate of survival (51% vs 48%) (Figure 4.3.A). Autopsy examination revealed a comparable rate of left ventricular rupture between the two genotypes post-MI (41% in WT and 39% in TIMP2$^{-/-}$) (Figure 4.3.B). Despite the similar survival rates, gross histological analysis of the hearts revealed a larger LV chamber size (Figure 4.4.A) and infarct size (Figure 4.4.B) in TIMP2$^{-/-}$ compared to WT mice at 1 week post-MI. This indicates greater infarct expansion in TIMP2$^{-/-}$ mice since the initial infarct size generated by ligation of the LAD was comparable between genotypes (46±5% in WT and 49±5% in TIMP2$^{-/-}$, measured at 1 day post-MI, P=0.1, n=6/genotype). In addition, brain natriuretic peptide (BNP), a disease marker known to correlate with the degree of LV wall stress,[14, 15] was more significantly elevated in the infarct and peri-infarct regions of TIMP2$^{-/-}$ hearts after 3 days, and in peri- and non-infarct regions at 1 week post-MI compared to the corresponding regions in WT-MI hearts (Figure 4.5.Ai-Aii). Lung water content, also a marker of severity of post-MI LV dysfunction, measured as the difference between wet and dry lung weights, was significantly higher in TIMP2$^{-/-}$ compared to WT mice at 1 week post-MI (Figure 4.5.B). These data collectively suggest that TIMP2 deficiency enhances the pathological cardiac response to MI.

4.4.3. TIMP2-deficient mice exhibit greater ventricular dilation and worsening of systolic function after MI

We evaluated cardiac function by echocardiography at 1week and 4 weeks post-MI in WT and TIMP2$^{-/-}$ mice. Sham-operated mice from either genotype served as baseline controls. All parameters representing cardiac structure and function were

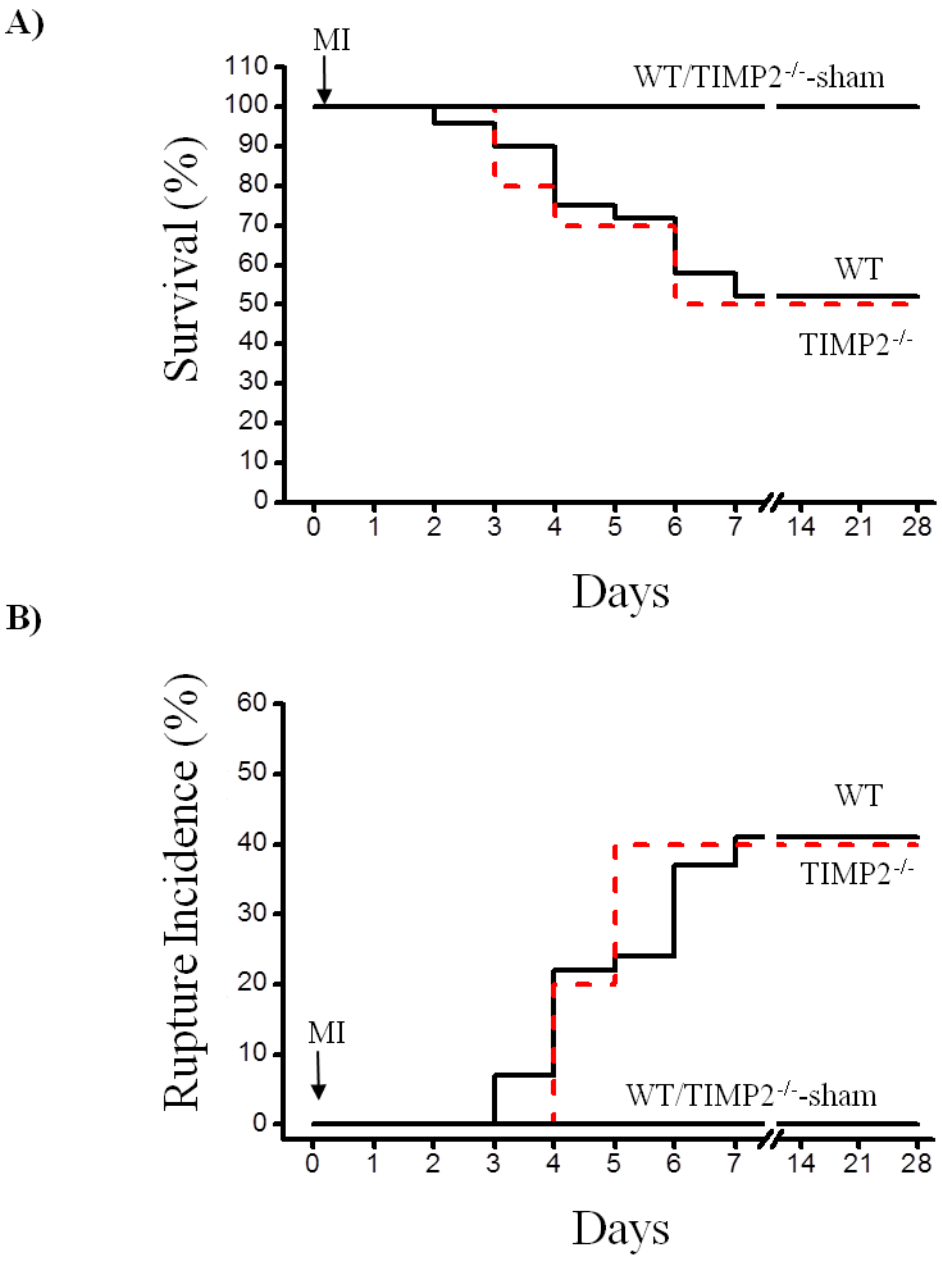

Figure 4.3. TIMP2 deficiency does not affect survival post-MI.

Total survival (A) and cumulative rupture incident (B) in WT (solid line, n=49) and TIMP2$^{-/-}$ (dashed line, n=56) mice post-MI.

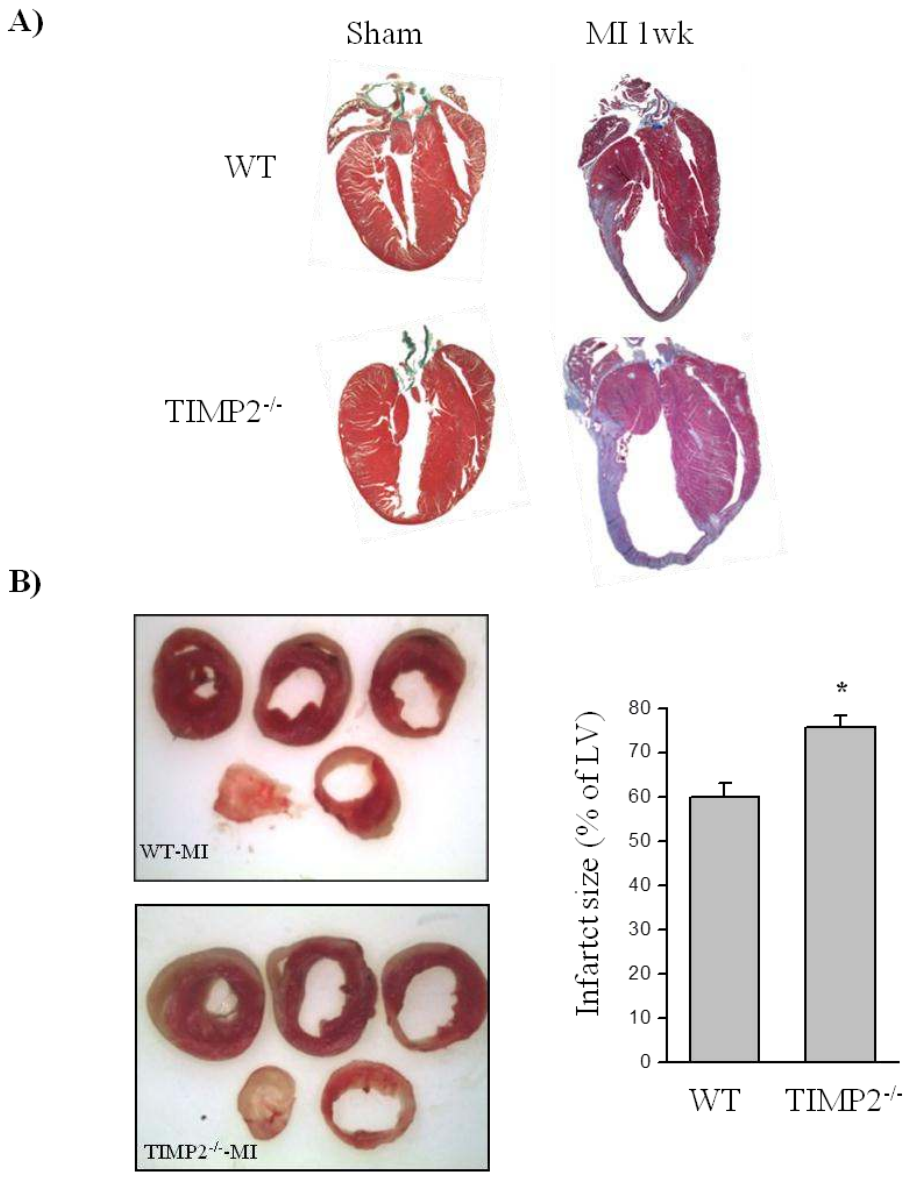

Figure 4.4. **TIMP2 deficiency leads to exacerbated left ventricular remodeling post-MI.**

A, Four-chamber view of trichrome-stained fixed hearts from WT and TIMP2$^{-/-}$ mice at 1 week post-sham or post-MI. B, Representative images of TTC-stained heart slices, and averaged infarct size in WT and TIMP2$^{-/-}$ mice at 1week post-MI (n=6/genotype). *p<0.05 compared to sham using Student's T-test analysis.

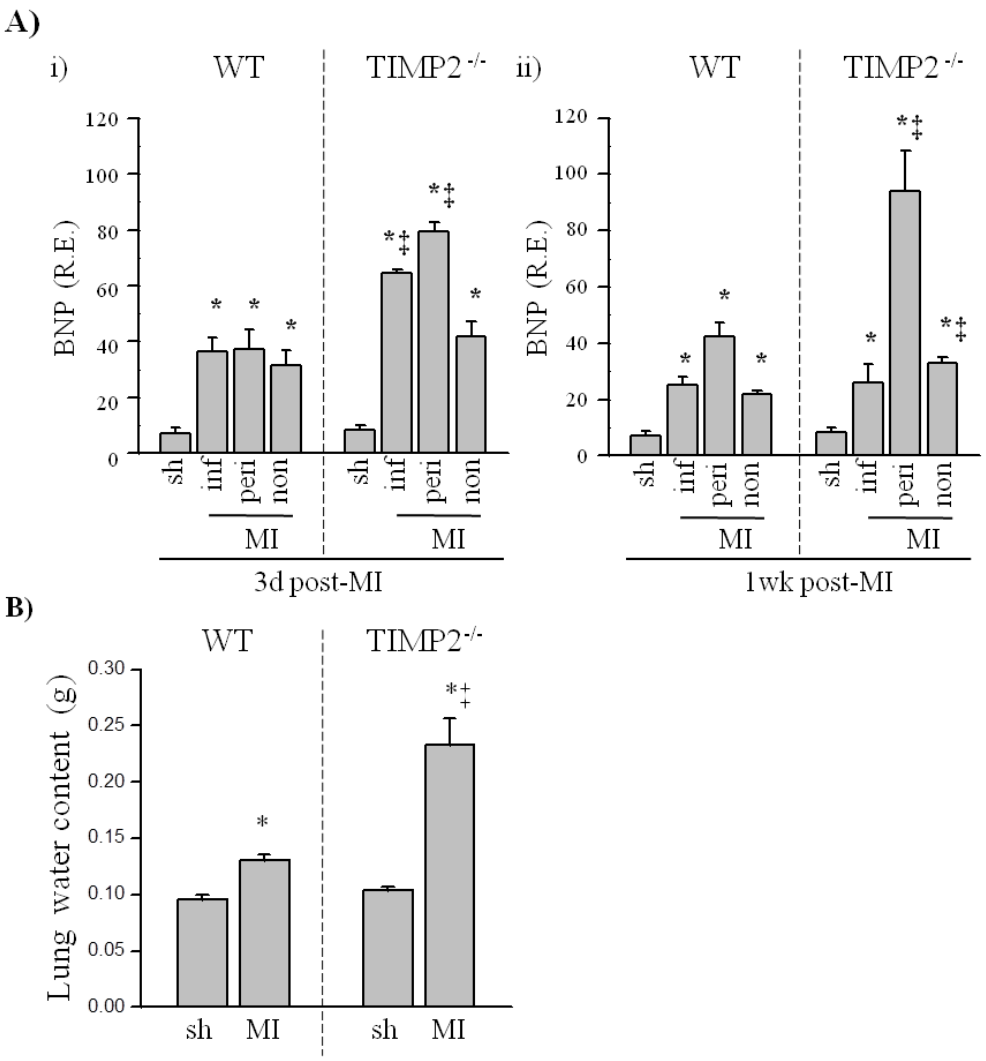

Figure 4.5. TIMP2 deficiency leads to more severe heart disease post-MI.

A, Brain natriuretic peptide (BNP) levels, a marker of disease progression, in sham, infarct (inf), peri-infarct (peri) and non-infarct (non) myocardium of WT and TIMP2$^{-/-}$ hearts at 3 days (i) and 1 week (ii) post-MI. B, Lung water content (wet weight – dry weight) in WT and TIMP2$^{-/-}$ mice at 1 week after sham or MI (n=5/group/genotype). R.E= Relative Expression. *p<0.05 compared to corresponding sham, ‡ p<0.05 compared to WT using two-way ANOVA analysis.

comparable between sham-operated TIMP2$^{-/-}$ and WT mice (Figure 4.6., Figure 4.7., and Table 4.1.). Representative parasternal long axis images from sham and post-MI hearts show a greater LV chamber dilation in TIMP2$^{-/-}$-MI compared to WT-MI heart (Figure 4.6.A). LVEDV and LVESV were significantly larger in TIMP2$^{-/-}$ compared to WT mice (Figures 4.6.Bi-Bii), while the reduction in EF was significantly greater in TIMP2$^{-/-}$ compared to WT mice (Figure 4.6.Biii). The LV dilation and dysfunction deteriorated more progressively in TIMP2$^{-/-}$ mice by 4 weeks post-MI (Table 4.1.).

WMSI is a novel and validated way of evaluating regional LV wall motion abnormalities post-MI. It incorporates wall motion of the infarct, peri- and non-infarct regions and contractility and represents the degree of adverse ventricular remodeling post-MI.[16] Sham-operated hearts have a WMSI of 1 indicating intact LV wall motion and contractility. An increase in WMSI (>1) indicates suppressed LV wall motion. TIMP2$^{-/-}$ hearts had significantly greater wall motion abnormalities at1 week post-MI compared to WT-MI mice (Figure 4.7.Ci), attributable primarily to worsening of midventricular and apical wall motion which extended into the basal anterior/anterolateral segments in the TIMP2$^{-/-}$-MI hearts (Figure 4.7.Cii). Tissue Doppler images from sham and post-MI hearts illustrate a marked reduction of systolic annular velocity (S'), a sensitive measure of systolic function, in the TIMP2$^{-/-}$-MI compared to WT-MI heart (Figure 4.7.B). Overall, TIMP2 deficiency resulted in exacerbated LV dilation, greater wall abnormalities and systolic dysfunction following MI.

4.4.4. TIMP2 deficiency leads to aberrant ECM degradation after MI

To determine the underlying mechanism of the adverse remodeling and dysfunction in TIMP2$^{-/-}$-MI mice, we first examined if absence of TIMP2 impacts the remodeling of myocardial ECM following MI. We chose an early time point of 3 days post-MI to examine the ECM structure in order to determine the early factors that lead to the exacerbated LV dilation and dysfunction in TIMP2$^{-/-}$ mice

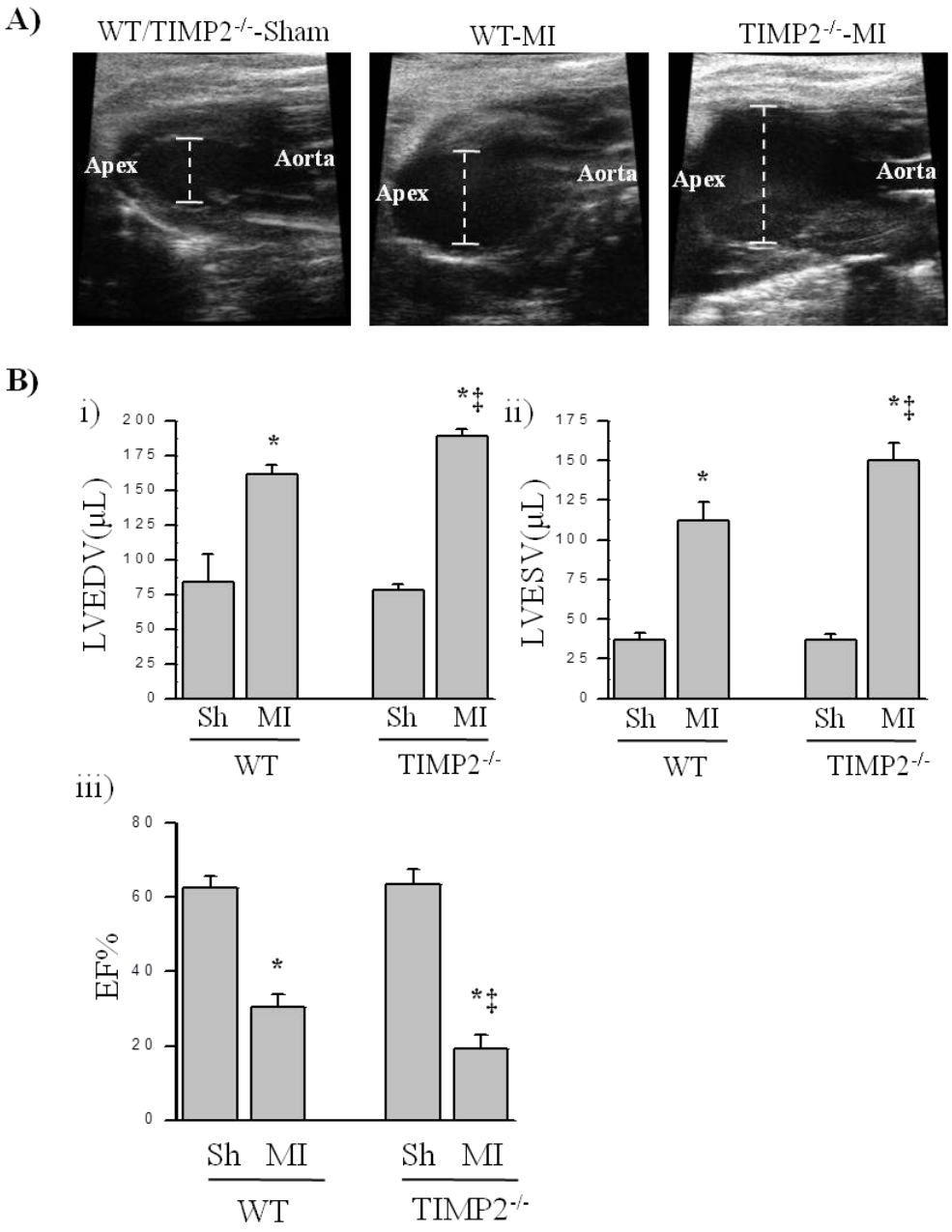

Figure 4.6. TIMP2$^{-/-}$ hearts display increased LV dilation and dysfunction at 1 week post-MI.

A, Representative parasternal long axis view from WT and TIMP2/ hearts after sham or 1 week post-MI. B, Averaged echocardiography parameters showing LV end-diastolic volume (LVEDV) (i), LV end-systolic volume (LVESV) (ii), and ejection fraction (EF) (iii). *$p<0.05$ compared to corresponding sham, ‡$p<0.05$ compared to WT using two-way ANOVA analysis.

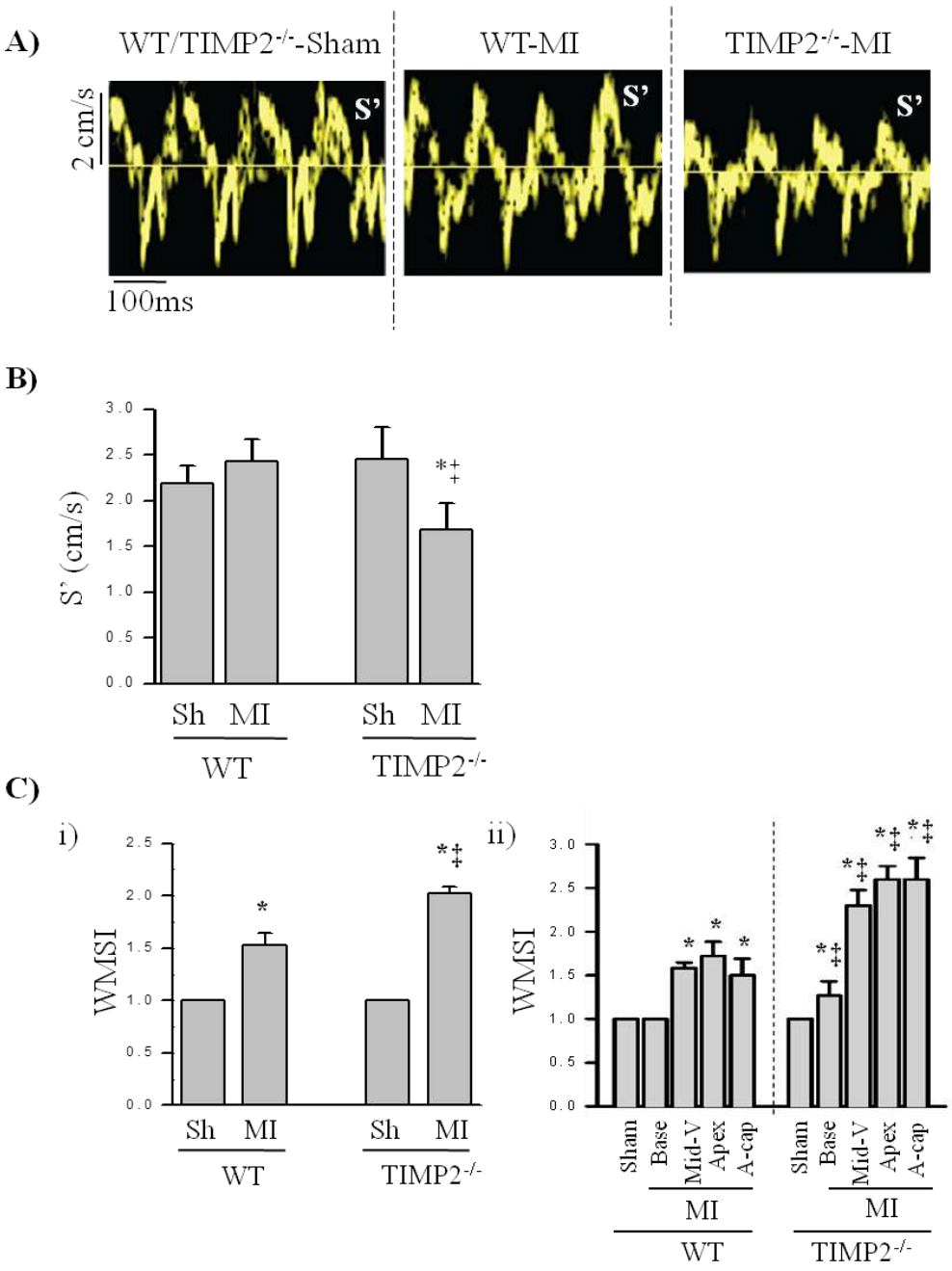

Figure 4.7. TIMP2$^{-/-}$ hearts display impaired LV systolic function at 1 week post-MI.

A, Representative tissue Doppler images from WT and TIMP2$^{-/-}$ hearts after sham or 1 week post-MI. B, Averaged echocardiography parameter annular systolic velocity (S'). C, LV Wall Motion Score Index (WMSI) (iii) and regional Wall Motion Scores (iv) in WT and TIMP2$^{-/-}$ mice at 1 week post-MI. *p<0.05 compared to corresponding sham, ‡p<0.05 compared to WT using two-way ANOVA analysis.

Table 4.1. Echocardiography parameters *in vivo* at 4 weeks post-MI.

	WT-Sham	WT-MI	TIMP2$^{-/-}$-Sham	TIMP2$^{-/-}$-MI
N	8	10	8	10
HR (bpm)	501±15	492±22	512±21	501±16
LVEDV (μL)	99.5±6.7	171.6±16.1	101.5±7.2	198±15.1*#
LVESV (μL)	19.2±2.3	34.5±3.9*	20.1±3.1	46.9±3.2*#
SV (μL)	19.9±1.8	15.1±2.7*	19.1±2.4	10.6.±2.3*#
EF (%)	60.7±4.9	41.8±5.3*	62.4±6.8	27.1±6.2*#

HR=Heart Rate; LVESV=LV End Systolic Volume; LVESP=LV End Systolic Pressure; SV=stroke volume; EF=Ejection Fraction. Values are presented as mean±SEM; *p<0.05 compared to corresponding sham-operated group; #p<0.05 compared with WT-MI group using two-way ANOVA analysis.

at later time points. We used and SHG/MPEF microscopy to visualize the fibrillar structure of the ECM in unfixed and unstained hearts. Highly ordered fibrillar collagens (Type I, II, III) produce SHG signals which can be visualized in fresh tissue without the need for exogenous labeling.[17-19] Other cell types and structures within the tissue generate MPEF because of their autofluorescence characteristics. The SHG emission spectrum (Figure 4.8.Ai) shows a strong signal manifested by a narrow peak at 440nm, exactly half of the pumping wavelength of 880 nm. This is consistent with the SHG being a frequency doubling optical process, in which photons interacting with anisotropic materials are effectively combined to form new photons with twice the energy.[17] The autofluorescence signal from the other

tissue components (e.g. different cells and vessels) was found to be very broad extending across the visible spectrum (Figure 4.8.Aii). Representative SHG images showing the myocardial fibrillar collagen matrix (red) overlaid with the MPEF images of autofluorescence (green) component are shown in Figure 4.8.A.

The structural arrangements of the collagen fibres and the fibrillar densities in sham-operated hearts from either genotype were comparable (Figure 4.8.B). However, by 3 days post-MI, the fibrillar structure of the ECM showed markedly reduced density and disarray in the infarct region, and to a lesser degree in the non-infarct region (Figure 4.8.B, top row). Interestingly, in TIMP2$^{-/-}$-MI hearts exhibited strikingly more excessive degradation and disarray of the collagen fibers in the infarct as well as the non-infarct myocardium compared to WT-MI hearts (Figure 4.8.B, bottom row). The stronger autofluorescence in the infarct areas is likely due to accumulated necrotic cells, lipofuscin, and blood-derived pigments.[20] Quantification of the fibrillar collagen revealed lower fibrillar collagen content in the infarct and non-infarct myocardium of both genotypes, whereas the reductions were significantly greater in TIMP2$^{-/-}$-MI hearts (Figure 4.8.C). These data indicate that TIMP2 deficiency leads to more severe degradation and adverse remodeling of the myocardial ECM structure following MI.

4.4.5. Exacerbated ventricular dilation and dysfunction in TIMP2$^{-/-}$-MI mice associated with heightened inflammation

Infiltration of inflammatory cells such as neutrophils and macrophages is an early tissue response to MI which contributes to the subsequent tissue remodeling and disease progression.[21] Staining for neutrophils and macrophages revealed a markedly higher number of these inflammatory cells in the TIMP2-deficient infarct and peri-infarct myocardium at 3 day and 1 week post-MI (Figure 4.9.Ai-

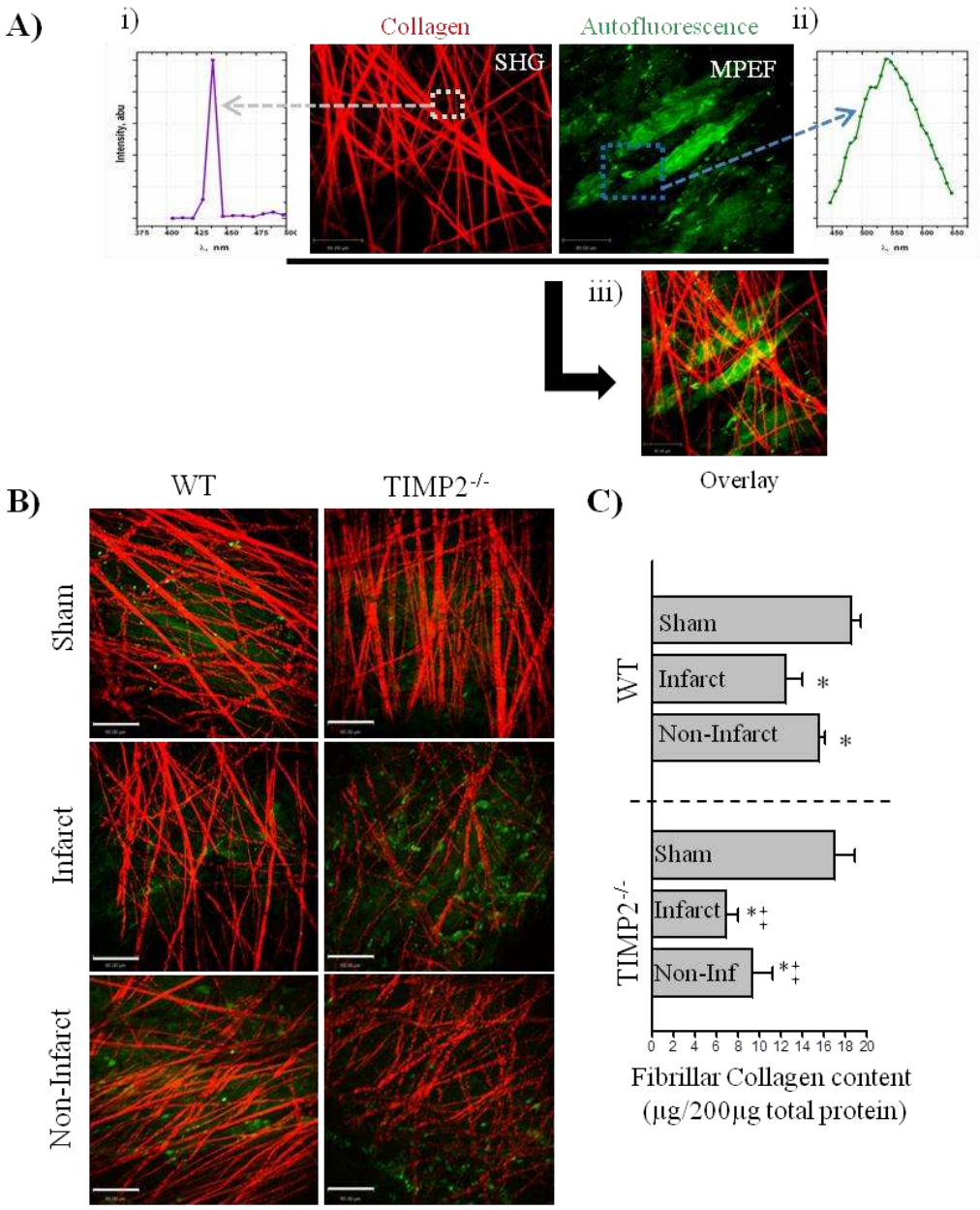

Figure 4.8. Excess degradation of the extracellular matrix fibrillar collagen in TIMP2$^{-/-}$ hearts post-MI

A, Second harmonic generation (SHG) (i) and multiphoton excitation fluorescence (MPEF) imaging (ii) were used to capture images of collagen fibers and endogenous autofluorescence, respectively. iii) Superimposed SHG and MPEF images. B, Representative images showing the density and arrangement of collagen fibres of the ECM in sham, infarct and non-infarct regions of WT and TIMP2$^{-/-}$ hearts. Scale bar=80µm. C, Fibrillar collagen content in WT and TIMP2$^{-/-}$ hearts. n=6/group/genotype. *p<0.05 compared to corresponding sham, ‡p<0.05 compared to WT using two-way ANOVA analysis.

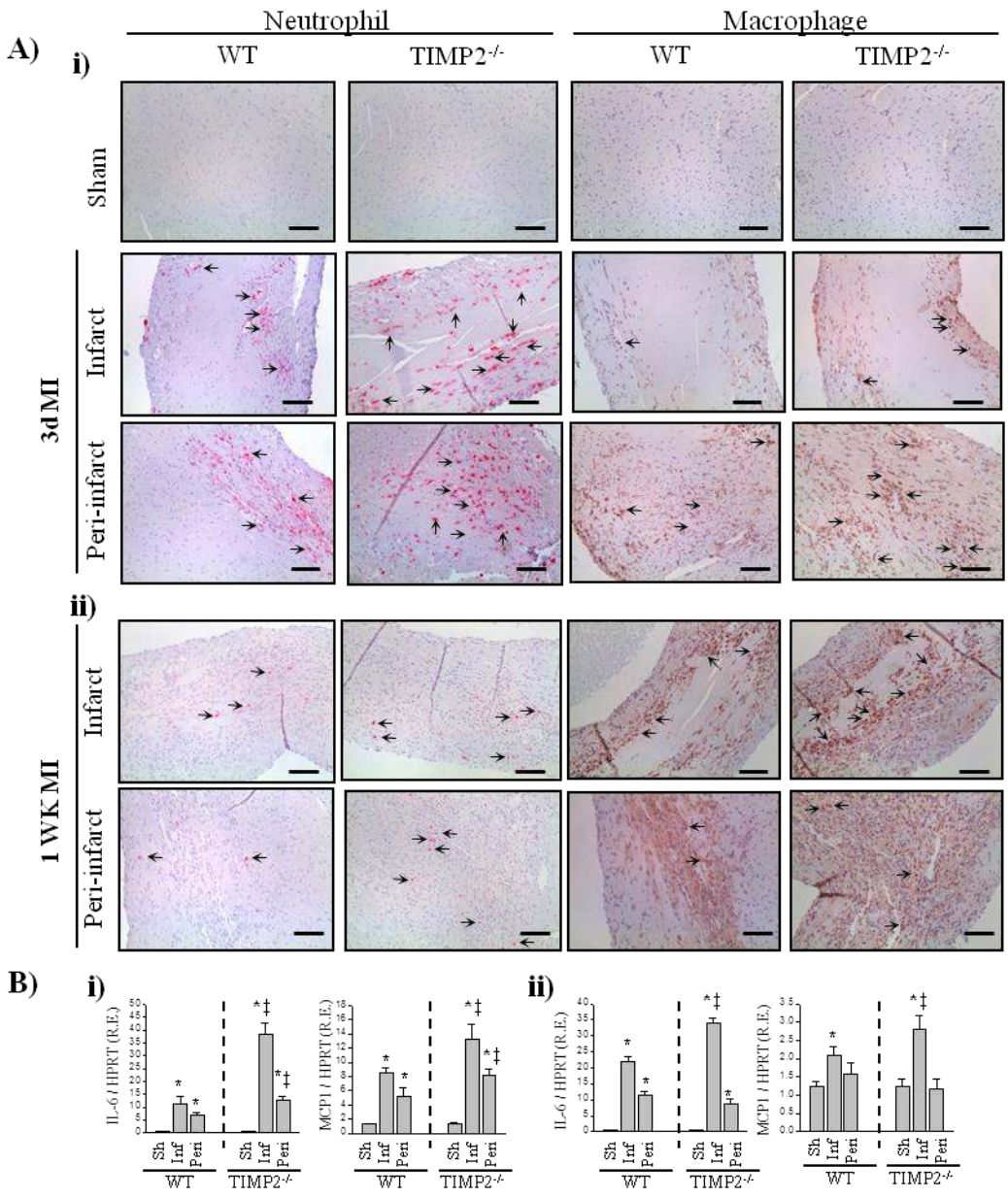

Figure 4.9. Increased inflammation in the TIMP2$^{-/-}$ hearts following MI.

A, Neutrophil and macrophage staining at 3 days (i) and 1 week post-MI (ii) in the infarct and peri-infarct regions of WT and TIMP2$^{-/-}$ hearts. B, Expression of inflammatory markers, interleukin-6 (IL6) and monocyte chemotactic protein -1 (MCP1), in the infarct (inf) and peri-infarct (peri) regions of WT and TIMP2$^{-/-}$ myocardium at 3 days (i) and 1 week post-MI (ii). Arrows point to positively stained neutrophils or macrophages. Scale bar=100μm. *p<0.05 compared to corresponding sham group, ‡ p<0.05 compared to WT using two-way ANOVA analysis.

Aii). At 1 week post-MI, the number of neutrophils and macrophages were noticeably reduced in both genotypes compared to 3 days post-MI (Figure 4.9.A). To further assess the extent of inflammation, we measured the expression of the inflammatory markers interleukin-6 and monocyte chemotactic protein-1 in these hearts. TIMP2$^{-/-}$ hearts showed a significantly greater increase in interleukin-6 and monocyte chemotactic protein-1 in the infarct and peri-infarct regions at 3 days post-MI (Figure 4.9.Bi), which persisted in the infarct regions at 1 week post-MI (Figure 4.9.Bii).

4.4.6. MMP2 activation is abrogated in TIMP2-deficient myocardium

Next, we investigated the molecular mechanism for the enhanced ECM degradation in TIMP2-deficient hearts post-MI. TIMP2 can activate or inhibit MMP2 in a dose-dependent manner.[22] As such, we first examined if TIMP2-deficiency influenced activation of MMP2 in the myocardium. MMP2 is produced as a proenzyme (72kDa) which then undergoes cell surface activation and is cleaved to its active (62 kDa) form.[23, 24] At 3 days post-MI, WT and TIMP2$^{-/-}$ hearts exhibited a similar increase in proMMP2 (72kDa) levels (Figure 4.10.A and 4.10.C). However, unlike WT hearts that showed a significant increase in cleaved MMP2 levels (62kDa), no cleaved MMP2 was detected in the TIMP2$^{-/-}$ myocardium (Figure 4.10.A and 4.10.D). MMP9 levels increased significantly in both groups, with a markedly greater increase in TIMP2$^{-/-}$-MI hearts (Figure 4.10.A, 4.10.B). Expression analyses for MMP9 and MMP2 showed that the mRNA levels of these MMPs remained generally unaltered in both genotypes, except for a significant increase in MMP9 in the infarct region of TIMP2$^{-/-}$ hearts. Hence, the rise in protein levels of these gelatinases as detected by zymography occurred through post-transcriptional regulations. A limitation of the gelatin zymography is that it does not reflect the interaction between the MMPs and TIMPs. We measured total gelatinase activity (using the EnzChek activity assay) and found it to be comparable between the two genotypes in all regions of the myocardium (Figure 4.10.F).

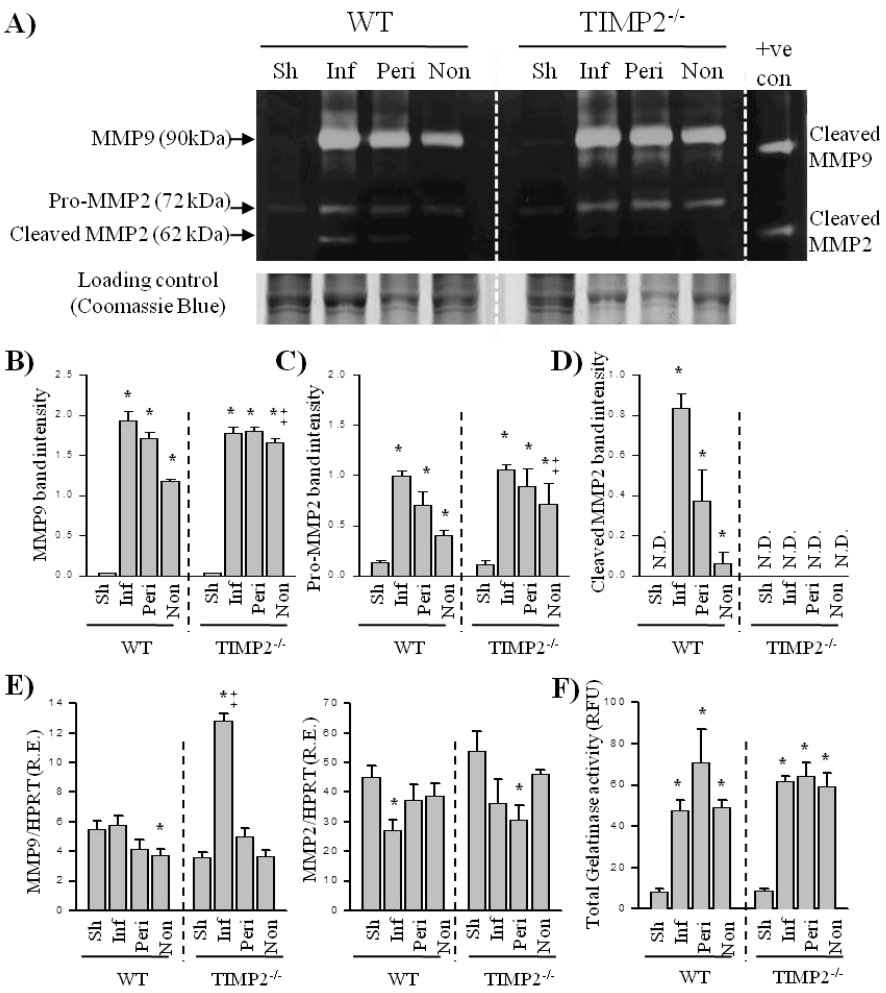

Figure 4.10. Lack of MMP2 activation, elevated MMP9 and unaltered gelatinase activity in TIMP2$^{-/-}$ hearts at 3 days post-MI.

A, Representative gelatin zymography showing MMP9, proMMP2 and cleaved MMP2 in sham, infarct, peri- and non-infarct myocardium of WT and TIMP2$^{-/-}$ hearts at 3 days post-MI. B-D, Averaged band intensity of MMP9, proMMP2 and cleaved MMP2 (normalized to the positive control) (n=5/group/genotype). E, mRNA expression of MMP9 and MMP2 in sham, infarct, peri- and non-infarct myocardium (n=8/group/genotype). F, Total gelatinase activity measured by fluorescence-based in vitro activity assay (n=6/group/genotype). N.D=Not Detectable, R.E= Relative Expression, RFU=Relative Fluorescent Units. *$p<0.05$ compared to corresponding sham, ‡ $p<0.05$ compared to WT using two-way ANOVA analysis.

At 1 week post-MI, MMP9 protein levels were significantly reduced in WT myocardium, but remained elevated in TIMP2$^{-/-}$ infarct and peri-infarct

regions and significantly greater than in WT-MI hearts (Figure 4.11.A and 4.11.B). Pro-and active MMP2 levels were strikingly elevated in the infarct and peri-infarct areas of WT-MI hearts, whereas no active MMP2 was detected in TIMP2$^{-/-}$ hearts (Figure 4.11.A and 4.11.C). Taqman RT-PCR showed a significant reduction in MMP9 mRNA levels in WT myocardium, but significant increase in the TIMP2$^{-/-}$-infarct region (Figure 4.11.E). MMP2 mRNA levels increased significantly and similarly in both genotypes at 1 week post-MI (Figure 4.11.E). We measure total gelatinase activity (using the EnzChek activity assay) and found a comparable increase in both genotypes post-MI (Figure 4.11.F). These data collectively indicate that the greater increase in MMP9 levels in TIMP2$^{-/-}$-MI hearts is counter-balanced by the lack of MMP2 activation in these hearts resulting in a similar overall increase in gelatinase activity in TIMP2$^{-/-}$ compared to WT hearts post-MI. These data provide the first in vivo evidence that TIMP2 is a critical molecule essential for MMP2 activation in the myocardium.

4.4.7. Collagenases are elevated in TIMP2$^{-/-}$-MI hearts

Since the similar levels of gelatinase activities between TIMP2$^{-/-}$ and WT myocardium could not explain the excess ECM degradation in the former group, we examined the activity of other MMPs. A number of collagenases have been shown to contribute to progression of heart disease.[3, 9] We found that total collagenase activity increased to a significantly greater level in TIMP2$^{-/-}$ hearts at 3 days (Figure 4.12.A) and 1 week post-MI (Figure 4.12.B) compared to WT. Expression analyses of a number of MMPs that contribute to the collagenase activity, showed that compared to WT hearts, MMP8 was increased more significantly in the peri-infarct, MMP13 in the peri- and non-infarct, and MT1-MMP in the infarct and peri-infarct regions of TIMP2$^{-/-}$ hearts at 3 days post-MI (Figure 4.12.Ci-Ciii). At 1 week post-MI, while expression of MMP8 decreased in WT hearts, it increased even further in TIMP2$^{-/-}$ hearts (Figure 4.12.Di). In addition, MMP13 was significantly greater in all regions, and MT1- MMP

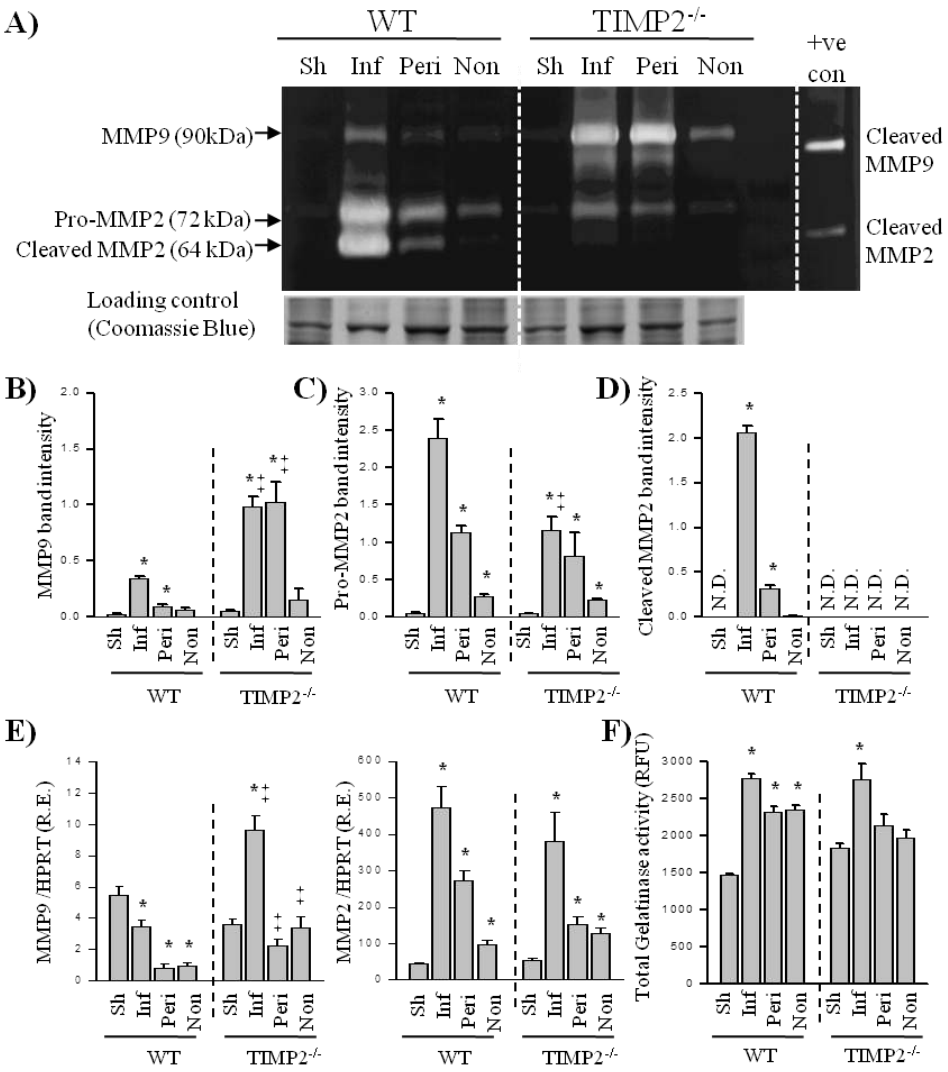

Figure 4.11. Lack of MMP2 activation, elevated MMP9 and unaltered gelatinase activity in TIMP2-deficient hearts at 1 week post-MI.

A, Representative gelatin zymography showing MMP9, proMMP2 and cleaved MMP2 in sham, infarct, peri- and non-infarct myocardium of WT and TIMP2$^{-/-}$ hearts at 1 week post-MI. B-D, Averaged band intensity of MMP9, proMMP2 and cleaved MMP2 (normalized to the positive control) (n=4/group/genotype). E, mRNA expression of MMP9 and MMP2 in sham, infarct, peri- and non-infarct myocardium (n=8/group/genotype). F, Total gelatinase activity measured by fluorescent-based in vitro activity assay (n=6/group/genotype). N.D= Not Detectable, R.E= Relative Expression, RFU=Relative Fluorescent Units. *p<0.05 compared to corresponding sham, ‡p<0.05 compared to WT using two-way ANOVA analysis.

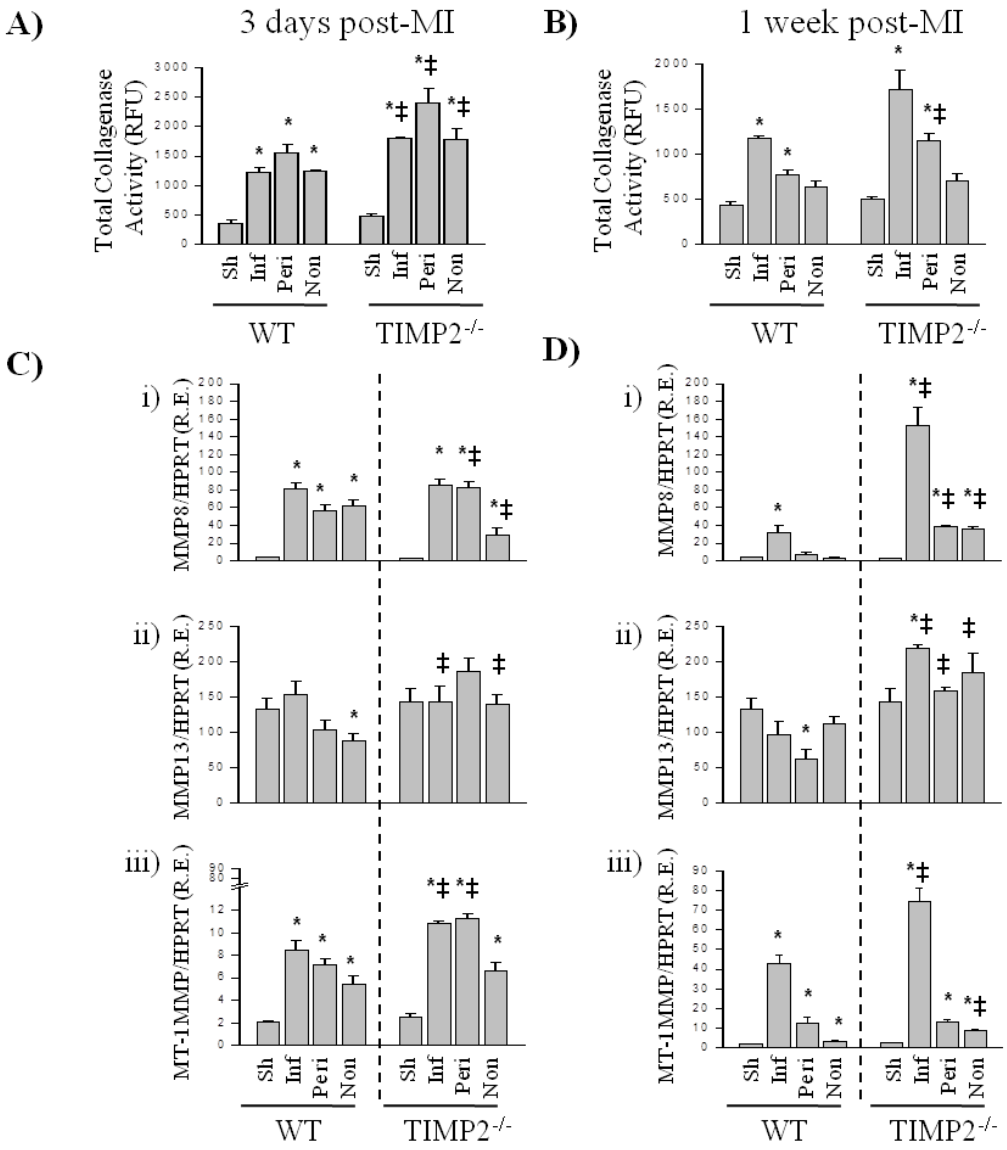

Figure 4.12. Enhanced activity and expression of collagenases in the TIMP2$^{-/-}$ and WT hearts post-MI.

A-B, Total collagenase activity in sham, infarct, peri-infarct, and non-infarct myocardium of WT and TIMP2$^{-/-}$ MI mice at 3 days (A) and 1 week post-MI (B). C-D, mRNA expression of collagenases, MMP8 (i), MMP13 (ii) and MT1-MMP (iii) in WT and TIMP2$^{-/-}$ hearts at 3 days (C) and 1 week (D) post-MI (n=6/group/genotype). RFU=Relative Fluorescent Units, R.E= Relative Expression. *p<0.05 compared to corresponding sham, ‡p<0.05 compared to WT using two-way ANOVA analysis.

in the infarct and non-infarct regions of TIMP2$^{-/-}$-MI hearts (Figure 4.12.Dii-Diii). Therefore, this marked elevation in expression and activity of collagenases in TIMP2-deficient hearts post-MI, could explain the aberrant degradation of the ECM collagen fibers and adverse LV remodeling in these mice.

4.4.8. MT1-MMP activity is significantly enhanced in the membrane fraction of TIMP2$^{-/-}$ hearts

MT1-MMP was one of the collagenases that was upregulated in TIMP2-MI myocardium, and is potently inhibited by TIMP2.[22] MT1-MMP is a membrane-bound MMP, and as such we examined levels and activity of this protease in the membrane fractions of the myocardium. We confirmed the purity of the membrane protein fractionation by blotting for a membrane protein, Toll-like receptor-4 (TLR4) as a positive control, and a cytoplasmic protein, caspase 3 as a negative control (Figure 4.13.). Coomassie blue staining was used as the loading control. Western blot analysis showed significantly higher MT1-MMP levels in the infarct and peri-infarct regions of TIMP2$^{-/-}$ myocardial tissue at 3 days (Figure 4.13.Ai) and 1 week post-MI (Figure 4.13.Aii).

We hypothesized that in the absence of TIMP2, activity of MT1-MMP would be more greatly increased. Using the antibody-based Biotrak activity assay which measures the activity specific to MT1-MMP without disrupting the MMP-TIMP interactions, we found that MI resulted in a rise in MT1-MMP activity in WT as well as TIMP2$^{-/-}$ hearts (Figure 4.13.B). However, this rise was significantly greater in the peri- and non-infarct regions of TIMP2$^{-/-}$ hearts at 3 days (Figure 4.13.Bi), and in the infarct and peri-infarct regions at 1 week (Figure 4.13.Bii) post-MI. We further confirmed that the detected activity is specific to MT1-MMP by demonstrating that recombinant TIMP2 (rTIMP2) completely blocked this activity to negligible levels, whereas rTIMP1 which is known to not inhibit MT-MMPs,[25] did not affect the MT-MMP activities (Figure 4.13.B).

We further investigated if the marked elevation in MT1-MMP activity in TIMP2$^{-/-}$-MI hearts was associated with degradation of other ECM components in

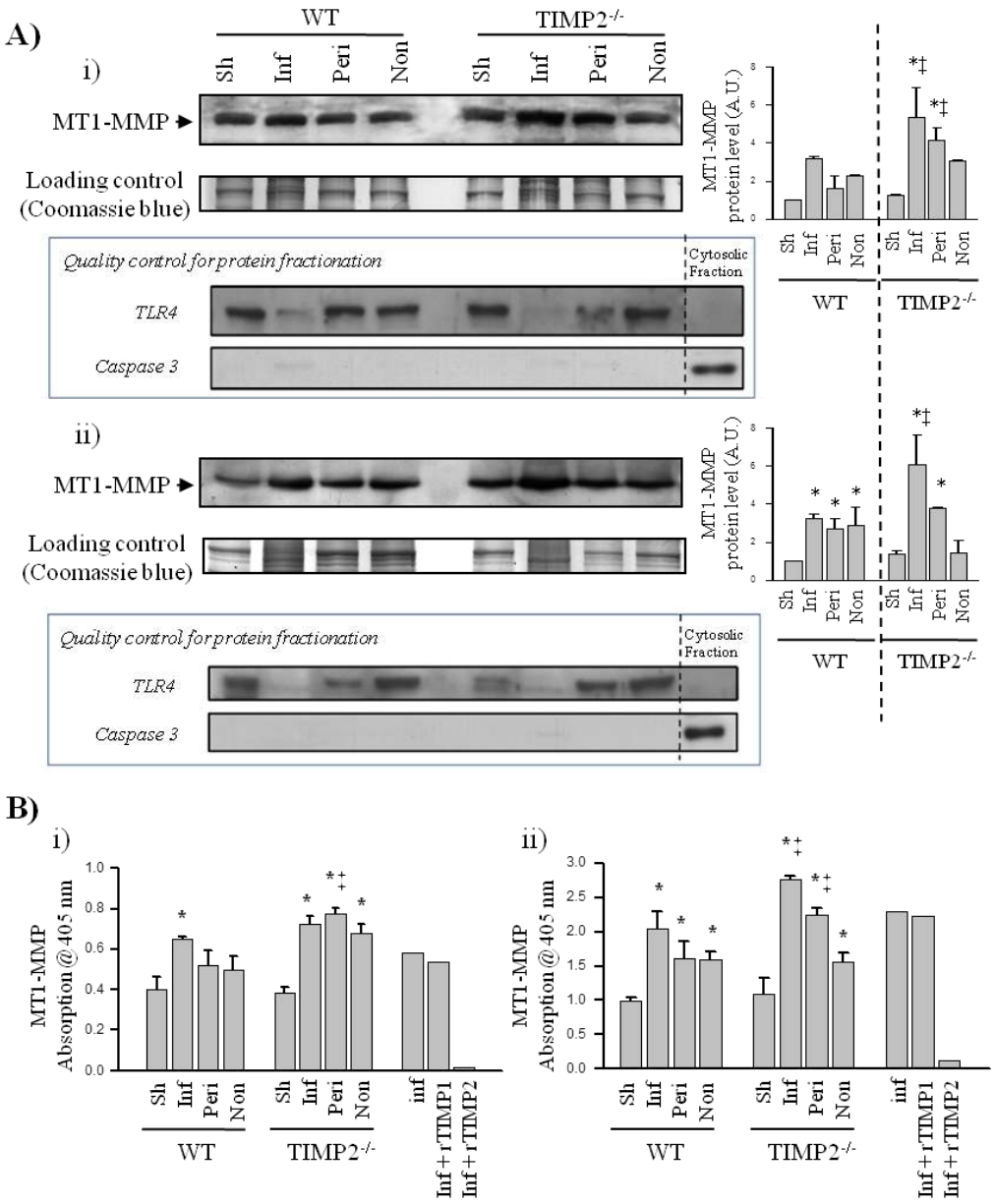

Figure 4.13. MT1-MMP levels and activity are significantly elevated in the membrane fraction of TIMP2$^{-/-}$-MI hearts.

A) Representative western blot for MT1-MMP (63kDa) in the membrane fraction WT and TIMP2$^{-/-}$ myocardium at 3 days (i) and 1 week (ii) post-MI. Toll-like receptor-4 (TLR4) and caspase-3 used as markers for quality control of subcelluar protein fractionation. Averaged protein levels are shown in bar graphs on the right (n=4/group/genotype). B) Activity of MT1-MMP on membrane fractions of WT and TIMP2$^{-/-}$ hearts at 3 days (i) and 1 week (ii) post-MI (n=6/group/genotype) . A.U.=Arbitrary Units, rTIMP1=recombinant TIMP1; rTIMP2=recombinant TIMP2. *p<0.05 compared to corresponding sham, ‡p<0.05 compared to WT using two-way ANOVA analysis.

A)

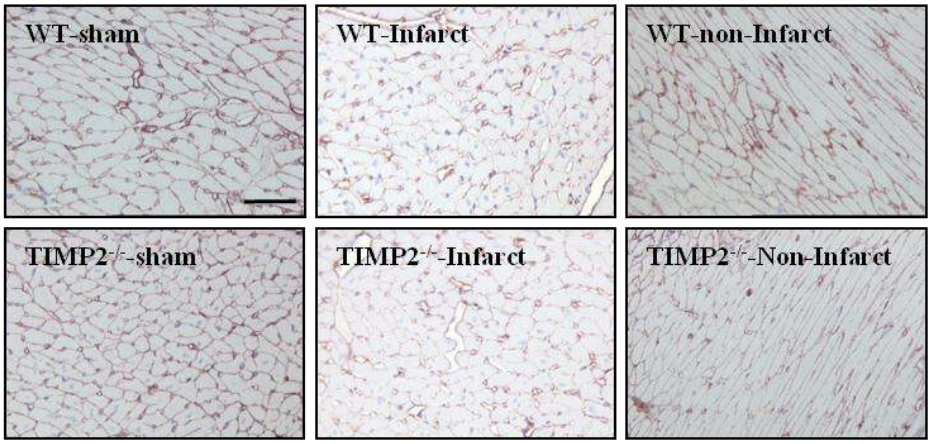

Figure 4.14. TIMP2$^{-/-}$-MI hearts show enhanced degradation of notable MT1-MMP-target laminin.

A, Laminin staining at 3 days post-MI of WT and TIMP2$^{-/-}$ sham, infarct, and non-infarcted myocardium. Scale bar=50µm

addition to collagen fibers (Figure 4.8). Immunostaining for laminin, another well known substrate for MT1-MMP action,[26, 27] showed a noticeable reduction in staining intensity in the infarct and non-infarct myocardium of TIMP2$^{-/-}$ compared to WT hearts at 3 days post-MI (Figure 4.14).

4.5. Discussion

4.5.1. TIMP2$^{-/-}$ mice exhibit pathological post-MI remodeling despite the lack of proMMP2 activation

TIMP2 and MT1-MMP are involved in cell surface activation of proMMP2 through formation of a trimolecular complex, MT1-MMP/TIMP2/proMMP2.[23, 24] MMP2 is a gelatinase and collagenase[28] that has been linked to a number of cardiomyopathies.[3, 8, 9] TIMP2 deficiency abolished MMP2 activation which was markedly increased in WT-MI infarct and peri-infarct myocardium. Our study clearly demonstrates that presence of TIMP2 is

absolutely essential for the cell surface activation of proMMP2 in the heart. Given the reported contribution of MMP2 in different cardiomyopathies,[3, 8, 9, 29-32] the exacerbated LV dilation and dysfunction in TIMP2$^{-/-}$-MI mice despite the lack of MMP2 activation is quite intriguing. Interestingly, increased MMP2 activation has been reported to underlie post-MI LV rupture,[33] and consistent with its lack of activation in TIMP2$^{-/-}$-MI hearts, we did not observe an elevated rate of LV rupture in these mice despite their severe remodeling and dysfunction compared to WT hearts post-MI.

4.5.2. Increased ECM degradation post-MI is associated with increased collagenase activity in the TIMP2$^{-/-}$ mice

Using the novel imaging technique of SHG/MPEF microscopy, we detected aberrant ECM remodeling characterized by lower density and enhanced disarray of the collagen fibres in the infarct and non-infarct regions of the TIMP2$^{-/-}$-MI hearts. The advantage of SHG over other imaging techniques is that it utilizes minimally manipulated tissue (unfixed and unstained), hence providing a more physiological presentation of the collagen fibre quality and arrangements. We also performed immunohistochemistry for laminin and found excess degradation of this ECM component in TIMP2$^{-/-}$-MI hearts. The aberrant degradation of the ECM structure was brought about by significantly enhanced collagenase activity in TIMP2$^{-/-}$-MI hearts driven largely by increased MT1-MMP activity.

4.5.3. TIMP2 inhibition of MT1-MMP is a critical regulator of post-MI remodeling

TIMP2 deficiency significantly deteriorated cardiac architecture and function following MI. We identified MT1-MMP as the primary protease whose activity is significantly augmented in the absence of TIMP2. The marked increase in MT1-MMP activity in TIMP2$^{-/-}$-MI hearts resulted from the increased protein levels as well as the absence of the inhibitory function of TIMP2 which potently inhibits MT1-MMP.[22, 34] In addition, MT1-MMP can mediate activation of other proMMPs, such as MMP13 (collagenase-3)[35, 36] which is also a potent collagenase

with broad substrate specificity, thereby amplifying the collagen degradation process. We used the BioTrak MT1-MMP specific activity assay to demonstrate the elevated activity of MT1-MMP in TIMP2-deficient myocardium, which was inhibited by rhTIMP2 but not by rhTIMP1, further demonstrating the TIMP2-dependence of this increased activity. Our study provides evidence that TIMP2 can regulate the activity of MT1-MMP, and can thereby serve as a therapeutic agent in heart disease.

4.5.4. Conclusions

This study is the first to demonstrate that TIMP2 is a key molecule in cardiac recovery from MI, and that the MMP-inhibitory function of TIMP2 is more critical than its MMP2-activating role in determining the fate of the myocardium in heart disease. Hence, TIMP2 replenishment in diseased myocardium could provide a potential therapy in reducing or preventing disease progression.

4.6. REFERENCES

1. Sutton MG, Sharpe N. Left ventricular remodeling after myocardial infarction: Pathophysiology and therapy. *Circulation*. 2000;101:2981-2988

2. Kassiri Z, Khokha R. Myocardial extra-cellular matrix and its regulation by metalloproteinases and their inhibitors. *Thromb Haemost*. 2005;93:212-219

3. Kassiri Z, Oudit GY, Sanchez O, Dawood F, Mohammed FF, Nuttall RK, Edwards DR, Liu PP, Backx PH, Khokha R. Combination of tumor necrosis factor-alpha ablation and matrix metalloproteinase inhibition prevents heart failure after pressure overload in tissue inhibitor of metalloproteinase-3 knock-out mice. *Circ Res*. 2005;97:380-390

4. Li YY, Feldman AM, Sun Y, McTiernan CF. Differential expression of tissue inhibitors of metalloproteinases in the failing human heart. *Circulation*. 1998;98:1728-1734

5. Tummalapalli CM, Heath BJ, Tyagi SC. Tissue inhibitor of metalloproteinase-4 instigates apoptosis in transformed cardiac fibroblasts. *J Cell Biochem*. 2001;80:512-521

6. Thomas CV, Coker ML, Zellner JL, Handy JR, Crumbley AJ, 3rd, Spinale FG. Increased matrix metalloproteinase activity and selective upregulation in lv myocardium from patients with end-stage dilated cardiomyopathy. *Circulation*. 1998;97:1708-1715

7. Webb CS, Bonnema DD, Ahmed SH, Leonardi AH, McClure CD, Clark LL, Stroud RE, Corn WC, Finklea L, Zile MR, Spinale FG. Specific temporal profile of matrix metalloproteinase release occurs in patients after myocardial infarction: Relation to left ventricular remodeling. *Circulation*. 2006;114:1020-1027

8. Spinale FG, Koval CN, Deschamps AM, Stroud RE, Ikonomidis JS. Dynamic changes in matrix metalloprotienase activity within the human myocardial interstitium during myocardial arrest and reperfusion. *Circulation*. 2008;118:S16-23

9. Spinale FG. Myocardial matrix remodeling and the matrix metalloproteinases: Influence on cardiac form and function. *Physiol Rev*. 2007;87:1285-1342

10. Creemers EE, Davis JN, Parkhurst AM, Leenders P, Dowdy KB, Hapke E, Hauet AM, Escobar PG, Cleutjens JP, Smits JF, Daemen MJ, Zile MR, Spinale FG. Deficiency of timp-1 exacerbates lv remodeling after myocardial infarction in mice. *Am J Physiol Heart Circ Physiol*. 2003;284:H364-371

11. Tian H, Cimini M, Fedak PW, Altamentova S, Fazel S, Huang ML, Weisel RD, Li RK. Timp-3 deficiency accelerates cardiac remodeling after myocardial infarction. *J Mol Cell Cardiol*. 2007;43:733-743

12. Kandalam V, Basu R, Abraham T, Wang X, Awad A, Wang W, Lopaschuk GD, Maeda N, Oudit GY, Kassiri Z. Early activation of matrix metalloproteinases underlies the exacerbated systolic and diastolic dysfunction in mice lacking timp3 following myocardial infarction. *Am J Physiol Heart Circ Physiol*. 2010;299:H1012-1023

13. Koskivirta I, Kassiri Z, Rahkonen O, Kiviranta R, Oudit GY, McKee TD, Kyto V, Saraste A, Jokinen E, Liu PP, Vuorio E, Khokha R. Mice with tissue inhibitor of metalloproteinases 4 (timp4) deletion succumb to induced myocardial infarction but not to cardiac pressure overload. *J Biol Chem*. 2010;285:24487-24493

14. Ang DS, Kong CF, Kao MP, Struthers AD. Serial bedside b-type natriuretic peptide strongly predicts prognosis in acute coronary syndrome independent of echocardiographic abnormalities. *Am Heart J*. 2009;158:133-140

15. Ang DS, Wei L, Kao MP, Lang CC, Struthers AD. A comparison between b-type natriuretic peptide, global registry of acute coronary events (grace) score and their combination in acs risk stratification. *Heart*. 2009

16. Zhang Y, Takagawa J, Sievers RE, Khan MF, Viswanathan MN, Springer ML, Foster E, Yeghiazarians Y. Validation of the wall motion score and myocardial performance indexes as novel techniques to assess cardiac function in mice after myocardial infarction. *Am J Physiol Heart Circ Physiol*. 2007;292:H1187-1192

17. Zipfel WR, Williams RM, Christie R, Nikitin AY, Hyman BT, Webb WW. Live tissue intrinsic emission microscopy using multiphoton-excited

native fluorescence and second harmonic generation. *Proc Natl Acad Sci U S A*. 2003;100:7075-7080

18. Palero JA, de Bruijn HS, van der Ploeg van den Heuvel A, Sterenborg HJ, Gerritsen HC. Spectrally resolved multiphoton imaging of in vivo and excised mouse skin tissues. *Biophys J*. 2007;93:992-1007

19. Abraham T, Carthy J, McManus B. Collagen matrix remodeling in 3-dimensional cellular space resolved using second harmonic generation and multi photon excitation fluorescence. *J Struct Biol*. 2009

20. Laflamme MA, Murry CE. Regenerating the heart. *Nat Biotechnol*. 2005;23:845-856

21. Jugdutt BI. Ventricular remodeling after infarction and the extracellular collagen matrix: When is enough enough? *Circulation*. 2003;108:1395-1403

22. Butler GS, Butler MJ, Atkinson SJ, Will H, Tamura T, Schade van Westrum S, Crabbe T, Clements J, d'Ortho MP, Murphy G. The timp2 membrane type 1 metalloproteinase "receptor" regulates the concentration and efficient activation of progelatinase a. A kinetic study. *J Biol Chem*. 1998;273:871-880

23. Strongin AY, Collier I, Bannikov G, Marmer BL, Grant GA, Goldberg GI. Mechanism of cell surface activation of 72-kda type iv collagenase. Isolation of the activated form of the membrane metalloprotease. *J Biol Chem*. 1995;270:5331-5338

24. Atkinson SJ, Crabbe T, Cowell S, Ward RV, Butler MJ, Sato H, Seiki M, Reynolds JJ, Murphy G. Intermolecular autolytic cleavage can contribute to the activation of progelatinase a by cell membranes. *J Biol Chem*. 1995;270:30479-30485

25. Lee MH, Rapti M, Murphy G. Unveiling the surface epitopes that render tissue inhibitor of metalloproteinase-1 inactive against membrane type 1-matrix metalloproteinase. *J Biol Chem*. 2003;278:40224-40230

26. Shen XM, Wu YP, Feng YB, Luo ML, Du XL, Zhang Y, Cai Y, Xu X, Han YL, Zhang X, Zhan QM, Wang MR. Interaction of mt1-mmp and laminin-5gamma2 chain correlates with metastasis and invasiveness in human esophageal squamous cell carcinoma. *Clin Exp Metastasis*. 2007;24:541-550

27. Ohtake Y, Tojo H, Seiki M. Multifunctional roles of mt1-mmp in myofiber formation and morphostatic maintenance of skeletal muscle. *J Cell Sci*. 2006;119:3822-3832

28. Collier IE, Wilhelm SM, Eisen AZ, Marmer BL, Grant GA, Seltzer JL, Kronberger A, He CS, Bauer EA, Goldberg GI. H-ras oncogene-transformed human bronchial epithelial cells (tbe-1) secrete a single metalloprotease capable of degrading basement membrane collagen. *J Biol Chem*. 1988;263:6579-6587

29. Schenke-Layland K, Stock UA, Nsair A, Xie J, Angelis E, Fonseca CG, Larbig R, Mahajan A, Shivkumar K, Fishbein MC, Maclellan WR. Cardiomyopathy is associated with structural remodelling of heart valve extracellular matrix. *Eur Heart J*. 2009

30. Lee JG, Dahi S, Mahimkar R, Tulloch NL, Alfonso-Jaume MA, Lovett DH, Sarkar R. Intronic regulation of matrix metalloproteinase-2 revealed by in vivo transcriptional analysis in ischemia. *Proc Natl Acad Sci U S A*. 2005;102:16345-16350

31. Zhou HZ, Ma X, Gray MO, Zhu BQ, Nguyen AP, Baker AJ, Simonis U, Cecchini G, Lovett DH, Karliner JS. Transgenic mmp-2 expression induces latent cardiac mitochondrial dysfunction. *Biochem Biophys Res Commun*. 2007;358:189-195

32. Tuysuz B, Mosig R, Altun G, Sancak S, Glucksman MJ, Martignetti JA. A novel matrix metalloproteinase 2 (mmp2) terminal hemopexin domain mutation in a family with multicentric osteolysis with nodulosis and arthritis with cardiac defects. *Eur J Hum Genet*. 2009;17:565-572

33. Matsumura S, Iwanaga S, Mochizuki S, Okamoto H, Ogawa S, Okada Y. Targeted deletion or pharmacological inhibition of mmp-2 prevents cardiac rupture after myocardial infarction in mice. *J Clin Invest*. 2005;115:599-609

34. Sato H, Kinoshita T, Takino T, Nakayama K, Seiki M. Activation of a recombinant membrane type 1-matrix metalloproteinase (mt1-mmp) by furin and its interaction with tissue inhibitor of metalloproteinases (timp)-2. *FEBS Lett*. 1996;393:101-104

35. Knauper V, Will H, Lopez-Otin C, Smith B, Atkinson SJ, Stanton H, Hembry RM, Murphy G. Cellular mechanisms for human procollagenase-3 (mmp-13) activation. Evidence that mt1-mmp (mmp-14) and gelatinase

a (mmp-2) are able to generate active enzyme. *J Biol Chem*. 1996;271:17124-17131

36. Elnemr A, Yonemura Y, Bandou E, Kinoshita K, Kawamura T, Takahashi S, Tochiori S, Endou Y, Sasaki T. Expression of collagenase-3 (matrix metalloproteinase-13) in human gastric cancer. *Gastric Cancer*. 2003;6:30-38

CHAPTER 5

Lack of Tissue Inhibitor of Metalloproteinases-2 leads to exacerbated left ventricular dysfunction and adverse extracellular matrix remodeling in response to biomechanical stress

Vijay Kandalam[1,2,4], Ratnadeep Basu[1,2,4], Linn Moore[1,2,4], Dong Fan[1,2,4], Xiuhua Wang[1,2,4], Diane M. Jaworski[5], Gavin Y. Oudit[1,2,3,4], Zamaneh Kassiri[1,2,4]

1Department of Physiology, 2Cardiovascular Research Centre, 3Division of Cardiology/Department of Medicine, 4Mazankowski Alberta Heart Institute, University of Alberta, Edmonton, AB., Canada; and 5Department of Anatomy and Neurobiology, University of Vermont, Burlington, VT.

Contributions:

VK (70%): Monitoring all animals, scheduling surgeries and functional data collection, tissue collection, data collection, and project planning. Collected all tissue, processed all tissue, and conducted majority of experiments and all data analysis. VK had a primary role in the writing of the manuscript and assembly of final figures.

RB : analysis of all acquired raw echocardiography data, LM: performed TIMP western blots for post-TAC samples with protein extraction, DF: Taqman on MMPi treatment portion of the project including RNA extraction, XW : performed Taqman RT-PCR and MMP activity assays; DMJ: performed integrin staining. GYO: worked in conjunction with RB to manage echocardiography analysis and interpretation, ZK: supervisor of VK, overall project planning and corresponding author.

A version of this chapter has been published. Kandalam et al. 2011. Circulation. 124(19): 2094-105.

5.1. Introduction

Increased afterload leading to excess biomechanical stress is a common cause of LV remodeling which leads to cardiac dysfunction and eventually heart failure.[1, 2] Adverse remodeling of the myocardial ECM, brought about by dysregulation in its turnover, is a key component of pressure overload-induced cardiomyopathy. This results in excess degradation and disruption of the ECM network structure, or accumulation of ECM proteins and formation of fibrotic lesions. Myocardial fibrosis is also a well-known cause of diastolic dysfunction and diastolic heart failure.[3-7] An imbalance in the function of MMPs and TIMPs occurs in heart disease leading to adverse ECM remodeling and TIMPs are emerging as critical regulators of this process.[8-13]

Among the four TIMPs,[14] TIMP2 has the unique property of activating MMP2 through formation of a trimolecular complex with proMMP2 and MT1-MMP. This function of TIMP2 is in addition to its ability to inhibit a number of MMPs. TIMP2 levels are increased in the hearts of patients with aortic valvular stenosis[15] and patients with pressure overloaded cardiomyopathy.[16] However, whether this rise in TIMP2 is a compensatory attempt by the heart to inhibit the elevated MMP activities, or it further contributes to disease progression by promoting activation of MMP2, remains to be determined. We investigated the role of TIMP2 in cardiac response to a pressure overload model of heart failure. Loss of TIMP2 resulted in adverse remodeling of the ECM and precipitous heart failure, while MMP inhibition prevented these unfavourable outcomes.

5.2. Objectives

The objective of this study is to investigate the role of TIMP2 in the cardiac response to pressure overload through the use of the TAC model in TIMP2-deficient mice to determine the extent and mechanism of cardiac remodeling in the absence of TIMP2 compared to WT. The aortic constriction will create a representative model of pressure overload, with increased afterload

against which the heart will work. Examining the remodeling process and mechanisms involved in the absence of TIMP2 will allow us to clarify whether TIMP2 has a protective or detrimental role in the heart subjected to an increase in biomechanical stress, thereby enabling us to determine a viable therapeutic approach to TIMP2-dependent regulation of ECM remodeling.

5.3. Methods

5.3.1. TAC procedure

At 8-10 weeks of age, mice were anesthetized and underwent transverse aortic constriction according to protocol in Section 2.2.2. Sham-operated mice were used as controls. Mice were allowed to recover and monitored as described in Section 2.4.1. MMPi was administered following the regimen described in Section 2.3.

5.3.2. *In vivo* imaging and analysis

Echocardiography was conducted to examine parameters pertaining to pressure overload analysis as described in Section 2.5.1, along with TMD (Section 2.5.2) and TDI (Section 2.5.3) for complete *in vivo* analysis of cardiac function.

5.3.3. Molecular and cellular analysis

Sham and post-TAC tissue was collected as described in Section 2.4.2., and processed for molecular (RNA in Section 2.8., protein in Section 2.9., and MMP activity in Section 2.11.), cellular (ECM-cell adhesion in Section 2.10.1.), histological (collagen in Section 2.6.2.1., and integrin-β1 in Section 2.7.1,), and morphological (LV morphology in Section 2.6.1.1., and collagen organization 2.6.2.4.) analysis.

5.4. Results

5.4.1. TIMP2-deficient mice exhibit more severe pressure overloaded cardiomyopathy

We first investigated how cardiac TIMPs change in response to pressure overload (TAC). We found that while TIMP1, TIMP3 and TIMP4 remained unaltered, TIMP2 protein levels increased significantly after 2 weeks (Figure 5.1.Ai-Aii) and 5 weeks (Figure 5.2.Ai-Aii) of TAC. To determine the precise role of TIMP2 in pressure overload-induced heart disease, we subjected mice lacking TIMP2 to pressure overload by TAC. After 2 weeks and 5 weeks, $TIMP2^{-/-}$-TAC hearts were larger than the parallel WT-TAC hearts (Figure 5.3.Ai) with greater myocardial hypertrophy as determined by larger LV weight-to-tibial length ratio (Figure 5.3.Aii) and cardiomyocyte cross-sectional area (Figure 5.3.Bi-ii) compared to WT-TAC group. $TIMP2^{-/-}$-TAC hearts also exhibited exacerbated adverse pathological remodeling as detected by a larger increase in mRNA expression of molecular markers of cardiac disease, brain natriuretic peptide, β-myosin heavy chain, and α-skeletal actin (Figure 5.4.Ai-Aiii). These results show that TIMP2 is upregulated in a pressure overload state, and that loss of TIMP2 exacerbates the adverse pathological myocardial remodeling.

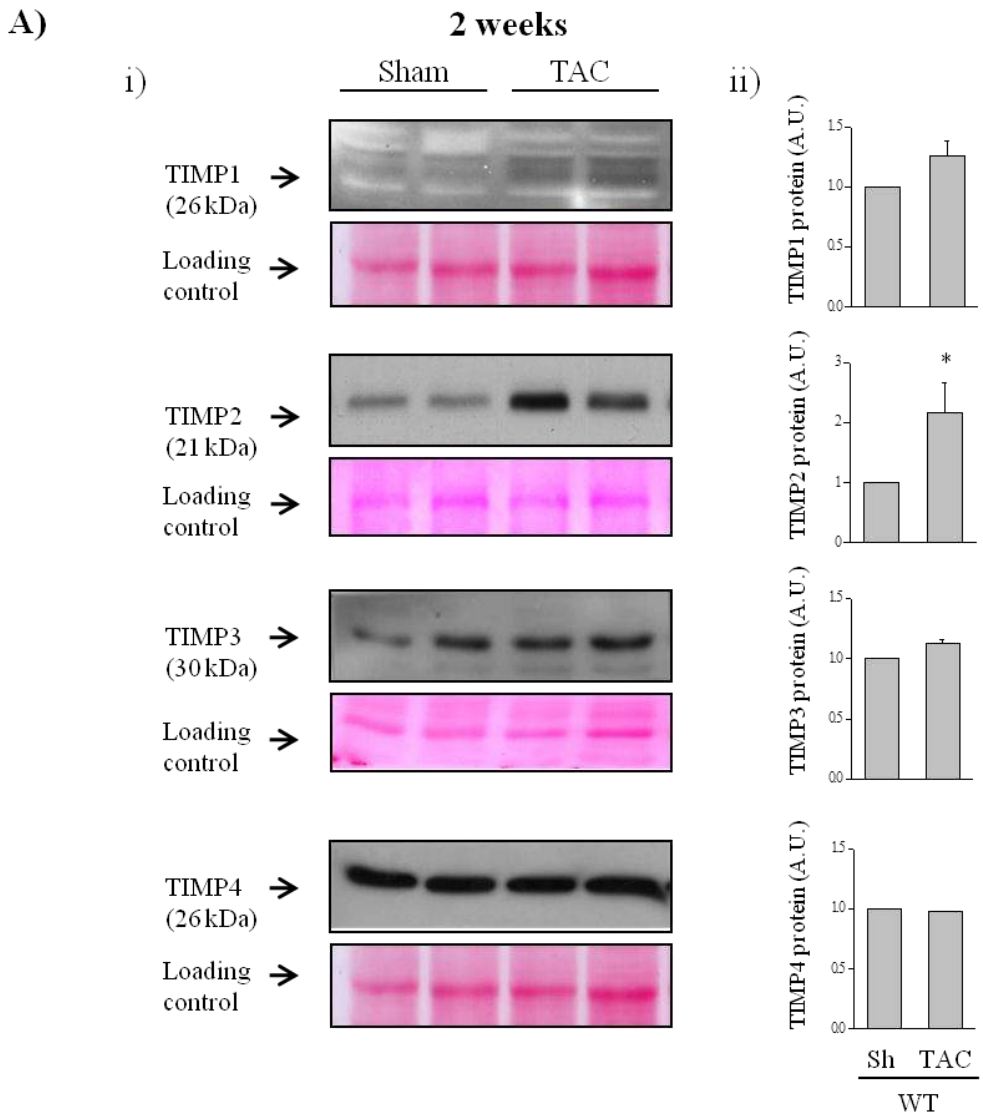

Figure 5.1. Pressure overload impacts each TIMP differently at 2 weeks after TAC.

A, Representative Western blot (i) and averaged protein quantification (ii) of TIMP1, TIMP2, TIMP3 and TIMP4 after 2 weeks of sham-operation or post-TAC. TAC=transverse aortic constriction. A.U.= arbitrary units. n=6/group. *p<0.05 compared to sham using Student's T-test analysis.

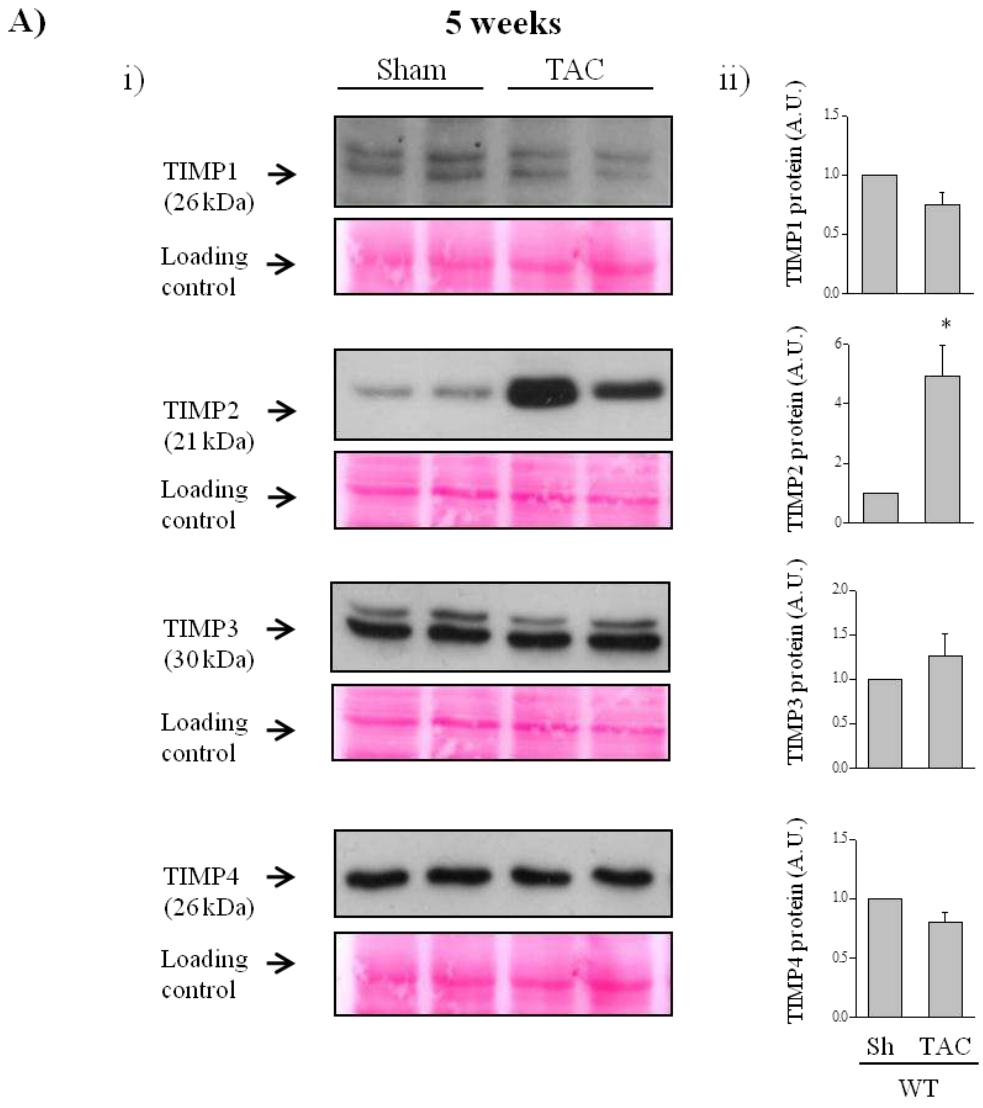

Figure 5.2. Pressure overload differentially impacts each TIMP at 5weeks post-TAC.

A, Representative Western blot (i) and averaged protein quantification (ii) of TIMP1, TIMP2, TIMP3 and TIMP4 after 5 weeks of sham-operation or post-TAC. TAC=transverse aortic constriction. A.U.= arbitrary units. n=6/group. *p<0.05 compared to sham using Student's T-test analysis.

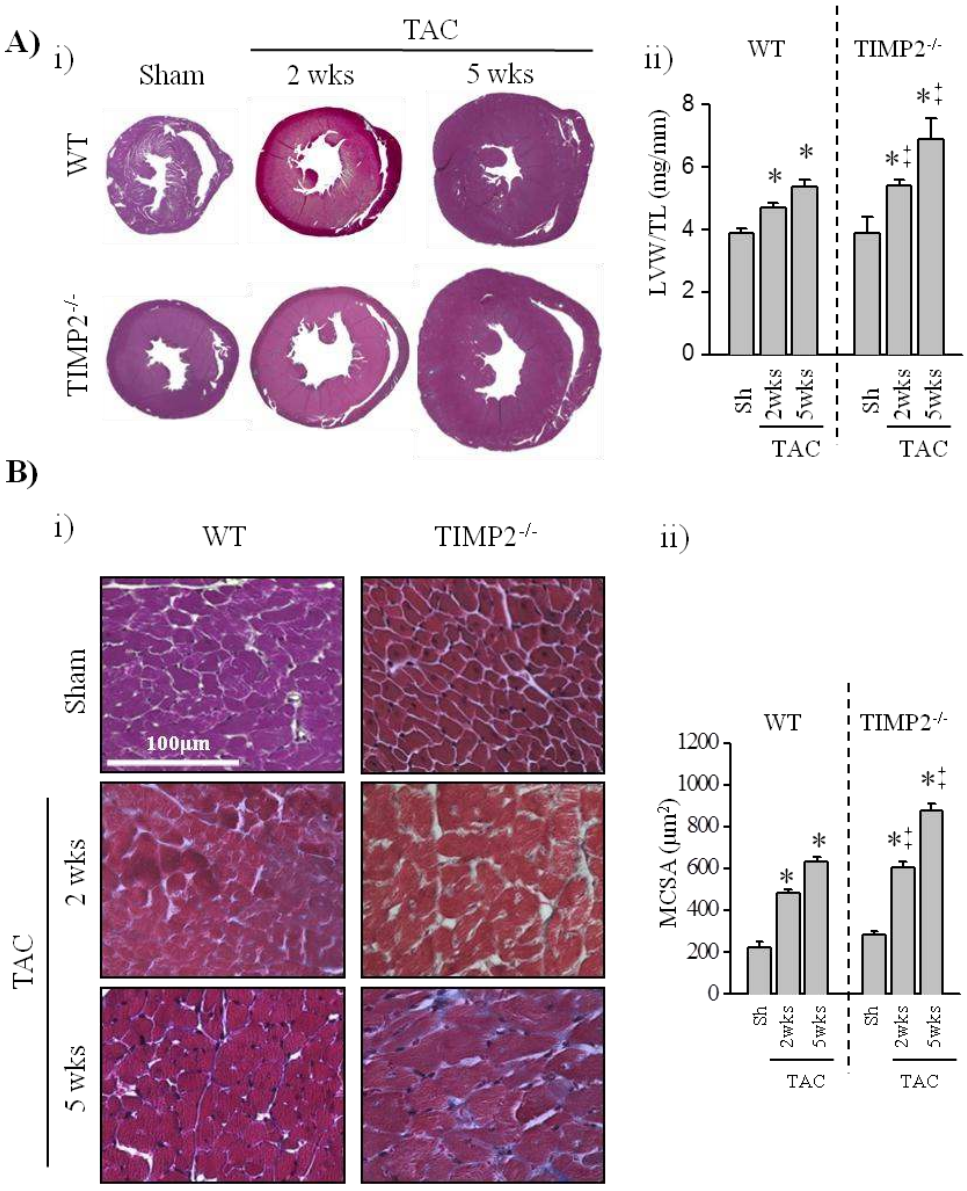

Figure 5.3. TIMP2-deficient mice display more severe cardiomyopathy following pressure overload.

A, Representative transverse cross-sections of trichrome-stained hearts (i) and LV weight-to-tibial length ratio (LVW/TL) (ii) of WT and TIMP2$^{-/-}$ hearts after sham, 2 weeks or 5 weeks of TAC. B, Representative images of cardiomyocyte cross-sections (i), and averaged myocyte cross-sectional area (MCSA) (n=100 myocytes/group) (ii) from each group. A.U.=arbitrary units. *p<0.05 compared to sham, ‡ p<0.05 compared to WT-TAC using two-way ANOVA analysis.

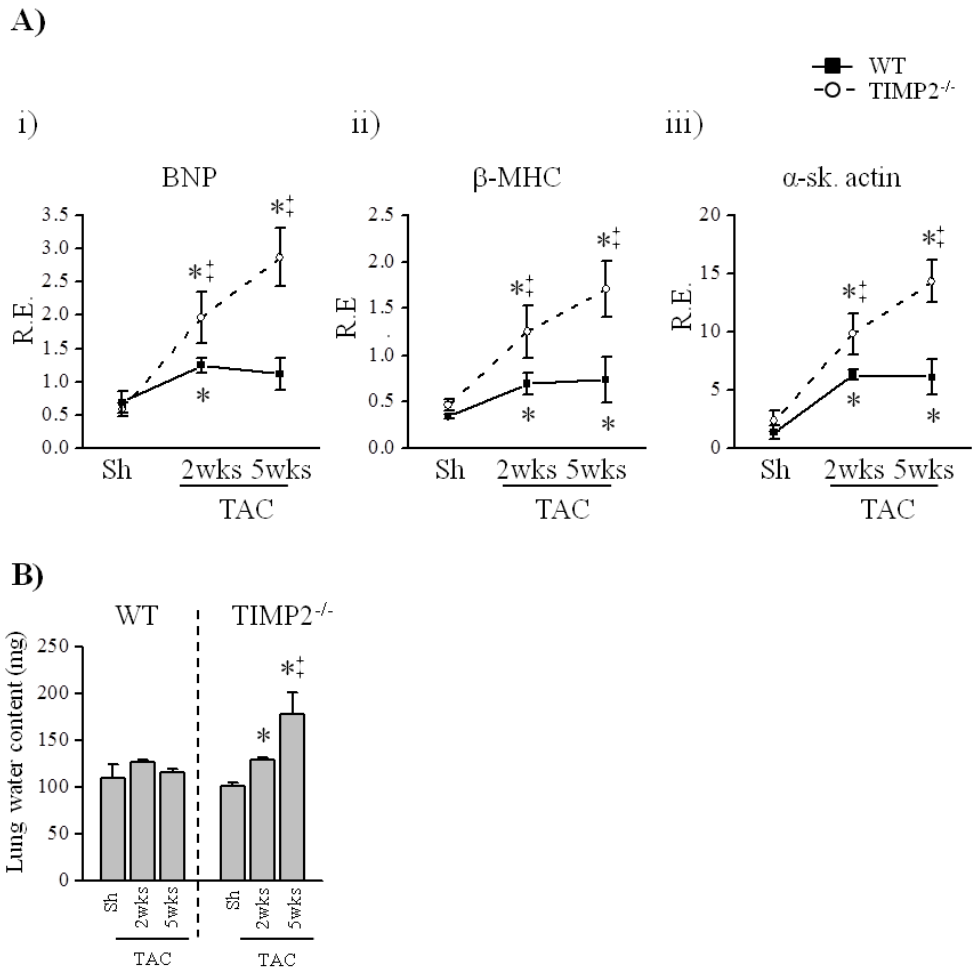

Figure 5.4. TIMP2$^{-/-}$ mice exhibit more severe heart disease in response to pressure overload.

A, mRNA expression of molecular markers of heart disease, brain natriuretic peptide (BNP) (i), beta-myosin heavy chain (β-MHC) (ii) and alpha-skeletal actin (α-Sk.Actin) (iii) in WT and TIMP2$^{-/-}$ hearts after sham or TAC (n=6/group). B, Lung water content (wet weight – dry weight) in WT and TIMP2$^{-/-}$ mice after sham or after 2 weeks or 5 weeks of TAC. n=8/group/genotype. R.E.=relative expression, *p<0.05 compared to sham, ‡ p<0.05 compared to WT-TAC using two-way ANOVA analysis

5.4.2. TIMP2-deficient mice exhibit exacerbated LV dysfunction post-TAC

Echocardiographic analysis of cardiac function revealed accelerated LV dilation and systolic dysfunction in TIMP2$^{-/-}$-TAC mice at 2 weeks post-TAC as

evident from B-mode (Figure 5.5.Ai) and M-mode images (Figure 5.5.Aii) showing reduced EF, greater LV end-diastolic diameter, and reduced velocity of circumferential shortening compared to WT-TAC mice (Figure 5.5.Bi-Biii). The E /E' ratio, a measure LV filling pressure, was markedly elevated in TIMP2$^{-/-}$-TAC mice (Figure 5.6.A, Bi and Table 5.1.). The left atrium was enlarged by 2-fold in TIMP2$^{-/-}$-TAC hearts (Figure 5.6.Bii, Table 5.1.) further indicating worsened systolic dysfunction in these mice. The systolic dysfunction in TIMP2$^{-/-}$-TAC mice exacerbated further by 5 weeks compared to the parallel WT-TAC group resulting in further elevation in E/E' and a restricted transmitral filling pattern. These deteriorations in cardiac function and elevated LV filling pressure lead to pulmonary edema in TIMP2$^{-/-}$ compared to WT mice post-TAC (Figure 5.4.B). Systolic and diastolic parameters were comparable in sham-operated WT and TIMP2$^{-/-}$ mice. These data indicate that TIMP2 is essential for an optimal adaptive functional response to increased biomechanical stress in the heart.

5.4.3. Lack of TIMP2 leads to excess myocardial fibrosis

Pressure overload triggered interstitial fibrosis in TIMP2$^{-/-}$, but not in WT mice, which became more severe and more prevalent by 5 weeks (Figure 5.7.A). The more severe fibrosis in TIMP2$^{-/-}$-TAC hearts was not due to increased expression of collagen type-I or type-III, the predominant components of fibrillar ECM, which were elevated similarly in both genotypes (Figure 5.7.Bi-Bii). We found that levels of SPARC, a protein that mediates extracellular stabilization of collagen fibres,[17, 18] were significantly elevated in TIMP2$^{-/-}$-TAC compared to WT-TAC hearts (Figure 5.7.Di-Dii). In addition, the greater myocardial fibrosis in TIMP2$^{-/-}$-TAC hearts was associated with higher expression of TIMP1, a well-known marker of fibrosis,[19-21] which increased progressively and to a markedly greater extent in TIMP2$^{-/-}$ compared to WT hearts post-TAC (Figure 5.7.C). Interestingly, an increase in TIMP1 levels was not observed at the protein level (Figure 5.1. and 5.2.) which indicates dissociation between transcription and

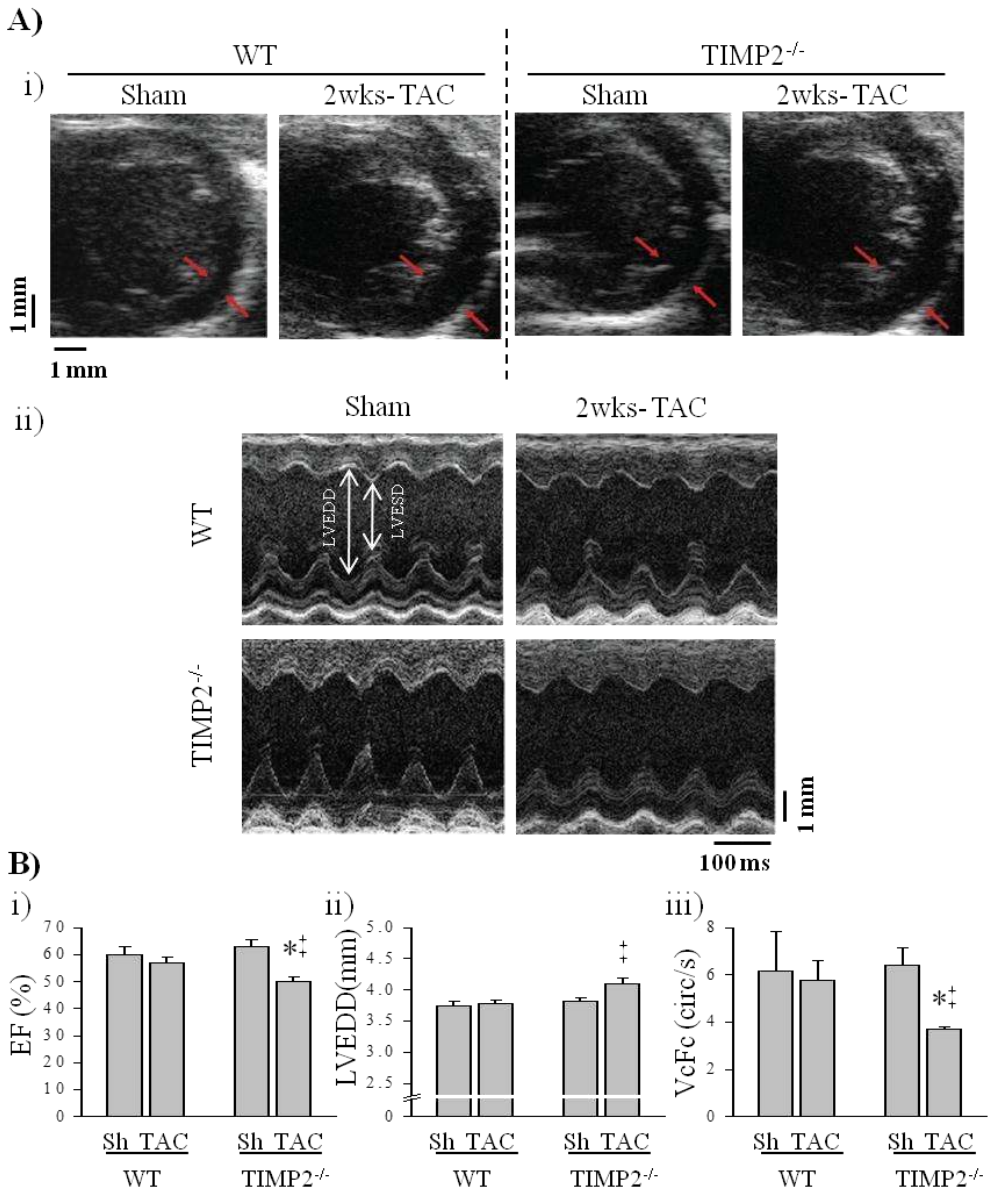

Figure 5.5. Exacerbated cardiac dysfunction in TIMP2$^{-/-}$ mice at 2 weeks post-TAC.

Echocardiographic images showing representative B-mode (A-i) and M-mode (A-ii) images from WT and TIMP2$^{-/-}$ mice at 2 weeks post-TAC or sham. B, Averaged parameters of cardiac contractility, ejection fraction (EF) (i), LV end-diastolic diameter (LVEDD) (ii), and velocity of circumferential fibre shortening (VcFC) (iii). (n=6/sham, 8-9/TAC). *p<0.05 compared to sham, ‡ p<0.05 compared to WT-TAC using two-way ANOVA analysis.

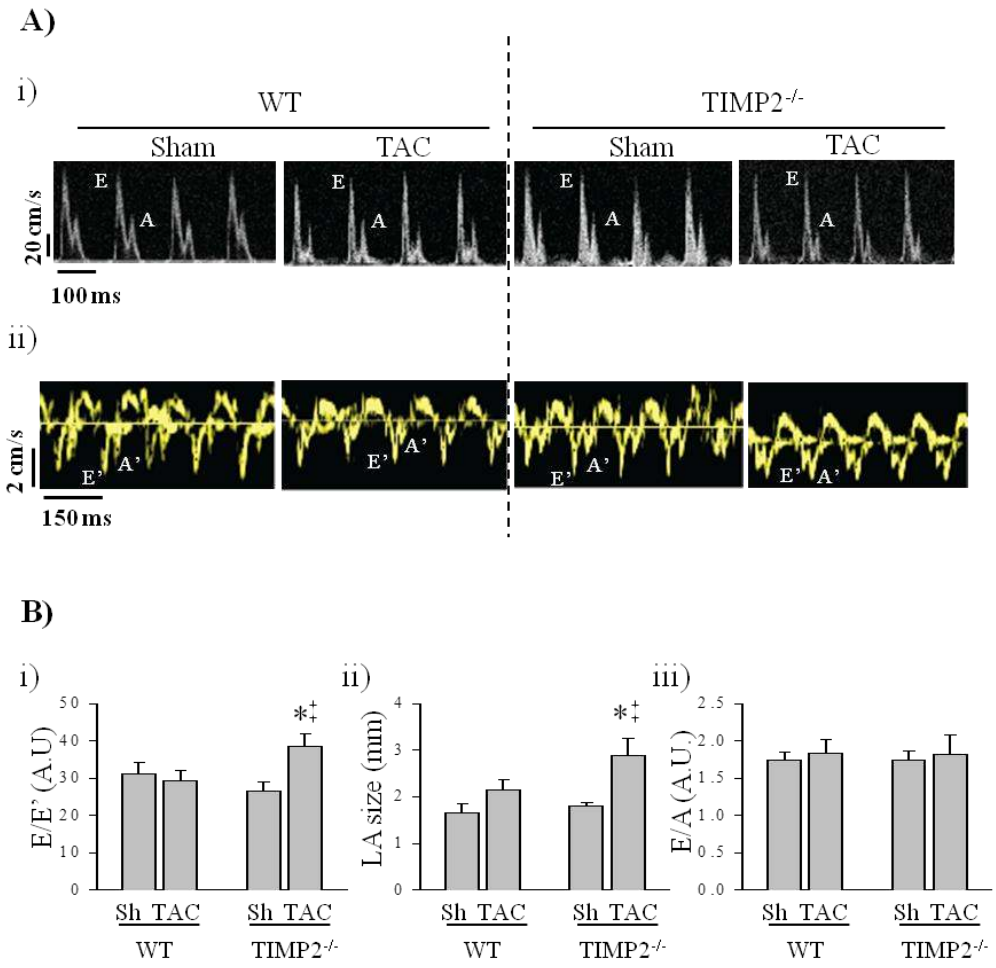

Figure 5.6. More severe cardiac dysfunction in TIMP2$^{-/-}$ mice at 2 weeks post-TAC.

A, Echocardiographic images showing representative Transmitral Valve (i), and Tissue Doppler images (ii). B, Averaged E-to-E' wave ratio (i), left atrial (LA) size (ii), and E-wave to A-wave ratio (iii). (n=6/sham, 8-9/TAC). *p<0.05 compared to sham, ‡ p<0.05 compared to WT-TAC using two-way ANOVA analysis.

Table 5.1. Echocardiographic assessment of systolic and diastolic function in WT and TIMP2$^{-/-}$ mice after sham, 2 weeks or 5 weeks after transverse aortic constriction (TAC), and after MMPi-treatment at 2 weeks and 5 weeks post-TAC.

	WT			TIMP2$^{-/-}$			TIMP2$^{-/-}$ + MMPi	
	Sham	**2wk-TAC**	**5wk-TAC**	**Sham**	**2wk-TAC**	**5wk-TAC**	**2wk-TAC**	**5wk-TAC**
n	6	9	9	6	9	6	10	8
HR (bpm)	483±12	469±10	472±16	472±14	465±21	467±20	488±14	471±11
LVEDD (mm)	3.74±0.08	3.78±0.05	4.09±0.09	3.81±0.07	4.10±0.10*‡	4.59±0.06*‡	3.90±0.05	4.03±0.17§
LVESD (mm)	2.57±0.06	2.64±0.07	3.19±0.13*	2.56±0.06	3.09±0.09*‡	3.81±0.07*‡	2.74±0.05§	2.94±0.18§
LVFS (%)	31.3±1.9	30.2±1.4	22±1.8*	32.8±1.9	24.6±1.0*‡	17±2.2*‡	29.7±1.6	27.1±2.4
LVEF (%)	60.2±3.0	57.1±1.9	47.5±2.5*	62.8±2.6	50.1±1.7*‡	31.5±4.1*‡	57.2±1.3§	53.0±3.6
VCFc (circ/s)	6.15±0.17	5.79±0.21	4.47±0.27*	6.43±0.41	3.70±0.12*‡	2.16±0.24*‡	5.38±0.28§	4.78±0.46§
LVPWT (mm)	0.66±0.05	0.86±0.03*	0.83±0.02*	0.65±0.05	0.87±0.03*	0.95±0.05*	0.75±0.02§	0.86±0.04
E-wave (mm/s)	749.3±28.4	755.6±24.1	708.1±25.6	761.4±23.5	770.5±38.2	821.8±48.1*‡	780.2±37.6§	715.6±44.2§
A-wave (mm/s)	429.8±15.2	409.8±18.3	444.6±11.5	443.5±24.3	421.2±45.6	207.1±81.5*‡	494.5±18.3§	458.2±51.3§
E/A ratio	1.74±0.11	1.84±0.18	1.59±0.12*	1.74±0.12	1.82±0.26	3.97±0.28*‡	1.62±0.11§	1.54±0.13§
DT (ms)	28.3±1.4	26.8±2.0	26.0±1.8	25.8±1.6	26.5±3.5	25.8±5.6	23.2±0.7§	29.0± 2.2
EWDR (mm/s^2)	26.5±2.1	28.2±2.3	27.2±2.0	29.4±3.2	29.1±2.8	31.8±4.8*‡	33.6±2.6§	24.71±2.4§
E′ (mm/s)	24.1±2.1	25.8±1.6	23.2±1.8	28.6±2.8	20.0±2.3*‡	15.4±5.4*‡	25.9±1.8§	25.0±3.4§
E/E′ ratio	31.1±3.3	29.3±2.8	30.5±3.2	26.6±2.4	38.5±3.6*‡	53.4±4.7*‡	30.1±1.9	28.6±2.2§
LA Size (mm)	1.66±0.19	2.14±0.24	2.50±0.20*	1.81±0.06	2.89±0.37*‡	2.99±0.21*‡	2.14±0.09§	2.22±0.12§

LVEDD= LV end diastolic diameter; LVESD=LV end systolic diameter; LVFS=LV fractional shortening; LVEF=LV ejection fraction; VCFc= Velocity of circumferential shortening corrected for heart rate; LVPWT=LV Posterior wall thickness. E-wave= early transmitral inflow velocity; A-wave=transmitral inflow velocity due to atrial contraction; DT=E-wave deceleration time; EWDR=E-wave deceleration rate (E-wave/DT); E′=early tissue Doppler velocity; LA=Left atrium.* $p<0.05$ compared to sham, ‡ $p<0.05$ compared to WT-TAC. § $p<0.5$ compared to TIMP2$^{-/-}$-TAC using two-way ANOVA analysis.

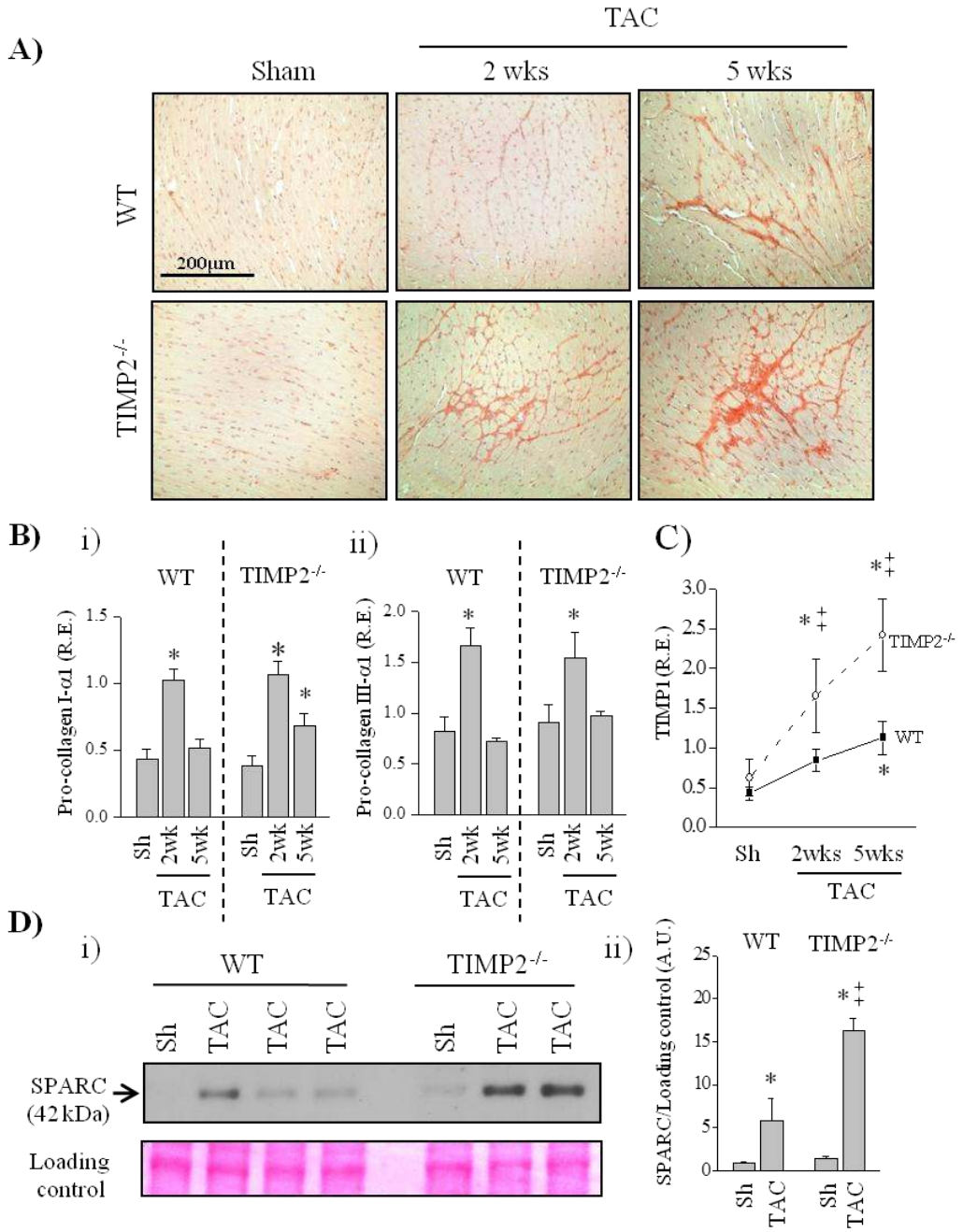

Figure 5.7. TIMP2 deficiency results in excess fibrosis post-TAC.

Picrosirius red staining of collagen (A), mRNA expression levels of procollagen I-α1 (B-i) and procollagen III-α1 (B-ii) of WT and TIMP2$^{-/-}$ hearts post-sham or TAC (n=6/group/genotype). C, mRNA expression levels of TIMP1 in WT and TIMP2$^{-/-}$ hearts post-TAC. D, Representative Western blot (i) and averaged protein levels (ii) for SPARC (secreted protein acidic and rich in cysteine) in WT and TIMP2$^{-/-}$ hearts post-sham and post-TAC (n=4-6/group/genotype). *p<0.05 compared to sham, ‡ p<0.05 compared to WT-TAC using two-way ANOVA analysis.

translation of this molecule. Hence, the increased myocardial fibrosis in TIMP2$^{-/-}$-TAC hearts is due to post-translational stabilization of collagen fibres rather than increased collagen production.

Detailed analysis of the ECM structure by scanning electron microscopy revealed a great degree of organization of the fibrillar ECM network in sham-operated hearts (Figure 5.8.Ai and Aiv). By 2 weeks post-TAC, this fibrillar arrangement started to become distorted in the WT hearts (Figure 5.8.Aii-iii), whereas TIMP2-TAC hearts showed a very severe and nonuniform disorganization of the ECM. While degraded ECM was detected in some areas (Figure 5.8.Av), other areas showed severe thickening of the ECM fibrillar structure (Figure 5.8.Avi). Clearly, loss of TIMP2 leads to both quantitative and qualitative alterations in the ECM network structure.

5.4.4. Collagenase activity is augmented in TIMP2$^{-/-}$-TAC hearts

Consistent with the critical role of TIMP2 in conversion of proMMP2 to active MMP2,[22] we found elevated levels of active MMP2 (64kDa) in WT, but not in TIMP2$^{-/-}$ hearts post-TAC (Figure 5.9.Ai and Aiv), while MMP9 levels increased similarly in both genotypes (Figure 5.9.Ai-Aii). Further, total collagenase activity was greater in TIMP2$^{-/-}$-TAC compared to WT-TAC hearts (Figure 5.10.A). Activity of MT1-MMP, a membrane-type MMP and a major collagenase that is potently inhibited by TIMP2,[12, 23, 24] was markedly greater in TIMP2$^{-/-}$-TAC compared to WT-TAC at 2 weeks post-TAC (Figure 5.10.B), although MT1-MMP protein levels remained unaltered at this time (Figure 5.10.Ci-Cii). These results show that TIMP2 is a critical negative regulator of collagenase activity, particularly MT1-MMP activity in the heart in a pressure overload state.

5.4.5. Cell-ECM adhesion is impaired in TIMP2$^{-/-}$-TAC hearts

The severe LV dilation and reduced systolic function with increased collagenase activity in TIMP2$^{-/-}$-TAC mice lead us to investigate if TIMP2 deficiency impacts the cell-ECM interaction. The cardiomyocyte-ECM

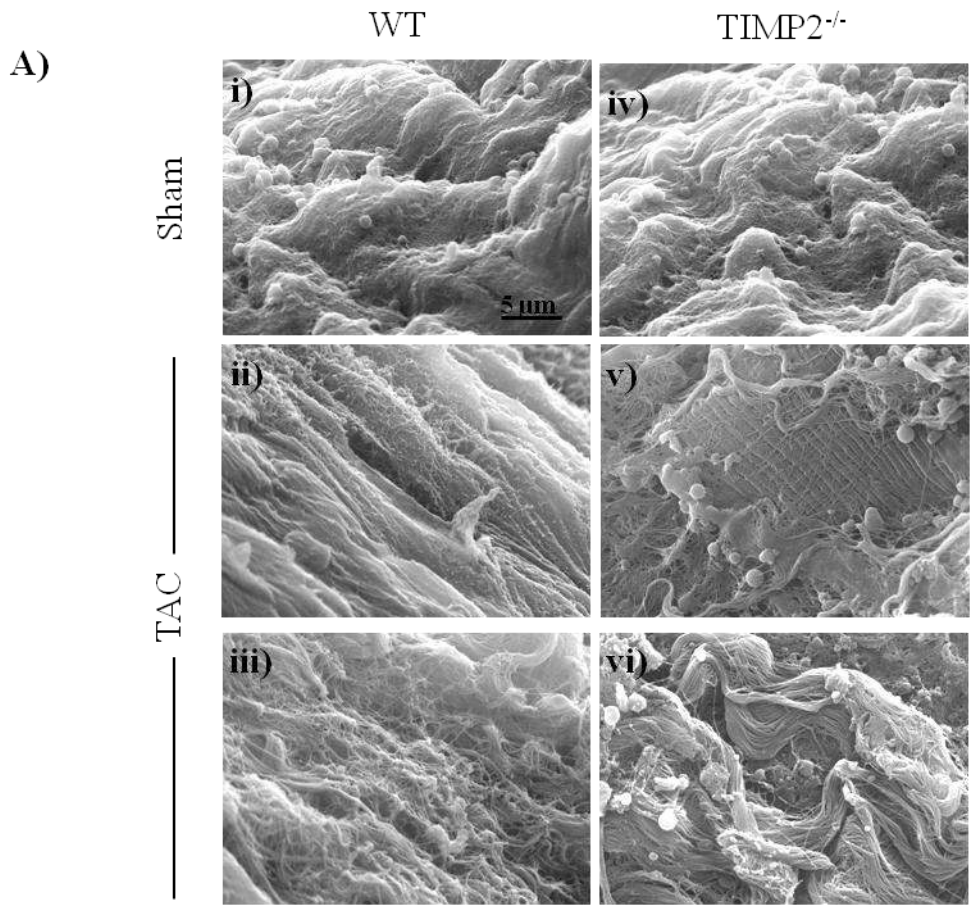

Figure 5.8. Lack of TIMP2 results in nonuniform ECM remodeling post-TAC.

A, Scanning Electron Microscopy showing the ECM structure in WT (i-iii) and TIMP2$^{-/-}$ (iv-vi) hearts 2 weeks post-sham or TAC.

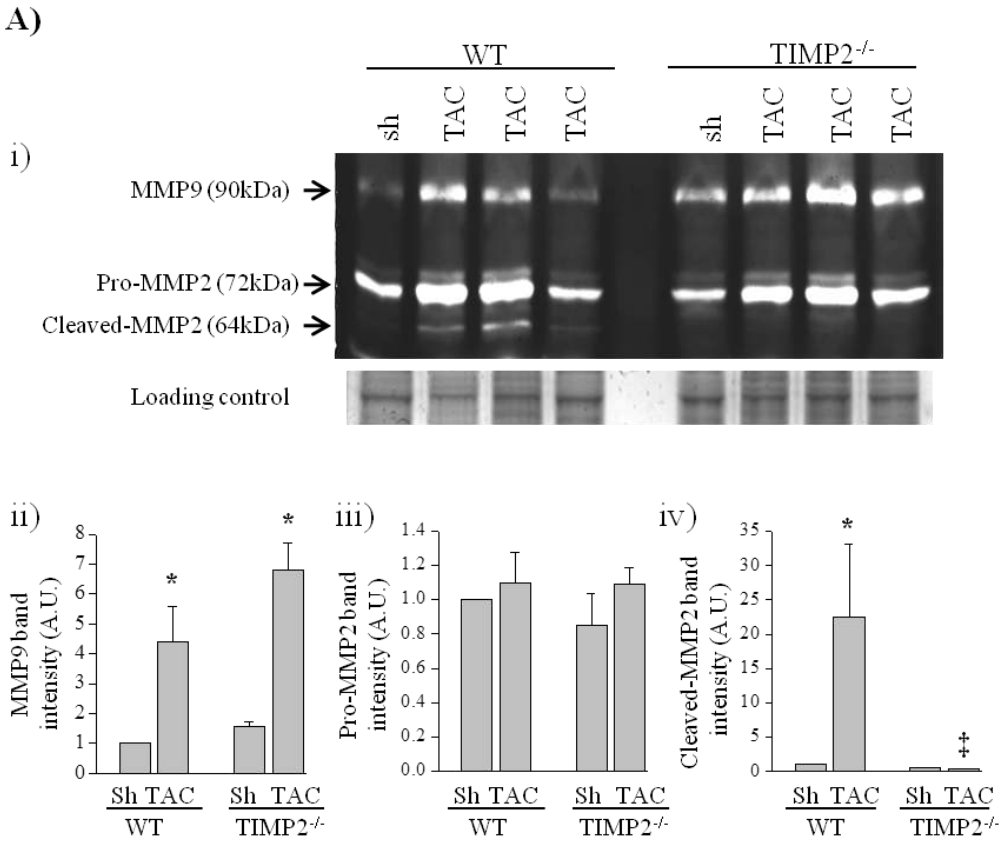

Figure 5.9. TIMP2$^{-/-}$ mice show an absence of MMP2 activation.

A, Gelatine zymography (i), band intensity for MMP9 (ii), proMMP2 (iii) and active MMP2 (iv) in WT and TIMP2$^{-/-}$ hearts at 2 weeks post-sham or TAC. Total collagenase activity (B) and specific MT1-MMP activity (C) in WT and TIMP2$^{-/-}$ hearts post-TAC/sham. Coomassie blue staining was used as loading control. n=6/group/genotype. *p<0.05 compared to sham, ‡ p<0.05 compared to WT-TAC using two-way ANOVA analysis.

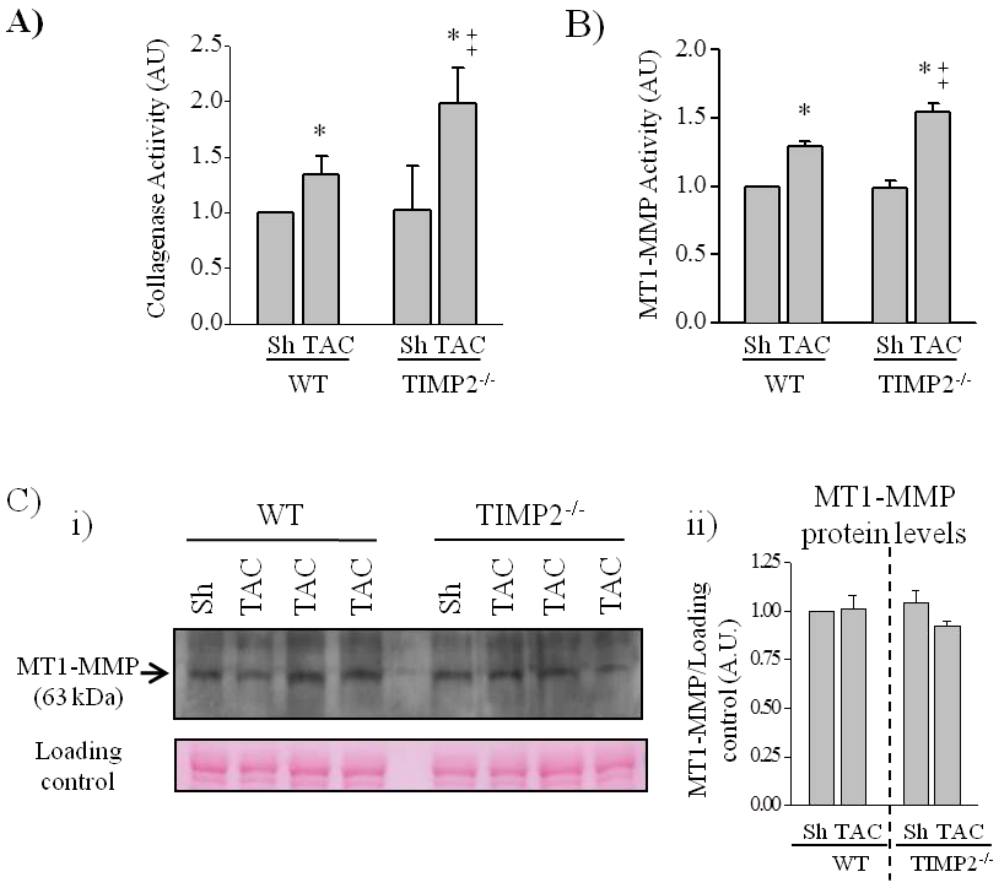

Figure 5.10. TIMP2$^{-/-}$ mice exhibited elevated collagenase activity.

A, Total collagenase activity and specific MT1-MMP activity (B) in WT and TIMP2$^{-/-}$ hearts 2 weeks post-TAC/sham. C, Representative Western blot (i) and averaged MT1-MMP protein levels (ii) on membrane protein fraction from WT and TIMP2$^{-/-}$ mice after sham or TAC. Ponceau red staining was used as loading control. n=4/sham, 6/TAC/genotype. AU=arbitrary units. *p<0.05 compared to sham, ‡ p<0.05 compared to WT-TAC using two-way ANOVA analysis.

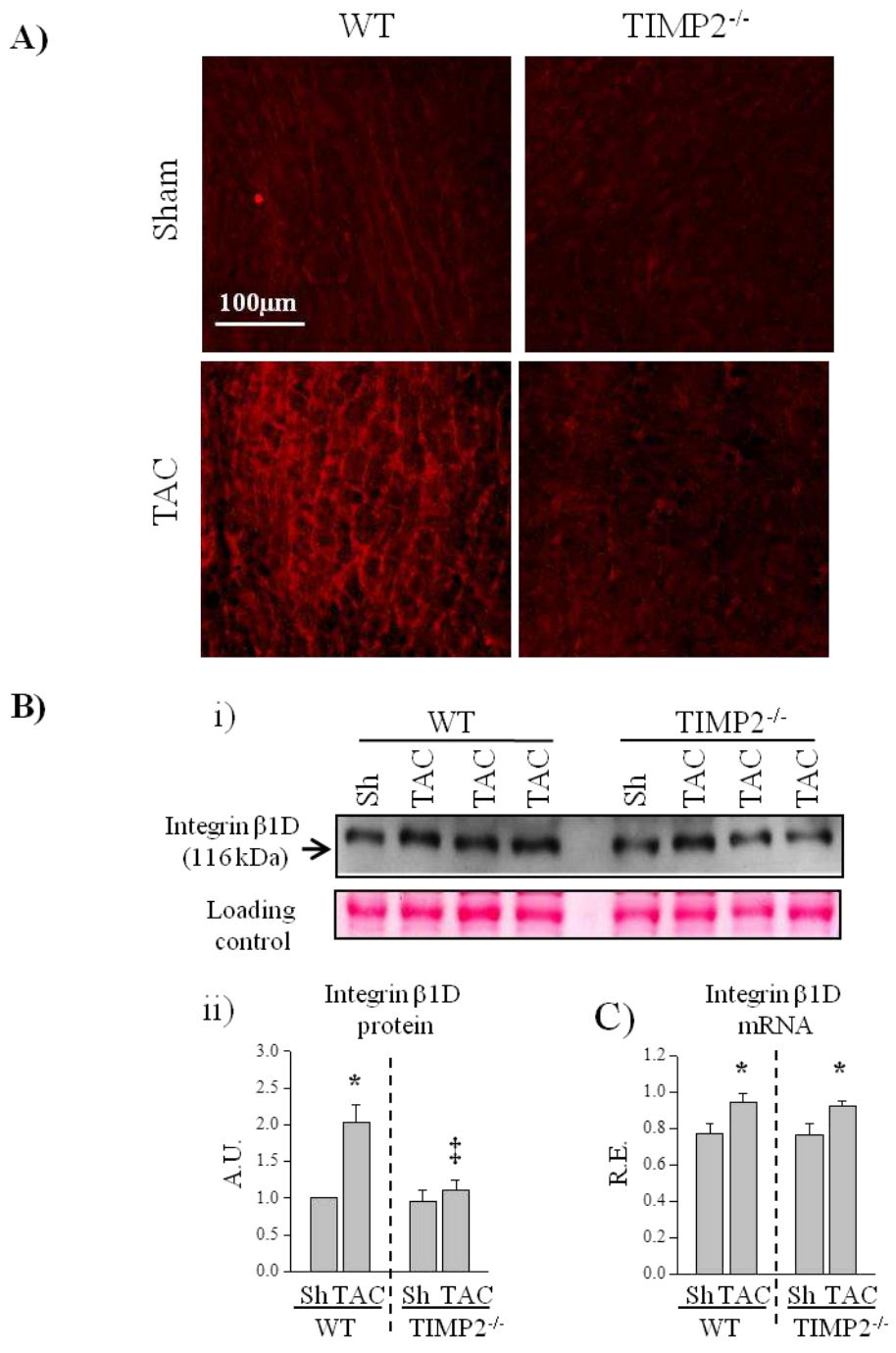

Figure 5.11. Myocyte-ECM interaction via integrin-β1 is diminished in TIMP2$^{-/-}$ mice following pressure overload.

A, Immunostaining and confocal imaging for integrin β1D at 2 weeks post-sham/TAC (n=4 group/genotype). B, Representative Western blot (i), averaged protein levels (ii), and mRNA expression levels of integrin β1D (C) in WT and TIMP2$^{-/-}$ hearts at 2 weeks post-sham/TAC (n=6/group). *p<0.05 compared to sham, ‡ p<0.05 compared to WT-TAC using two-way ANOVA analysis.

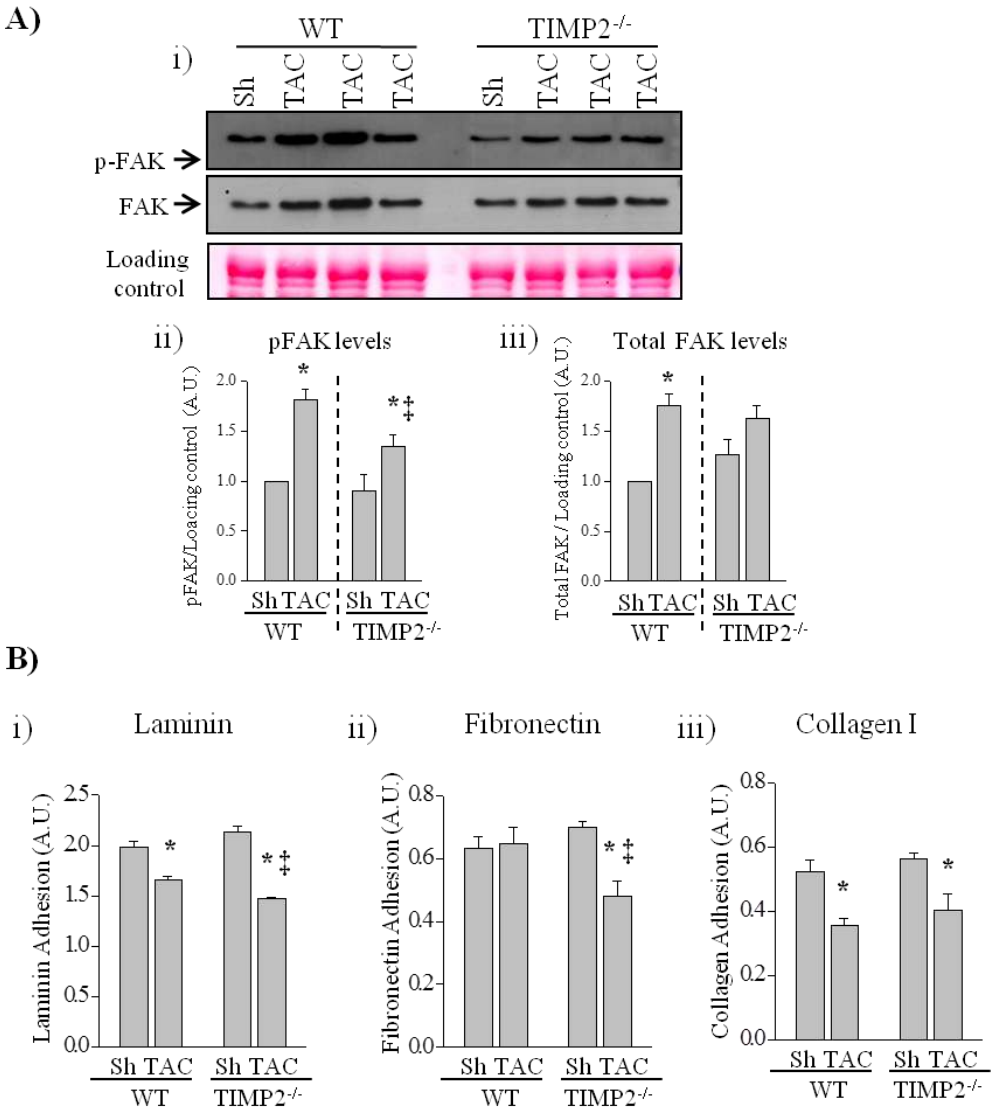

Figure 5.12. Reduced integrin-β1 expression in TIMP2$^{-/-}$ mice following pressure overload impairs mechanosignaling and myocyte-ECM adhesion.

A, Representative Western blots for phospho-FAK, total FAK (i) and averaged p-FAK (ii) and total FAK (iii) protein levels (n=9/group). B, In vitro cell-ECM adhesion assay showing the adhesion of cardiomyocytes from WT and TIMP2$^{-/-}$ hearts post-sham/TAC to laminin (i), fibronectin (ii) or collagen type-I (iii) (n=3 hearts/group). *p<0.05 compared to sham, ‡ p<0.05 compared to WT-TAC using two-way ANOVA analysis.

connections are primarily mediated by integrins.[25-27] Immunostaining (Figure 5.11.A) and western blot analysis on the membrane protein fraction (Figure 5.11.Bi-Bii) showed elevated integrin β1D levels post-TAC in WT, but not in TIMP2$^{-/-}$ hearts, whereas its mRNA levels increased similarly between the two genotypes (Figure 5.11.C). Integrins act as biomechanical sensors and convert mechanical stress, to biochemical signals.[27, 28] One of the well-known intracellular signalling pathways activated by integrin β1 is phosphorylation of focal adhesion kinase (FAK).[29-31] Consistent with reduced integrin β1 levels in the TIMP2$^{-/-}$-TAC cardiomyocyte membranes, p-FAK levels were significantly lower in these hearts compared to WT-TAC hearts (Figure 5.12.Ai-Aii). *In vitro* cell-adhesion assay further revealed that while cardiomyocytes from either genotype post-TAC showed similar impairment in adhesion to collagen type I, there was a greater impairment of cell adhesion to laminin and fibronectin by TIMP2$^{-/-}$-TAC cardiomyocytes (Figure 5.12.B). This indicates that loss of TIMP2 leads to selective loss of integrin β1D resulting in reduced FAK phosphorylation, and thereby compromising cardiomyocyte adhesion to the ECM.

5.4.6. Inhibition of MMPs ameliorated myocardial hypertrophy and fibrosis, and LV dysfunction in TIMP2$^{-/-}$-TAC mice

In order to examine if absence of TIMP2 and the resulting uncontrolled proteolytic activities underlie the worsened LV dilation and dysfunction following pressure overload in these mice, we treated TIMP2$^{-/-}$-TAC mice with an MMPi, PD166793, which has also been demonstrated to efficiently inhibit the membrane type MMP, MT1-MMP.[32, 33] Total collagenase activity (Figure 5.13.A) and MT1-MMP activity (Figure 5.13.B) were markedly reduced in MMPi-treated TIMP2$^{-/-}$-TAC hearts up to 5 weeks post-TAC. This suppression of MMP activity was accompanied by lack of LV hypertrophy (Figure 5.14.Ai-ii) and interstitial fibrosis (Figure 5.14.B). In addition, at 5 weeks post-TAC, MMPi-treated TIMP2$^{-/-}$ mice showed no systolic dysfunction as indicated by preserved LV contractility (EF and VcFc) and lack of LV dilation (LVEDD) (Figure 5.15. Ai-Aiv), as well as a marked reduction in LV filling pressure estimated by E/E' ratio,

normalized LA size and restoration of a normal transmitral filling pattern (Figure 5.16.Ai-Av). As such, early and persistent suppression of the increased MMP activity in the TIMP2-null setting rescued the pathological cardiac remodeling and systolic dysfunction

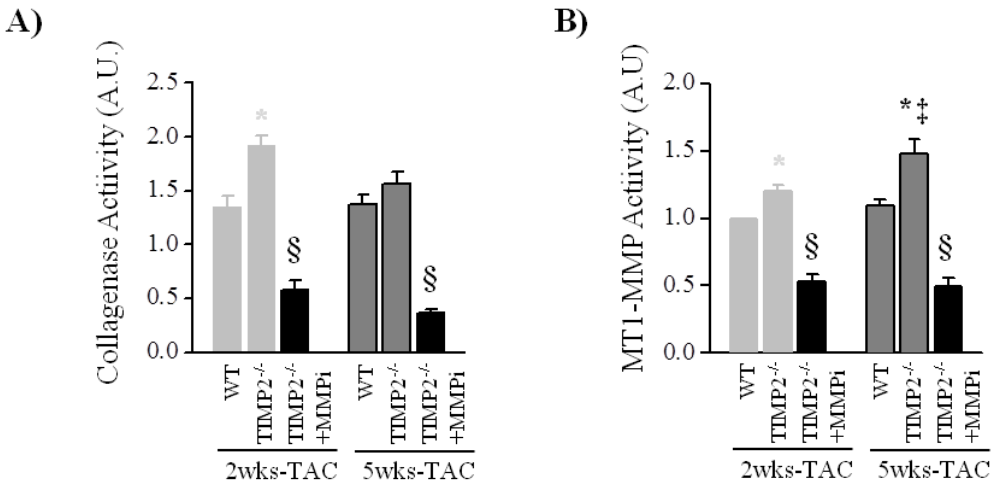

Figure 5.13. MMPi-treatment of TIMP2$^{-/-}$-TAC mice effectively reduced protease activities.

Total collagenase (A), and specific MT1-MMP activities (B) in TIMP2$^{-/-}$-MMPi hearts at 2 weeks and 5 weeks post-TAC (n=6). The data from 2 weeks post-TAC are repeated in light grey color to allow for comparison with the MMPi-treated groups. *p<0.05 compared to sham, ‡ p<0.05 compared to WT-TAC. § p<0.05 compared to TIMP2$^{-/-}$-TAC using two-way ANOVA analysis.

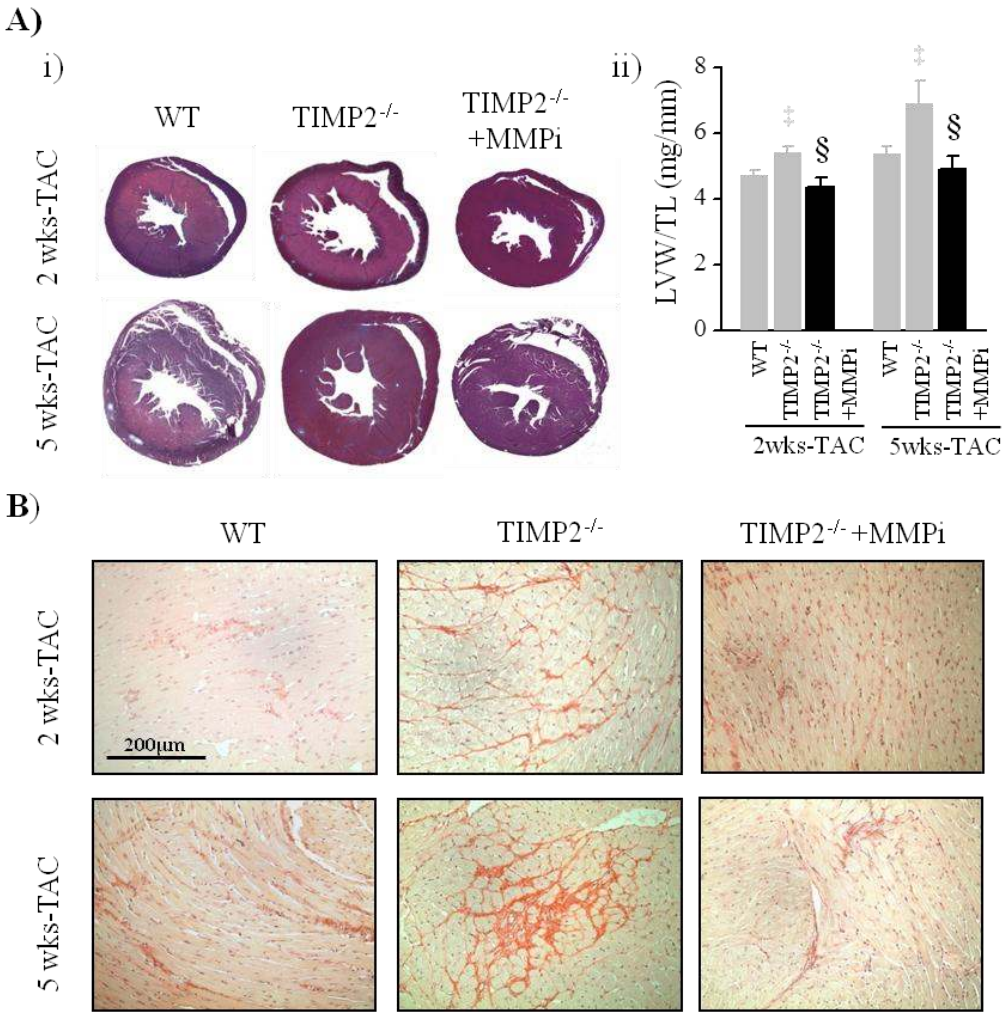

Figure 5.14. MMPi-treatment of TIMP2$^{-/-}$-TAC mice lead to reduced myocardial hypertrophy and fibrosis.

A, Transverse cross-sectional images of hearts (i), and heart weight-to-tibial length ratio (ii) in TIMP2$^{-/-}$-MMPi compared to other groups. B, Picrosirius Red staining showing lack of fibrosis in TIMP2$^{-/-}$-MMPi hearts at 5 weeks post-TAC. The data from 2 weeks post-TAC are repeated in light grey color to allow for comparison with the MMPi-treated groups. *$p<0.05$ compared to sham, ‡ $p<0.05$ compared to WT-TAC. § $p<0.05$ compared to TIMP2$^{-/-}$-TAC using two-way ANOVA analysis.

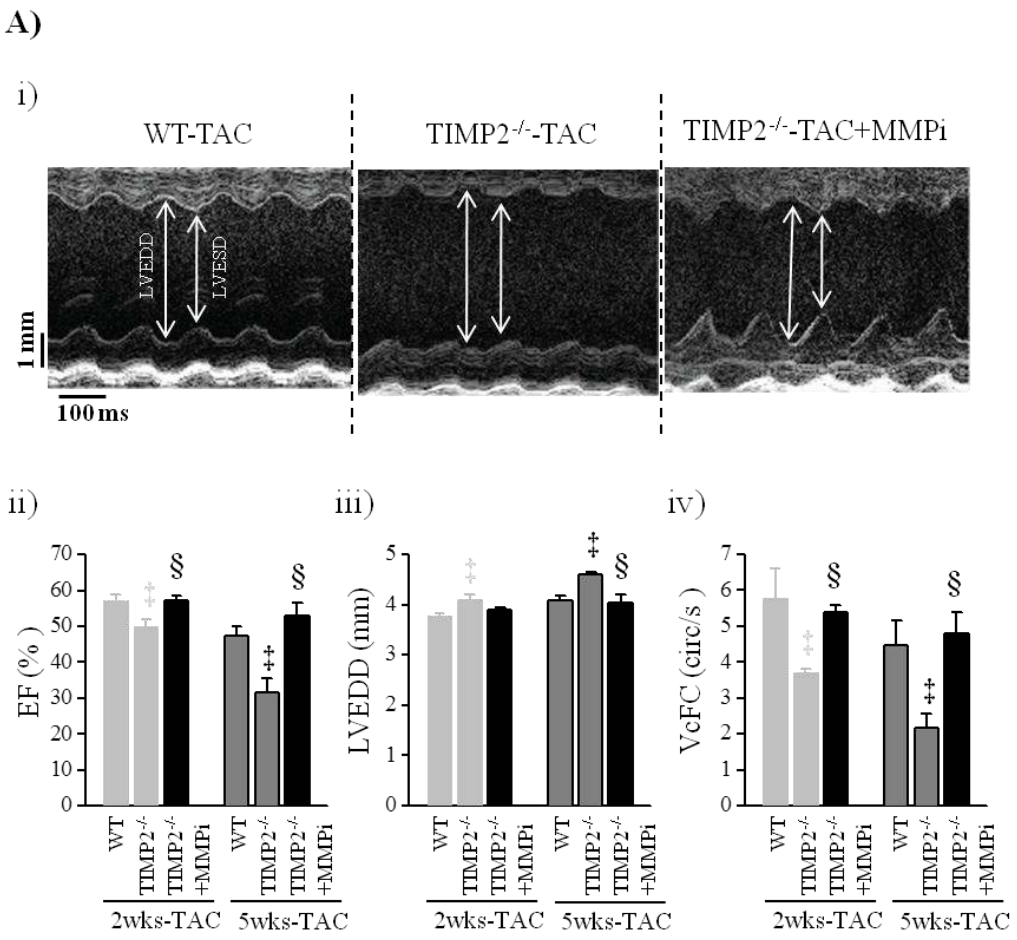

Figure 5.15. The severe cardiac dysfunction and dilation in TIMP2$^{-/-}$-TAC mice was blocked with MMP-inhibition *in vivo*.

A, Representative M-mode images (i) and averaged parameters of cardiac systolic function, ejection fraction (EF) (ii), LV end-diastolic diameter (LVEDD) (iii) and velocity of circumferential shortening (VCFc) (iv) in TIMP2$^{-/-}$ mice treated with MMPi at 2 weeks and 5 weeks post-TAC compared to WT and untreated TIMP2$^{-/-}$ mice (n=6/sham, 8-12/TAC). *p<0.05 compared to sham, ‡ p<0.05 compared to WT-TAC. § p<0.05 compared to TIMP2$^{-/-}$-TAC. The data from 2 weeks post-TAC are repeated in light grey color to allow for comparison with the MMPi-treated groups using two-way ANOVA analysis.

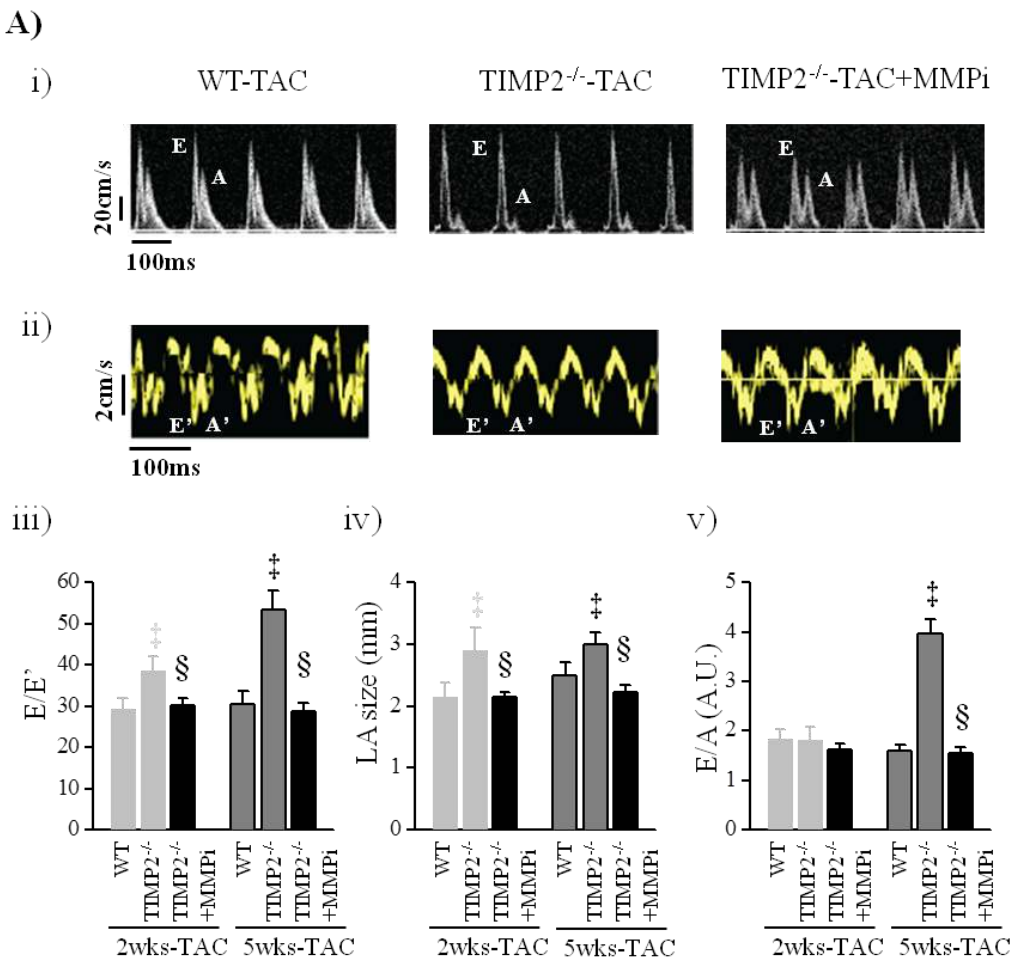

Figure 5.16. MMP-inhibition ameliorated the cardiac diastolic dysfunction in TIMP2$^{-/-}$-TAC mice *in vivo*.

A, Transmitral valve (i) and Tissue Doppler images (ii) , and averaged parameters of LV filling and LA size (iii-v) in TIMP2$^{-/-}$ mice treated with MMPi at 2 weeks and 5 weeks post-TAC compared to WT and untreated TIMP2$^{-/-}$ mice (n=6/sham, 8-12/TAC). *p<0.05 compared to sham, ‡ p<0.05 compared to WT-TAC. § p<0.05 compared to TIMP2$^{-/-}$-TAC. The data from 2 weeks post-TAC are repeated in light grey color to allow for comparison with the MMPi-treated groups using two-way ANOVA analysis.

5.5. Discussion

5.5.1. Increased MT1-MMP activity is linked to pathological cardiac fibrosis in TIMP2$^{-/-}$ mice post-TAC

The worsened LV dilation and dysfunction in TIMP2$^{-/-}$ mice following pressure overload was accompanied by a greater increase in total collagenase activity, and particularly MT1-MMP compared to parallel WT hearts. The important inhibitory function of TIMP2 against MT1-MMP has been reported in myocardial infarction.[12] MT1-MMP has also been linked to fibrosis, one of the characteristics of pressure overload cardiomyopathy,[3, 34] as cardiac-specific overexpression of MT1-MMP led to myocardial fibrosis.[32, 35] MT1-MMP also promotes invasion of fibroblasts, the collagen-producing cells, through its focal collagenolytic activity necessary for supporting tissue invasion.[36] We found that TIMP2$^{-/-}$-TAC mice exhibit excess myocardial fibrosis, associated with elevated SPARC levels resulting in stabilization of the collagen fibres, rather than increased collagen production. MT1-MMP has been shown to trigger myocardial fibrosis by increasing the expression of collagens.[32, 35] Our study provides evidence for a novel profibrotic role for MT1-MMP through post-translational stabilization of the collagen fibres rather than increased production of collagens.

5.5.2. MMP inhibition of upregulated collagenase activity ameliorated the negative outcomes of TIMP2 deficiency

We further demonstrate that inhibition of the upregulated MMPs including MT1-MMP,[9, 11, 37] ameliorated the myocardial fibrosis and hypertrophy which culminated in a marked improvement in the systolic dysfunction in TIMP2$^{-/-}$-TAC mice. Hence, the negative outcomes of TIMP2 deficiency are in fact due to lack of its MMP-inhibitory function and the resulting uncontrolled proteolytic activities in disease. As such, the rise in TIMP2 levels following pressure overload, as also observed in patients,[15, 16] is likely an adaptive response to dampen the elevated proteolytic activities that occur in heart disease.

5.5.3. TIMP2$^{-/-}$ -TAC hearts exhibit a loss of integrin-β1D and ECM adhesion from increased degradation by MT1-MMP

The biomechanical stress exerted on the heart is transmitted to the ECM. Integrins are cell surface receptors that mediate the cell-ECM adhesion and convert the extracellular biomechanical stress to intracellular biochemical signalling. Integrin β1D levels increase during the compensatory phase of cardiac response to pressure overload.[26, 38] In contrast, in TIMP2$^{-/-}$ hearts, protein levels of integrin β1D did not increase following pressure overload despite a comparable increase in integrin β1D mRNA levels. Consistently, TIMP2$^{-/-}$-TAC cardiomyocytes showed impaired adhesion to fibronectin, a basement membrane protein that cross-links with the integrins, and to laminin, the molecule that connects the ECM to the integrins. TIMP2 has been reported to regulate integrin β1 expression in skeletal muscle.[39] Although we found that TIMP2 deficiency did not alter integrin β1 mRNA expression in the heart post-TAC, the reduced integrin β1 protein levels suggest its proteolytic degradation in TIMP2$^{-/-}$-TAC hearts which correlates with the higher collagenase and MT1-MMP activities in these hearts.

MT1-MMP is a strong candidate among MMPs to mediate degradation of the integrin structure since it colocalizes to the cell membrane in proximity to the ECM-binding integrins,[26, 40, 41] , although contribution of other MMPs such as MMP13 cannot be entirely excluded. Consistent with our finding of exacerbated cardiac hypertrophy and fibrosis in TIMP2$^{-/-}$-TAC mice, cardiac specific deletion of integrin β1 resulted in cardiac fibrosis and heart failure, as well as intolerance to pressure overload,[42] while loss of FAK signaling in the heart lead to worsening of hypertrophy and fibrosis following pressure overload.[43] The impaired cardiomyocyte-ECM connections due to reduced levels of integrin-β1D in the TIMP2$^{-/-}$-TAC mice exacerbate the dilated cardiomyopathy in these mice. Our study provides a novel role for TIMP2 in the link between cardiomyocyte-ECM interaction and post-translational regulation of integrin-β1 in the heart.

5.5.4. Conclusions

Our study provides a novel insight into the role of TIMP2 in pressure overloaded cardiomyopathy, and the molecular mechanisms for fibrosis, ECM integrity and cardiomyocyte-ECM interaction. In addition, this study completes the analysis of the role of each TIMP in cardiac recovery from pressure overload. Unlike TIMP1[44] and TIMP4[45] which do not impact cardiac response to pressure overload, TIMP3-deficiency severely exacerbates this process.[9, 21] Hence, TIMP2 and TIMP3 have emerged as key players in pressure overloaded cardiomyopathy, although they each function through a different mechanism. Confirmation of these findings in patients is essential in order to address the interspecies differences, and it could lead to implementing therapeutic approaches to replenish TIMP2 and/or TIMP3 to improve the outcomes in cardiac response to biomechanical stress.

5.6. References

1. Toischer K, Rokita AG, Unsold B, Zhu W, Kararigas G, Sossalla S, Reuter SP, Becker A, Teucher N, Seidler T, Grebe C, Preuss L, Gupta SN, Schmidt K, Lehnart SE, Kruger M, Linke WA, Backs J, Regitz-Zagrosek V, Schafer K, Field LJ, Maier LS, Hasenfuss G. Differential cardiac remodeling in preload versus afterload. *Circulation*. 2010;122:993-1003

2. Drazner MH. The progression of hypertensive heart disease. *Circulation*. 2011;123:327-334

3. Creemers EE, Pinto YM. Molecular mechanisms that control interstitial fibrosis in the pressure-overloaded heart. *Cardiovasc Res*. 2011;89:265-272

4. Weidemann F, Herrmann S, Stork S, Niemann M, Frantz S, Lange V, Beer M, Gattenlohner S, Voelker W, Ertl G, Strotmann JM. Impact of myocardial fibrosis in patients with symptomatic severe aortic stenosis. *Circulation*. 2009;120:577-584

5. Towbin JA. Scarring in the heart--a reversible phenomenon? *N Engl J Med*. 2007;357:1767-1768

6. Jellis C, Martin J, Narula J, Marwick TH. Assessment of nonischemic myocardial fibrosis. *J Am Coll Cardiol*. 2010;56:89-97

7. Gradman AH, Wilson JT. Hypertension and diastolic heart failure. *Curr Cardiol Rep*. 2009;11:422-429

8. Dixon JA, Spinale FG. Myocardial remodeling: Cellular and extracellular events and targets. *Annu Rev Physiol*. 2011;73:47-68

9. Kassiri Z, Oudit GY, Sanchez O, Dawood F, Mohammed FF, Nuttall RK, Edwards DR, Liu PP, Backx PH, Khokha R. Combination of tumor necrosis factor-alpha ablation and matrix metalloproteinase inhibition prevents heart failure after pressure overload in tissue inhibitor of metalloproteinase-3 knock-out mice. *Circ Res*. 2005;97:380-390

10. Kassiri Z, Khokha R. Myocardial extra-cellular matrix and its regulation by metalloproteinases and their inhibitors. *Thromb Haemost*. 2005;93:212-219

11. Kandalam V, Basu R, Abraham T, Wang X, Awad A, Wang W, Lopaschuk GD, Maeda N, Oudit GY, Kassiri Z. Early activation of matrix metalloproteinases underlies the exacerbated systolic and diastolic dysfunction in mice lacking timp3 following myocardial infarction. *Am J Physiol Heart Circ Physiol*. 2010;299:H1012-1023

12. Kandalam V, Basu R, Abraham T, Wang X, Soloway PD, Jaworski DM, Oudit GY, Kassiri Z. Timp2 deficiency accelerates adverse post-myocardial infarction remodeling because of enhanced mt1-mmp activity despite lack of mmp2 activation. *Circ Res*. 2010;106:796-808

13. Spinale FG. Myocardial matrix remodeling and the matrix metalloproteinases: Influence on cardiac form and function. *Physiol Rev*. 2007;87:1285-1342

14. Brew K, Nagase H. The tissue inhibitors of metalloproteinases (timps): An ancient family with structural and functional diversity. *Biochim Biophys Acta*. 2010;1803:55-71

15. Fielitz J, Leuschner M, Zurbrugg HR, Hannack B, Pregla R, Hetzer R, Regitz-Zagrosek V. Regulation of matrix metalloproteinases and their inhibitors in the left ventricular myocardium of patients with aortic stenosis. *J Mol Med*. 2004;82:809-820

16. Heymans S, Schroen B, Vermeersch P, Milting H, Gao F, Kassner A, Gillijns H, Herijgers P, Flameng W, Carmeliet P, Van de Werf F, Pinto YM, Janssens S. Increased cardiac expression of tissue inhibitor of metalloproteinase-1 and tissue inhibitor of metalloproteinase-2 is related to cardiac fibrosis and dysfunction in the chronic pressure-overloaded human heart. *Circulation*. 2005;112:1136-1144

17. Bradshaw AD, Sage EH. Sparc, a matricellular protein that functions in cellular differentiation and tissue response to injury. *J Clin Invest*. 2001;107:1049-1054

18. Bornstein P, Sage EH. Matricellular proteins: Extracellular modulators of cell function. *Curr Opin Cell Biol*. 2002;14:608-616

19. Meier H, Bullinger J, Deten A, Marx G, Rabald S, Zimmer HG, Briest W. Tissue inhibitor of matrix metalloproteinase-1 in norepinephrine-induced remodeling of the mouse heart. *Cell Physiol Biochem*. 2007;20:825-836

20. Swiderski RE, Dencoff JE, Floerchinger CS, Shapiro SD, Hunninghake GW. Differential expression of extracellular matrix remodeling genes in a

murine model of bleomycin-induced pulmonary fibrosis. *Am J Pathol*. 1998;152:821-828

21. Kassiri Z, Defamie V, Hariri M, Oudit GY, Anthwal S, Dawood F, Liu P, Khokha R. Simultaneous tgfbeta-tnf activation and cross-talk cause aberrant remodeling response and myocardial fibrosis in tissue inhibitor of metalloproteinase 3 deficient heart. *J Biol Chem*. 2009

22. Strongin AY, Collier I, Bannikov G, Marmer BL, Grant GA, Goldberg GI. Mechanism of cell surface activation of 72-kda type iv collagenase. Isolation of the activated form of the membrane metalloprotease. *J Biol Chem*. 1995;270:5331-5338

23. Lauer-Fields JL, Broder T, Sritharan T, Chung L, Nagase H, Fields GB. Kinetic analysis of matrix metalloproteinase activity using fluorogenic triple-helical substrates. *Biochemistry*. 2001;40:5795-5803

24. Hurst DR, Schwartz MA, Ghaffari MA, Jin Y, Tschesche H, Fields GB, Sang QX. Catalytic- and ecto-domains of membrane type 1-matrix metalloproteinase have similar inhibition profiles but distinct endopeptidase activities. *Biochem J*. 2004;377:775-779

25. Manso AM, Kang SM, Ross RS. Integrins, focal adhesions, and cardiac fibroblasts. *J Investig Med*. 2009;57:856-860

26. Manso AM, Elsherif L, Kang SM, Ross RS. Integrins, membrane-type matrix metalloproteinases and adams: Potential implications for cardiac remodeling. *Cardiovasc Res*. 2006;69:574-584

27. Ingber DE. Cellular basis of mechanotransduction. *Biol Bull*. 1998;194:323-325; discussion 325-327

28. Lal H, Verma SK, Foster DM, Golden HB, Reneau JC, Watson LE, Singh H, Dostal DE. Integrins and proximal signaling mechanisms in cardiovascular disease. *Front Biosci*. 2009;14:2307-2334

29. Laser M, Willey CD, Jiang W, Cooper Gt, Menick DR, Zile MR, Kuppuswamy D. Integrin activation and focal complex formation in cardiac hypertrophy. *J Biol Chem*. 2000;275:35624-35630

30. Torsoni AS, Constancio SS, Nadruz W, Jr., Hanks SK, Franchini KG. Focal adhesion kinase is activated and mediates the early hypertrophic response to stretch in cardiac myocytes. *Circ Res*. 2003;93:140-147

31. Franchini KG, Torsoni AS, Soares PH, Saad MJ. Early activation of the multicomponent signaling complex associated with focal adhesion kinase induced by pressure overload in the rat heart. *Circ Res*. 2000;87:558-565

32. Spinale FG, Escobar PG, Mukherjee R, Zavadzkas JA, Saunders SM, Jeffords LB, Leone AM, Beck C, Bouges S, Stroud RE. Cardiac-restricted overexpression of membrane type-1 matrix metalloproteinase in mice: Effects on myocardial remodeling with aging. *Circulation Heart Failure*. 2009;2:351-360

33. Deschamps AM, Yarbrough WM, Squires CE, Allen RA, McClister DM, Dowdy KB, McLean JE, Mingoia JT, Sample JA, Mukherjee R, Spinale FG. Trafficking of the membrane type-1 matrix metalloproteinase in ischemia and reperfusion: Relation to interstitial membrane type-1 matrix metalloproteinase activity. *Circulation*. 2005;111:1166-1174

34. Tsang W, Lang RM. Myocardial fibrosis in severe aortic stenosis. *Curr Cardiol Rep*.12:196-198

35. Spinale FG, Mukherjee R, Zavadzkas JA, Koval CN, Bouges S, Stroud RE, Dobrucki LW, Sinusas AJ. Cardiac restricted overexpression of membrane type-1 matrix metalloproteinase causes adverse myocardial remodeling following myocardial infarction. *J Biol Chem*. 2010;285:30316-30327

36. Sabeh F, Li XY, Saunders TL, Rowe RG, Weiss SJ. Secreted versus membrane-anchored collagenases: Relative roles in fibroblast-dependent collagenolysis and invasion. *J Biol Chem*. 2009;284:23001-23011

37. Peterson JT, Hallak H, Johnson L, Li H, O'Brien PM, Sliskovic DR, Bocan TM, Coker ML, Etoh T, Spinale FG. Matrix metalloproteinase inhibition attenuates left ventricular remodeling and dysfunction in a rat model of progressive heart failure. *Circulation*. 2001;103:2303-2309

38. Babbitt CJ, Shai SY, Harpf AE, Pham CG, Ross RS. Modulation of integrins and integrin signaling molecules in the pressure-loaded murine ventricle. *Histochem Cell Biol*. 2002;118:431-439

39. Lluri G, Langlois GD, Soloway PD, Jaworski DM. Tissue inhibitor of metalloproteinase-2 (timp-2) regulates myogenesis and beta1 integrin expression in vitro. *Exp Cell Res*. 2008;314:11-24

40. Seeland U, Selejan S, Engelhardt S, Muller P, Lohse MJ, Bohm M. Interstitial remodeling in beta1-adrenergic receptor transgenic mice. *Basic Res Cardiol*. 2007;102:183-193

41. Gonzalo P, Moreno V, Galvez BG, Arroyo AG. Mt1-mmp and integrins: Hand-to-hand in cell communication. *Biofactors*. 2010;36:248-254

42. Shai SY, Harpf AE, Babbitt CJ, Jordan MC, Fishbein MC, Chen J, Omura M, Leil TA, Becker KD, Jiang M, Smith DJ, Cherry SR, Loftus JC, Ross RS. Cardiac myocyte-specific excision of the beta1 integrin gene results in myocardial fibrosis and cardiac failure. *Circ Res*. 2002;90:458-464

43. Peng X, Kraus MS, Wei H, Shen TL, Pariaut R, Alcaraz A, Ji G, Cheng L, Yang Q, Kotlikoff MI, Chen J, Chien K, Gu H, Guan JL. Inactivation of focal adhesion kinase in cardiomyocytes promotes eccentric cardiac hypertrophy and fibrosis in mice. *J Clin Invest*. 2006;116:217-227

44. Johnson RR, Hapke E, Hendrick JW, Parkhurst AM, dowdy KB, Holder JR, Zile MR. Chronic pressure overload: Effects of gene deletion of the tissue inhibitor of the matrix metalloproteinase type 1 (timp-1) on hypertrophic remodeling. Abs # 2125. *Circulation suppl.* 2002;106:II-427

45. Koskivirta I, Kassiri Z, Rahkonen O, Kiviranta R, Oudit GY, McKee TD, Kyto V, Saraste A, Jokinen E, Liu PP, Vuorio E, Khokha R. Mice with tissue inhibitor of metalloproteinases 4 (timp4) deletion succumb to induced myocardial infarction but not to cardiac pressure overload. *J Biol Chem*. 2010;285:24487-24493

CHAPTER 6

DISCUSSION

Determining the interactions involved in cardiac ECM turnover during the process of cardiac remodeling has been proven to be a focal point of understanding the progression of heart disease. The identification and characterization of the MMPs and TIMPs as regulators of the ECM balance has encouraged deeper investigation into the ECM regulatory process. My interest to study the complexity of ECM remodeling in response to myocardial infarction in comparison to cardiac pressure overload-induced cardiomyopathies was focused on determining the role of two independent, highly expressed TIMPs, TIMP2 and TIMP3 which possess different and unique properties, in these disease models and identifying the relationship between ECM remodeling and the observed functional outcome.

6.1. Summary of important findings

With TIMP3 deficiency, we observed increased mortality predominantly due to LV rupture starting at 3 days post-MI, and a larger infarct size at 1 week in the surviving mice. We found the collagen network in disarray in the infarct region likely contributing to the worsened dilation and increased rupture incidence. There was an early increase in MMP2 and MMP9 levels throughout the TIMP3$^{-/-}$ myocardium at 1 day post-MI with increased gelatinase and collagenase activity, primarily in the infarct and peri-infarct regions. Furthermore, there was a considerable increase in neutrophil infiltration in the TIMP3$^{-/-}$ infarct and peri-infarct regions at 3 days, with a concomitant increase in inflammation-associated MMP expression. MMPi administration improved survival and reduced rupture incidence to levels greater than in the WT, as well as preserving systolic and diastolic function which was exacerbated in the TIMP3$^{-/-}$ mice at 1 week post-MI.

The lack of TIMP2 in myocardial infarction and in pressure overload cardiomyopathy provided us with distinct yet overlapping patterns of TIMP2-dependent remodeling, with both studies demonstrating that the presence of

TIMP2 is required for adaptive cardiac response to disease. Loss of TIMP2 in the setting of myocardial infarction displayed worsened cardiac dysfunction and dilation post-MI, with an increase in infarct expansion with similar incidence of infarct rupture compared to WT mice. TIMP2$^{-/-}$ MI-hearts exhibited reduced and disordered collagen matrix structure in all regions compared to the WT heart, along with increased inflammatory cell infiltration. The absence of cleaved-MMP2 in the TIMP2$^{-/-}$ hearts and comparable total gelatinase activity in both genotypes was offset by increased mRNA expression of the critical cardiac collagenases (MMP8, MMP13, and MT1-MMP), with greater collagenase activity in the TIMP2$^{-/-}$ mice determined to be a result of a significant contribution by MT1-MMP activity and possibly the other collagenases.

The pressure overloaded heart in the absence of TIMP2 also displayed exacerbated dysfunction and dilation, with increased hypertrophy compared to WT-TAC hearts at 2 weeks. Upon closer examination, we observed considerable fibrosis throughout the myocardium in a nonuniform pattern. There was a lack of proMMP2 activation which is consistent with the MI model and an increase in total collagenase and MT1-MMP-specific activity. In addition to altered ECM structure, we found a loss of integrin-β1D at the cell membrane in the TIMP2$^{-/-}$-TAC myocardium which was accompanied by reduced downstream signaling and impaired cardiomyocyte adhesion to matrix substrates *in vitro*. Pharmacological MMPi administration starting at one-day prior to TAC and continued to end-point dampened the adverse dilation and hypertrophy, and preserved cardiac function to WT-TAC levels which was sustained until 5 weeks post-TAC.

6.2. Distinct TIMP-dependent remodeling patterns are evident in MI versus cardiac pressure overloaded hearts

MI triggers alterations in the structure and composition of the myocardial ECM that eventually leads to adverse myocardial remodeling. The remodeling process begins with degradation of the existing ECM, loss of normal collagen

struts, and reduced cross-linking within the ischemic region very early post-MI[1, 2]. Among the TIMPs, TIMP2 and its role in development and progression of cardiomyopathy has been the least studied. Since TIMP2 has two opposing functions, as an activator and an inhibitor of MMPs, it is uncertain how a change in TIMP2 levels will impact the tissue response to MI or pressure overload. The role of TIMP3, although its impact has been partially characterized previously in an experimental MI model[3], remains unexplored with regards to identifying the critical mechanisms leading to the early functional decline and increased LV rupture associated with its loss. The findings from our study shed light on the immediate onset of the remodeling process regulated by TIMP3 inhibition, and its critical contribution to disease progression.

Excess biomechanical stress, secondary to hypertension or aortic valve stenosis, remains an important cause of systolic and diastolic failure[4]. The mechanical stress exerted on the heart by pressure overload is transmitted to the extracellular matrix and the cell-ECM connections. Hence, the integrity of the ECM and its interaction with the cardiomyocytes is critical in optimal cardiac response to pressure overload. We found that TIMP2-deficient mice exhibit severe dysfunction with significant myocardial remodeling, hypertrophy and fibrosis, which was detected in WT hearts post-TAC to a much lesser degree. Cardiac pressure overload did not impact cardiac remodeling or dysfunction in mice lacking TIMP1[5] or TIMP4[6], but lead to precipitous dilated cardiomyopathy and early heart failure in TIMP3-deficient mice[7, 8]. These findings collectively indicate a distinct key role for TIMP2 and TIMP3 as critical TIMPs in the cardiac response to biomechanical stress.

A direct comparison between the post-infarct activation of MMPs with that following pressure overload cannot be made since myocardial infarction is rapid onset (ischemia and necrosis of the LV tissue is induced by ligation of the supplying coronary artery), whereas pressure overload imposes a gradual pressure burden on the left ventricle. As such, myocardial infarction triggers a rapid (within hours)[9] and transient induction of a number of MMPs, primarily those

produced by inflammatory markers, MMP8, MMP9 and MMP12, as well as other collagenases, MMP2 and MT1-MMP. On the other hand, molecular changes induced by pressure overload occur gradually (days)[10] and will persist through the development of disease.

6.3. Diverse maladaptive cellular responses lead to the loss of myocardial contractility in the TIMP2- and TIMP3-deficient mice in the disease heart

Injury to the myocardium results in a number of cellular transformations that can lead to local or overall structural damage. Following MI, myocardial necrosis in the ischemic area resulted in the thinning of the ventricular wall and scar formation. The initial infarct size was found to be comparable between the TIMP2$^{-/-}$, TIMP3$^{-/-}$ and the WT mice indicating that LAD-ligation affected the same downstream myocardial area in all strains. However, the greater infarct size expansion seen in the TIMP2$^{-/-}$ and TIMP3$^{-/-}$ mice compared to the WT mice correlated with increased dilation of the LV. The causal factors behind this expansion are likely diverse, ranging from malformed and destabilized interstitial environment, increased susceptibility of peri-infarct myocyte necrosis, inflammation, and vascular impairment as inferences. The increased dilation altered the hemodynamics of the LV with respect to ventricular volume and pressure, thereby further compromising the optimal relationship between these two parameters for both systolic and diastolic function.

Preserving adhesion of the viable myocardium with the ECM has been found to be important to maintain proper myocardial function in a synchronous fashion[11]. Irrespective of the abnormality, whether it is ECM disruption or a myocardium-anchoring defect, the end result is the inability for myocytes to attach to their surrounding environment for structural or communication purposes. This was evident in the TIMP2$^{-/-}$-TAC model with the loss of integrin-β1. Integrins are the cell surface mediators for myocyte communication and attachment with the ECM. The β1D integrin isoform has been found to respond

rapidly to changes to the myocardium, notably in the event of mechanical stress from pressure overload[11], especially relevant as it is an abundant and unique isoform of the β1 family subclass found specifically in striated muscle such as in cardiac and skeletal muscle[12]. In addition to responding positively during pressure overload, it has been determined that this integrin is very much essential for proper cardiac response to mechanical stress, as these conditional knockout mice did not adapt well when subjected to TAC[13]. The concept of a disrupted myocyte-matrix interface network resulting in myocyte rearrangement and misalignment, or slippage, is not unique and has been found to be relevant to heart disease and development of heart failure[14-19]. Myocyte slippage is a factor considered to be involved in the impairment of systolic function[14, 20], and also a contributor to dilation as myocytes slide out of their original location and over one another thereby elongating ventricle dimensions[21].

The greater dilation that is observed in the TIMP2$^{-/-}$-TAC hearts compared to WT is intriguing as this dilation was accompanied by an enhanced myocardial hypertrophy as determined by greater LV weight relative to tibial length and also an increase in myocyte CSA. The classical concept of early hypertrophy serving as an adaptive response to cardiac stress has been challenged while examining the outcome of TIMP2 deficiency in the pressure overloaded heart, adding to the debate about its beneficial value. The presence of a more severe hypertrophic myocardium at 2 weeks post-TAC in the TIMP2$^{-/-}$ mice is correlated with reduced functional capacity of these hearts. This is not purely a result of the increased hypertrophy, as there are other alterations of the myocardium and ECM that we propose are collectively detrimental to cardiac function, but it is interesting to see that the hypertrophy observed could not compensate for these alterations and may possibly be contributing to the decline. One of the major improvements after MMPi administration was the normalization of hypertrophy in the TIMP2$^{-/-}$-TAC hearts with preserved function, indicating that hypertrophy may be directly linked to ECM changes and related intracellular signaling, or possibly as an indirect response to the functional decline as a result of adverse ECM remodeling leading to improper myocardium functioning triggering hypertrophy to compensate.

6.4. The role of MMPs and TIMPs in matrix remodeling (disruption and fibrosis) is a complex process

ECM remodeling typically involves a two part process, the degradation of existing ECM and the reassembly with new matrix components thereafter, generally classified as ECM turnover[22, 23]. The actions of MMPs and TIMPs in ECM remodeling for a long time were thought to be clear and well established. The canonical theory is that MMPs are the proteolytic enzymes that degrade ECM components leading to the reduction of ECM content, and that TIMPs prevent this process thereby allowing for ECM accumulation. The imbalance of these actions was thought to be the decisive step in pathological ECM remodeling in disease. However, our studies have revealed that the process of ECM remodeling in disease is more complex and in fact multidimensional, with temporal and condition-dependent aspects.

The classic paradigm was apparent in our myocardial infarction model, especially pertaining to the actions attributable to the unregulated overall MMP activity in TIMP3$^{-/-}$-MI hearts and upregulation of total collagenase and MT1-MMP activities in the TIMP2$^{-/-}$ hearts post-MI. The degradation of the ECM was evident in the infarct and peri-infarct regions as visualized through SHG imaging in the TIMP2- and TIMP3-deficient myocardium. A loss of ECM structure was also detected very early in the TIMP3$^{-/-}$ heart post-TAC[8] within hours or even a week post-TAC. The contradiction to this classical notion is evident in pressure overload-induced aberrant ECM remodeling in the TIMP2$^{-/-}$ heart with dispersed areas of fibrotic lesions situated among degraded regions, which was also seen at later stages in the TIMP3$^{-/-}$ TAC, associated with TGF-β involvement[24]. A fundamental event leading to fibrosis, aside from altered synthesis, was proposed to be a shift in the balance towards TIMP inhibition of MMP activity (TIMPs >> MMPs)[25]. This is interesting in light of the different TIMPs typically showing distinct and sometimes opposing expression patterns in response to disease[26, 27]. It is important to note that in certain stages of a particular disease, such as post-MI[28] and hypertensive heart failure[29], there can be a parallel increase in both MMP and

TIMP levels with the inhibitory effect from TIMPs on MMPs being superior to the MMPs' proteolytic activity leading to a net reduction in proteolytic activity, without an actual reduction in MMP levels. In the MI models, MMP2-deletion resulted in less incidence of rupture post-MI[30], and along with others we have shown that TIMP3$^{-/-}$ mice experience greater cardiac infarct rupture[31, 32] supporting the notion that inhibition of MMP activity can protect against the degradation and instability in the newly forming infarct. However, it has been reported that MT1-MMP overexpression resulted in increased fibrosis in all myocardial regions post-MI[33], MMP9$^{-/-}$mice display less collagen in the infarcted region post-MI[34], and MMP2 deficiency ameliorates TAC-induced interstitial fibrosis found in WT mice[35]. These reports collectively suggest that upregulated MMP levels have the potential to act contrary to the general belief, and to promote collagen accumulation, thereby indicating a role for TIMPs in preventing fibrosis.

The activation of profibrotic factors could play a considerable role in ECM remodeling and pathology. Ventricular stiffness is dependent on fibrillar collagen content and cross-linking[36], and prevention of the cross-linking process has been found to alleviate ventricular stiffness at baseline pharmacologically[37] and in cardiac pressure overload[38]. Angiotensin II (AngII) has been well-documented to stimulate fibroblasts to trigger collagen synthesis[39, 40], as well as induce regulators of ECM structure[41-43]. Factors such as TGF-β, and fibroblast growth factor can stimulate fibroblast activity, which have been found to be released and/or activated through increased MMP activity[33, 44, 45] leading to increased expression and synthesis of ECM components. Without a difference in procollagen Iα or IIIα mRNA expression between TIMP2$^{-/-}$ or TIMP3$^{-/-}$-MI or TAC hearts in comparison to their WT counterpart, we found lower density and disrupted collagen structure in the TIMP2$^{-/-}$-MI and TIMP3$^{-/-}$-MI, and a nonuniform ECM assembly in the TIMP2$^{-/-}$-TAC with areas of considerable fibrosis in response to pressure overload. These ECM conditions show that collagen expression and synthesis are only partially responsible for ECM integrity, and that the post-translational modifications by increased MMP degradation or alternatively

strengthening of the ECM have a strong influence on the ECM stability. The loss of ECM structural integrity seen in both TIMP2$^{-/-}$-MI and TIMP3$^{-/-}$-MI can be linked to the increased MMP activity, whereas we found the fibrosis in the absence of TIMP2 in the pressure overloaded heart to be linked to increased SPARC and matricellular processing for collagen post-translational modification[38], which we have found to be considerably increased post-TAC in the TIMP2$^{-/-}$ hearts.

6.5. TIMP2 and TIMP3 exert differential effects post-MI

TIMPs are critical in the outcome of ECM turnover and remodeling in health and in disease[27, 46]. MMP activities post-MI have been demonstrated to be differentially regulated by TIMP2 and TIMP3. According to our findings, the loss of TIMP2 results in a significantly greater upregulation of collagenase activity compared to sham-operated controls and WT-MI mice, whereas absence of TIMP3 resulted in an early and greater increase in both gelatinase and collagenase activities at 1 day post-MI , which was also observed with TIMP3 deficiency post-TAC[8]. The similar increase in gelatinase activity between WT and TIMP2$^{-/-}$-MI hearts may be attributable to the balance between the loss of activated MMP2 and the concomitant increase in MMP9 levels compared to WT-MI, in contrast to the increase in levels of both gelatinases (MMP2 and MMP9) seen in the TIMP3$^{-/-}$-MI myocardium. TIMP3 also regulates collagenase activities, possibly due to tight regulation of MMP2 which has been found to possess collagenase behavior[47] and possibly MT1-MMP, a potent membrane-bound collagenase[48, 49]. To summarize, TIMP2 deficiency results in the lack of MMP2 activation, as opposed to increased MMP2 activation within 1 day post-MI in TIMP3$^{-/-}$ mice. MMP2 has been reported to be a key factor in post-MI LV rupture[30], and as such could partly explain the differential impact of TIMP2 deficiency and TIMP3 deficiency in post-MI rupture incidence.

TIMP2 and TIMP3 appear to also display differential spatial expression patterns, particularly in response to disease. In contrast to the WT-MI where we found a drastic loss of TIMP3 protein levels in the ischemic myocardium compared to healthy control myocardium, we found the opposite expression pattern of TIMP2 protein levels throughout the WT-MI regions. Notably, there was a relatively greater TIMP2 level in the WT-infarcted myocardial region with a decline further remote from the ischemic zone post-MI, and an overall upregulation of myocardial TIMP2 levels in response to pressure overload. We interpret the loss of TIMP3 in the infarct region of the LV post-MI as a major cause of instability in this region, as $TIMP3^{-/-}$-mice exhibited increased infarct ECM degradation and rupture incidence indicating a prominent role for TIMP3 in infarct stability and proper scar formation. TIMP2-deficient mice exhibit comparable LV rupture incidence compared to the WT mice despite the far more severe LV dilation and dysfunction, similar to the resultant loss of function in the $TIMP3^{-/-}$ mice. In addition, TIMP2 upregulation in the infarct area of TIMP3-deficient hearts was not sufficient to decrease the rate of LV rupture in these mice. These findings indicate that while TIMP2 deficiency primarily affected the remodeling and function of the non-infarct myocardium, the lack of TIMP3 exerted a global effect influencing the infarct as well as the non-infarct myocardium.

6.6. MMP2 activity has a variable role in ECM remodeling during heart disease

TIMP2 is highly expressed in the heart and its levels are upregulated in patients with pressure overload cardiomyopathy[25, 50]. TIMP2 plays a dual role as an activator of proMMP2[51, 52], as well as an inhibitor of a number of MMPs[53]. We have determined that TIMP2 is essential for cell surface activation of proMMP2 in the myocardium. TIMP3 has a broad-spectrum MMP inhibitory role which includes MMP2 inhibition. However, in contrast to TIMP2, TIMP3 is uniquely inhibitory to the cell surface activation process of proMMP2[54]. Consistently, we

observed an increase in MMP2 activation to the cleaved-form in the TIMP3$^{-/-}$-MI myocardium. MMP2 has been traditionally classified as a gelatinase, with recent evidence demonstrating collagenase properties[47, 55, 56] and it has been linked to a number of cardiomyopathies[8, 57, 58]. The variability in establishing and attributing a clear level of importance to MMP2 in the ECM remodeling process stems from some inconsistencies between its presence and the resultant ECM remodeling occurring during heart disease in these experimental models.

MMP2 is a known type IV collagenase[55], but it has been found to possess potential triple helicase capacity to degrade collagen type I[47, 59]. Classically known to degrade denatured type I[60], which is commonly referred to as gelatin, this ability to participate in type I collagenolysis contributes to its total collagenase activity. Additionally, MMP2 has been considered to act synergistically to increase the collagenolytic activity of MT1-MMP[61]. With respect to the cell surface activation of proMMP2, despite a significant increase in the activity of MT1-MMP, no cleavage of proMMP2 to its 64kDa form was detected in the TIMP2$^{-/-}$ myocardium *in vivo*. Biochemical studies have shown that proMMP2 can be activated by MT2- and MT3-MMP in a TIMP2-independent fashion[62].

MMP2 has also been shown to trigger fibrosis through releasing the ECM-bound latent TGF-β thereby inducing collagen synthesis[7, 63]. Consistent with this finding, cardiac overexpression of active MMP2 leads to severe myocardial fibrosis, along with hypertrophy and impaired systolic function, with an additional increase in myocyte fragmentation and the recruitment of other MMPs[64]. The effect of MMP2-deletion in minimizing injury and ameliorating disease progression has been well documented[30, 35, 65, 66], although there seems to be evidence that MMP2-deletion may infact potentially exacerbate inflammation-based diseases[67, 68], adding to the complexity and variability of predicting the role of MMP2. MI[69] and the pressure overloaded heart[35] have both shown preservation of cardiac morphology and function in the absence of MMP2,

indicating that its presence may be injurious as opposed to adaptive in response to disease.

Experimental models of both TIMP2$^{-/-}$- and TIMP3$^{-/-}$-MI exhibit precipitous decline in function as a result of considerably enhanced ECM remodeling, however the polar opposite effects of MMP2 activation that we observed creates confusion regarding the importance of this MMP in the observed phenotypes. The fact that the increased presence or complete absence of MMP2 can result in similar functional outcomes is intriguing, clearly indicating that although there is a lack of activated MMP2 in the TIMP2$^{-/-}$ model, the absence of TIMP2 creates a considerable void in the regulation of other MMPs in the remodeling process which compensate for the abolished MMP2, such as increased MT1-MMP activity. The confounding dilemma in establishing the role of MMP2 stems from having to take into account the compensatory upregulation of other MMPs due to its own upregulation or by its removal from the overall proteolytic balance, as both scenarios are possible. One must consider the context of MMP2 activity, as there are demonstrated intracellular MMP2 processes that can contribute to cardiac dysfunction[70, 71] due to intracellular MMP2 activation from increased oxidative agents present in pressure overload[72] or MI[73], or by intracellular MMP2 phosphorylation regulating its activity[74]. There are also temporal patterns of expression and the essential duties in ECM turnover that need to be taken into consideration when assessing its overall impact in remodeling and the prospect of limiting its activity.

6.7. MT1-MMP is a critical regulatory factor in cardiac ECM remodeling

MT1-MMP is a potent collagenase[75, 76], which also targets other ECM components such as fibronectin[77, 78], laminin[77, 79], and proteoglycans[80, 81]. In fact, transmembrane-deletion mutant (soluble) MT1-MMP also possesses potent proteolytic activity towards a large number of ECM molecules[82]. A unique role of MT1-MMP is that it is involved in the activation of proMMP2 through the

formation of a trimolecular complex with TIMP2[51]. MT1-MMP has also demonstrated the capacity to activate proMMP13 at the cell surface[83, 84], thereby further contributing to the proteolytic activities in a tissue, although MT1-MMP has a much greater triple-helical peptidase activity than other interstitial collagenases such as MMP1 or MMP13[85, 86]. A direct interaction between TIMP2 and the catalytic domain of MT1-MMP indicates that TIMP2 could act as a highly specific inhibitor of MT1-MMP[87]; however it is important to note that TIMP3 has also been found to exhibit effective inhibition of MT1-MMP[48], possibly at a lesser extent[49].

The absence of TIMP2 in our experimental MI and pressure overload models have shown a greater increase in MT1-MMP mRNA, protein, and activity compared to parallel WT mice, which correlates with our finding of increased total collagenase activity in the absence of TIMP2. We were able to prevent this elevated proteolysis by using a pharmacological MMP inhibitor that reduced both activity and mRNA expression, thereby significantly protecting the heart from extensive adverse ventricular remodeling exhibited in the untreated mice. This illustrates the significant contribution that MT1-MMP has in total collagenase activity in the heart, and the importance of sufficient inhibitory control for preserving adequate ventricular form and function. Although the pharmacological inhibitor that we used (PD166793) is not a specific inhibitor of MT1-MMP, it has been shown to also inhibit this membrane-bound MMP[88]. Of course, a more targeted inhibition of MT1-MMP would have been ideal, however in the absence of a specific pharmacological inhibitor and since MT1-MMP-deficient mice die shortly after birth due to a loss of viability as a result of severe developmental abnormalities[89], our options were limited. To date, MT1-MMP cardiac-specific overexpression in mice has been examined in various contexts such as in aging[90] and in disease[33]. Other approaches, such as the utilization of cre-lox technology for cardiac-specific conditional deletion of MT1-MMP would serve as a suitable alternative.

In mice lacking TIMP3 we examined mRNA expression levels of various MMPs post-MI and similarly discovered an increase in MT1-MMP mRNA expression that is consistent with earlier findings in pressure overloaded TIMP3$^{-/-}$ hearts[8]. Recently, it has been reported that MT1-MMP overexpression results in severe cardiomyopathy[76]. MT1-MMP is elevated in fibroblasts from patients with cardiomyopathies and has been shown to contribute to heart disease[91]. These findings indicate that both TIMP2 and TIMP3 may collectively regulate this highly dynamic protease, which under disease states has been found to be upregulated, greatly influential, and may contribute to fibrosis post-MI[33]. As such, an increase in MT1-MMP activity is inevitably associated with elevated MMP2 activation, unless when TIMP2 is lacking. Hence, the TIMP2$^{-/-}$ mice provide an exciting model to examine the outcomes of MT1-MMP activation in the absence of MMP2 activation, with further work required to distinguish the role of MT1-MMP with the loss of TIMP3.

In addition to its role in cardiac ECM remodeling, MT1-MMP has demonstrated a significant role in angiogenesis in both a vascular ECM-dependent[92] and -independent[93] fashion. A characteristic of MT1-MMP that is relevant to both endothelial cells and cardiomyocytes is its localization with membrane integrin complexes. As we have demonstrated in the TIMP2-deficient mice, there is a strong likelihood of the increased MT1-MMP activity being responsible for the proteolytic processing of adjacent cell surface integrins in the TIMP2$^{-/-}$-TAC heart. The importance of integrins in cellular adhesion and communication is well-established; the interaction between MT1-MMP and integrins on various cell types in the absence of TIMP2- or TIMP3-specific regulation will allow us to discriminate how MMPs-TIMPs regulate myocardial cell adhesion or conversely endothelial cell migration.

6.8. Inflammation is an important catalyst of ECM remodeling post-MI

There is a delicate balance between inflammation and ECM remodeling (Chapter 1.4.1). The upregulation of MMP9 in the TIMP2- and TIMP3-deficient MI hearts are consistent with the more severe inflammation in these hearts as MMP9 levels are often used as markers of severity of inflammation in different inflammatory diseases including sepsis[94]. Fragments of ECM proteins can attract inflammatory cells[95], and initial degradation of collagen fibers has been shown to precede inflammation post-MI[58]. Degradation products of collagen type I, such as the Pro-Gly-Pro (PGP) peptide that is produced by MMP9[96] and MMP8[97], can serve as neutrophil chemoattractants in vivo[98]. In addition, TIMP3 has been reported to constrain neutrophil influx in the lung through inhibiting MMPs[99]. Hence, the severe inflammation in TIMP2$^{-/-}$ and TIMP3$^{-/-}$ myocardium further indicates excess damage to the ECM structural components in these mice post-MI and likely attracts further infiltration.

The heightened inflammation itself in these MI hearts compared to WT-MI could also explain the significantly higher levels of MMP8 and MMP9, the two MMPs that are produced by neutrophils, which can in turn facilitate neutrophil migration[97]. Recent studies have shown that a high neutrophil count is correlated with a higher incidence of adverse cardiac events in patients with acute MI[100] and that the neutrophil-to-lymphocyte ratio serves as an independent predictor of cardiac death in patients with stable coronary artery disease[101]. Inflammatory cells can produce a number of MMPs (including MMP8, MMP9, and MMP12) that will further mediate ECM degradation and overall adverse tissue remodeling[102-104]. The greater neutrophil infiltration in the TIMP-deficient hearts is consistent with elevated levels of MMP8, MMP9, and MMP12 in these hearts. Inflammation and elevated MMP9 levels have also been linked to LV rupture in patients and in animal models[105-107]. In addition, mice lacking MMP9 are protected against LV rupture post-MI[105] and exhibit improved LV dilation and dysfunction post-MI[34], suggesting that the increase in MMP9 in mice lacking TIMP2 or TIMP3 post-MI leaves it susceptible to unfavourable outcomes.

Further evidence indicating the need to regulate inflammation was reported with the overexpression of an NFκB-inhibitor to antagonize the proinflammatory signaling in the rat-MI model, which reduced MMP expression and increased TIMP expression and was linked to preventing dilation and preserving function post-MI[108]. This correlates with the concept of an inherent protection by TIMPs in the heart and the importance of adequate containment of upregulated MMPs, as well as corroborating the potential detrimental effects of excessive inflammation post-MI.

6.9. MMP dysregulation is a significant culprit in the adverse cardiac remodeling after injury, and therefore needs to be strategically neutralized

The TIMP3$^{-/-}$-MI and TIMP2$^{-/-}$-TAC studies examined the beneficial effects of early pharmacological MMPi treatment, which would supplement our understanding of the complexity of balancing the ECM remodeling process. Continuous MMPi treatment attenuated the adverse LV remodeling in mice[109] and in pigs[88] following MI. In addition to the TIMP2$^{-/-}$-TAC study in which we administered continuous MMPi starting from one day pretreatment before TAC, we demonstrate that the beneficial effects of MMPi treatment during the first 2 days post-MI, following 2 days pretreatment, persist to prevent adverse LV remodeling, infarct expansion, and LV rupture up to 1 week post-MI. Targeting the early rise in MMP activities post-MI is particularly important, since we have demonstrated that levels of TIMPs (TIMP2, TIMP3, and TIMP4) are also reduced early post-MI. In addition, this could also explain the unsuccessful outcome of the PREMIER trial, where STEMI patients received PG-116800, an MMPi, 48–72 h after the onset of MI[110]. There exist inherent difficulties with the implementation of MMP inhibitors as exhibited by recent unsuccessful trials such as the PREMIER trial. Perhaps an earlier treatment window could have been more beneficial.

We realize that pre-treatment with MMPi poses limitations in clinical applications. However, the aim of this study is the 'proof of concept' to demonstrate that the very early rise in MMP activities is what drives the later LV adverse remodeling and dysfunction. The previous reports on MMP inhibition post-MI[88, 109] employed continuous MMPi-treatment during the course of the study. Contrary to this approach, in our study we stopped the MMPi treatment 2 days after MI, and evaluated the cardiac architecture and function at 1 week after MI. Our study presents important information about the beneficial effects of early MMP inhibition lasting beyond the time of treatment if applied appropriately.

6.10. Study Limitations

6.10.1. The TIMP-deficient mice are whole-body knockouts

Although TIMP2 deletion has no effects on viability or fertility of the mice in the C57BL/6 background[111], there have been reports of developmental motor deficits in the TIMP2$^{-/-}$ mice that are evident within the first two postnatal weeks, and are not as apparent by one month[112]. However we have not found any baseline defects in cardiovascular structure or function in mice lacking TIMP2 or TIMP3 at the young age. The use of TIMP-knockout mice has been feasible and effective for the purposes of these studies. Due to our study of the direct effects on the heart from cardiac-directed procedures, LAD-ligation or aortic constriction, we are not overly concerned about extraneous factors. These concerns are further mitigated by the use of these mice at an early age (8-12 weeks), as certain heart defects are unlikely to develop and become apparent by this time, which we have examined with baseline cardiac function and molecular studies between the WT and TIMP2$^{-/-}$- or TIMP3$^{-/-}$-mice. As we are working with these mice at a timepoint well before the age of two-years where TIMP3$^{-/-}$ mice have been reported to exhibit dilated cardiomyopathy[113], we assume that these long-term changes do not affect our study. Alternatives to total-body knockout mice would include using a conditional TIMP-knockout with cardiac-specific TIMP-deletion

with an additional inducible feature to trigger TIMP-deletion prior to, upon, or after induction of cardiac injury. A TIMP2 or TIMP3 gene knockdown method would suppress expression of the respective TIMP, or the investigation of the heterozygous TIMP mouse expressing partial protein levels could also be informative to a certain degree.

Lack of TIMP2 as well as TIMP3 resulted in enhanced inflammation post-MI. Since inflammatory cells originate from the bone marrow, a whole body knockout mouse will not allow us to differentiate between the cardiac-specific events versus the invasive properties of the bone marrow cells in mediating the inflammatory response. To directly address this point, bone-marrow transplantation can introduce bone marrow of a desired genotype into a mouse that has a different genotype in the rest of its body, especially the cells of the heart. Therefore, there are two sources of influence, the mouse and its tissues, and secondly the bone marrow. Using a WT and a $TIMP^{-/-}$knockout mouse, a clear *in vivo* understanding through a full study can be done by manipulating the combinations of which variable possess what genotype to ascertain the role of the of the protein of interest with respect to its cellular host.

The contribution from each source is difficult to ascertain as both sources (the heart tissue and the bone marrow) possess the same genotype, whereas now all tissues, including the heart, possess a genotype different from that of the bone marrow that produces the inflammatory cells. This would allow isolation of a single source of MMPs and TIMPs . As such, a chimera possessing the heart tissue or marrow of a WT background will need to have the other material from a knockout, and marrow transplantation is more feasible than that of an organ.

6.10.2. Experimental disease model

Advancement from cells in culture as a test system to the use of genetically modified animal and disease models in vivo, with the incorporation of cellular research, has changed the way research is conducted and applied. The mouse *in vivo* models of heart disease are acceptable models with many

fundamental advantages such as short gestation period and greater litter size compared to larger mammals. An additional advantage of the mouse models is the genetic-manipulation of the sequenced mouse genome to delete or to incorporate exogenous genetic material to create a variety of genetically-modified mice. To briefly summarize our surgical methods, for MI we ligated the LAD coronary artery which is the major coronary vessel supplying the myocardium of the LV. Pressure overload was induced by constricting the aorta at its transverse segment. The concern that arises from using the mouse model for this type of invasive and extensive procedure is the degree of injury and resulting pathology. The severity of disease produced in the mouse may be at a much larger extent than generally experienced by man, or even other species in experimental models due to the extent of insult on a relatively small organ compared to the heart size in other animals. Complete transmural MI in the mouse MI model is typically created from the LAD ligation procedure, and aortic constriction typically achieves relatively high pressure gradients against which the heart works against. There is general concern whether the results from the mouse model and other small animals can be translated to the clinical setting. The severity of injury and resultant morbidity and mortality are an extreme example to delineate the processes underlying the pathology and requires further examination of the proposed mechanisms.

6.10.3. Oxidative stress and intracellular MMP regulation

One aspect of MMP regulation that has been briefly addressed, but may be significant in our analysis of MMPs and TIMPs regulating ECM remodeling are the intracellular activation and activities of MMPs[71, 114]. The canonical theory about MMPs is that they are secreted in precursor zymogen form for activation through a range of processes, either through other proteases[115], other MMPs involved in the activation process[83], or through the involvement of specific TIMPs[111]. Of all of the MMPs, MT1-MMP was found to be activated intracellularly through the actions of the protease furin[116, 117] in the cytoplasm prior to establishing its transmembrane position. It has been proposed that

intracellular MMP activation through any one of a number of causes may lead to the degradation of various intracellular targets including mechanical or structural proteins[66, 118]. Various oxidative species have been determined to be involved as a primary agents for this intracellular activation[114, 119] and cellular damage, such as peroxynitrite[120] or hydroxyl radical[121], and also need to be assessed based on their source, whether it is from xanthine oxidase, NADPH oxidase[122], or mitochondrial damage[73, 123] as examples. The exposure of the catalytic site of the MMP enables proteolytic activity from the MMP. Our lab has reported that superoxide is a mediator of the transient induction of MMPs from cardiomyocytes from acute TNF treatment[124]. Two considerations that arise from this are that intracellular activation may be contributing to the phenotype through a mechanism of intracellular degradation that we are not accounting for, and secondly, the MMP activities (collagenase and gelatinase) that we report in these mice could partially be originating from intracellular sources.

6.10.4. Demographics and care of the mice

The main attributes of the mice and their living environment that impact our objective to create conditions that are representative of actual heart disease are the age of the mice, their sex, and their diet and conditions under which the mice are cared for. The age of the subject provides a variable that has both advantages and disadvantages that will influence the focus of the study. It has been found that there exists an age-dependent pattern of ECM remodeling[125] that may in itself contribute to the remodeling process in response to MI, thereby potentially either negating or amplifying the innate response. There is a reasonable argument that can be made that heart disease has a greater likelihood of occurring in the aging population as opposed to younger individuals, therefore assessing older animals would be more representative. By using younger animals our objective was to focus on changes that occur due to our specific genetic and surgical manipulations to identify specific ECM remodeling patterns and mechanisms of heart disease, not to observe a broader impact with confounding factors such as age-related ECM regulatory changes and age-associated cardiac functional and structural

alterations[126]. Our exclusive use of male mice as subjects was to similarly delineate the mechanisms of heart disease development independent of confounding factors unique to females, in particular hormonal influence. Lastly, the conditions under which our mice were cared for were pristine prior to and post-surgery, as is the case with most scientific research in an optimal laboratory setting. Although this is to eliminate confounding factors, it represents a lifestyle that may not be conducive to typical heart disease incidence, thereby omitting highly influential behavioural variables, although our specific and accurate simulation of heart disease for a large part should offset this issue.

6.10.5. *In vivo* assessment of cardiac function in mice

Assessing cardiac function in anesthetized animals has its inherent limitations, such as the potential direct or indirect effects that the anesthetic may have on cardiac function while the animal is in this state of anesthesia. The main purpose of using anesthesia is to sedate and immobilize the animal, thereby obtaining resting measurements with minimal difficulty. There is evidence the type of anesthetic agent used can have differential effects on cardiac function in mice[127] or rats[128], with the direct influence on the heart rate of the animal seemingly a predominant cause of this alteration. The use of low levels of isoflurane (0.75-1% in 100% oxygen) limits the effects, as isoflurane has also been found to be the more reproducible in repeat studies compared to other agents[127], indicating a higher degree of reliability. The alternative methods of *in vivo* cardiac functional imaging would be to attempt this on conscious animals, which would limit data collection as it would not allow the user to capture precise images for analysis, or to use invasive hemodynamics that despite its high level of precision and accuracy also experiences the issues of anesthesia and additionally is a terminal process which would not allow for any time-course studies of a particular animal. Overall, the methods used in the studies presented in this thesis for *in vivo* assessment of cardiac function in mice are the most optimal and feasible of options.

6.10.6. In vitro assays for measuring MMP activation and activity

Two methods of MMP analyses that are commonly used are the gelatin-based zymography and the *in vitro* MMP activity assays. Each method presents limitations to accomplishing its intended goal. The gelatin zymography is used to analyze the levels of the gelatinases MMP2 and MMP9 present in the tissue sample by electrophoresis through a gelatin-based polyacrylamide gel, with the degradation of gelatin by commonly known gelatinases (MMP2 and MMP9) creating gelatin-free bands that appear clear (or white) upon staining of the gel with coomassie blue. This technique cannot be used to evaluate the activity of MMP2 or MMP9 (based on the size of the clear bands in the gel). This is because through the process of protein extraction and electrophoresis, the MMP-TIMP interaction is disrupted, thereby the contribution of TIMPs in inhibiting the activity of these MMPs is not reflected on the gelatin zymography gel. Additionally, the 72kDa form of MMP2 that appears on the gel can either be an inactive precursor of the cleaved activated form, or an activated molecule through the exposure of the catalytic site in the absence of the truncation process. In the gelatin zymography, this 72kDa molecule will be activated through the denaturing effect of SDS present in the gel, thereby not allowing for differentiation of inactive pro-MMP2 (or pro-MMP9) and activated forms of these MMPs. As such, all the data obtained from gelatin zymographies are herein presented to indicate levels of MMP2 and MMP9, and conversion of pro-MMP2 to its cleaved form which is mediated by TIMP2 (and MT1-MMP).

The *in vitro* MMP activity assay is a fluorescent substrate-based assay that relies on measurement of the release of fluorescence from the degradation of the fluorescent-tagged collagen or gelatin substrates by collagenases or gelatinases present in protein extracts. The protein extraction buffer used for this assay contains milder detergents (compared to the RIPA buffer used for gelatin zymography) and is meant to maintain the TIMP-MMP interaction. Although there is no definitive way to confirm if this interaction is indeed preserved, we have found that by using RIPA extraction buffer (or any other SDS-containing

extraction buffer) in this assay, we were not able to obtain the typical curves that are indicative of enzymatic activity. Having said that, whether 100% of the protein-protein interactions remain intact remains unknown.

6.11. Future Directions

6.11.1. Role of TIMPs in angiogenesis

MI and pressure overload induced hypertrophy both create conditions where the existing viable vasculature is most probably insufficient to supply the working myocardium enough to sustain cardiac function, requiring the initiation of angiogenesis. Largely through the application of genetic MMP-modification in mice, MMPs have been implicated in promoting angiogenesis in a variety of settings, most notably in cancer[129] and ischemia[130], in mostly a proangiogenic capacity except with some variability with regard to the actions of MMP9[131-133]. MMPs have been found to be directly involved in the development of angiogenesis, through the processes of proteolysis of existing basement-membrane ECM and the synthesis of new matrix components[134, 135]. Moreover, additional roles of MMPs include increasing availability of growth factors and cytokines, and enabling mobilization and migration of various cell types[136]. TIMP2 and TIMP3 have both been shown to inhibit a broad-spectrum of MMPs, which would consequently impair angiogenesis. There is also the possibility that MMP activity may result in the regression and loss of vasculature under certain conditions, especially pertaining to MT1-MMP[137]. Determining the extent of MMP-dependence of the anti-angiogenic properties of TIMPs, and differentiating between the roles of each TIMP in this process would be beneficial to understanding the balance between MMPs and TIMPs in establishing adaptive vasculature in response to disease and under what conditions it is optimal. Additionally, aside from the ability of TIMPs to inhibit MMPs, there have been novel findings that TIMPs can affect the downstream signaling from the proangiogenic VEGFR2 growth factor receptor independent of its MMP-

inhibitory capacity, through TIMP2 interaction with the endothelial cell membrane-bound adjacent α3β1 integrin complex[138] or TIMP3 interacting directly with the VEGFR2 receptor[139]. The use of TIMP-deficient mice to determine the different roles of TIMPs in angiogenesis is an effective and unexplored approach, especially through the application of *in vitro*, *ex vivo*, and *in vivo* analyses.

6.11.2. TIMP3/TACE/TNFα axis in myocardial infarction

The role of TNFα in heart disease has been investigated through the use of TNFα-deficient mouse models of MI[140] and pressure overload[141] to demonstrate an injurious role attributed to this cytokine leading to adverse cardiac remodeling. The deletion of TNFα improved the outcomes in these disease models, suggesting that the investigation of upstream regulators of TNFα may serve as potential therapeutic targets. The activation of TNFα via TACE /ADAM17 has been described earlier, and in addition to inhibiting a large number of MMPs, TIMP3 also inhibits TACE, which is responsible for the cell surface shedding of TNF and activation of its downstream signaling[142, 143]. Our lab has reported that the activation of the TNF pathway induces a number of MMPs in cardiomyocytes within 1 h of treatment[124], and is therefore a pathway that would benefit from further exploration. In the pressure overloaded heart, it has been determined that TNFα-ablation can rescue the phenotype observed in the TIMP3-deficient heart post-TAC[8], and in combination with pharmacological MMP inhibition complete rescue can be achieved. A recent report has found contradicting results suggesting a beneficial effect of TNFα in the pressure overloaded heart related to placental growth factor, based on the establishment of an adaptive inflammatory response through the TIMP3-TACE axis[144]. The duality of the roles of TNF receptor 1 (TNFR1) and receptor 2 (TNFR2) to serve as injurious and protective signaling mediators, respectively, as well as serving as a possible TACE targets, further requires investigation of the role of TIMP3 in the cytokine regulation, inflammation, and ultimately cell fate related to myocardial infarction. TNF receptors are critical mediators of the immune response[145] and are considered to be regulated by TACE in its ectodomain sheddase capacity[146].

In addition to monitoring TIMP3 and TNFα, examination of TACE can be accomplished through the use of TACE cardiac-specific knockout mice using cre-lox technology, as TACE whole-body knockouts ($TACE^{-/-}$) die at birth[147] with adverse fetal cardiac development and modeling[148]. A limitation of investigating the TIMP3-TACE interaction in myocardial infarction is of the broad spectrum of actions by TACE, as TNFα activation is only one aspect of its role. By using cardiac-specific TACE knockout mice, in essence we can simulate a TIMP3-overexpression environment to understand ultimately how TIMP3 is involves in this cytokine system, and the extent of its contribution. Looking immediately downstream from TIMP3 is an effective approach because it allows for observation of mechanisms that balance changes in TNFα activation and TNFR involvement. Investigating the interaction between TIMP3 and TACE, also the noncanonical aspects of TACE's TNFα regulation may be worth exploring.

6.11.3. TIMP replenishment

An alternative approach that needs to be investigated and propelled forward involves establishing balanced ECM remodeling via the introduction of TIMPs, in particular TIMP2 and TIMP3, to the myocardium either independently or in a concerted fashion. The perceived problems with introducing TIMPs was initially based on ineffective experimental delivery methods and also that the TIMP protein has a short half-life within the myocardium and would not have the desired prolonged effect. Adenoviral-based gene expression is a possible avenue, however with immunological risks associated with it. Ideally, a cell-based treatment targeted at overexpressing specific factors is likely the most desirable approach, as stem cells themselves would be more readily accepted into the cellular environment, along with the potential intrinsic reparative benefits associated with them. Currently, studies attempting to combine both gene-transfer and cell-therapy to generate TIMP-overexpressing stem cells have exhibited positive results[149], although more research is necessary as there have been only preliminary results with inadequate controls utilized to clearly delineate therapeutic benefits attributable to the specific treatment.

6.11.4. Studies on females

The studies completed for this thesis all included the exclusive use of male C57BL/6 mice to examine heart disease in WT and TIMP2- or TIMP3-deficient mice. The purpose of this was to identify the underlying mechanisms of heart disease development pertaining to the effect of TIMP-deficiency, which likely would have been altered in female patients in a hormone-dependent manner; hence female mice were not used. There is considerable literature that supports the theory that male and female rodents respond differently to heart disease[150, 151], likely due to the protective effects of estrogen in disease[152, 153] and conditionally with replacement therapy in aging[154, 155]. There is also evidence of a gender-specific differential expression pattern for genes associated with hypertrophy and collagen synthesis in aortic stenosis patients experiencing cardiac pressure overload[156], with higher collagen I along with a distinct hypertrophy pattern combining to have a significant effect on ventricular dimensions. As ECM turnover has demonstrated to be susceptible to sex-dependent factors, it would be informative and useful to clarify these mechanisms to protect women from deleterious cardiac remodeling. The impact of the proteolytic balance with respect to TIMP regulation in female mice should be investigated in parallel with male subjects and also in the context of age-related hormonal changes.

6.12. Challenges for clinical translation

The translation of preclinical discoveries to clinical application is a great challenge, especially when considering work with smaller animals. The minor variation in cardiovascular physiology among different species allows for careful comparison of molecular or cellular processes between animal models and the patient. Despite prevailing skepticism of the true translational potential and disconnect between the scientific and clinical communities, there remains anticipation that the next great finding will hold the key to treating and possibly reversing heart disease or heart failure. Great strides have been made to add to the

traditionally accepted therapies that exist for heart disease, but the recent scientific discoveries will not come to fruition for many years to come. Additionally, there is likely not one cure-all for heart disease, particularly heart failure when addressing the disease from a systolic or diastolic dysfunction perspective with each having its unique characteristic processes. The attempts to develop an effective therapy have varied from reliable upstream targets[157, 158] to novel highly specific downstream targets[159] to determine the most successful approach.

ECM and MMP regulation have been strongly considered as therapeutic targets for intervention[160-162]. The problem that arises is that there does not exist one absolute universal pattern of ECM remodeling that covers all heart diseases as the ECM structure is highly dynamic and dependent on a variety of conditions, with excess ECM degradation typically linked to myocardium-ECM disconnect leading to systolic dysfunction, whereas diastolic dysfunction is associated with the development of interstitial fibrosis within the myocardium impairing passive relaxation. Diastolic dysfunction has been identified as an important and independent prognostic marker of adverse outcome in patients with heart disease[163, 164]. The requirement for a successful ECM-based therapy would be to establish the most favorable balance for ECM remodeling in an injury-specific context using commonalities in remodeling patterns in order to stabilize and adapt the ECM to preserve optimal function.

6.13. Conclusions

The findings reported in this thesis present the complexity and relative unpredictability that underlies a significant aberrant shift in the balance of the cardiac ECM proteolysis system comprised primarily of the MMPs and TIMPs. In these studies, the removal of two specific TIMPs, namely TIMP2 and TIMP3, was to determine the causal role of these TIMPs in the cardiac response to injury or stress. We found that TIMP2 and TIMP3 play distinct roles in the cardiac response to MI versus pressure overload. TIMP2 and TIMP3 in the heart

significantly regulate MMP activity, which if left unchecked has demonstrated the capacity to drastically impair cellular adaptive processes, alter ventricular morphology, and inevitably exacerbate cardiac function. In addition, TIMP2 serves a critical role in sustaining the myocyte-ECM interaction by preventing integrin degradation by MT1-MMP. The study of ECM biology related to heart disease is a growing field with rapid progress made in the last decade pertaining to the MMP-TIMP balance. The therapeutic potential of preserving and possibly enhancing ECM viability is evident and needs to be further explored to augment current clinical interventions.

6.14. References

1. Jugdutt BI, Joljart MJ, Khan MI. Rate of collagen deposition during healing and ventricular remodeling after myocardial infarction in rat and dog models. *Circulation*. 1996;94:94-101

2. Jugdutt BI. Limiting fibrosis after myocardial infarction. *N Engl J Med*. 2009;360:1567-1569

3. Tian H, Cimini M, Fedak PW, Altamentova S, Fazel S, Huang ML, Weisel RD, Li RK. Timp-3 deficiency accelerates cardiac remodeling after myocardial infarction. *J Mol Cell Cardiol*. 2007;43:733-743

4. Drazner MH. The progression of hypertensive heart disease. *Circulation*. 2011;123:327-334

5. Johnson RR, Hapke E, Hendrick JW, Parkhurst AM, dowdy KB, Holder JR, Zile MR. Chronic pressure overload: Effects of gene deletion of the tissue inhibitor of the matrix metalloproteinase type 1 (timp-1) on hypertrophic remodeling. Abs # 2125. *Circulation suppl.* 2002;106:II-427

6. Koskivirta I, Kassiri Z, Rahkonen O, Kiviranta R, Oudit GY, McKee TD, Kyto V, Saraste A, Jokinen E, Liu PP, Vuorio E, Khokha R. Mice with tissue inhibitor of metalloproteinases 4 (timp4) deletion succumb to induced myocardial infarction but not to cardiac pressure overload. *J Biol Chem*. 2010;285:24487-24493

7. Kassiri Z, Defamie V, Hariri M, Oudit GY, Anthwal S, Dawood F, Liu P, Khokha R. Simultaneous tgfbeta-tnf activation and cross-talk cause aberrant remodeling response and myocardial fibrosis in tissue inhibitor of metalloproteinase 3 deficient heart. *J Biol Chem*. 2009

8. Kassiri Z, Oudit GY, Sanchez O, Dawood F, Mohammed FF, Nuttall RK, Edwards DR, Liu PP, Backx PH, Khokha R. Combination of tumor necrosis factor-alpha ablation and matrix metalloproteinase inhibition prevents heart failure after pressure overload in tissue inhibitor of metalloproteinase-3 knock-out mice. *Circ Res*. 2005;97:380-390

9. St John Sutton M, Lee D, Rouleau JL, Goldman S, Plappert T, Braunwald E, Pfeffer MA. Left ventricular remodeling and ventricular arrhythmias after myocardial infarction. *Circulation*. 2003;107:2577-2582

10. Yarbrough WM, Mukherjee R, Ikonomidis JS, Zile MR, Spinale FG. Myocardial remodeling with aortic stenosis and after aortic valve replacement: Mechanisms and future prognostic implications. *J Thorac Cardiovasc Surg*. 2012;143:656-664

11. Babbitt CJ, Shai SY, Harpf AE, Pham CG, Ross RS. Modulation of integrins and integrin signaling molecules in the pressure-loaded murine ventricle. *Histochem Cell Biol*. 2002;118:431-439

12. Zhidkova NI, Belkin AM, Mayne R. Novel isoform of beta 1 integrin expressed in skeletal and cardiac muscle. *Biochem Biophys Res Commun*. 1995;214:279-285

13. Shai SY, Harpf AE, Babbitt CJ, Jordan MC, Fishbein MC, Chen J, Omura M, Leil TA, Becker KD, Jiang M, Smith DJ, Cherry SR, Loftus JC, Ross RS. Cardiac myocyte-specific excision of the beta1 integrin gene results in myocardial fibrosis and cardiac failure. *Circ Res*. 2002;90:458-464

14. Olivetti G, Capasso JM, Sonnenblick EH, Anversa P. Side-to-side slippage of myocytes participates in ventricular wall remodeling acutely after myocardial infarction in rats. *Circ Res*. 1990;67:23-34

15. Weisman HF, Bush DE, Mannisi JA, Weisfeldt ML, Healy B. Cellular mechanisms of myocardial infarct expansion. *Circulation*. 1988;78:186-201

16. Zimmerman SD, Criscione J, Covell JW. Remodeling in myocardium adjacent to an infarction in the pig left ventricle. *Am J Physiol Heart Circ Physiol*. 2004;287:H2697-2704

17. Gupta S, Prahash AJ, Anand IS. Myocyte contractile function is intact in the post-infarct remodeled rat heart despite molecular alterations. *Cardiovasc Res*. 2000;48:77-88

18. Weber KT. Cardiac interstitium in health and disease: The fibrillar collagen network. *J Am Coll Cardiol*. 1989;13:1637-1652

19. Francis GS. Pathophysiology of chronic heart failure. *Am J Med*. 2001;110 Suppl 7A:37S-46S

20. D'Armiento J. Matrix metalloproteinase disruption of the extracellular matrix and cardiac dysfunction. *Trends Cardiovasc Med*. 2002;12:97-101

21. Beltrami CA, Finato N, Rocco M, Feruglio GA, Puricelli C, Cigola E, Quaini F, Sonnenblick EH, Olivetti G, Anversa P. Structural basis of end-stage failure in ischemic cardiomyopathy in humans. *Circulation*. 1994;89:151-163

22. Lindsey ML, Mann DL, Entman ML, Spinale FG. Extracellular matrix remodeling following myocardial injury. *Ann Med*. 2003;35:316-326

23. Shirwany A, Weber KT. Extracellular matrix remodeling in hypertensive heart disease. *J Am Coll Cardiol*. 2006;48:97-98

24. Kassiri Z, Defamie V, Hariri M, Oudit GY, Anthwal S, Dawood F, Liu P, Khokha R. Simultaneous transforming growth factor beta-tumor necrosis factor activation and cross-talk cause aberrant remodeling response and myocardial fibrosis in timp3-deficient heart. *J Biol Chem*. 2009;284:29893-29904

25. Heymans S, Schroen B, Vermeersch P, Milting H, Gao F, Kassner A, Gillijns H, Herijgers P, Flameng W, Carmeliet P, Van de Werf F, Pinto YM, Janssens S. Increased cardiac expression of tissue inhibitor of metalloproteinase-1 and tissue inhibitor of metalloproteinase-2 is related to cardiac fibrosis and dysfunction in the chronic pressure-overloaded human heart. *Circulation*. 2005;112:1136-1144

26. Li YY, McTiernan CF, Feldman AM. Interplay of matrix metalloproteinases, tissue inhibitors of metalloproteinases and their regulators in cardiac matrix remodeling. *Cardiovasc Res*. 2000;46:214-224

27. Moore L, Fan D, Basu R, Kandalam V, Kassiri Z. Tissue inhibitor of metalloproteinases (timps) in heart failure. *Heart Fail Rev*. 2011

28. Peterson JT, Li H, Dillon L, Bryant JW. Evolution of matrix metalloprotease and tissue inhibitor expression during heart failure progression in the infarcted rat. *Cardiovasc Res*. 2000;46:307-315

29. Li H, Simon H, Bocan TM, Peterson JT. Mmp/timp expression in spontaneously hypertensive heart failure rats: The effect of ace- and mmp-inhibition. *Cardiovasc Res*. 2000;46:298-306

30. Matsumura S, Iwanaga S, Mochizuki S, Okamoto H, Ogawa S, Okada Y. Targeted deletion or pharmacological inhibition of mmp-2 prevents cardiac rupture after myocardial infarction in mice. *J Clin Invest*. 2005;115:599-609

31. Kandalam V, Basu R, Abraham T, Wang X, Awad A, Wang W, Lopaschuk GD, Maeda N, Oudit GY, Kassiri Z. Early activation of matrix metalloproteinases underlies the exacerbated systolic and diastolic dysfunction in mice lacking timp3 following myocardial infarction. *Am J Physiol Heart Circ Physiol*. 2010;299:H1012-1023

32. Hammoud L, Lu X, Lei M, Feng Q. Deficiency in timp-3 increases cardiac rupture and mortality post-myocardial infarction via egfr signaling: Beneficial effects of cetuximab. *Basic Res Cardiol*. 2011;106:459-471

33. Spinale FG, Mukherjee R, Zavadzkas JA, Koval CN, Bouges S, Stroud RE, Dobrucki LW, Sinusas AJ. Cardiac restricted overexpression of membrane type-1 matrix metalloproteinase causes adverse myocardial remodeling following myocardial infarction. *J Biol Chem*. 2010;285:30316-30327

34. Ducharme A, Frantz S, Aikawa M, Rabkin E, Lindsey M, Rohde LE, Schoen FJ, Kelly RA, Werb Z, Libby P, Lee RT. Targeted deletion of matrix metalloproteinase-9 attenuates left ventricular enlargement and collagen accumulation after experimental myocardial infarction. *J Clin Invest*. 2000;106:55-62

35. Matsusaka H, Ide T, Matsushima S, Ikeuchi M, Kubota T, Sunagawa K, Kinugawa S, Tsutsui H. Targeted deletion of matrix metalloproteinase 2 ameliorates myocardial remodeling in mice with chronic pressure overload. *Hypertension*. 2006;47:711-717

36. Covell JW. Factors influencing diastolic function. Possible role of the extracellular matrix. *Circulation*. 1990;81:III155-158

37. Kato S, Spinale FG, Tanaka R, Johnson W, Cooper Gt, Zile MR. Inhibition of collagen cross-linking: Effects on fibrillar collagen and ventricular diastolic function. *Am J Physiol*. 1995;269:H863-868

38. Bradshaw AD, Baicu CF, Rentz TJ, Van Laer AO, Boggs J, Lacy JM, Zile MR. Pressure overload-induced alterations in fibrillar collagen content and myocardial diastolic function: Role of secreted protein acidic and rich in cysteine (sparc) in post-synthetic procollagen processing. *Circulation*. 2009;119:269-280

39. Chen K, Chen J, Li D, Zhang X, Mehta JL. Angiotensin ii regulation of collagen type i expression in cardiac fibroblasts: Modulation by ppar-gamma ligand pioglitazone. *Hypertension*. 2004;44:655-661

40. Lee AA, Dillmann WH, McCulloch AD, Villarreal FJ. Angiotensin ii stimulates the autocrine production of transforming growth factor-beta 1 in adult rat cardiac fibroblasts. *J Mol Cell Cardiol*. 1995;27:2347-2357

41. Odenbach J, Wang X, Cooper S, Chow FL, Oka T, Lopaschuk G, Kassiri Z, Fernandez-Patron C. Mmp-2 mediates angiotensin ii-induced hypertension under the transcriptional control of mmp-7 and tace. *Hypertension*. 2011;57:123-130

42. Arenas IA, Xu Y, Lopez-Jaramillo P, Davidge ST. Angiotensin ii-induced mmp-2 release from endothelial cells is mediated by tnf-alpha. *Am J Physiol Cell Physiol*. 2004;286:C779-784

43. Eagleton MJ, Ballard N, Lynch E, Srivastava SD, Upchurch GR, Jr., Stanley JC. Early increased mt1-mmp expression and late mmp-2 and mmp-9 activity during angiotensin ii induced aneurysm formation. *J Surg Res*. 2006;135:345-351

44. Gomez-Duran A, Mulero-Navarro S, Chang X, Fernandez-Salguero PM. Ltbp-1 blockade in dioxin receptor-null mouse embryo fibroblasts decreases tgf-beta activity: Role of extracellular proteases plasmin and elastase. *J Cell Biochem*. 2006;97:380-392

45. Tatti O, Vehvilainen P, Lehti K, Keski-Oja J. Mt1-mmp releases latent tgf-beta1 from endothelial cell extracellular matrix via proteolytic processing of ltbp-1. *Exp Cell Res*. 2008;314:2501-2514

46. Kassiri Z, Khokha R. Myocardial extra-cellular matrix and its regulation by metalloproteinases and their inhibitors. *Thromb Haemost*. 2005;93:212-219

47. Aimes RT, Quigley JP. Matrix metalloproteinase-2 is an interstitial collagenase. Inhibitor-free enzyme catalyzes the cleavage of collagen fibrils and soluble native type i collagen generating the specific 3/4- and 1/4-length fragments. *J Biol Chem*. 1995;270:5872-5876

48. Will H, Atkinson SJ, Butler GS, Smith B, Murphy G. The soluble catalytic domain of membrane type 1 matrix metalloproteinase cleaves the propeptide of progelatinase a and initiates autoproteolytic activation. Regulation by timp-2 and timp-3. *J Biol Chem*. 1996;271:17119-17123

49. Zhao H, Bernardo MM, Osenkowski P, Sohail A, Pei D, Nagase H, Kashiwagi M, Soloway PD, DeClerck YA, Fridman R. Differential inhibition of membrane type 3 (mt3)-matrix metalloproteinase (mmp) and

mt1-mmp by tissue inhibitor of metalloproteinase (timp)-2 and timp-3 rgulates pro-mmp-2 activation. *J Biol Chem*. 2004;279:8592-8601

50. Fielitz J, Leuschner M, Zurbrugg HR, Hannack B, Pregla R, Hetzer R, Regitz-Zagrosek V. Regulation of matrix metalloproteinases and their inhibitors in the left ventricular myocardium of patients with aortic stenosis. *J Mol Med*. 2004;82:809-820

51. Strongin AY, Collier I, Bannikov G, Marmer BL, Grant GA, Goldberg GI. Mechanism of cell surface activation of 72-kda type iv collagenase. Isolation of the activated form of the membrane metalloprotease. *J Biol Chem*. 1995;270:5331-5338

52. Butler GS, Butler MJ, Atkinson SJ, Will H, Tamura T, Schade van Westrum S, Crabbe T, Clements J, d'Ortho MP, Murphy G. The timp2 membrane type 1 metalloproteinase "receptor" regulates the concentration and efficient activation of progelatinase a. A kinetic study. *J Biol Chem*. 1998;273:871-880

53. Brew K, Nagase H. The tissue inhibitors of metalloproteinases (timps): An ancient family with structural and functional diversity. *Biochim Biophys Acta*. 2010;1803:55-71

54. English JL, Kassiri Z, Koskivirta I, Atkinson SJ, Di Grappa M, Soloway PD, Nagase H, Vuorio E, Murphy G, Khokha R. Individual timp deficiencies differentially impact pro-mmp-2 activation. *J Biol Chem*. 2006;281:10337-10346

55. Collier IE, Wilhelm SM, Eisen AZ, Marmer BL, Grant GA, Seltzer JL, Kronberger A, He CS, Bauer EA, Goldberg GI. H-ras oncogene-transformed human bronchial epithelial cells (tbe-1) secrete a single metalloprotease capable of degrading basement membrane collagen. *J Biol Chem*. 1988;263:6579-6587

56. Patterson ML, Atkinson SJ, Knauper V, Murphy G. Specific collagenolysis by gelatinase a, mmp-2, is determined by the hemopexin domain and not the fibronectin-like domain. *FEBS Lett*. 2001;503:158-162

57. Spinale FG, Koval CN, Deschamps AM, Stroud RE, Ikonomidis JS. Dynamic changes in matrix metalloprotienase activity within the human myocardial interstitium during myocardial arrest and reperfusion. *Circulation*. 2008;118:S16-23

58. Spinale FG. Myocardial matrix remodeling and the matrix metalloproteinases: Influence on cardiac form and function. *Physiol Rev*. 2007;87:1285-1342

59. Tam EM, Moore TR, Butler GS, Overall CM. Characterization of the distinct collagen binding, helicase and cleavage mechanisms of matrix metalloproteinase 2 and 14 (gelatinase a and mt1-mmp): The differential roles of the mmp hemopexin c domains and the mmp-2 fibronectin type ii modules in collagen triple helicase activities. *J Biol Chem*. 2004;279:43336-43344

60. Murphy G, McAlpine CG, Poll CT, Reynolds JJ. Purification and characterization of a bone metalloproteinase that degrades gelatin and types iv and v collagen. *Biochim Biophys Acta*. 1985;831:49-58

61. Ohuchi E, Imai K, Fujii Y, Sato H, Seiki M, Okada Y. Membrane type 1 matrix metalloproteinase digests interstitial collagens and other extracellular matrix macromolecules. *J Biol Chem*. 1997;272:2446-2451

62. Morrison CJ, Overall CM. Timp independence of matrix metalloproteinase (mmp)-2 activation by membrane type 2 (mt2)-mmp is determined by contributions of both the mt2-mmp catalytic and hemopexin c domains. *J Biol Chem*. 2006;281:26528-26539

63. Yu Q, Stamenkovic I. Cell surface-localized matrix metalloproteinase-9 proteolytically activates tgf-beta and promotes tumor invasion and angiogenesis. *Genes Dev*. 2000;14:163-176

64. Bergman MR, Teerlink JR, Mahimkar R, Li L, Zhu BQ, Nguyen A, Dahi S, Karliner JS, Lovett DH. Cardiac matrix metalloproteinase-2 expression independently induces marked ventricular remodeling and systolic dysfunction. *Am J Physiol Heart Circ Physiol*. 2007;292:H1847-1860

65. Kunugi S, Shimizu A, Kuwahara N, Du X, Takahashi M, Terasaki Y, Fujita E, Mii A, Nagasaka S, Akimoto T, Masuda Y, Fukuda Y. Inhibition of matrix metalloproteinases reduces ischemia-reperfusion acute kidney injury. *Lab Invest*. 2011;91:170-180

66. Ali MA, Cho WJ, Hudson B, Kassiri Z, Granzier H, Schulz R. Titin is a target of matrix metalloproteinase-2: Implications in myocardial ischemia/reperfusion injury. *Circulation*. 2010;122:2039-2047

67. Westermann D, Savvatis K, Lindner D, Zietsch C, Becher PM, Hammer E, Heimesaat MM, Bereswill S, Volker U, Escher F, Riad A, Plendl J,

Klingel K, Poller W, Schultheiss HP, Tschope C. Reduced degradation of the chemokine mcp-3 by matrix metalloproteinase-2 exacerbates myocardial inflammation in experimental viral cardiomyopathy. *Circulation*. 2011;124:2082-2093

68. Garg P, Rojas M, Ravi A, Bockbrader K, Epstein S, Vijay-Kumar M, Gewirtz AT, Merlin D, Sitaraman SV. Selective ablation of matrix metalloproteinase-2 exacerbates experimental colitis: Contrasting role of gelatinases in the pathogenesis of colitis. *J Immunol*. 2006;177:4103-4112

69. Hayashidani S, Tsutsui H, Ikeuchi M, Shiomi T, Matsusaka H, Kubota T, Imanaka-Yoshida K, Itoh T, Takeshita A. Targeted deletion of mmp-2 attenuates early lv rupture and late remodeling after experimental myocardial infarction. *Am J Physiol Heart Circ Physiol*. 2003;285:H1229-1235

70. Schulz R. Intracellular targets of matrix metalloproteinase-2 in cardiac disease: Rationale and therapeutic approaches. *Annu Rev Pharmacol Toxicol*. 2007;47:211-242

71. Butler GS, Overall CM. Updated biological roles for matrix metalloproteinases and new "intracellular" substrates revealed by degradomics. *Biochemistry*. 2009;48:10830-10845

72. Takimoto E, Champion HC, Li M, Ren S, Rodriguez ER, Tavazzi B, Lazzarino G, Paolocci N, Gabrielson KL, Wang Y, Kass DA. Oxidant stress from nitric oxide synthase-3 uncoupling stimulates cardiac pathologic remodeling from chronic pressure load. *J Clin Invest*. 2005;115:1221-1231

73. Ide T, Tsutsui H, Hayashidani S, Kang D, Suematsu N, Nakamura K, Utsumi H, Hamasaki N, Takeshita A. Mitochondrial DNA damage and dysfunction associated with oxidative stress in failing hearts after myocardial infarction. *Circ Res*. 2001;88:529-535

74. Sariahmetoglu M, Crawford BD, Leon H, Sawicka J, Li L, Ballermann BJ, Holmes C, Berthiaume LG, Holt A, Sawicki G, Schulz R. Regulation of matrix metalloproteinase-2 (mmp-2) activity by phosphorylation. *FASEB J*. 2007;21:2486-2495

75. Gioia M, Monaco S, Fasciglione GF, Coletti A, Modesti A, Marini S, Coletta M. Characterization of the mechanisms by which gelatinase a, neutrophil collagenase, and membrane-type metalloproteinase mmp-14

recognize collagen i and enzymatically process the two alpha-chains. *J Mol Biol*. 2007;368:1101-1113

76. Spinale FG, Escobar PG, Mukherjee R, Zavadzkas JA, Saunders SM, Jeffords LB, Leone AM, Beck C, Bouges S, Stroud RE. Cardiac-restricted overexpression of membrane type-1 matrix metalloproteinase in mice: Effects on myocardial remodeling with aging. *Circulation Heart Failure*. 2009;2:351-360

77. Ohtake Y, Tojo H, Seiki M. Multifunctional roles of mt1-mmp in myofiber formation and morphostatic maintenance of skeletal muscle. *J Cell Sci*. 2006;119:3822-3832

78. Takino T, Saeki H, Miyamori H, Kudo T, Sato H. Inhibition of membrane-type 1 matrix metalloproteinase at cell-matrix adhesions. *Cancer Res*. 2007;67:11621-11629

79. Shen XM, Wu YP, Feng YB, Luo ML, Du XL, Zhang Y, Cai Y, Xu X, Han YL, Zhang X, Zhan QM, Wang MR. Interaction of mt1-mmp and laminin-5gamma2 chain correlates with metastasis and invasiveness in human esophageal squamous cell carcinoma. *Clin Exp Metastasis*. 2007;24:541-550

80. Su G, Blaine SA, Qiao D, Friedl A. Membrane type 1 matrix metalloproteinase-mediated stromal syndecan-1 shedding stimulates breast carcinoma cell proliferation. *Cancer Res*. 2008;68:9558-9565

81. Barbolina MV, Stack MS. Membrane type 1-matrix metalloproteinase: Substrate diversity in pericellular proteolysis. *Semin Cell Dev Biol*. 2008;19:24-33

82. Pei D, Weiss SJ. Transmembrane-deletion mutants of the membrane-type matrix metalloproteinase-1 process progelatinase a and express intrinsic matrix-degrading activity. *J Biol Chem*. 1996;271:9135-9140

83. Knauper V, Will H, Lopez-Otin C, Smith B, Atkinson SJ, Stanton H, Hembry RM, Murphy G. Cellular mechanisms for human procollagenase-3 (mmp-13) activation. Evidence that mt1-mmp (mmp-14) and gelatinase a (mmp-2) are able to generate active enzyme. *J Biol Chem*. 1996;271:17124-17131

84. Knauper V, Bailey L, Worley JR, Soloway P, Patterson ML, Murphy G. Cellular activation of prommp-13 by mt1-mmp depends on the c-terminal domain of mmp-13. *FEBS Lett*. 2002;532:127-130

85. Hurst DR, Schwartz MA, Ghaffari MA, Jin Y, Tschesche H, Fields GB, Sang QX. Catalytic- and ecto-domains of membrane type 1-matrix metalloproteinase have similar inhibition profiles but distinct endopeptidase activities. *Biochem J*. 2004;377:775-779

86. Lauer-Fields JL, Broder T, Sritharan T, Chung L, Nagase H, Fields GB. Kinetic analysis of matrix metalloproteinase activity using fluorogenic triple-helical substrates. *Biochemistry*. 2001;40:5795-5803

87. Zucker S, Drews M, Conner C, Foda HD, DeClerck YA, Langley KE, Bahou WF, Docherty AJ, Cao J. Tissue inhibitor of metalloproteinase-2 (timp-2) binds to the catalytic domain of the cell surface receptor, membrane type 1-matrix metalloproteinase 1 (mt1-mmp). *J Biol Chem*. 1998;273:1216-1222

88. Mukherjee R, Brinsa TA, Dowdy KB, Scott AA, Baskin JM, Deschamps AM, Lowry AS, Escobar GP, Lucas DG, Yarbrough WM, Zile MR, Spinale FG. Myocardial infarct expansion and matrix metalloproteinase inhibition. *Circulation*. 2003;107:618-625

89. Holmbeck K, Bianco P, Caterina J, Yamada S, Kromer M, Kuznetsov SA, Mankani M, Robey PG, Poole AR, Pidoux I, Ward JM, Birkedal-Hansen H. Mt1-mmp-deficient mice develop dwarfism, osteopenia, arthritis, and connective tissue disease due to inadequate collagen turnover. *Cell*. 1999;99:81-92

90. Spinale FG, Escobar GP, Mukherjee R, Zavadzkas JA, Saunders SM, Jeffords LB, Leone AM, Beck C, Bouges S, Stroud RE. Cardiac-restricted overexpression of membrane type-1 matrix metalloproteinase in mice: Effects on myocardial remodeling with aging. *Circ Heart Fail*. 2009;2:351-360

91. Spruill LS, Lowry AS, Stroud RE, Squires CE, Mains IM, Flack EC, Beck C, Ikonomidis JS, Crumbley AJ, McDermott PJ, Spinale FG. Membrane-type-1 matrix metalloproteinase transcription and translation in myocardial fibroblasts from patients with normal left ventricular function and from patients with cardiomyopathy. *Am J Physiol Cell Physiol*. 2007;293:C1362-1373

92. Collen A, Hanemaaijer R, Lupu F, Quax PH, van Lent N, Grimbergen J, Peters E, Koolwijk P, van Hinsbergh VW. Membrane-type matrix metalloproteinase-mediated angiogenesis in a fibrin-collagen matrix. *Blood*. 2003;101:1810-1817

93. Sounni NE, Devy L, Hajitou A, Frankenne F, Munaut C, Gilles C, Deroanne C, Thompson EW, Foidart JM, Noel A. Mt1-mmp expression promotes tumor growth and angiogenesis through an up-regulation of vascular endothelial growth factor expression. *FASEB J*. 2002;16:555-564

94. Lorente L, Martin MM, Labarta L, Diaz C, Sole-Violan J, Blanquer J, Orbe J, Rodriguez JA, Jimenez A, Borreguero-Leon JM, Belmonte F, Medina JC, Lliminana MC, Ferrer-Aguero JM, Ferreres J, Mora ML, Lubillo S, Sanchez M, Barrios Y, Sierra A, Paramo JA. Matrix metalloproteinase-9, -10, and tissue inhibitor of matrix metalloproteinases-1 blood levels as biomarkers of severity and mortality in sepsis. *Crit Care*. 2009;13:R158

95. Adair-Kirk TL, Senior RM. Fragments of extracellular matrix as mediators of inflammation. *Int J Biochem Cell Biol*. 2008;40:1101-1110

96. Malik M, Bakshi CS, McCabe K, Catlett SV, Shah A, Singh R, Jackson PL, Gaggar A, Metzger DW, Melendez JA, Blalock JE, Sellati TJ. Matrix metalloproteinase 9 activity enhances host susceptibility to pulmonary infection with type a and b strains of francisella tularensis. *J Immunol*. 2007;178:1013-1020

97. Lin M, Jackson P, Tester AM, Diaconu E, Overall CM, Blalock JE, Pearlman E. Matrix metalloproteinase-8 facilitates neutrophil migration through the corneal stromal matrix by collagen degradation and production of the chemotactic peptide pro-gly-pro. *Am J Pathol*. 2008;173:144-153

98. Weathington NM, van Houwelingen AH, Noerager BD, Jackson PL, Kraneveld AD, Galin FS, Folkerts G, Nijkamp FP, Blalock JE. A novel peptide cxcr ligand derived from extracellular matrix degradation during airway inflammation. *Nat Med*. 2006;12:317-323

99. Gill SE, Huizar I, Bench EM, Sussman SW, Wang Y, Khokha R, Parks WC. Tissue inhibitor of metalloproteinases 3 regulates resolution of inflammation following acute lung injury. *Am J Pathol*. 2010;176:64-73

100. Takahashi T, Hiasa Y, Ohara Y, Miyazaki S, Ogura R, Suzuki N, Hosokawa S, Kishi K, Ohtani R. Relationship of admission neutrophil count to microvascular injury, left ventricular dilation, and long-term outcome in patients treated with primary angioplasty for acute myocardial infarction. *Circ J*. 2008;72:867-872

101. Papa A, Emdin M, Passino C, Michelassi C, Battaglia D, Cocci F. Predictive value of elevated neutrophil-lymphocyte ratio on cardiac

mortality in patients with stable coronary artery disease. *Clin Chim Acta*. 2008;395:27-31

102. Cuadrado E, Ortega L, Hernandez-Guillamon M, Penalba A, Fernandez-Cadenas I, Rosell A, Montaner J. Tissue plasminogen activator (t-pa) promotes neutrophil degranulation and mmp-9 release. *J Leukoc Biol*. 2008;84:207-214

103. Owen CA, Hu Z, Lopez-Otin C, Shapiro SD. Membrane-bound matrix metalloproteinase-8 on activated polymorphonuclear cells is a potent, tissue inhibitor of metalloproteinase-resistant collagenase and serpinase. *J Immunol*. 2004;172:7791-7803

104. Van Lint P, Libert C. Matrix metalloproteinase-8: Cleavage can be decisive. *Cytokine Growth Factor Rev*. 2006;17:217-223

105. Heymans S, Luttun A, Nuyens D, Theilmeier G, Creemers E, Moons L, Dyspersin GD, Cleutjens JP, Shipley M, Angellilo A, Levi M, Nube O, Baker A, Keshet E, Lupu F, Herbert JM, Smits JF, Shapiro SD, Baes M, Borgers M, Collen D, Daemen MJ, Carmeliet P. Inhibition of plasminogen activators or matrix metalloproteinases prevents cardiac rupture but impairs therapeutic angiogenesis and causes cardiac failure. *Nat Med*. 1999;5:1135-1142

106. Kawakami R, Saito Y, Kishimoto I, Harada M, Kuwahara K, Takahashi N, Nakagawa Y, Nakanishi M, Tanimoto K, Usami S, Yasuno S, Kinoshita H, Chusho H, Tamura N, Ogawa Y, Nakao K. Overexpression of brain natriuretic peptide facilitates neutrophil infiltration and cardiac matrix metalloproteinase-9 expression after acute myocardial infarction. *Circulation*. 2004;110:3306-3312

107. van den Borne SW, Cleutjens JP, Hanemaaijer R, Creemers EE, Smits JF, Daemen MJ, Blankesteijn WM. Increased matrix metalloproteinase-8 and -9 activity in patients with infarct rupture after myocardial infarction. *Cardiovasc Pathol*. 2009;18:37-43

108. Trescher K, Bernecker O, Fellner B, Gyongyosi M, Schafer R, Aharinejad S, DeMartin R, Wolner E, Podesser BK. Inflammation and postinfarct remodeling: Overexpression of ikappab prevents ventricular dilation via increasing timp levels. *Cardiovasc Res*. 2006;69:746-754

109. Rohde LE, Ducharme A, Arroyo LH, Aikawa M, Sukhova GH, Lopez-Anaya A, McClure KF, Mitchell PG, Libby P, Lee RT. Matrix metalloproteinase inhibition attenuates early left ventricular enlargement

after experimental myocardial infarction in mice. *Circulation*. 1999;99:3063-3070

110. Hudson MP, Armstrong PW, Ruzyllo W, Brum J, Cusmano L, Krzeski P, Lyon R, Quinones M, Theroux P, Sydlowski D, Kim HE, Garcia MJ, Jaber WA, Weaver WD. Effects of selective matrix metalloproteinase inhibitor (pg-116800) to prevent ventricular remodeling after myocardial infarction: Results of the premier (prevention of myocardial infarction early remodeling) trial. *J Am Coll Cardiol*. 2006;48:15-20

111. Wang Z, Juttermann R, Soloway PD. Timp-2 is required for efficient activation of prommp-2 in vivo. *J Biol Chem*. 2000;275:26411-26415

112. Jaworski DM, Soloway P, Caterina J, Falls WA. Tissue inhibitor of metalloproteinase-2(timp-2)-deficient mice display motor deficits. *J Neurobiol*. 2006;66:82-94

113. Fedak PW, Smookler DS, Kassiri Z, Ohno N, Leco KJ, Verma S, Mickle DA, Watson KL, Hojilla CV, Cruz W, Weisel RD, Li RK, Khokha R. Timp-3 deficiency leads to dilated cardiomyopathy. *Circulation*. 2004;110:2401-2409

114. Ali MA, Schulz R. Activation of mmp-2 as a key event in oxidative stress injury to the heart. *Front Biosci*. 2009;14:699-716

115. Lee E, Vaughan DE, Parikh SH, Grodzinsky AJ, Libby P, Lark MW, Lee RT. Regulation of matrix metalloproteinases and plasminogen activator inhibitor-1 synthesis by plasminogen in cultured human vascular smooth muscle cells. *Circ Res*. 1996;78:44-49

116. Remacle AG, Rozanov DV, Fugere M, Day R, Strongin AY. Furin regulates the intracellular activation and the uptake rate of cell surface-associated mt1-mmp. *Oncogene*. 2006;25:5648-5655

117. Yana I, Weiss SJ. Regulation of membrane type-1 matrix metalloproteinase activation by proprotein convertases. *Mol Biol Cell*. 2000;11:2387-2401

118. Sawicki G, Leon H, Sawicka J, Sariahmetoglu M, Schulze CJ, Scott PG, Szczesna-Cordary D, Schulz R. Degradation of myosin light chain in isolated rat hearts subjected to ischemia-reperfusion injury: A new intracellular target for matrix metalloproteinase-2. *Circulation*. 2005;112:544-552

119. Kandasamy AD, Chow AK, Ali MA, Schulz R. Matrix metalloproteinase-2 and myocardial oxidative stress injury: Beyond the matrix. *Cardiovasc Res*. 2010;85:413-423

120. Wang W, Sawicki G, Schulz R. Peroxynitrite-induced myocardial injury is mediated through matrix metalloproteinase-2. *Cardiovasc Res*. 2002;53:165-174

121. Kinugawa S, Tsutsui H, Hayashidani S, Ide T, Suematsu N, Satoh S, Utsumi H, Takeshita A. Treatment with dimethylthiourea prevents left ventricular remodeling and failure after experimental myocardial infarction in mice: Role of oxidative stress. *Circ Res*. 2000;87:392-398

122. Kuroda J, Ago T, Matsushima S, Zhai P, Schneider MD, Sadoshima J. Nadph oxidase 4 (nox4) is a major source of oxidative stress in the failing heart. *Proc Natl Acad Sci U S A*. 2010;107:15565-15570

123. Kowaltowski AJ, de Souza-Pinto NC, Castilho RF, Vercesi AE. Mitochondria and reactive oxygen species. *Free Radic Biol Med*. 2009;47:333-343

124. Awad AE, Kandalam V, Chakrabarti S, Wang X, Penninger JM, Davidge ST, Oudit GY, Kassiri Z. Tumor necrosis factor induces matrix metalloproteinases in cardiomyocytes and cardiofibroblasts differentially via superoxide production in a pi3kgamma-dependent manner. *Am J Physiol Cell Physiol*. 2010;298:C679-692

125. Lindsey ML, Goshorn DK, Squires CE, Escobar GP, Hendrick JW, Mingoia JT, Sweterlitsch SE, Spinale FG. Age-dependent changes in myocardial matrix metalloproteinase/tissue inhibitor of metalloproteinase profiles and fibroblast function. *Cardiovasc Res*. 2005;66:410-419

126. Cheng S, Fernandes VR, Bluemke DA, McClelland RL, Kronmal RA, Lima JA. Age-related left ventricular remodeling and associated risk for cardiovascular outcomes: The multi-ethnic study of atherosclerosis. *Circ Cardiovasc Imaging*. 2009;2:191-198

127. Roth DM, Swaney JS, Dalton ND, Gilpin EA, Ross J, Jr. Impact of anesthesia on cardiac function during echocardiography in mice. *Am J Physiol Heart Circ Physiol*. 2002;282:H2134-2140

128. Stein AB, Tiwari S, Thomas P, Hunt G, Levent C, Stoddard MF, Tang XL, Bolli R, Dawn B. Effects of anesthesia on echocardiographic

assessment of left ventricular structure and function in rats. *Basic Res Cardiol*. 2007;102:28-41

129. Foda HD, Zucker S. Matrix metalloproteinases in cancer invasion, metastasis and angiogenesis. *Drug Discov Today*. 2001;6:478-482

130. Cheng XW, Kuzuya M, Nakamura K, Maeda K, Tsuzuki M, Kim W, Sasaki T, Liu Z, Inoue N, Kondo T, Jin H, Numaguchi Y, Okumura K, Yokota M, Iguchi A, Murohara T. Mechanisms underlying the impairment of ischemia-induced neovascularization in matrix metalloproteinase 2-deficient mice. *Circ Res*. 2007;100:904-913

131. Lindsey ML, Escobar GP, Dobrucki LW, Goshorn DK, Bouges S, Mingoia JT, McClister DM, Jr., Su H, Gannon J, MacGillivray C, Lee RT, Sinusas AJ, Spinale FG. Matrix metalloproteinase-9 gene deletion facilitates angiogenesis after myocardial infarction. *Am J Physiol Heart Circ Physiol*. 2006;290:H232-239

132. Pozzi A, LeVine WF, Gardner HA. Low plasma levels of matrix metalloproteinase 9 permit increased tumor angiogenesis. *Oncogene*. 2002;21:272-281

133. Johnson C, Sung HJ, Lessner SM, Fini ME, Galis ZS. Matrix metalloproteinase-9 is required for adequate angiogenic revascularization of ischemic tissues: Potential role in capillary branching. *Circ Res*. 2004;94:262-268

134. Stetler-Stevenson WG. Matrix metalloproteinases in angiogenesis: A moving target for therapeutic intervention. *J Clin Invest*. 1999;103:1237-1241

135. Rundhaug JE. Matrix metalloproteinases and angiogenesis. *J Cell Mol Med*. 2005;9:267-285

136. van Hinsbergh VW, Koolwijk P. Endothelial sprouting and angiogenesis: Matrix metalloproteinases in the lead. *Cardiovasc Res*. 2008;78:203-212

137. Aplin AC, Zhu WH, Fogel E, Nicosia RF. Vascular regression and survival are differentially regulated by mt1-mmp and timps in the aortic ring model of angiogenesis. *Am J Physiol Cell Physiol*. 2009;297:C471-480

138. Seo DW, Li H, Guedez L, Wingfield PT, Diaz T, Salloum R, Wei BY, Stetler-Stevenson WG. Timp-2 mediated inhibition of angiogenesis: An mmp-independent mechanism. *Cell*. 2003;114:171-180

139. Qi JH, Ebrahem Q, Moore N, Murphy G, Claesson-Welsh L, Bond M, Baker A, Anand-Apte B. A novel function for tissue inhibitor of metalloproteinases-3 (timp3): Inhibition of angiogenesis by blockage of vegf binding to vegf receptor-2. *Nat Med*. 2003;9:407-415

140. Sun M, Dawood F, Wen WH, Chen M, Dixon I, Kirshenbaum LA, Liu PP. Excessive tumor necrosis factor activation after infarction contributes to susceptibility of myocardial rupture and left ventricular dysfunction. *Circulation*. 2004;110:3221-3228

141. Sun M, Chen M, Dawood F, Zurawska U, Li JY, Parker T, Kassiri Z, Kirshenbaum LA, Arnold M, Khokha R, Liu PP. Tumor necrosis factor-alpha mediates cardiac remodeling and ventricular dysfunction after pressure overload state. *Circulation*. 2007;115:1398-1407

142. Amour A, Slocombe PM, Webster A, Butler M, Knight CG, Smith BJ, Stephens PE, Shelley C, Hutton M, Knauper V, Docherty AJ, Murphy G. Tnf-alpha converting enzyme (tace) is inhibited by timp-3. *FEBS Lett*. 1998;435:39-44

143. Black RA, Rauch CT, Kozlosky CJ, Peschon JJ, Slack JL, Wolfson MF, Castner BJ, Stocking KL, Reddy P, Srinivasan S, Nelson N, Boiani N, Schooley KA, Gerhart M, Davis R, Fitzner JN, Johnson RS, Paxton RJ, March CJ, Cerretti DP. A metalloproteinase disintegrin that releases tumour-necrosis factor-alpha from cells. *Nature*. 1997;385:729-733

144. Carnevale D, Cifelli G, Mascio G, Madonna M, Sbroggio M, Perrino C, Persico MG, Frati G, Lembo G. Placental growth factor regulates cardiac inflammation through the tissue inhibitor of metalloproteinases-3/tumor necrosis factor-alpha-converting enzyme axis: Crucial role for adaptive cardiac remodeling during cardiac pressure overload. *Circulation*. 2011;124:1337-1350

145. Xanthoulea S, Pasparakis M, Kousteni S, Brakebusch C, Wallach D, Bauer J, Lassmann H, Kollias G. Tumor necrosis factor (tnf) receptor shedding controls thresholds of innate immune activation that balance opposing tnf functions in infectious and inflammatory diseases. *J Exp Med*. 2004;200:367-376

146. Murthy A, Defamie V, Smookler DS, Di Grappa MA, Horiuchi K, Federici M, Sibilia M, Blobel CP, Khokha R. Ectodomain shedding of egfr ligands and tnfr1 dictates hepatocyte apoptosis during fulminant hepatitis in mice. *J Clin Invest*. 2010;120:2731-2744

147. Peschon JJ, Slack JL, Reddy P, Stocking KL, Sunnarborg SW, Lee DC, Russell WE, Castner BJ, Johnson RS, Fitzner JN, Boyce RW, Nelson N, Kozlosky CJ, Wolfson MF, Rauch CT, Cerretti DP, Paxton RJ, March CJ, Black RA. An essential role for ectodomain shedding in mammalian development. *Science*. 1998;282:1281-1284

148. Shi W, Chen H, Sun J, Buckley S, Zhao J, Anderson KD, Williams RG, Warburton D. Tace is required for fetal murine cardiac development and modeling. *Dev Biol*. 2003;261:371-380

149. Angoulvant D, Fazel S, Weisel RD, Lai TY, Fedak PW, Chen L, Rafati S, Seneviratne CK, Degousee N, Li RK. Cell-based gene therapy modifies matrix remodeling after a myocardial infarction in tissue inhibitor of matrix metalloproteinase-3-deficient mice. *J Thorac Cardiovasc Surg*. 2009;137:471-480

150. Douglas PS, Katz SE, Weinberg EO, Chen MH, Bishop SP, Lorell BH. Hypertrophic remodeling: Gender differences in the early response to left ventricular pressure overload. *J Am Coll Cardiol*. 1998;32:1118-1125

151. Wang M, Tsai BM, Crisostomo PR, Meldrum DR. Tumor necrosis factor receptor 1 signaling resistance in the female myocardium during ischemia. *Circulation*. 2006;114:I282-289

152. Voloshenyuk TG, Gardner JD. Estrogen improves timp-mmp balance and collagen distribution in volume-overloaded hearts of ovariectomized females. *Am J Physiol Regul Integr Comp Physiol*. 2010;299:R683-693

153. Wang M, Wang Y, Weil B, Abarbanell A, Herrmann J, Tan J, Kelly M, Meldrum DR. Estrogen receptor beta mediates increased activation of pi3k/akt signaling and improved myocardial function in female hearts following acute ischemia. *Am J Physiol Regul Integr Comp Physiol*. 2009;296:R972-978

154. Xu Y, Arenas IA, Armstrong SJ, Davidge ST. Estrogen modulation of left ventricular remodeling in the aged heart. *Cardiovasc Res*. 2003;57:388-394

155. Jazbutyte V, Hu K, Kruchten P, Bey E, Maier SK, Fritzemeier KH, Prelle K, Hegele-Hartung C, Hartmann RW, Neyses L, Ertl G, Pelzer T. Aging reduces the efficacy of estrogen substitution to attenuate cardiac hypertrophy in female spontaneously hypertensive rats. *Hypertension*. 2006;48:579-586

156. Villar AV, Llano M, Cobo M, Exposito V, Merino R, Martin-Duran R, Hurle MA, Nistal JF. Gender differences of echocardiographic and gene expression patterns in human pressure overload left ventricular hypertrophy. *J Mol Cell Cardiol*. 2009;46:526-535

157. Pfeffer JM, Pfeffer MA, Mirsky I, Braunwald E. Regression of left ventricular hypertrophy and prevention of left ventricular dysfunction by captopril in the spontaneously hypertensive rat. *Proc Natl Acad Sci U S A*. 1982;79:3310-3314

158. Pfeffer JM, Pfeffer MA, Braunwald E. Influence of chronic captopril therapy on the infarcted left ventricle of the rat. *Circ Res*. 1985;57:84-95

159. Malik FI, Hartman JJ, Elias KA, Morgan BP, Rodriguez H, Brejc K, Anderson RL, Sueoka SH, Lee KH, Finer JT, Sakowicz R, Baliga R, Cox DR, Garard M, Godinez G, Kawas R, Kraynack E, Lenzi D, Lu PP, Muci A, Niu C, Qian X, Pierce DW, Pokrovskii M, Suehiro I, Sylvester S, Tochimoto T, Valdez C, Wang W, Katori T, Kass DA, Shen YT, Vatner SF, Morgans DJ. Cardiac myosin activation: A potential therapeutic approach for systolic heart failure. *Science*. 2011;331:1439-1443

160. Spinale FG, Coker ML, Bond BR, Zellner JL. Myocardial matrix degradation and metalloproteinase activation in the failing heart: A potential therapeutic target. *Cardiovasc Res*. 2000;46:225-238

161. Lee RT. Matrix metalloproteinase inhibition and the prevention of heart failure. *Trends Cardiovasc Med*. 2001;11:202-205

162. Creemers EE, Cleutjens JP, Smits JF, Daemen MJ. Matrix metalloproteinase inhibition after myocardial infarction: A new approach to prevent heart failure? *Circ Res*. 2001;89:201-210

163. Moller JE, Pellikka PA, Hillis GS, Oh JK. Prognostic importance of diastolic function and filling pressure in patients with acute myocardial infarction. *Circulation*. 2006;114:438-444

164. Persson H, Lonn E, Edner M, Baruch L, Lang CC, Morton JJ, Ostergren J, McKelvie RS. Diastolic dysfunction in heart failure with preserved

systolic function: Need for objective evidence:Results from the charm echocardiographic substudy-charmes. *J Am Coll Cardiol*. 2007;49:687-694